

Enzymatic Degradation and Drug Release Behavior of Dense Collagen Implants

Dissertation

zur Erlangung des Doktorgrades
der Fakultät für Chemie und Pharmazie
der Ludwig-Maximilians-Universität München

vorgelegt von
Iris Metzmacher
aus München

München 2005

ERKLÄRUNG:

Diese Dissertation wurde im Sinne von § 13 Abs. 3 bzw. 4 der Promotionsordnung vom 29. Januar 1998 von Herrn Prof. Dr. Wolfgang Frieß betreut.

EHRENWÖRTLICHE VERSICHERUNG

Diese Dissertation wurde selbstständig, ohne unerlaubte Hilfe angefertigt.

München, den 28. September 2005



.....
(Iris Metzmacher)

Dissertation eingereicht am: 30. September 2005

1. Gutachter: Prof. Dr. Wolfgang Frieß

2. Gutachter: Prof. Dr. Karsten Mäder

Tag der mündlichen Prüfung: 25. Oktober 2005

Acknowledgments

This thesis was written at the Department of Pharmacy, Pharmaceutical Technology and Biopharmaceutics at the Ludwig-Maximilians-University in Munich. The co-operation of several other parties contributed to the development of this work.

I would like to express my gratitude to my supervisor Prof. Dr. Wolfgang Frieß who gave me the opportunity to join his working group and greatly encouraged my interest in the field of biomaterials. I very much enjoyed the scientific discussions (which often developed into conversations about many other topics), his ongoing interest in my work and his scientific and personal advice. Thanks for providing such an outstanding working climate.

I would also like to extend my appreciation to Prof. Dr. Gerhard Winter who has created a very pleasant working atmosphere at the institute and who originally engaged my interest in pharmaceutical technology during my study of pharmacy in Munich.

Over the years I was accompanied by Dr. Florin Radu and PD Dr. Markus Bause from the Institute of Applied Mathematics at the Friedrich-Alexander University of Erlangen-Nuremberg (working group of Prof. Dr. Peter Knabner). Based on our cooperation in describing the drug release from dense collagen devices, a close working partnership developed. Thanks for giving me a small insight into the wide (and sometimes very confusing) field of mathematics and the chance to see problems through different eyes. I really enjoyed this broadening of my scientific horizons.

I am indebted to Prof. Dr. Karsten Mäder who introduced me to the secrets of ESR and who spent a lot of time making my investigations possible. In his working group at the Department of Pharmacy, Pharmaceutical Technology and Biopharmaceutics at the Martin-Luther-University in Halle/Saale, I would like to thank Kerstin Schwarz who performed the in vitro ESR investigations and who provided every detail I needed to deal with the data. I would also like to acknowledge Martin Bastrop who guided me through my in vivo measurements. Thanks to the whole group for the warm welcome and the very pleasant stay in Halle/Saale.

The in vivo investigations were performed in co-operation with the working group of Prof. Dr. Dr. Stefan Schultze-Mosgau (Department of Oral and Maxillofacial Surgery/Plastic Surgery at the Friedrich-Schiller-University, Jena). Dr. Falk Wehrhan is

acknowledged for his support, even if the stress of the clinical work limited the time available for discussions.

Dr. Martin Abel and Dr. Peter Ruth (both Lohmann & Rauscher GmbH & Co. KG, Rengsdorf) are acknowledged for their scientific advice concerning the binding studies on collagen wound dressings.

At the LMU Munich, I'm grateful to Prof. Dr. Joachim Rädler for the opportunity to use the FCS at the Institute of Experimental Physics. Special thanks go to Dr. Laura Rusu and Dr. Simon Keller who spent many hours with me at the spectrometer to perform the measurements.

For the challenging investigation of the diffusion coefficient inside the implants, I would like to thank Dr. André Pampel (Department of Physics and Earth Science, Group of Physics of Dielectric Solids at the University Leipzig) for his great efforts.

I would like to thank all my colleagues who shared the time with me at our institute. Imke Leitner who supported me whenever I needed help and all the other members of the "Frießens" for their friendship and support. Special thanks go to my lab partners Andreas Rutz and Dr. Daniel Schwartz who made the years in B.0.003 a pleasant short-time stay and who always helped me when things weren't working the way they should. I am grateful for the assistance of Dr. Silke Mohl and Dr. Roland Schmidt who answered every question patiently.

Guido, Mama, Papa and Gernot, thanks a lot for your love and support; I will always remember the words "If you try hard enough, everything is possible!".

There is not enough space to acknowledge all of the contributions to this work. Many thanks go to all who contributed in one or another way to my work, but were not explicitly listed here. This does not reduce my appreciation in any way.

Last but not least, I would like to thank the DFG for financially supporting this thesis and Innocoll GmbH, Saal/Donau and Lohmann & Rauscher GmbH & Co. KG, Rengsdorf for providing the collagen materials.

“As far as the laws of mathematics refer to reality, they are not certain, as far as they are certain, they do not refer to reality.”

Albert Einstein (1879-1955)

Table of Contents

1	INTRODUCTION	1
1.1	Classification of Polymers for Controlled Drug Release Devices	2
1.2	Classifications of Biodegradable Polymers	5
1.2.1	Origin of Polymer – Collagen: a Natural Polymer	5
1.2.1.1	Structure of Collagen	7
1.2.1.2	Cross-linking of Collagen	9
1.2.1.3	Collagen as a Biomaterial	12
1.2.2	Mechanism of Degradation	14
1.2.2.1	In vitro Degradation of Collagen	16
1.2.2.2	In vivo Degradation of Collagen	20
1.2.3	Mechanism of Drug Release	25
1.2.3.1	Erosion Controlled Drug Release	27
1.2.3.2	Drug Release from Collagen Devices	28
1.3	Introduction to Mathematical Models	30
1.3.1	Enzymatic Reaction	33
1.3.1.1	Adsorption	35
1.3.1.2	Degradation	37
1.3.2	Drug Release from Biodegradable Devices	42
1.3.2.1	Diffusion Controlled Drug Release	42
1.3.2.2	Swelling Controlled Drug Release	43
1.3.2.3	Erosion Controlled Drug Release	43
2	GOALS OF THIS THESIS	50
3	MATERIALS AND METHODS	52
3.1	Materials	52
3.1.1	Collagen	52
3.1.2	Wound Dressings	52

3.1.3	Enzymes	52
3.1.3.1	Collagenase	52
3.1.3.2	Gelatinase A	53
3.1.3.3	Gelatinase B	53
3.1.4	Model Compounds	54
3.1.5	Reagents and Buffers	55
3.2	Methods	57
3.2.1	Matrix Preparation	57
3.2.1.1	Collagen Powder	57
3.2.1.2	Collagen Mini-rods	57
3.2.1.3	DHT Cross-linking	59
3.2.1.4	EDC Cross-linking	60
3.2.1.5	Lyophilization	60
3.2.2	Characterization of the Collagen Matrices	61
3.2.2.1	Macroscopic Studies	61
3.2.2.2	Scanning Electron Microscopy (SEM)	61
3.2.2.3	Determination of Density	61
3.2.2.4	Karl-Fischer Titration	61
3.2.2.5	Differential Scanning Calorimetry (DSC)	62
3.2.2.6	Swelling Studies	62
3.2.2.7	Pulsed Field Gradient Nuclear Magnetic Resonance Spectroscopy (PFG-NMR)	62
3.2.3	Characterization of the Model Drugs	63
3.2.3.1	Sodium Dodecyl Sulphate Polyacrylamide Gel Electrophoresis (SDS- PAGE)	63
3.2.3.2	Fluorescence Correlation Spectroscopy (FCS)	63
3.2.4	Characterization of the Enzymatic Reaction	64
3.2.4.1	Determination of Enzyme Activity	64
3.2.4.1.1	FALGPA Assay	64
3.2.4.1.2	EnzChek® Gelatinase / Collagenase Assay Kit	64
3.2.4.2	Binding studies	64
3.2.4.3	Sorption Studies	65
3.2.4.4	Determination of the Degradation Constants	65
3.2.5	In vitro Degradation Studies	66
3.2.6	In vitro Release Studies	66

3.2.6.1	FITC Dextrans	66
3.2.6.2	BSA	66
3.2.7	In vivo Studies	67
3.2.7.1	Electron Spin Resonance Spectroscopy (ESR)	67
3.2.7.2	Histology	67
3.2.8	Mathematical Discretization	68
4	RESULTS AND DISCUSSION	69
4.1	Characterization of Collagen Matrices	69
4.1.1	Characterization of Dry Collagen Matrices	69
4.1.1.1	Matrix Density	70
4.1.1.2	Differential Scanning Calorimetry (DSC)	74
4.1.2	Transport of Water in Collagen Matrices	77
4.1.2.1	Swelling of Collagen Matrices	77
4.1.2.1.1	Swelling Without Addition of Collagenase	78
4.1.2.1.2	Swelling in the Presence of Collagenase	87
4.1.2.2	Diffusion Coefficient of Water in Minirods	91
4.1.3	Summary	93
4.2	Characterization of Degradation	94
4.2.1	Time Dependency of Activity of MMPs	95
4.2.2	Enzymatic Binding Studies on Collagenous Materials	98
4.2.2.1	Development of Test Conditions	98
4.2.2.2	Gelatinase B (MMP-9)	100
4.2.2.3	Gelatinase A (MMP-2)	101
4.2.2.4	Bacterial Collagenase (CHC)	105
4.2.3	Determination of Sorption Isotherms	109
4.2.4	Determination of Degradation Constants	114
4.2.5	Summary	116
4.3	In vitro Release of FITC Dextran	118
4.3.1	Diffusion Coefficient of FITC Dextrans	119
4.3.2	Influence of Experimental Setup	120
4.3.2.1	Variation in Concentration of Collagenase	120
4.3.2.2	Variation in Time of Collagenase Addition	123

4.3.3	Influence of Collagen Raw Material	125
4.3.3.1	Variation in Pretreatment of Collagen Material	125
4.3.3.2	Variation in Animal Source	126
4.3.3.3	Variation in Cross-linking	127
4.3.3.3.1	Variation in EDC Cross-linking Ratio	129
4.3.3.3.2	Variation in Cross-linking Method	132
4.3.4	Influence of Matrix Dimensions	133
4.3.4.1	Variation in Length of Minirods	133
4.3.4.2	Variation in Diameter of Minirods	135
4.3.5	Influence of FITC Dextran	137
4.3.5.1	Variation in Molecular Weight	137
4.3.5.2	Variation in Drug Concentration	144
4.3.6	Summary	146
4.4	In vitro and in vivo Release of PCA-BSA	148
4.4.1	Introduction to Electron Spin Resonance (ESR) Spectroscopy	148
4.4.1.1	Physical Principles	148
4.4.1.2	Samples	152
4.4.1.3	Spectra Analysis	153
4.4.2	Labeling of BSA	156
4.4.3	In vitro Release of BSA	158
4.4.4	In vivo Release of BSA	163
4.4.5	Biocompatibility	167
4.4.6	Summary	176
4.5	Mathematical Model of the Erosion Controlled Drug Release from Collagen Devices	178
4.5.1	Model Development	178
4.5.2	Additional Parameters Needed for the Model	184
4.5.2.1	Dependency of k_2 on the Enzyme Concentration	184
4.5.2.2	Correlation Between Immobile Drug and Degraded Collagen	187
4.5.3	Data used for Fitting the Model	189
4.5.4	Elaboration of the Implemented Parameters	190
4.5.4.1	Sorption Parameters	190
4.5.4.1.1	Type of Sorption Isotherm	190
4.5.4.1.2	Freundlich Sorption Exponent n	191

4.5.4.1.3 Sorption Rate k_1	193
4.5.4.2 Degradation Parameters	194
4.5.4.2.1 Degradation Rate k_2	194
4.5.4.2.2 Dependency of the Degradation Rate on the ES Complex Concentration (γ)	195
4.5.4.3 Parameters of the Drug Release	196
4.5.4.3.1 FITC Dextran 70 Immobilization Inside the Collagen Minirods	196
4.5.4.3.2 Diffusion Coefficients of FITC Dextran 70 and Collagenase	198
4.5.4.3.3 Matrix Dimensions	199
4.5.5 Comparison of Modeled and Experimental Data	200
4.5.5.1 FITC dextran 70 Release from Equine non Cross-linked Minirods	200
4.5.5.2 FITC dextran 70 Release from Bovine Corium EDC 1 Cross-linked Minirods	203
4.5.6 Summary	208
5 FINAL SUMMARY	210
6 REFERENCE LIST	215

List of Abbreviations

a_n	hyperfine coupling constant
APMA	p-aminophenylmercuricacetate
B_0	magnetic field
BCA	bicinchoninic acid
BSA	bovine serum albumin
CHC	Clostridium histolyticum collagenase
DDS	drug delivery system
DHT	dehydrothermal
DMSO	dimethyl sulfoxide
DSC	differential scanning calorimetry
EDC	1-ethyl-3-(3-dimethylaminopropyl)carbodiimide
EMR	electron magnetic resonance
EPR	electron paramagnetic resonance
ESR	electron spin resonance
EVAc	poly(ethylene-co-(vinyl acetate))
FALGPA	furylacryloyl-leucine-glycine-proline-alanine
FCS	fluorescence correlation spectroscopy
FITC	fluorescein isothiocyanate
G-CSF	granulocyte colony stimulating factor
Gly	glycine
GTA	glutaraldehyde
HE	hemalaun and eosin
hGH	human growth hormone
HMDIC	hexamethylene diisocyanate
HSA	human serum albumin

IEP	isoelectric point
k_{cat}	degradation rate
K_M	Michaelis-Menten constant
MMP	matrix metalloproteinase
MMP-2	gelatinase A
MMP-9	gelatinase B
MT-MMP	membrane-type matrix metalloproteinase
NHS	N-hydroxysuccinimide
NMR	nuclear magnetic resonance
ORC	oxidized regenerated cellulose
PCA	3-carboxy-2,2,5,5-tetramethyl-1-pyrrolidinyloxy
PFG-NMR	pulsed field gradient nuclear magnetic resonance
PLA	poly(lactic acid)
PLGA	poly(lactic acid-co-glycolic acid)
r_H	hydrodynamic radius
r.h.	relative humidity
rh-BMP 2	recombinant human bone morphogenetic protein 2
SD	standard deviation
SDS-PAGE	sodium dodecyl sulphate polyacrylamide gel electrophoresis
SEM	scanning electron microscopy
TEMPOL	4-hydroxy-2,2,6,6-tetramethylpiperidinyloxy
TGF	transforming growth factor
TIMP	tissue inhibitor of metalloproteinases
TLC	thin layer chromatography
T_m	melting temperature
Tris	tris(hydroxymethyl)aminomethane

1 Introduction

Drug delivery is a challenging part in pharmaceutical sciences. Especially, delivery of proteins is of interest, since these molecules are high potential therapeutics for e.g. cancer, contraception, diabetes and vaccination. Proteins are used for local and systemic therapy and administration could be oral, nasal, transdermal, rectal, ocular, bucal or parenteral (Sinha et al.; 2003). When given e.g. orally, proteins are often poorly bioavailable, due to rapid degradation, deactivation at acidic pH values and poor adsorption in the gastrointestinal tract. Therefore, the most convenient way for drug delivery to achieve high bioavailability is the parenteral route (Ranade et al.; 2003). Therapeutic effectiveness can be achieved by multiple injections, resulting in a problem of compliance, or by providing controlled or sustained release devices which release drugs in well-defined pharmacokinetic profiles (Sinha et al.; 2003). This second approach was even practiced before the word “pharmacy” existed. Aztecs, Mayans, Incas and people in Mesopotamia, Egypt and China developed macroscopic delivery systems containing polymers, commonly waxes, to extend the action mechanism of drugs and to improve features such as site specificity (Mainardes et al.; 2004). In 1937, Deanesly et al. presented the first controlled drug delivery system for hormonal implantation, containing pure crystalline estrogen pellets (Dash et al.; 1998). Nowadays, one of the most important features of drug delivery, going beyond release kinetics, is to enhance patient compliance by improving therapeutic efficacy and reducing toxic side effects. This can be achieved by providing implantable controlled release drug delivery systems (DDS). Drug release is either controlled by a polymer or polymeric membrane (polymeric DDS) or by mechanical ways like in pumps (mechanical DDS) (Danckwerts et al.; 1991). A major application field of pumps is diabetes (Ranade et al.; 2003). A certain insulin level is needed at all times which otherwise can be maintained only by multiple injections per day (circulation half live of insulin < 25min; (Siegel et al.; 1984)). Different types of pumps are used, e.g. infusion pumps or mircopumps (Dash et al.; 1998).

Another type of pump which attracted attention, is an osmotic based system developed from Alza Corporation (Alzet[®]). It is approved in the US for the treatment of prostate cancer by delivery of leuprolide acetate (Viadur[®]). However, an unrestricted use is limited by high costs and the eventual need of surgical removal (Weadock; 1986). Polymeric DDS are either monolithic or reservoir-type devices which are prepared from biodegradable or non-biodegradable polymers (Dash et al.; 1998). These DDS are used for local and systemic therapy.

1.1 Classification of Polymers for Controlled Drug Release Devices

A wide range of polymers for parenteral drug delivery are available (see Table 1-1) (Pillai et al.; 2001; Saltzman; 2001). Due to this overwhelming variety, many approaches for classification were taken. One main feature is biodegradability.

A classification of degradable and non-degradable polymers can be made by applying the Deborah number (Göpferich; 1997a). Degradable polymers have small Deborah numbers with values approaching zero (time of degradation is much shorter than human lifetime), whereas non-degradable polymers have large values (time of degradation can exceed human lifetime). Another definition for degradable materials can be based on the degradation of the material during application or immediately afterwards (Göpferich; 1996).

Table 1-1 Representative list of polymers used in drug delivery (modified from (Mohl; 2004; Pillai et al.; 2001; Saltzman; 2001; Shastri; 2003))

Classification	Examples
NATURAL POLYMERS	
Proteins	albumin, collagen, gelatin
Polysaccharides	agarose, alginate, carrageenan, cellulose, chitin, chitosan, cyclodextrin, dextran, hyaluronic acid, starch

Lipids	cholesterol, triglycerides
SYNTHETIC POLYMERS	
Biodegradable	
Polyesters	poly(lactic acid), poly(glycolic acid), copolymers of lactide/glycolide, poly(ϵ -caprolactone), poly(β -hydroxy butyrate), poly(β -malic acid), poly(dioxanone)
Polyanhydrides	poly(sebacic acid), poly(adipic acid), poly(terephthalic acid) and various copolymers
Polyamides	poly(imino carbonate), poly(amino acid)
Phosphorous-based polymers	poly(phosphazene), poly(phosphate), poly(phosphonate)
Others	poly(orthoester), poly(urethane), poly(cyanoacrylate), poly(ethylene glycol), poly(dihydropyran), poly(acetal)
Non-biodegradable	
Cellulose derivatives	carboxymethyl cellulose, cellulose acetate, cellulose acetate propionate, ethyl cellulose, hydroxypropyl methyl cellulose
Silicones	poly(dimethylsiloxane), colloidal silica
Acrylic polymers	poly(methacrylate), poly(methylmethacrylate), poly(hydroxy(ethylmethacrylate))
Others	poly(ethylene-co-(vinyl acetate)), poloxamer, poly(vinylpyrrolidone), poloxamine, poly(propylene)

One of the first implants, prepared by Folkman and Long in 1964, was a poly(dimethylsiloxane) tubing loaded with isoproterenol (Heller; 1984). This polymer was tolerated well during implantation in dogs, but a severe limitation was its non biodegradability. At the end of therapy, the depleted implant matrix remains inside the body or has to be removed surgically and non-biodegradable

potentially toxic fragments could stay behind (Ranade et al.; 2003). Hence, these polymers are suitable for implants when the removal is easy, such as ocular or vaginal implants or for artificial replacement of failing body parts in which long term resistance and excellent mechanical properties are desired (Shastri; 2003). Beyond this, for special applications, e.g. contraception (Implanon[®]), non-biodegradable polymers are used as drug delivery systems as well. Another limitation is the mechanism of drug release. Since most of the drug is released by diffusion, controlled release of molecules with molecular weights over 7.5kDa and/or poor solubility in the polymer can be difficult (Sinha et al.; 2003). This problem was overcome by Langer and Folkman in 1976 who achieved a reproducible three month delivery of macromolecules up to 2×10^6 Da from so-called “sandwich” pellets. These pellets consist of a polymer-drug core which is coated with the pure polymer e.g. poly(ethylene-co-(vinyl acetate) (EVAc)) to retard drug diffusion (Langer et al.; 1978).

Consequently, development of biodegradable polymer drug matrices has become increasingly important over the last 30 years (Pillai et al.; 2001). The first documented study was performed by Yolles et al. in 1970, who investigated the drug release of cyclazocine from a poly(lactic acid) (PLA) implant. The polymer is degraded to lactic acid, its natural metabolite, and disappears from the implant site without surgical removal (Heller; 1984).

Before going into details on biodegradable polymers, some terms have to be defined. Biodegradable or bioerodible reactions involve biological systems (Siepmann et al.; 2001). Biodegradable polymers are defined as polymers which are eroded in vivo, either enzymatically or non-enzymatically, into biocompatible, non-toxic products which are subsequently removed via normal metabolic pathways from the implant site (Ranade et al.; 2003; Sinha et al.; 2003). Often biocompatibility is defined by the degradation products and not necessarily by the polymer itself (Uhrich et al.; 1999). Biodegradable polymers can be subdivided by their material source (see 1.2.1) or by their mechanism of erosion (see 1.2.3). Erosion is considered as a physical phenomenon related to dissolution and diffusion processes (Mainardes et al.; 2004), in which the polymer bulk loses material, such as mono- or oligomers or parts of the

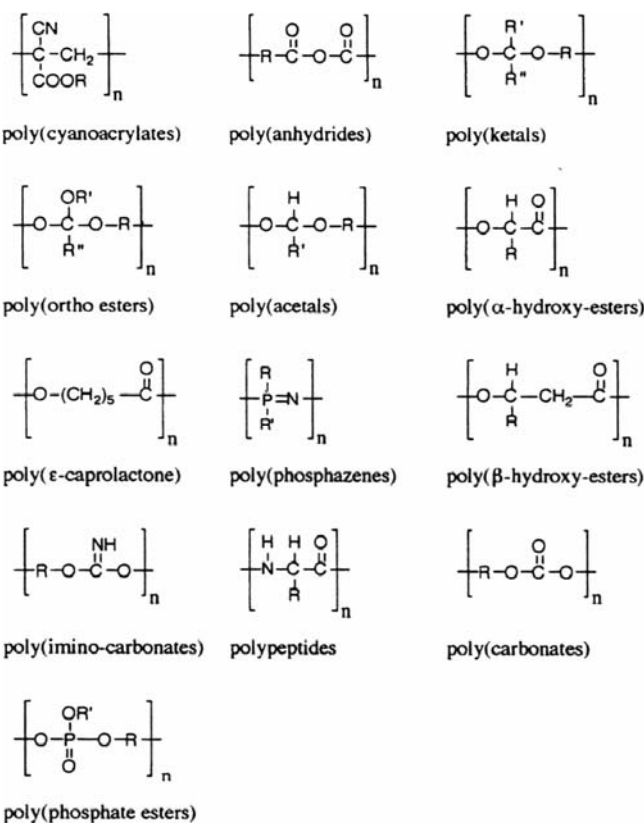
polymer backbone or bulk. In contrast, degradation is a chemical process that is restricted to the scission of the polymer chain resulting in mono- or oligomers. Consequently, degradation is a necessary condition for erosion (Göpferich; 1997a).

1.2 Classifications of Biodegradable Polymers

1.2.1 Origin of Polymer – Collagen: a Natural Polymer

Besides natural polymers, many synthetic biodegradable polymers, such as poly(esters), poly(amides), poly(anhydrides), poly(orthoesters) and poly(cyanoacrylates) are used as biodegradable matrices (see Table 1-1, Table 1-2).

Table 1-2 Functional groups of biodegradable polymers (Göpferich; 1997a)



Their advantage is, that large quantities with predictable and reproducible physicochemical properties, adapted to distinct applications, can be produced and purified (Cleland; 1997; Ranade et al.; 2003). On the other hand, for production organic solvents and high temperatures may be necessary (Cleland; 1997), and polymerization by-products, like non-reacted monomers or organic solvents, can have negative effects on drug release and biocompatibility.

The most extensively investigated subgroup are poly(esters), especially aliphatic poly(esters), like poly(lactic acid), poly(glycolic acid) and copolymers of lactic and glycolic acid. Consequently, the current “gold standard” of biodegradable polymers is poly(lactic acid-co-glycolic acid) (PLGA) (Pillai et al.; 2001). The advantages of these polymers are their good biocompatibility, because degradation products are natural metabolites, e.g. lactic and glycolic acid, and easy manufacturing. A wide variety of modifications by using racemic or optical active monomers for preparation of homo- and copolymers can be easily achieved (Uhrich et al.; 1999). Poly(esters) are used as rate controlling membranes or monolithic devices for delivery of narcotic antagonists, contraceptives, anticancer and antimalarial drugs (Sinha et al.; 2003). However, the release rate is difficult to predict because non-enzymatic bulk hydrolysis of ester linkages takes place. Additionally, an initial burst release and another burst after complete matrix erosion can occur. Consequently, a release mechanism with different stages is proposed for PLA and/or PLGA microspheres (Sinha et al.; 2003). To improve release kinetics, PLGA devices can be coated with pure polymer, stabilizing buffer salts can be added or the polymer itself can be modified (Sinha et al.; 2003). Apart from this complex release mechanism, PLGA has some further limitations for protein delivery. For the manufacturing of PLGA devices either organic solvents or elevated temperatures are needed which may cause harm to the incorporated proteins (Cleland; 1997). Furthermore, proteins can become unstable during release due to a change in environmental conditions (e.g. fast hydration of the matrix or decrease in pH caused by acidic erosion products) (Mohl; 2004).

Natural polymers, also named biopolymers, can be divided into polysaccharides (e.g. alginate, cellulose, chitosan, hyaluronic acid and starch), proteins (e.g.

albumin, collagen, gelatin) and lipids (e.g. triglycerides) (see Table 1-1). They are attractive as drug delivery materials because commercial quantities are available and the possibility of performing a variety of chemical modifications. As given by their name, they are natural products with good biocompatibility. On the other hand, because of their natural origin, batch to batch variations in polymer composition and difficulties in purification can occur (Pillai et al.; 2001). A frequently used biopolymer is collagen. Its attractiveness is its natural source, more precisely it is found in vertebrates to a great extent. Hence, in general it is well tolerated, biodegradable, biocompatible, non-toxic and shows low immunogenicity and antigenicity. Wound repair and cellular penetration are enhanced and degradation leads to well tolerated physiological compounds with haemostatic properties (Frieß; 1999; Gorham; 1991). Beyond this, its structural, chemical, physical and immunological properties are well documented (Sinha et al.; 2003).

1.2.1.1 Structure of Collagen

Collagen is the major structural protein in vertebrates, accounting approximately 30% of complete body protein (Frieß; 1999), and is predominantly located in the extracellular matrix (Brinckmann et al.; 2005). Different collagen types are necessary to meet the demands of different kinds of connective tissue. Currently, 27 collagen types have been isolated (Brinckmann et al.; 2005). Of those, 21 types are characterized in detail and divided into eight subgroups (Gelse et al.; 2003). Type I collagen is predominant in higher order animals and is found e.g. in bone, skin and tendon.

Due to these special requirements, collagen shows a very characteristic triple-helical structure with unusual strength and stability (Frieß; 1999). The sequence of amino acids is characterized by a repetitive unit: Gly-X-Y. The absence of a side chain in glycine, results in the formation of a typical left-handed triple helix as closest packing with glycine orientated into the core. The X- and Y-positions can be any amino acid, however, the X-position is occupied almost exclusively by proline, whereas hydroxyproline is found predominantly in the Y-position (Gorham; 1991). The stabilization of the triple helix is attributed to a limited

rotation along the backbone, based on the heterocyclic structure of the imino acids, intramolecular van der Waals interactions between imino acids and on the inductive effect of the OH-group of hydroxyproline (Brinckmann et al.; 2005). Three triple helical polypeptides, named α -chains, form a rope-like right-handed supercoil with a length of approximately 300nm and a diameter of 1.5nm. The supercoil is stabilized by hydrogen bonds between glycine and proline located in neighboring chains and by an extensive water network which can form hydrogen bonds between several carbonyl and hydroxyl peptide residues (Brinckmann et al.; 2005). Furthermore, amino acids in the X- and Y-positions are able to participate in intermolecular stabilization, e.g. by hydrophobic interactions or interactions between charged residues (Brinckmann et al.; 2005). This helical part is flanked by short non-helical domains (9-26 amino acids), the so called telopeptides, which play an important role in fibril formation and natural cross-linking. Instead of the repeating unit Gly-X-Y, a high variation in amino acids is available which is responsible for most of the immunological responses (Piez; 1985). At this level, the collagen supercoil is known as tropocollagen. Type I collagen is composed of two $\alpha 1$ (I) and one $\alpha 2$ (I) chains, containing approximately 1050 amino acids each. New data show that besides the telopeptides, tropocollagens still contain the N- and C-terminal propeptide sequences, also called non-collagenous domains (Brinckmann et al.; 2005). These domains are responsible for correct chain alignment and triple helix formation. The propeptides are removed before fibril formation and regulate the fibril formation process. Tropocollagens are staggered longitudinally and bilaterally by inter- and intramolecular cross-links into microfibrils (4 to 8 tropocollagens) and further into fibrils. This periodic arrangement is characterized by a gap of 40nm between succeeding collagen molecules and by a displacement of 67nm. The fibrils organize into fibers which in turn can form large fiber bundles (see Figure 1-1). Fibers and fiber bundles are stabilized by intermolecular cross-links (Frieß; 1998).

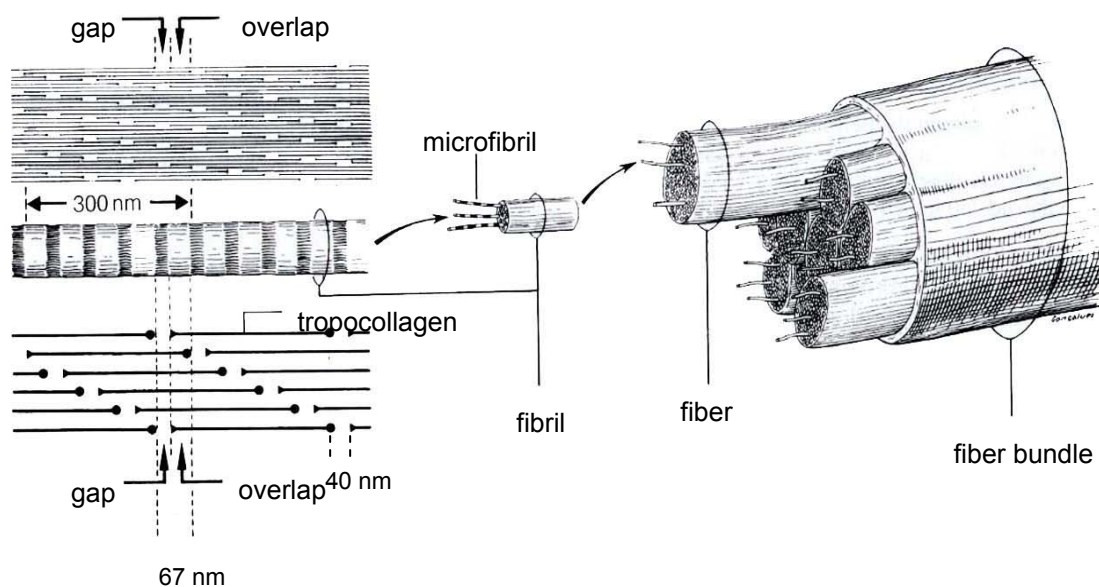


Figure 1-1 Structure of collagen (modified from (Junqueira et al.; 1996))

1.2.1.2 Cross-linking of Collagen

Collagen is predominantly isolated and purified from skin or tendon, even though it is ubiquitously present in vertebrates. For DDSs either soluble or insoluble collagen can be used. The choice of collagen has a great influence on the matrix durability *in vivo* (Frieß; 1999). During collagen biosynthesis (see 1.2.1.1), natural cross-links are created at the stage of fibril formation. After enzymatic transformation of lysine and hydroxylysine into their aldehydes, telopeptides are linked intrachainly by aldol condensation. Intermolecular bonds between telopeptides and the helical region of another collagen molecule are formed by aldimine formation between aldehydes and the ϵ -amino groups of lysine and hydroxylysine residues and subsequent stabilization by amadori rearrangement. These intermolecular linkages are still reactive and can develop additional cross-links with histidine, lysine and hydroxylysine (Frieß; 1998). Insoluble collagen is more appropriate to enhance the resistance of collagenous DDSs, because the original primary to tertiary structures with intact collagen fibers and telopeptides are still present, whereas (parts of the) telopeptides are

removed by enzymatic, acidic or alkali treatment in soluble collagen materials (Ruszczak et al.; 2003).

Table 1-3 Overview over cross-linking methods for collagen material

Chemical cross-linking	
Aldehydes e.g. glutaraldehyde (GTA)	Charulatha et al.; 2003, Cheung et al. ; 1984, Frieß; 1999, Geiger; 2001, Gilbert; 1988b, Gorham; 1991, Jayakrishnan et al.; 1996, Khor; 1997, Olde Damink et al.; 1995, Weadock et al.; 1984
Acyl azide	Charulatha et al.; 2003, Frieß; 1999, Gorham; 1991, Khor; 1997, Petite et al.; 1990
Carbodiimides e.g. 1-ethyl-3-(3-dimethylamino-propyl)carbodiimide (EDC)	Frieß; 1999, Geiger; 2001, Gorham; 1991, Khor; 1997, Olde Damink et al.; 1996, Park et al.; 2002, Pieper et al.; 1999, Weadock et al.; 1984, Zeeman et al.; 1999
Hexamethylene diisocyanate	Frieß; 1999, Geiger; 2001, Gorham; 1991, Khor; 1997
Poly-epoxy-compounds	Frieß; 1999, Khor; 1997, Tang et al.; 1995, Zeeman et al.; 1999
Physical cross-linking	
Dehydrothermal treatment (DHT)	Frieß; 1999, Geiger; 2001, Gilbert; 1988b, Gorham; 1991, Gorham et al.; 1992, Pieper et al.; 1999, Wang et al.; 1994, Weadock et al.; 1984, Weadock et al.; 1995, Weadock et al.; 1996
UV irradiation	Frieß; 1999, Gilbert; 1988b, Weadock et al.; 1984, Weadock et al.; 1995, Weadock et al.; 1996

Further increase in mechanical and chemical stability and in consequence reduced biodegradability and swelling can be achieved by additional exogenous cross-linking. This kind of cross-linking mainly takes place in the helical parts of

collagen because most commonly carboxyl groups of aspartic and glutamic acids and ϵ -amino groups of lysine and hydroxylysine residues are involved which are hardly found in the telopeptides (Zeeman et al.; 1999). Different ways of cross-linking, either chemical or physical, have been carried out and often the method is prescribed by the target application (see Table 1-3) (Frieß; 1999; Gorham; 1991; Hendriks et al.; 1998).

Chemical cross-linking is based on the additional formation of ionic or covalent bonds (Gorham; 1991). Aldehydes have a long tradition as cross-linking reagents. Especially treatment with GTA is intensively used. Besides its good efficiency, this cross-linking method is fast, inexpensive and mechanical properties are enhanced (Frieß; 1999; Jayakrishnan et al.; 1996). But due to polymerization of GTA, cross-linking is sometimes restricted to the surface of the device and a heterogeneous cross-linking structure can occur (Cheung et al.; 1984). Additionally, GTA is incorporated into the new linkage and non-reacted GTA can cause local incompatibility, inflammation, encapsulation and calcification, going along with limited cell ingrowth (Jayakrishnan et al.; 1996; Weadock et al.; 1984). Hence, non-toxic, water soluble substances which only facilitate the reaction, without becoming part of the new linkage, are needed. Such reagents are acyl azides and carbodiimides. Carbodiimides, e.g. EDC, couple carboxyl groups of glutamic or aspartic acid with amino groups of lysine or hydroxylysine residues. Reaction efficacy is increased by addition of N-hydroxysuccinimide (NHS) which prevents side reactions of the intermediate (Frieß; 1999; Gorham; 1991; Olde Damink et al.; 1996b). Because EDC can only couple groups within a distance of 1nm, this treatment enhances intra- and interhelical linkages, but no intermicrofibrillar cross-links (Zeeman et al.; 1999). EDC cross-linked collagens show reduced calcification, no cytotoxicity and slow enzymatic degradation (Khor; 1997; Pieper et al.; 1999; van Wachem et al.; 1994b).

Apart from chemical treatments, physical procedures have been developed (Frieß; 1999). Optimized DHT cross-linking of collagenous material is performed under vacuum at 110°C for 5d (Wang et al.; 1994). If the water content is below 0.1% (w/w) (Gilbert; 1988b), interchain amide formation or esterification occur

as a consequence of condensation of amino acid side chains (Weadock et al.; 1984). However, partial denaturation, detectable by trypsin digestion, accompanies this treatment (Weadock et al.; 1996). To minimize denaturation effects, DHT cross-linking has to be performed after removal of residual moisture. Distances between neighboring molecules are reduced after cross-linking, which is reflected in lower flexibility, less swelling, slower degradation and higher mechanical stability (Wang et al.; 1994). Advantages of this method are the absence of substances with toxic potential, the reduction of the microbiological burden (Geiger; 2001) and the preservation of the three dimensional matrix structure (Weadock; 1986). On the other hand partial denaturation may cause a faster degradation in vivo and if cross-linking is performed on the final product, incorporated drugs may lose their activity due to thermal instability or temperature induced reactions with collagen (Frieß; 1999; Gorham; 1991).

1.2.1.3 Collagen as a Biomaterial

Collagen was first employed as a biomaterial in medical surgery in the late 19th century (Burke et al.; 1983; Silver et al.; 1997). Subsequently, it was used in many other medical applications, e.g. as wound dressings, hemostats or in cardiovascular, plastic or neurosurgery (see Table 1-4). Most commonly, collagen type I is used in medical devices (Silver et al.; 1997). Device production is uncomplicated and is performed in water without applying high temperatures resulting in a variety of matrix forms, such as coatings, fibers, films, fleeces, implants, injectable solutions and dispersions, membranes, meshes, powders, sheets, sponges, tapes and tubes. Additionally, its properties can be adapted to the desired requirements by additional cross-linking (Frieß; 1999; Gorham; 1991; Silver et al.; 1997). However, shape instability due to swelling, poor mechanical strength and low elasticity in vivo may limit its unrestricted usage. Further limitations are possible antigenic responses, tissue irritations and variations in release kinetics (Sinha et al.; 2003).

Table 1-4 Some medical applications of collagen (modified from (Frieß; 1999; Fujioka et al.; 1998; Gilbert; 1988b; Gorham; 1991; Pachence et al.; 1987; Silver et al.; 1997; Weadock; 1986))

Specialty	Applications
Cardiology	heart valves
Dermatology	soft tissue augmentation
Surgery	hemostatic agent plasma expander suture wound dressing and repair skin replacement (artificial skin) nerve repair and conduits blood vessel prostheses
Orthopaedic	bone, tendon and ligament repair cartilage reconstruction
Ophthalmology	corneal graft, vitreous implants artificial tears tape and retinal reattachment contact lenses
Urology	dialysis membrane sphincter repair
Vascular	vascular graft, Vessel replacement angioplasty
Others	biocoatings cell culture organ replacement skin test

Nevertheless, collagen is used as a drug delivery matrix in cancer treatment, contraception, ophthalmology, orthopedics, periodontology, tissue repair and for the delivery of proteins (see Table 1-5). Except for protein delivery, these

applications are all used for local drug delivery (Frieß; 1998). Comprehensive reviews of collagen applications are given in (Frieß; 1998; Gorham; 1991).

Table 1-5 Drug delivery from collagen devices (modified from (Frieß; 1999; Fujioka et al.; 1998; Silver et al.; 1997; Weadock; 1986))

Application Field	Drug
Ophthalmology	amphotericin B, antibiotics, cyclosporine, 5-fluorouracil, non-steroidal anti-inflammatory drugs, pilocarpine, steroids
Parenteral	antibiotics, antineoplastic agents, bone morphogenetic proteins, contraceptives, growth factors, insulin, interferons, interleukins, medroxyprogesterone
Dermal	antibiotics, cosmetics, local anesthetics, retinol, tretinoin

1.2.2 Mechanism of Degradation

In general, erosion can be divided into four steps: hydration, loss of mechanical strength, loss of integrity and finally mass loss (Ranade et al.; 2003). The critical step therein is hydration, or more precisely degradation. Biodegradation is affected by properties of the polymer, like the type of the chemical bond, crystallinity, molecular weight and the ability of water uptake, and environmental factors, e.g. pH (Göpferich; 1997a). The polymer degradation mechanisms were classified by several investigators (see Figure 1-2) (Gombotz et al.; 1995; Heller; 1984; Kamath et al.; 1993). Heller distinguished between three types of degradation mechanisms (Heller; 1984). Type I occurs in water soluble polymers which have been made insoluble by covalent cross-linking. Consequently, water penetration into the device leads to swelling which is limited by the degree of cross-linking. The active agent must be only slightly water soluble or a macromolecule if drug release should be erosion controlled. Otherwise, drugs would be released by diffusion (see also 1.2.3).

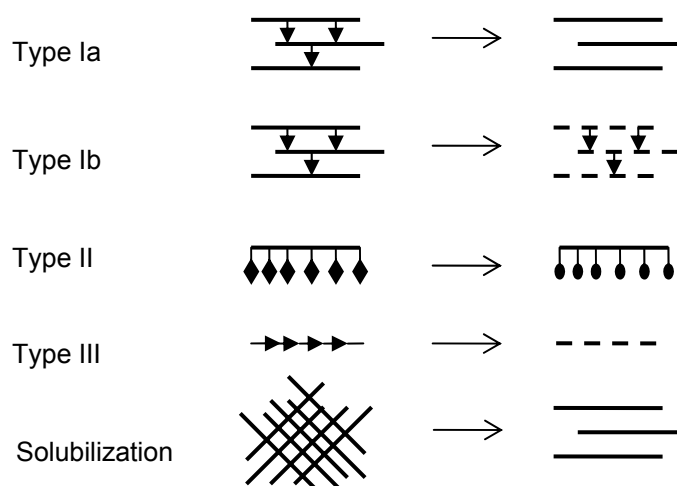


Figure 1-2 Mechanism of polymer degradation (modified from (Gombotz et al.; 1995; Heller; 1984))

Type I degradation can be subdivided into two groups. Either it takes place by cleaving the cross-links (type Ia) or by digestion of the polymer backbone (type Ib) (see Figure 1-2). Type Ia results in fragments which have to be further degraded, whereas cleavage products of type Ib have relatively low molecular weight. Gombotz et al. mentioned these two degradation pathways as well (Gombotz et al.; 1995). Polymers with unstable linkages in the water insoluble polymer backbone are equal to Heller's type Ib polymers. After either chemical or enzymatic cleavage, the resulting fragments are water soluble and have a lower molecular weight. Type Ia was defined by Gombotz et al. as degradation of a network of covalently or ionically cross-linked monomers. After digestion of unstable linkages, water soluble fragments are released. Their molecular weight depends on the density of cleavable bonds. Cross-linked collagen or gelatin are degraded by this mechanism (Gombotz et al.; 1995).

Degradation type II refers to polymers that are initially water insoluble. Hydrolysis, ionization or protonation of a pendant group is necessary before these polymers become water soluble (Heller; 1984). If solely type II degradation occurs, materials are only suitable for topical applications due to

high molecular weight degradation products. However, often a combination of type II and III degradation takes place, resulting in smaller fragments because of additional cleavage in the backbone (= type III) and polymers are appropriate for implants (Heller; 1984). Normally, combinations, e.g. of type Ia with type III occur with an initial cleavage of cross-links and subsequent backbone digestion. Such combined degradation mechanism occur in aliphatic poly(esters), poly(amides), poly(cyanoacrylates), poly(anhydrides), poly(acetals) and poly(orthoesters) (Heller; 1984).

Besides these degradation mechanisms, polymers, like non cross-linked gelatin, hyaluronic acid or polysaccharides, can be degraded by solubilization (Gombotz et al.; 1995). The polymer itself does not disintegrate and its molecular weight remains constant. The simplest form of solubilization is water diffusion into the polymer which leads to swelling and finally dissolution (Kamath et al.; 1993).

1.2.2.1 In vitro Degradation of Collagen

As described above, degradation of collagen requires water and enzyme penetration and digestion of linkages. Collagen swells to a certain extent by exposure to water. But due to its special sterical arrangement, native collagen can only be digested completely when collagenases participate. These enzymes are unique because they are able to cleave collagen in its undenatured helical regions at physiological pH and temperature (Harrington; 1996). If this general definition is used, collagenases which cleave one time across all three chains, like tissue collagenases, as well as collagenases making multiple scissions per chain, like collagenase from *Clostridium histolyticum* (CHC), are included (Seifter et al.; 1971). Non-specific proteinases, like pepsin, can only attack the telopeptides or denatured helical regions of collagen (Weiss; 1976). Hence, these enzymes are responsible for further degradation down to amino acids.

For in vitro experiments CHC is often used, because this enzyme was the only one available in adequate purified quantities for a long time (Seifter et al.; 1971) due to lower costs in production compared to tissue collagenases. These types

of collagenase are only present in tissue at very low levels and tightly bound to collagen (Woessner; 1991). Furthermore, CHC is easier to handle because no activation step is required and it has a broader spectrum than tissue collagenases, cleaving all types of collagen with no preference for a special collagen substrate (Welgus et al.; 1983). Last but not least, despite different cleavage sites (Mallya et al.; 1992), its specificity is quite similar to that of human neutrophil and fibroblast collagenase, which is important for in vivo / in vitro - correlation (Mookhtiar et al.; 1992). Scission occurs between Y and glycine at a -P-Y-Gly-P- sequence within the helical apolar regions, with P representing proline or hydroxyproline. Depending on the collagen type about 150-200 cleaves per chain can be made (Seifter et al.; 1971).

Up to now, seven forms of CHC are known (Mookhtiar et al.; 1992). All seven enzymes contain zinc and calcium and consist of one polypeptide chain with one active site. The zinc (II) atom is located in the active site and is therefore essential for catalysis, whereas the calcium (II) atoms are required to stabilize the enzyme conformation and consequently the enzymatic activity (Bond et al.; 1984). On the basis of their primary and secondary structure, their substrate specificity and their way of attack, CHCs can be divided into two classes. Class I contains α -, β -, γ -, and η -collagenase and firstly attacks the collagen triple helix near the ends. After cleavage at the C-terminal end, a cut near the N-terminus follows, before collagen is successively degraded into smaller fragments (see Figure 1-3a). Class II consists of δ -, ϵ - and ζ - collagenase and cleaves the tropocollagen in its center to produce two fragments. Further digestion of the bigger fragment follows (see Figure 1-3b) (French et al.; 1992; Mookhtiar et al.; 1992). Consequently, class II CHC better resembles tissue collagenases, which cleave collagen in a TC^A and a TC^B fragment (Seifter et al.; 1971; Welgus et al.; 1980).

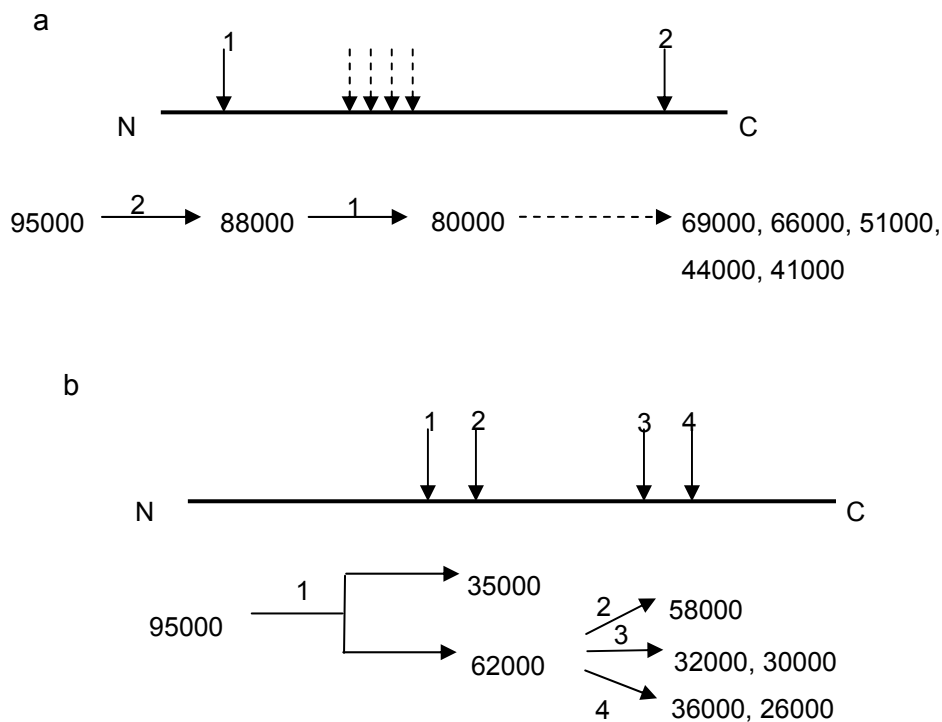


Figure 1-3 Schematic illustration of collagen cleavage by class I (a) and class II (b) CHC; numbers denote the molecular weight of resulting fragments (modified from (French et al.; 1992))

Moving along the polypeptide chain, collagenase recognizes its specific binding sites (see Figure 1-4). Thereby, the calcium (II) atoms of collagenase and the structural arrangement of collagen play a fundamental role. If collagenase binds to collagen, calcium ions interact with collagen residues, the conformation of the enzyme changes and positions in vicinity of the zinc atom become available to bind collagen amino acids. Due to the typical helical form of collagen, the cleavage sequence $-P-Y-Gly-P-$ forms a pocket with Y and glycine at the bottom. The zinc (II) atom of the enzymatic active site is thought to form a linkage with glycine and digestion can occur (Seifter et al.; 1971; Seifter et al.; 1970). Fields et al. detected enriched imino acids at the specific binding site for tissue collagenases, resulting in a stiff and thermally stable collagen region. This section is followed by a less thermally stable helical part which is more mobile due to depletion of imino acids. The helix can be unwound easily and the enzyme gains access to the cleavage site (Fields et al.; 1992). A similar

observation was made by Federman et al., who detected substantial unwinding of the triple helix during gelatin degradation by gelatinase A and B (Federman et al.; 2002). However, not all cleavage sites of CHC have a deficiency in imino acids. This suggests that digestion sites for bacterial collagenases exhibit not simply local disorder, but rather can adopt non-helical conformations and that local conformations at the cleavage site are more important than the amino acid sequence (French et al.; 1992). After scission, CHC can move on along the same collagen chain up to the next cleavage site (see Figure 1-4) (Gaspers et al.; 1994), whereas tissue collagenases have to switch to the next triple helix. Degradation by collagenases does not result in complete digestion down to individual amino acids (Mandl et al.; 1953). This subsequent digestion is catalyzed by non-specific proteinases.

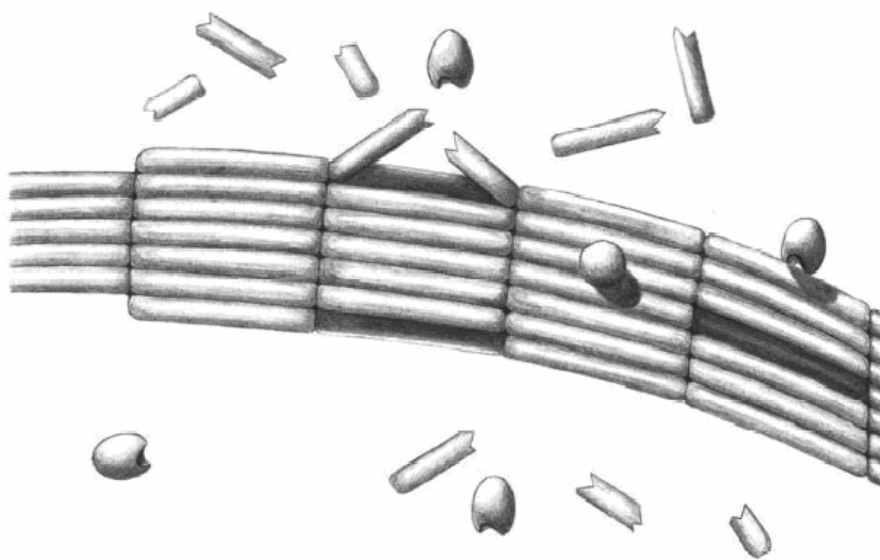


Figure 1-4 Schematic illustration of the proposed mechanism of the action of bacterial collagenase (Paige et al.; 2002)

Collagen fibrils are degraded in a non-specific manner, with no preferential cleavage site in the interior or at the ends of fibrils (see Figure 1-4) (Paige et al.; 2002). Paige et al. observed that fibril diameter and length decreases uniformly. It was concluded that collagenase is too large to penetrate into the fibrils and

that digestion can only occur at the fibril surface (Okada et al.; 1992a; Paige et al.; 2002). Hence, degradation rate is directly correlated to substrate molecules available on the surface. If collagen forms fibers and fiber bundles, tropocollagens within get inaccessible and degradation rate is even more reduced (Steven; 1976).

1.2.2.2 In vivo Degradation of Collagen

In vivo, degradation of collagen is more complex than in vitro. Collagen implants are infiltrated by various inflammatory cells, e.g. fibroblasts, macrophages or neutrophils, which cause contraction of the implant and secrete collagen degrading enzymes. Infiltration depends on properties of the implant, such as shape, porosity and degree of cross-linking, implantation site and individual enzyme levels (Gorham; 1991). Connective tissue, for example, is digested by the interplay of four different classes of proteinases which are either stored within cells or released when required. Cystein and aspartic proteinases degrade connective tissue intracellularly at acidic pH values, whereas serine and matrix metalloproteinases (MMP) act extracellularly at neutral pH values (Shingleton et al.; 1996). Furthermore, non-enzymatic degradation mechanisms, e.g. hydrolysis, participate in collagen breakdown (Okada et al.; 1992a). For degradation of the extracellular matrix, mainly MMPs are responsible. These enzymes represent a family of structurally and functionally related zinc-containing endopeptidases which degrade almost all extracellular matrix and basement membrane proteins (Wall et al.; 2002). Especially their catalytic domains are characterized by high sequence and structural homology (Overall; 1991). Up to now, 24 different MMPs and four tissue inhibitors of metalloproteinases (TIMP) are characterized (Yoshizaki et al.; 2002). According to their primary structure and substrate specificity, MMPs are divided into five sub-classes (see Table 1-6).

Table 1-6 MMP family (modified from (Yoshizaki et al.; 2002))

Group	MMP	Substrates
Collagenases		
Collagenase-1 (interstitial)	MMP-1	collagen types I, II, III, VII, X, casein
Collagenase-2 (neutrophil)	MMP-8	collagen types I, II, III, VII, X, casein
Collagenase-3	MMP-13	collagen types I, II, III, VII, X, casein
Collagenase-4 (Xenopus)	MMP-18	not known
Gelatinases		
Gelatinase A	MMP-2	collagen types I, IV, V, VII, IX, gelatin types I, IV, V, X, elastin, fibronectin, laminin V
Gelatinase B	MMP-9	collagen types I, III, IV, V, VII, gelatin types I, IV, V, X, elastin, laminin V
Stromelysins		
Stromelysin-1	MMP-3	collagen types I, III, IV, IX, X, gelatin, pro-MMP-1, fibronectin, laminin, proteoglycan
Matrilysin	MMP-7	gelatin, fibronectin, pro-MMP-1, transferrin
Stromelysin-2	MMP-10	collagen types III, IV, IX, X, gelatin, pro-MMP-1, elastin, laminin, proteoglycan
Stromelysin-3	MMP-11	collagen types II, IV, V, gelatin, elastin, fibronectin, α -1-antiproteinase
Metalloelastase	MMP-12	elastin

Membrane-type MMPs		
MT1-MMP	MMP-14	pro-MMP-2, gelatin and collagens
MT2-MMP	MMP-15	pro-MMP-2
MT3-MMP	MMP-16	pro-MMP-2
MT4-MMP	MMP-17	not known
Non-classified MMPs		
No trivial name	MMP-19	not known
Enamelysin	MMP-20	not known
XMMP (Xenopus)	MMP-21	not known
CMMP (Chicken)	MMP-22	not known
No trivial name	MMP-23	not known
No trivial name	MMP-24	not known

In human, five major MMPs have been identified, namely MMP-1, 2, 3, 8 and 9 (Netzel-Arnett et al.; 1991). Besides MMP-8, which is stored in specific granules of neutrophils, and membrane-type MMPs (MT-MMP), which are integral membrane cell (glyco)proteins, all other MMPs are synthesized if required (Imai et al.; 1998).

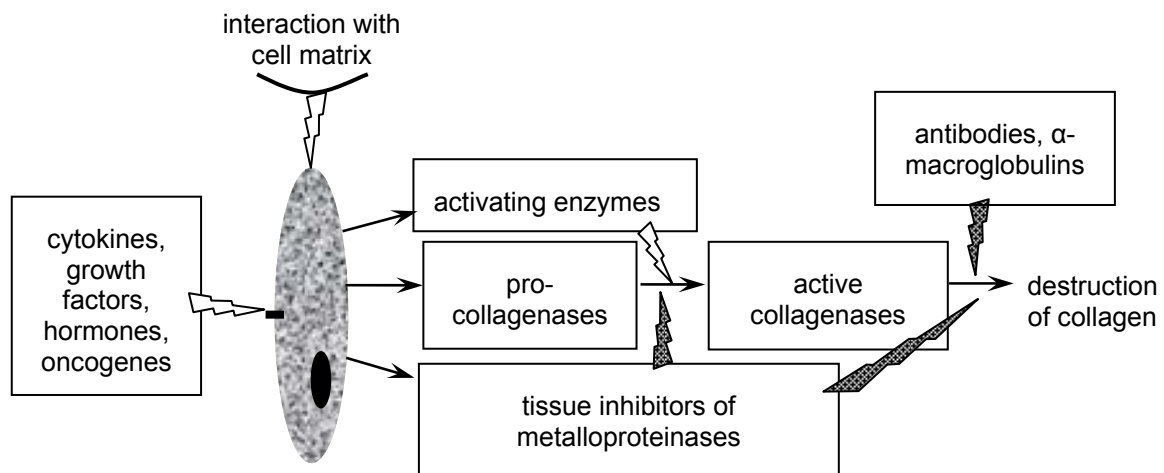


Figure 1-5 Control of MMP-1 activity (⚡ activation; ⚡ inhibition; modified from (Birkedal-Hansen et al.; 1993; He et al.; 1989; Shingleton et al.; 1996)

MMP expression is induced by various cytokines, e.g. interleukin-1, and growth factors (see Figure 1-5) (Shingleton et al.; 1996). MMPs are secreted as latent inactive pro-enzymes (= zymogens) which have to be activated before they have complete proteolytic activity (Overall; 1991). Four amino acids (three histidines and one cysteine) are coordinated to the zinc atom in the active center of zymogens (Birkedal-Hansen et al.; 1993). For activation, a “cysteine switch model” is proposed (see Figure 1-6). The linkage to the cysteine residue is thought to be cleaved and a water molecule, which must be the fourth substituent in the active enzyme, can bind (Nagase et al.; 1999; Woessner; 1991). In vivo, zymogens are activated by removal of a pro-peptide by proteinases, like plasmin or stromelysin, followed by a second activation step provoked by proteinases or autocatalysis (Shingleton et al.; 1996). Additionally, activation is controlled by TIMPs, which can prevent activation of zymogens and/or action of activated MMPs (see Figure 1-5). In vitro, trypsin and organomercurials can be used for activation as well (Overall; 1991). Physical agents unfold the structure, the zinc-cysteine contact breaks and the pro-peptide is cleaved autocatalytically (Woessner; 1991).

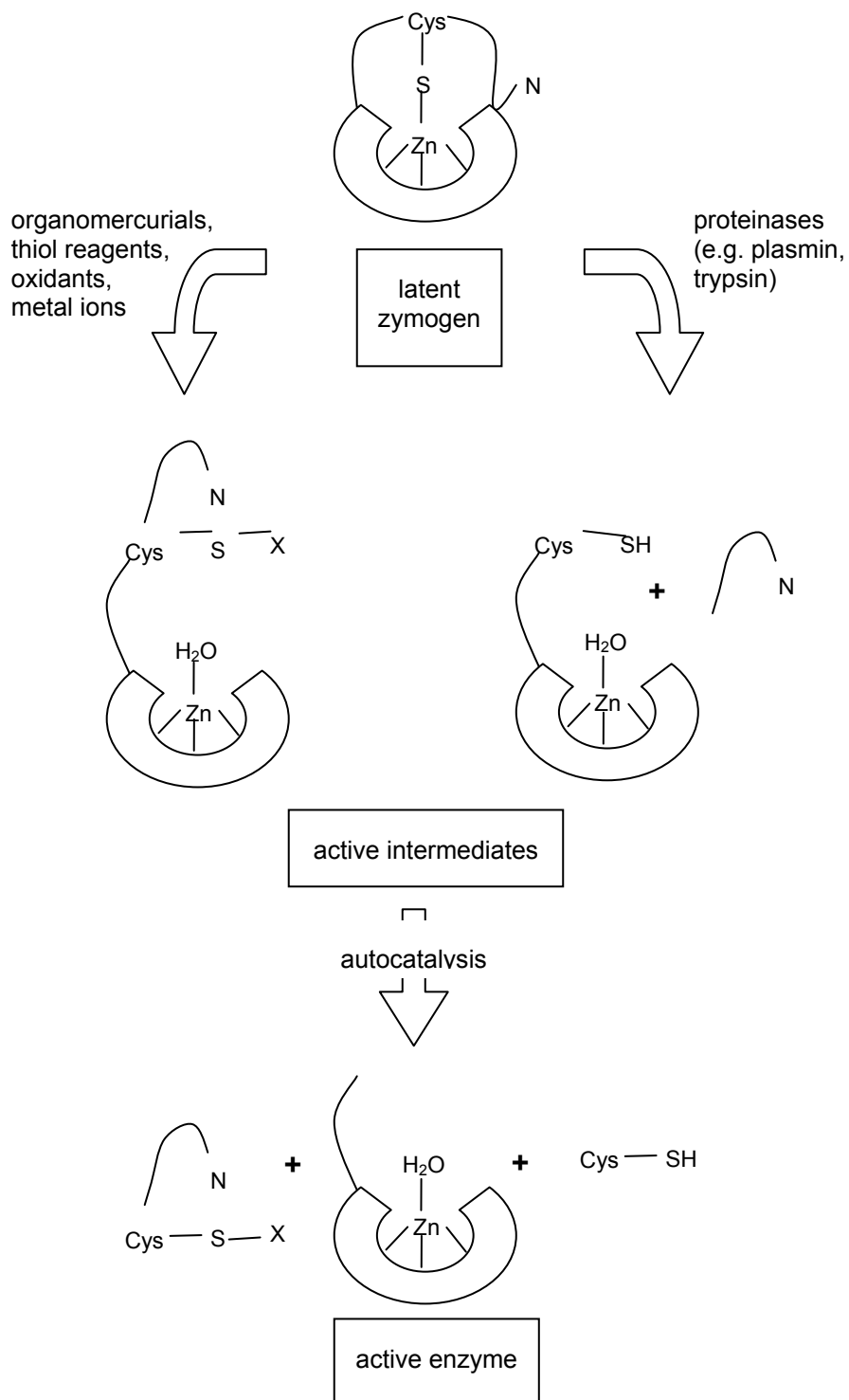


Figure 1-6 Cysteine switch model (modified from (Birkedal-Hansen et al.; 1993; Woessner; 1991))

Tissue collagenases cleave tropocollagen at one single site, producing TC^A and TC^B fragments about three-quarters and one-quarter of the original molecule size. After that initial cleavage, the helical fragments spontaneously denature at body temperature and are subsequently further digested by other proteinases (Mallya et al.; 1992). This secondary degradation can take place extracellularly or intracellularly after phagocytosis (Harris, Jr. et al.; 1974). Apart from collagenases, gelatinases play an important role in collagen degradation. Besides further degradation of initially cleaved collagen, gelatinases can degrade native collagen type I, IV, V and VII (Aimes et al.; 1995; Okada et al.; 1995; Overall; 1991). Furthermore, levels of gelatinases are considered to be a good index whether inflammation is present or not, because high concentrations are only available when a normal remodeling process is disrupted (Tregrove et al.; 1999; Wysocki et al.; 1993).

1.2.3 Mechanism of Drug Release

Looking more closely at the drug release mechanism, one has to focus first of all on the structure of the device. For parenteral depot delivery systems, either implants or microparticles are used. The active agent can be surrounded by a rate-controlling biodegradable membrane, e.g. in microcapsules, or uniformly distributed throughout the biodegradable polymer giving monolithic devices (Heller; 1984) such as microspheres, cylinders, films or beads. In the first case, drug release is predictable whenever the membrane erodes after complete drug delivery. Nevertheless, if the polymer is degraded before the complete drug is liberated, a dramatic change in release profile occurs (dose dumping). Drug release from monolithic devices is based on diffusion, swelling, matrix erosion or combinations (see Figure 1-7) (Göpferich; 1997a).

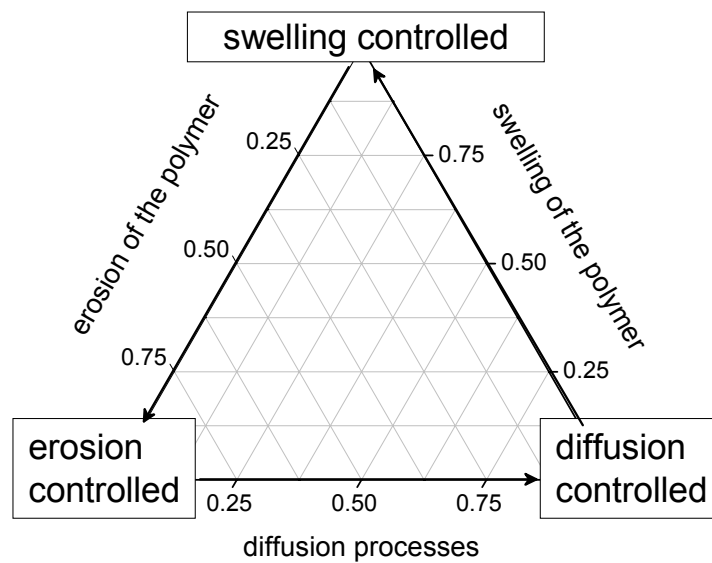


Figure 1-7 Possible drug release mechanism from degradable polymer devices (modified from (Winzenburg et al.; 2004))

For example PLGA microspheres combine different drug release mechanism. Initially, the release is controlled by desorption of the drug from the device surface, followed by drug diffusion through porous channels. The formation of these channels is influenced by the swelling rate of the microspheres. Afterwards, drug release is governed by diffusion through the intact and water swollen polymer barriers. This release phase is strongly dependent on the polymer properties, such as hydrophilicity and crystallinity. Finally, degradation and erosion of the polymer affect the drug delivery by formation of additional pores. Beyond this, the release mechanism can be influenced by physical properties of the polymer which further complicates the release kinetics (Gombotz et al.; 1995; Sinha et al.; 2003).

If drug release is diffusion controlled, delivery is described for monolithic devices by either Fick's second law (drug loading is lower than drug solubility in the polymer) or by the Higuchi equation (drug loading is higher than drug solubility in the polymer) (Kanjickal et al.; 2004).

1.2.3.1 Erosion Controlled Drug Release

When erosion is faster than drug diffusion, drug release is controlled by erosion. Distinction between two erosion mechanisms can be made. Erosion can take place throughout the whole matrix, referred as homogeneous or bulk erosion, or can be restricted to the device surface, named heterogeneous or surface erosion (see Figure 1-8). Mathematical models for drug delivery are discussed in more detail in section 1.3.2.

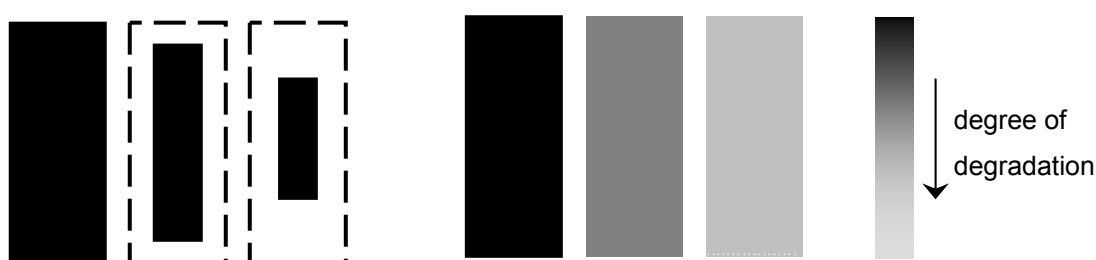


Figure 1-8 Principles of surface (left) and bulk (right) erosion (modified from (von Burkersroda et al.; 2002))

Bulk erosion is very complex because water uptake is much faster than polymer degradation. The entire device is rapidly hydrated and digestion can take place throughout the complete matrix. This results in simultaneous drug diffusion and matrix erosion (Siepmann et al.; 2001). Consequently, the molecular weight of the matrix decreases steadily and the permeability of the device increases over time. However, the device retains its original shape and mass, until up to approximately 90% is degraded. Then solubilization and mass loss starts (Sinha et al.; 2003). The release rate is difficult to predict, especially if the matrix disintegrates before drug is released completely (Heller; 1984).

If surface erosion occurs, water penetration is slow compared to the polymer degradation rate. Degradation takes place only at the matrix boundaries and not in the core of the polymer (Siepmann et al.; 2001). Thus, except for the boundaries, the chemical integrity of the device is preserved and a consistent degradation rate of the polymer is the result (Heller; 1984). In general, the active agent is entangled within the matrix. Since only minimal diffusion occurs,

prediction of release rate is easier because drug is released by zero-order kinetics. Therefore, surface erosion is considered as the preferable erosion mechanism in many cases, because it is highly reproducible, the degradation rate can be manipulated by just changing the surface area and water labile drugs are protected within the device (Uhrich et al.; 1999).

For most biodegradable drug systems, especially for hydrophilic matrices, both erosion mechanisms occur together (Gilbert; 1988b). The relative extent depends on the chemical backbone of the polymer (Mainardes et al.; 2004). Polymers which contain reactive functional groups, e.g. poly(anhydrides) or poly(orthoesters), tend towards fast degradation, i.e. surface erosion, whereas polymers with less reactive functional groups, e.g. PLGA or poly(cyanoacrylates), commonly show bulk erosion (Siepmann et al.; 2001). However, von Burkersroda et al. showed that this general assumption is not applicable without restrictions. For example, depending on device dimensions, bulk eroding materials can undergo surface erosion if the critical dimensions are exceeded (von Burkersroda et al.; 2002). The other extremes are formulations of nano- and microparticles in which similar degradation processes occur irrespectively of the type of polymer (Uhrich et al.; 1999).

1.2.3.2 Drug Release from Collagen Devices

Hydrogels, like non cross-linked collagen or gelatin, hyaluronic acid or polysaccharide systems, show a combination of swelling and erosion controlled drug release. The initial release rate is controlled by diffusion through water filled channels which depends on the swelling rate of the polymer. If degradation occurs, the release rate becomes additionally erosion dependent (Gombotz et al.; 1995). Drug liberation of hydrophilic drugs from collagen films, gels and dense DDSs is mainly diffusion and erosion controlled (see Figure 1-9). Due to swelling of collagen matrices, high water contents up to approximately 90% (w/w) are found in the swollen systems (Frieß; 1999) and diffusion through water filled channels can occur (Gilbert et al.; 1988a; Maeda et al.; 1999).

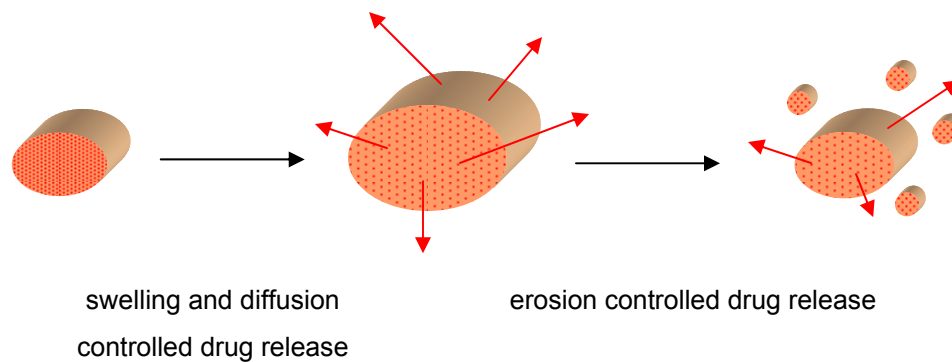


Figure 1-9 Schematic illustration of drug release from collagen minirods (\rightarrow drug release)

After a short lag time, resulting from swelling, the first part of release is characterized by a Higuchi dependent release kinetic (Frieß et al.; 1996b; Gilbert et al.; 1990; Maeda et al.; 1999). When drugs are bound to collagen or when macromolecules are incorporated into the delivery system, release may be additionally dependent on matrix degradation. However, swelling and diffusional release have the greater impact on release (Radu et al.; 2002). Different strategies in order to reduce diffusion controlled release were developed (Frieß; 1998). In general, drying a collagen-drug-mixture shows better sustained release properties than a collagen matrix which is soaked with the drug solution. Increasing the concentration of collagen results in an increase in viscosity of the swollen devices and reduces drug diffusion (Fujioka et al.; 1995). By changing the mesh size of fibrillar collagen gels, diffusional drug release of macromolecules can be controlled, since diffusion becomes hindered when the mesh size of the gel approaches the drug size (Rosenblatt et al.; 1989). The same result is obtained by increasing the cross-linking density: drug release by diffusion is restrained and delivery controlled by erosion becomes more important since tortuosity increases (Frieß et al.; 1996b; Gilbert et al.; 1988a). For drugs with smaller molecular weight, diffusional release from gels can be controlled by the extent of non-fibrillar collagen, because of a lower effective pore size of these gels compared to fibrillar gels (Wallace et al.; 2003).

Charge interactions between drug and collagen have a great influence on diffusional drug liberation as well. Diffusion is slowed down by electrostatic interactions (Singh; 1994). The extent is dependent on the type of collagen, due to different amino acid compositions, the collagen preparation, e.g. use of succinylated collagen, and the incorporated drug itself, e.g. antibiotics, which can also be charged (Frieß; 1998; Singh; 1994). Another strategy is to control release by changing the matrix dimensions. Release from dense extruded collagen devices is dependent on the length and the diameter of the rods. By decreasing the length and/or diameter of the extrudate a faster release was observed (Sano et al.; 2003). Beyond this, drug loading and drug hydrophilicity effect release as well. Higher drug loads or incorporation of larger drug particles lead to an increase in drug release due to formation of more and/or larger cavities (Gilbert et al.; 1990). The collagen matrix becomes more porous, the diffusion barrier decreases and the release is enhanced (Maeda et al.; 1999). Sparingly water soluble drugs are incorporated into collagen devices as crystals and have to be dissolved prior to release, resulting in lower delivery rates (Wallace et al.; 2003). Additionally, the liberation may be prolonged, if diffusion through more hydrophobic collagen parts plays a role (Silver et al.; 1997).

1.3 Introduction to Mathematical Models

Mathematical models of drug delivery systems can be used to provide information about diffusion processes, matrix degradation and drug release. If an adequate model is chosen, insights into the effects of varying parameters which influence the drug delivery, such as size and shape of the drug device and the drug-polymer ratio, can be given (Kanjickal et al.; 2004; Siepmann et al.; 2001). Consequently, these models contribute to a better understanding of processes occurring during drug release and can facilitate the optimization of existing drug delivery systems and the development of new systems without performing a multiplicity of experiments. A mathematical model describing drug release from dense collagen drug devices has to consider the three phases: swelling, diffusion and erosion (see 1.2.3.2).

In vivo, collagen is degraded enzymatically (see 1.2.2.2). Therefore, some basics of enzymatic reactions are presented, before mathematical models are discussed in more detail (nomenclature see Table 1-7).

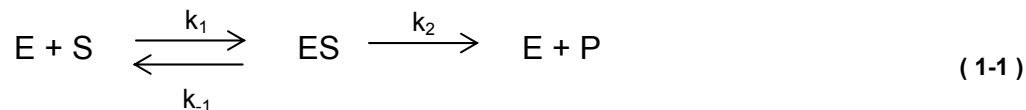
Table 1-7 Nomenclature

a	half thickness of a film or radius of a sphere or cylinder
A	surface area of the device
B	surface erosion rate constant
C_0	initial drug load
C_s	solubility of the drug in the polymer
d_0	initial diameter of a cylinder
D	diffusion coefficient of a substance
D_0	diffusion coefficient of a substance in the undegraded matrix
$[E_0]$	concentration of total enzyme
$[E]$	concentration of free enzyme
$[E_a]$	concentration of adsorbed enzyme
$[ES]$	concentration of enzyme-substrate complex
f	fractional drug release rate
J	flux of a substance
k_1	rate constant of formation of the ES complex
k_{-1}	rate constant of dissociation of the ES complex
k_2	catalysis rate
k_a	degradation rate of easily hydrolysable substrate
k_{ad}	rate of adsorption
k_b	degradation rate of more difficult hydrolysable substrate
k_{de}	rate of desorption

K'	half saturation constant
K_D	adsorption constant
K_M	Michaelis-Menten constant
l_0	initial length of a cylinder
m_{ad}	weight after degradation
m_{bd}	weight before degradation
n	Freundlich sorption exponent
M_∞	amount of released drug at matrix exhaustion
M_S	amount of substrate to bind one mole enzyme
M_t	amount of released drug at time t
p_0	drug permeability through the matrix before erosion
$[P]$	concentration of product
$[S_0]$	concentration of total substrate
$[S]$	concentration of unbound substrate
$[S_a]$	concentration of easily hydrolysable substrate
$[S_b]$	concentration of more difficult hydrolysable substrate
t	time
v_i	net sum of synthesis and degradation rate
V_0	initial reaction rate
α	fraction of total enzyme which can bind to the substrate
δ	relative separation between erosion and diffusion fronts
μ_{\max}	maximum reaction rate
ρ_0	density of the matrix before hydrolysis

1.3.1 Enzymatic Reaction

Enzyme catalyzed reactions are regarded as reactions in which an enzyme-substrate complex (ES) is formed. The enzyme (E) binds to the substrate (S), converts the substrate into the product (P) and finally is released to be available as free enzyme again. This assumption was first made by Brown in 1892. Henri improved this approach in 1903 by more precise mathematical and chemical terms. He inserted equilibrium between free enzyme, enzyme-substrate complex and enzyme-product complex. By measuring the initial reaction rates of invertase in 1913, Michaelis and Menten came to a similar equation as Henri and provided the basis for modern enzymology (Cornish-Bowden; 1999). Nowadays, enzymatic reactions are described particularly by using the Michaelis-Menten equation. Assuming a reversible reaction between substrate and enzyme at early stages the following reaction takes place:



with k_1 the rate constant of formation of the ES complex, k_{-1} the rate constant of dissociation of the ES complex and k_2 the catalysis rate. In most cases, the final step is regarded as irreversible because only the degradation can be catalyzed by the enzyme (Tzafriri et al.; 2002).

The initial reaction rate can be described by

$$V_0 = \frac{\mu_{\max} * [S]}{[S] + K_M} \quad (1-2)$$

The Michaelis-Menten constant K_M is the substrate concentration at which the reaction rate is half of the maximum rate (μ_{\max}). Michaelis-Menten kinetics describe reactions with saturation phenomena such as enzymatic reactions. Looking closer at enzymatic reactions, this kinetic is used to describe the degradation of soluble substrates (Bailey; 1986). However, many enzymatic reactions occur in heterogeneous systems. Examples for the action of soluble enzymes on insoluble substrates are the hydrolysis of collagen, cellulose and starch or the digestion of food in animal intestine (Lee et al.; 1980). The most

distinct difference to the reaction with soluble substrates is the formation of the enzyme-substrate complex. For digestion of insoluble substrates this can only be achieved by diffusion of the enzyme towards the insoluble substrate and adsorption onto its surface. For a better understanding of these degradation mechanisms, going far beyond the original Michaelis-Menten kinetics, the degradation equations of collagen and cellulose will be discussed in more detail.

Gaspers et al. investigated the behavior of bacterial collagenase on FALGPA (furylacryloyl-leucine-glycine-proline-alanine) attached to glass (Gaspers et al.; 1994; Gaspers et al.; 1995). Initially, diffusion limited adsorption was observed, followed by lateral movement of collagenase on the surface towards reaction sites. During this process, the enzyme remains irreversibly adsorbed onto the surface, as was observed by Welgus et al. for human fibroblast collagenase (Welgus et al.; 1980). Collagenase is adsorbed by many weak physical bonds. The sum of interactions results in irreversible adsorption. During hydrolysis or migration along the collagen molecule, only few physical bonds are cleaved which are not sufficient to release collagenase from the surface. After disengagement, new links are formed nearby, resulting in enzymatic movement (Gaspers et al.; 1994). Collagenase remains active after adsorption and enzymatic conversion can occur (Gaspers et al.; 1995). Hence, degradation of collagen takes place in three steps: after diffusion of collagenase towards the collagen substrate, the enzyme has to adsorb onto the collagen surface and subsequently degradation can occur (see Figure 1-10).

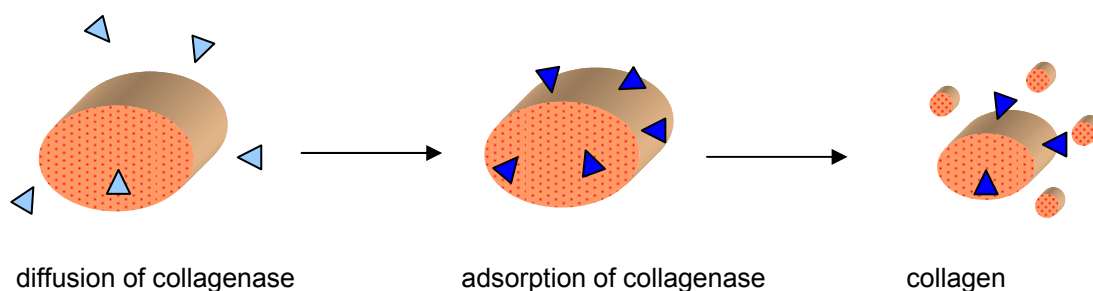


Figure 1-10 Schematic illustration of degradation of collagen matrices (\triangle free collagenase, \blacktriangle adsorbed collagenase)

1.3.1.1 Adsorption

The prerequisite step for degradation of insoluble substrates is the adsorption of the enzyme. In general, adsorption is defined as adhesion of gas or liquid molecules onto a solid or liquid surface. Different approaches for describing this phenomenon have been taken. One of the simplest was proposed by Langmuir in 1916, who investigated the adsorption of gases onto solids. The resulting equation corresponds closely to the Michaelis-Menten equation (Cornish-Bowden; 1999). Adsorbed molecules do not interact with themselves on the surface and affinity to all surface sites is the same (McLaren et al.; 1970). The number of adsorption sites per area are constant and only one molecule can adsorb per adsorption site which results in the formation of a monolayer of adsorbed molecules (Martin et al.; 1983). Adsorption can be described by:

$$\frac{[E_a]}{[S_0]} = \frac{K_D [E]}{1 + K_D [E]} \quad \text{with} \quad K_D = \frac{k_{ad}}{k_{de}} \quad (1-3)$$

The distribution between two phases is defined by the adsorption constant K_D , which is the ratio of adsorption rate (k_{ad}) to desorption rate (k_{de}).

In contrast, the Freundlich isotherm describes a multiplicity of adsorption sites which differ in their energy (Rubingh et al.; 1992). The more adsorption sites are occupied, the lower is the required adsorption energy because interactions between adsorbed molecules take place (Haas; 2002). This results in a parabolic isotherm without a maximum in adsorption:

$$\frac{[E_a]}{[S_0]} = K_D [E]^n \quad (1-4)$$

with n a chemical-specific constant.

However, strictly spoken, the above mentioned adsorption isotherms are applicable only to small solute molecules. Therefore, more complex adsorption kinetics may have to be taken into account for the adsorption of enzymes (McLaren; 1963) as for example a combination of Langmuir and Freundlich:

$$\frac{[E_a]}{[S_0]} = \frac{K_D [E]^n}{1 + K_D [E]^n} \quad (1-5)$$

Both, Freundlich and Langmuir, sorption isotherms are used to describe the enzymatic adsorption on insoluble substrates (McLaren et al.; 1970).

Adsorption of human skin fibroblast collagenase on a fibrillar collagen gel is already completed after 12-15 minutes at 37°C (Welgus et al.; 1980). Consequently, the assumption that adsorption is faster than the enzymatic reaction is correct. McLaren et al. postulated that the adsorbed enzyme does not interact with itself on the surface and that the affinity to all reaction sites is the same. Therefore, they assumed a Langmuir sorption isotherm for gelatin degradation by trypsin (McLaren et al.; 1970). This assumption was affirmed by Welgus et al., who observed a linear Lineweaver-Burk plot for bound to free human fibroblast collagenase, indicating that all binding sites on collagen are equal (Welgus et al.; 1980). On the other hand, with data from Tsuk et al. (Tsuk et al.; 1961), McLaren suggested a Freundlich isotherm for gelatin degradation by trypsin, because Tsuk et al. observed that a higher surface area was covered with enzyme than the actual substrate surface area (McLaren; 1963; Schurr et al.; 1966). For collagen degradation by bacterial collagenase, the more appropriate approach seems to be the Freundlich isotherm, as was described by Rubingh et al. (Rubingh et al.; 1992). They investigated the degradation of Azocoll, a collagen-dye conjugate, by three different enzymes and obtained Freundlich sorption isotherms. This is in agreement with Gaspers et al. who postulated a non-uniformity of adsorption states of bacterial collagenase during degradation of FALGPA attached to glass (Gaspers et al.; 1994).

Adsorption of cellulase on cellulose can be divided in two sorption phases. Within the first 5-10 minutes, fast adsorption occurs which is followed by a slower uptake for several hours which results in equilibrium between adsorption and desorption. This equilibrium is described by first-order kinetics. Thereafter, a slight release of cellulase can be observed indicating digestion of cellulose. The active enzymes bind stronger than inactive enzymes (Ghose et al.; 1979),

as was also observed for collagenase (Gaspers et al.; 1994). The Langmuir isotherm was used as a general characterization of the adsorption (Lee et al.; 1980; McLaren et al.; 1970). However, in 1988 Steiner et al. could demonstrate that adsorption results in a multimolecular layer of enzymes (Steiner et al.; 1988). They distinguished between equations for low and high surface coverage when low substrate concentration is used. The equations are based on the law of mass action, the Michaelis-Menten equation, assuming reversible adsorption. For low surface coverage

$$\frac{[ES]}{[E_0]} = \frac{\alpha[S_0]}{K' + [S_0]} \quad (1-6)$$

is valid, where $K' = K_M * M_S$ representing the half saturation constant and α the fraction of total enzyme which can bind to the substrate (Steiner et al.; 1988). In 1974, Kim demonstrated that the initially adsorbed amount of cellulase is primarily responsible for the degradation of cellulose and is proportional to the initial hydrolysis rate (Lee et al.; 1980). This strengthened the assumption, that adsorption is the prerequisite step for degradation of insoluble substrates. Consequently, adsorption of bacterial collagenase on the surface of collagen can be included into the mathematical model by incorporation of a Freundlich sorption isotherm.

1.3.1.2 Degradation

After the enzyme adsorption, degradation of collagen can start. Collagen monomers in solution are digested according to the Michaelis-Menten kinetics. In contrast, degradation of fibrillar collagen depends on its age. Freshly reconstituted collagen fibrils behave similarly to diluted tropocollagens (Tzafirri et al.; 2002) because cross-links can still be hydrolyzed rather easily. Degradation of fibrillar collagen samples with more stable bonds or a higher degree of cross-linking is hyperbolically dependent on enzyme concentration (Steven; 1976). This anomaly is related to hindered enzymatic penetration into the fibril resulting in protection of collagen molecules within the fibrils (Steven; 1976; Tzafirri et al.; 2002).

Based on the Michaelis-Menten equation, McLaren proposed different approaches to describe the digestion of insoluble substrates, depending on whether the enzyme can penetrate into the substrate or not (McLaren et al.; 1970). Assuming that the reaction rate is not exclusively dependent on the initial enzyme concentration, but on the concentration of adsorbed enzyme, he inserted enzyme adsorption on the surface of the substrate into the Michaelis-Menten equation (McLaren et al.; 1970). This assumption was affirmed by Rubingh et al. who observed a lag-time before linear degradation occurred. This delay was attributed to the establishment of a surface equilibrium concentration (Rubingh et al.; 1992). For a cross-linked insoluble gelatin gel it was assumed that enzymes, e.g. trypsin, are unable to penetrate into the substrate. Hence, enzymatic action is restricted to the surface. Because degradation products are soluble and will be removed from the surface, new surface areas will be exposed and degradation becomes surface dependent (Tsuk et al.; 1961). Based on these observations, McLaren developed a model in which Langmuir adsorption is combined with degradation (McLaren et al.; 1970). This equation is valid when adsorption is faster than degradation and desorption is the slowest step.

$$V_0 = \frac{k^n [E_0] A}{[E_0] + K_D^{-1}} \quad (1-7)$$

k^n denotes the degradation rate, $K_D^{-1} = K_M$ and $E_0 = E + E_a$. It must be pointed out that not all adsorbed enzyme molecules must inevitably build an enzyme-substrate complex ($E_a \geq ES$) because adsorption can also occur at sites which can not be cleaved (McLaren et al.; 1970). By using data from Tsuk et al. (Tsuk et al.; 1961), more enzymes than a monolayer can be adsorbed and a Freundlich adsorption isotherm is valid:

$$V_0 = k^n K_D [E]^n \quad (1-8)$$

with $n = 0.43$ as a geometrical interpretation based on the Freundlich isotherm (McLaren; 1963). Gyani defined four extremes of n . When adsorption between

two immiscible liquids is investigated, $n = 1$ is valid. In contrast, $n = 2/3$ presents complete surface coverage of a smooth solid. When $n = 1/3$ is observed, only adsorption on edges and cracks of the solids takes place and only distinct points are covered when $n = 0$ (Gyani; 1945). If n is between $1/3$ and $2/3$, adsorption on edges and cracks and surface adsorption occur simultaneously. If $n > 2/3$, penetration of the solute into the solid can take place (McLaren; 1963).

Other assumptions were pursued by Okada et al. (Okada et al.; 1992a) and Tzafirri (Tzafirri et al.; 2002) who investigated the degradation of collagen fibers. Okada et al. assumed that erosion of Catgut is exclusively surface erosion and concluded that the square root of fiber mass $\sqrt{\frac{m_{ad}}{m_{bd}}}$ decreases linearly with time and depends on the initial diameter d_0 and density ρ_0 of the matrix (Okada et al.; 1992a):

$$\sqrt{\frac{m_{ad}}{m_{bd}}} = 1 - \frac{k}{\frac{d_0}{2} \rho_0} t \quad (1-9)$$

Tzafirri jeopardized this linearity and the validity of adsorption isotherms on erodible surfaces. He developed a model for degradation of sparsely fibrillar collagen gels by human skin fibroblast collagenase based on the Michaelis-Menten and diffusion equations (Tzafirri et al.; 2002). It was assumed that degradation is the rate-limiting step, that the erosion process is confined to the surface of fibrils, that only one specific cleavage site per fibril exists, and that enzyme and product diffusion are instantaneously compared to the time scale of degradation. By applying a quasi-steady-state assumption a model was developed which is dependent on four model parameters. Based on data from Welgus et al. (Welgus et al.; 1980), Tzafirri used a Langmuir adsorption to simulate adsorption, which is significantly faster than degradation. A linear relationship of the square root of fiber mass and time was found. K_M and k_{cat} (turnover number) of human skin fibroblast collagenase were determined and it

was concluded that this model is also valid for bacterial collagenase which cleaves at more than just one site (Tzafiriri et al.; 2002). However, this interesting model can not be used for our dense collagen devices which show fibril surface erosion and matrix bulk erosion.

Suga et al. developed a model for degradation of cross-linked dextran spheres. They also combined the Michaelis-Menten equation with diffusion equations for the enzyme and released substrate fragments (Suga et al.; 1975).

Degradation of cellulose is more complex than digestion of collagen. On the one hand three major synergistic enzymes (endoglucanases, exoglucanases and β -glucosidases) catalyze the reaction, and on the other hand competitive and non-competitive product inhibition by cellubiose and/or glucose is observed. Several models were proposed, assuming a pseudo-first-order enzymatic reaction with adsorption as a prerequisite step (Lee et al.; 1980; Sattler et al.; 1989). Esterbauer et al. observed a two phase degradation resulting from an initial fast digestion followed by a slower one. Consequently, a distinction between easily hydrolysable cellulose S_a and more difficult digestible parts of the substrate S_b was made. This reflected the structural properties of the substrate, such as pore size, adsorption properties or accessibility (Esterbauer et al.; 1984). Based on these observations, Sattler et al. developed a simple model to describe the relation between extent of hydrolysis, enzyme dosage and reaction time (Sattler et al.; 1989). Simplification can be made by setting the initial substrate concentration as $S_0 = S_a + S_b$, if the substrate consists of 100% reactable molecules. They detected that both, the adsorbed amount of enzyme and the enzyme-substrate ratio at fixed reaction times follow a Langmuir dependency. Hence, a hyperbolic function must also be valid for the enzymatic degradation at these time points. Combining all observations, the digestion of cellulose can be described as:

$$\frac{[P]}{[S_0]} = \frac{\left(1 - \frac{[S_a]}{[S_0]e^{-k_a t}} - \frac{[S_b]}{[S_0]e^{-k_b t}}\right)[E]}{K + [E]} \quad (1-10)$$

where K indicates an independent constant for reaction times longer than 2 hours. The degradation rate of the more difficult digestible parts of the substrate, k_b , increases steadily with higher enzyme dosages leading to the conclusion that S_b is not saturated with enzyme during the enzymatic reaction. Consequently, a limited case of simple Michaelis-Menten kinetics can only be accepted for the digestion of S_a , with K_M smaller than the enzyme concentration (Sattler et al.; 1989).

Other approaches are based on the Michaelis-Menten kinetic. In 1965, Amemura et al. applied this kinetic directly to an insoluble cellulase-cellulose system. They concluded that the initial hydrolysis rate is not limited by adsorption or penetration phenomena, and that there is a constant number of binding sites. The model was improved by including terms for accessibility of cellulose and product inhibition (Lee et al.; 1980). McLaren adapted the Michaelis-Menten equation to the hydrolysis of insoluble substrates by referring the initial rate to the amount of adsorbed enzyme (McLaren et al.; 1970). For the hydrolysis of cellulose by cellulase a Freundlich isotherm was assumed. K and n can be determined from adsorption isotherms. An increase in n , was attributed to a deeper enzymatic penetration into the swollen polymer (McLaren; 1963). McLaren's model can only be used for simple cellulose-cellulase reactions because substrate multiplicity, product inhibition and mode of action of cellulose are ignored (Lee et al.; 1980), but is of general interest to approach models for collagen materials.

Further developments were made by Huang, who combined the enzymatic adsorption and the Michaelis-Menten kinetics with equations for competitive inhibition (Huang; 1975). For adsorption a fast process based on the Langmuir isotherm was assumed. A very complex model was developed by Kim which takes into account enzyme adsorption, formation and dissociation of the enzyme-substrate complex, product inhibition and enzyme deactivation (Lee et al.; 1980).

In conclusion, mathematical modeling of degradation of insoluble collagen by bacterial collagenase is quite challenging, because normal Michaelis-Menten

kinetics is not sufficient to describe the complete enzymatic conversion correctly. Based on the Michaelis-Menten mechanism, equations for collagen degradation need to be developed, which take into account enzymatic adsorption phenomena and diffusion of collagenase and degraded collagen fragments. Some complex aspects described for the cellulose-cellulase system, such as substrate multiplicity, product inhibition or special mode of enzymatic action, need not be considered for a collagen degradation model.

1.3.2 Drug Release from Biodegradable Devices

As already pointed out in section 1.1, delivery of drugs from biodegradable polymers got into focus within the last decades, because patient compliance can be improved compared to non-biodegradable polymeric matrices. However, drug release is more complex than from non-biodegradable DDSs. Various mathematical models have been developed, because biodegradable polymers exhibit significant chemical and physiochemical differences (Siepmann et al.; 2001). Consequently, it is important to reassess the chosen mathematical model for every drug device, even if only the geometry changes.

1.3.2.1 Diffusion Controlled Drug Release

Diffusion controlled drug release is extensively dependent on the structure of the device. In reservoir systems, the rate limiting step is the diffusion through a polymer membrane which surrounds the drug containing core. The release J of a drug a is governed by Fick's first law (Kanjickal et al.; 2004).

$$J_a = -D_a \frac{dC_a}{dz} \quad (1-11)$$

The drug release from monolithic systems, which contain dissolved or dispersed drug throughout the entire device, is dependent on the solubility of the drug in the polymer and the drug load. If drug loading is below the drug solubility limit, the release by diffusion can be described by Fick's second law (Kanjickal et al.; 2004).

$$\frac{dC_a}{dt} = D_a \frac{d^2 C_a}{dz^2} \quad (1-12)$$

If the drug load C_0 is higher than the solubility of the drug in the polymer C_s , the release is expressed by the Higuchi model (Siepmann et al.; 2001).

$$M_t = A \sqrt{D(2C_0 - C_s)C_s t} \quad (1-13)$$

1.3.2.2 Swelling Controlled Drug Release

Besides diffusion controlled drug release (Case I transport), the other extreme of diffusional behavior is drug release controlled by swelling (Case II transport). In Case II transport, swelling at the liquid front is the rate limiting factor because the mobility of the solvent is higher than the rearrangement of the polymer structure. For classifying the character of mass transport either the Deborah number, the swelling interface number or the power law can be used. All three distinguish between Case I and II and anomalous transport (Kanjickal et al.; 2004).

A transition between models of swelling and erosion controlled drug release was proposed by Lee, who developed an analytical solution for thin, surface eroding films, with a thickness of $2a$, based on the movement of a swelling and an erosion front (with a relative separation δ) within the device. This theory predicts a zero-order release for surface eroding matrices (with a surface erosion rate constant B) when the initial drug load C_0 becomes much larger than drug solubility in the polymer C_s (Siepmann et al.; 2001).

$$\frac{M_t}{M_\infty} = \delta + \frac{B \cdot a}{D} \cdot \tau - \delta \frac{C_s}{C_0} \left(\frac{1}{2} + \frac{a_3}{6} \right) \quad (1-14)$$

1.3.2.3 Erosion Controlled Drug Release

Mathematical modeling of erosion controlled drug release is more challenging than the above mentioned models, because besides mass transfer, chemical reactions have to be considered. This kind of models can be divided in two

principle categories. The first ones, named empirical models, assume a single zero-order process to control drug release. Besides easy handling, they are of advantage if only one material is used. However, they fail if specific physicochemical processes have to be taken into account. Then, mechanistic models can be applied which also consider the underlying physical and chemical properties, e.g. diffusion mass transfer. These models are quite complex compared to empirical models, but more accurate and powerful (Siepmann et al.; 2001).

Empirical models were proposed from Hopfenberg and Cooney for drug release controlled by surface erosion (Kanjickal et al.; 2004; Siepmann et al.; 2001). Both investigated the effect of polymer matrix geometry. Hopfenberg assumed that the drug release rate is proportional to the device surface and that all mass transfer processes result in one single zero-order process. A general model for surface erosion of slabs, cylinders and spheres with drug release as rate-limiting step was developed.

$$\frac{M_t}{M_\infty} = 1 - \left[1 - \frac{k_0 t}{C_0 a} \right]^{sf} \quad (1-15)$$

with k_0 a rate constant and sf a “shape factor” set as 1 (slab), 2 (cylinder) and 3 (sphere), respectively. This equation leads to zero-order drug release kinetics for slabs and to declining release rates with time for cylinders and spheres (Heller; 1984; Kanjickal et al.; 2004). Cooney established a more detailed model for surface eroding cylinders and spheres. He assumed that dissolution from non-porous homogeneous solids is covered by two main steps, detachment of an atom, molecule or ion from the solid surface, followed by diffusion through an adjacent stationary solvent layer into the incubation medium. Additionally, drug release is thought to be proportional to the surface area. This results in a single zero-order process for drug release, described by the following equation:

$$f = \frac{(d_0 - 2Kt)^2 + 2(d_0 - 2Kt)(l_0 - 2Kt)}{d_0^2 + 2d_0l_0} \quad (1-16)$$

K is a constant and f the ratio of instantaneous drug release rate to the initial drug release rate. For slabs (l_0/d_0 approaches 0), a constant dissolution rate was found. Good differentiation can be made between rod like cylinders ($l_0/d_0 \gg 1$), with relative drug release rates approaching zero up to drug exhaust, and disc like cylinders ($l_0/d_0 \ll 1$), with relative drug release rates remaining finite until the end (Kanjickal et al.; 2004; Siepmann et al.; 2001).

Going one step further, descriptions of physical, chemical and physicochemical processes, which control drug delivery, can be incorporated in mechanistic models. Consequently, these models provide more information on the mechanism of drug release. Approaches were made with models with partial differential equations and simplified discrete models (Siepmann et al.; 2001).

Heller established a model that describes the drug delivery from bulk eroding, water insoluble polymers digested by backbone cleavage (Heller; 1984). Assuming first-order kinetics for degradation, the model is based on the Higuchi equation. Additionally, a relationship between drug permeability at the beginning p_0 and during erosion due to an increase in permeability of the matrix undergoing erosion is inserted. In the beginning, drug release rate decreases because diffusion path length increases. Subsequently, the rate increases due to an increase of matrix permeability. This results in an expression for quantifying drug release from thin, bulk eroding films with an initial drug load C_0 above drug solubility in the polymer

$$\frac{dM_t}{dt} = \frac{A}{2} \sqrt{\frac{2p_0^{Kt} C_0}{t}} \quad (1-17)$$

where K is a first-order degradation constant (Heller; 1984; Siepmann et al.; 2001).

Thombre et al. proposed a model for poly(orthoester) slabs which are degraded by an autocatalysis mechanism based on Fick's second law (Thombre et al.; 1985). They assumed perfect sink conditions and that diffusivities change continuously as a function of hydrolysis. However, description of the

microstructure of the device was not included into this model. The diffusion of four species i , occurring during degradation, was described as:

$$\frac{\partial C_{0i}}{\partial t} = \frac{\partial}{\partial x} \left(D_i(x, t) \frac{\partial C_{0i}}{\partial x} \right) + v_i \quad (1-18)$$

with

$$D_i = D_{0i} \exp \left[\frac{\mu (C_D^0 - C_D)}{C_D^0} \right] \quad (1-19)$$

and x is the space variable, μ a dimensionless constant (Siepmann et al.; 2001), C_D^0 the concentration of undegraded and C_D the concentration of the degraded substrate at time t .

Charlier et al. investigated the release rate of mifepristone from bulk eroding PLGA films (Charlier et al.; 2000). They observed an early drug delivery according to Higuchi, assuming that the diffusion coefficient does not change in the matrix because no degradation takes place. Subsequently, homogeneous erosion, following first-order kinetics, starts. The diffusion coefficient becomes dependent on the polymer molecular weight and the release rate no longer obeys the Higuchi kinetics. These observations were combined and gave the following equation (valid for $(C_0 \gg C_S)$):

$$M_t = A \sqrt{\frac{2C_0 C_S D_0 (e^{kt} - 1)}{k}} \quad (1-20)$$

where $F = A \sqrt{2C_0 C_S D_0}$ and k is the degradation constant. This equation was divided into an early release phase ($M_t = F \sqrt{t}$) and a release for later time points ($M_t = F \sqrt{\frac{e^{kt} - 1}{k}}$) (Charlier et al.; 2000).

The release of chlorhexidine gluconate from a cross-linked gelatin chip was modeled by Tzafirri using a finite element method (Tzafirri; 2000). Tzafirri assumed a fully swollen matrix undergoing bulk erosion, a drug load composed

of a mobile and immobile drug pool, and that most of the drug is released prior to erosion. The mobile drug can diffuse freely after hydration of the matrix, whereas the immobile drug can only diffuse after matrix degradation. Consequently, the release of mobile and immobile drug was modeled separately. Constant diffusion coefficients, independent of degradation, were applied because only small drugs were considered in this model. Immobilization can be chemical (conjugation to the polymer backbone) or physical (steric hindrance). Due to proportionality of immobilized drug and substrate concentration, an immobilizing capacity of the polymer was defined which is equal to the number of hindering cross-links per mole of fully swollen substrate for physical immobilization. Hence, the release rate becomes proportional to the degradation rate. Degradation was assumed to follow the Michaelis-Menten kinetics, because the fully swollen matrix does not restrict enzyme penetration (Tzafiriri; 2000).

Macromolecular drug release from bulk eroding PLGA microparticles was modeled by Batycky et al. (Batycky et al.; 1997). A microstructural model was used, assuming micropores in the sphere surface which coalesced to mesopores during degradation. Distinction between burst release, dependent on drug desorption from the particle surface and already existing mesopores, and drug release by Fickian diffusion through newly formed mesopores was made. Before the second phase could occur, an “induction phase”, necessary for formation of additional mesopores by coalescing of micropores, was implemented. However, effects of pH and interactions between protein and polymer were not implemented (Batycky et al.; 1997).

Another subclass of mechanistic models is based on the Monte-Carlo-simulation, first mentioned by Zygourakis in the late 1980's. A two-dimensional grid is generated for the device to simulate the polymer microstructure with each cell representing drug, polymer, solvent and a pore void, respectively. The rate-limiting step is thought to be the detachment of molecules from the surface. Consequently, this model was used for simulating drug release from surface eroding devices. As soon as a cell comes into contact with the solvent, its lifetime starts to decrease and it finally dissolves instantaneously (Kanjickal et

al.; 2004; Siepmann et al.; 2001). These simulations were verified by Göpferich, who inserted several parameters, e.g. crystallinity, shape and porosity of the device. Last but not least, mass transport processes like diffusion were incorporated by including Fick's second law. Hence, simulations were extended to bulk eroding systems and mass loss and degradation can be simulated individually (Göpferich; 1997b). Further improvement was achieved by Siepmann et al., who proposed a "comprehensive" model for bulk eroding microparticles which covers the initial burst, the subsequent zero-order release and the final rapid drug delivery (Siepmann et al.; 2002).

In this thesis a mechanistic model for the drug release from dense matrices prepared from insoluble collagen type I was to be developed. Since, drug delivery from collagen devices is governed by two simultaneously occurring mechanisms, swelling and erosion controlled release (see 1.2.3.2), both had to be incorporated into the model. Diffusional release was adapted from Radu et al. (Radu et al.; 2002). Swelling and diffusion controlled drug release of indomethacin and gentamicin from dense collagen devices were described by assuming Fickian diffusion and concentration dependent diffusion coefficients of water and drugs (Radu et al.; 2002). These equations were transferred to higher molecular weight drugs, like FITC dextran 70. For erosion controlled drug release, a combination of bulk and surface erosion was taken as a basis and a model similar to Tzafirri appeared to be suitable (Tzafirri; 2000; Tzafirri et al.; 2002). Figure 1-11 summarizes the mathematical modeling approach.

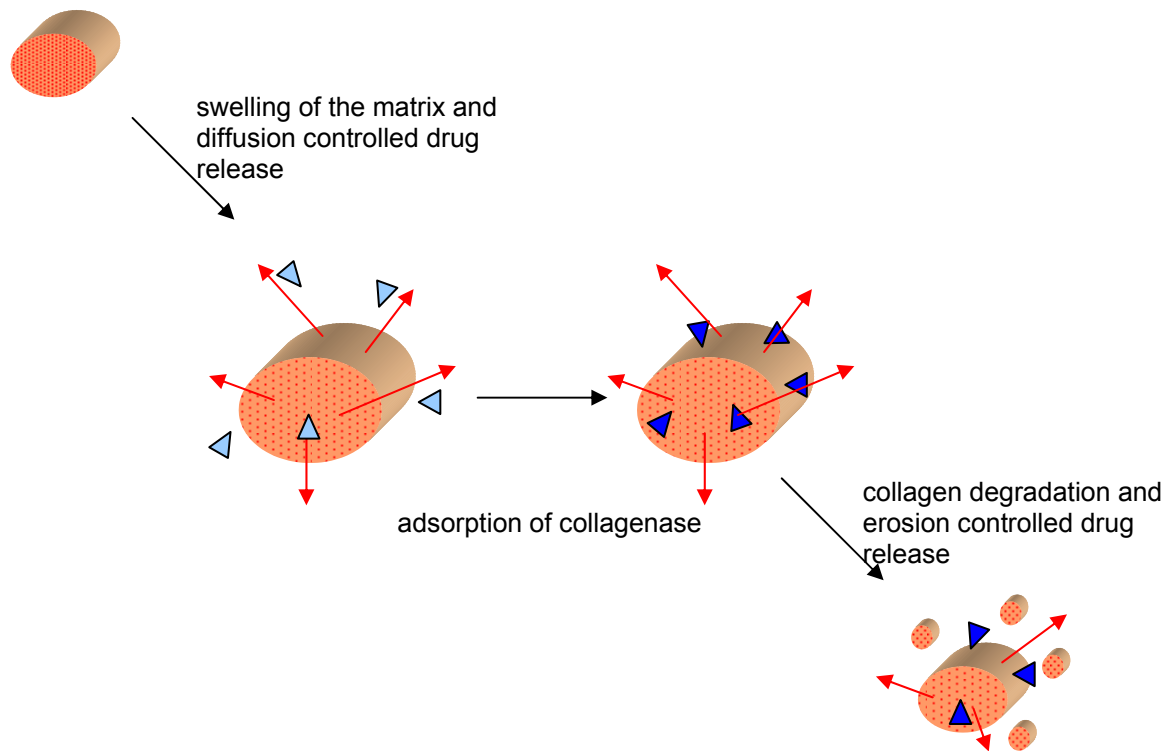


Figure 1-11 Schematic illustration of the mathematical model of dense collagen matrices (\rightarrow drug release, \triangle free collagenase, \blacktriangle adsorbed collagenase)

2 Goals of this thesis

The aim of this thesis was to characterize the drug release from dense collagen matrices. For this purpose, a biodegradable device based on insoluble collagen had to be developed and the delivery of higher molecular weight compounds, e.g. dextrans and proteins, was investigated. Since drug release is covered by swelling, diffusion and erosion mechanisms (Frieß et al.; 1996b; Radu et al.; 2002), a more fundamental understanding of these processes is needed to adopt and prolong delivery properties. Focus was put on the description of the enzymatic matrix erosion and its influence on drug release. Based on the collected data, a mathematical model had to be developed, in cooperation with the Institute of Applied Mathematics in Erlangen, which describes both, the drug release and the degradation of dense collagen implants in one model. To our knowledge, until this new model was presented, these processes are only implemented separately for collagen drug devices. Either the drug release from cross-linked hydrolyzed gelatin matrices (Tzafriri; 2000), the drug release controlled by diffusion from dense collagen devices (Radu et al.; 2002) or the degradation of a sparse fibrillar collagen gel by human skin fibroblast collagenase (Tzafriri et al.; 2002) were described in literature.

In summary, the following targets were postulated:

- (I) Development and characterization of a dense drug delivery system based on insoluble collagen.
- (II) Characterization of the collagen degradation by bacterial collagenase.
- (III) Investigation and characterization of the in vitro matrix degradation/erosion of the developed dense drug delivery systems in the presence of bacterial collagenase.
- (IV) Investigation and characterization of the in vitro drug release of model drug compounds and/or proteins from the developed dense drug delivery systems.

- (V) Development of a mathematical model, on the basis of the experimental results obtained from (I) – (IV), to simulate simultaneously drug release and matrix erosion of dense collagen devices.
- (VI) Investigation of the biocompatibility and the in vivo drug release from the developed dense drug delivery systems.

3 Materials and Methods

3.1 Materials

3.1.1 Collagen

Three different qualities of insoluble collagen type I were used. An equine and a bovine collagen flavor were obtained from Innocoll GmbH (Saal/Donau, Germany). Both were derived from tendon and provided as lyophilized material. A more detailed characterization of these two materials was performed by Schlapp (Schlapp; 2001). For comparison, a second bovine collagen was provided from Lohmann & Rauscher GmbH & Co. KG (Rengsdorf, Germany). This material was extracted from corium and had a slightly higher IEP of 6.7 compared to the other two materials (equine: 6.5; bovine tendon: 6.4). The bovine corium material was obtained as a 1% (w/w) aqueous dispersion and was subsequently lyophilized to improve storage stability (see 3.2.1.5).

3.1.2 Wound Dressings

Two wound dressings, containing bovine corium collagen type I were investigated. Suprasorb[®] C (Lohmann & Rauscher GmbH & Co. KG, Rengsdorf, Germany), consisting exclusively of collagen and a wound dressing containing collagen and oxidized regenerated cellulose (ratio 45/55; Promogran[®], Johnson & Johnson Medical Limited, Gargrave, Skipton, UK).

3.1.3 Enzymes

3.1.3.1 Collagenase

Bacterial collagenase from *Clostridium histolyticum* (CHC) was obtained from Sigma Aldrich Chemie GmbH (Taufkirchen, Germany). This crude collagenase is a lyophilized mixture of all seven known forms of collagenase (α : 68 kDa; β : 115 kDa; γ : 79 kDa; η : 130 kDa; δ : 100 kDa; ϵ : 110 kDa and ζ : 125 kDa) (Mookhtiar et al.; 1992) and contained additionally 35 units/mg solid caseinase activity. The activity of collagenase was 1.2 units/mg solid referred to the

hydrolysis of FALGPA (1 unit hydrolyzes 1 μ mol of FALGPA (furylacryloyl-leucine-glycine-proline-alanine) per minute at pH 7.5 in the presence of calcium ions) (Sigma Aldrich; 1998).

3.1.3.2 Gelatinase A

Matrix metalloproteinase 2 (MMP-2; gelatinase A) was purchased from Roche Diagnostics GmbH (Penzberg, Germany) and from Sigma Aldrich Chemie GmbH (Taufkirchen, Germany). Both qualities of MMP-2 were isolated from human fibrosarcoma cells. After activation with 2.5mM APMA (p-aminophenylmercuriacetate) (30min at 37°C) the specific activity was 200 units/mg referring to hydrolysis of collagen type IV (Roche Diagnostics; 2004b) for the Roche enzyme. In literature, no data for the activity of the Sigma enzyme was available. We determined an activity which was only 1.14 units/mg.

3.1.3.3 Gelatinase B

Matrix metalloproteinase 9 (MMP-9; gelatinase B) was also purchased from Roche Diagnostics GmbH (Penzberg, Germany). The enzyme was isolated from human blood. After activation with trypsin (10min at 37°C) and subsequent stop of activation with aprotinin (10min at 37°C), the specific activity was ≥ 200 mU/mg referring to hydrolysis of DNP-peptide (Roche Diagnostics; 2004a).

3.1.4 Model Compounds

Table 3-1 Model compounds

Model Drug	Description	Supplier
Bovine Serum Albumin (BSA)	catalogue # A-6793	Sigma Aldrich Chemie GmbH (Taufkirchen, Germany)
FITC dextran 20	catalogue # FD-20S	Sigma Aldrich Chemie GmbH (Taufkirchen, Germany)
FITC dextran 70	catalogue # FD-70S	Sigma Aldrich Chemie GmbH (Taufkirchen, Germany)
FITC dextran 150	catalogue # 46946	Sigma Aldrich Chemie GmbH (Taufkirchen, Germany)

For electron spin resonance (ESR) investigations, BSA was spin-labeled. Labeling was performed according to the protocol of Katzhendler et al. (Katzhendler et al.; 2000a): 160mg 3-carboxy-2,2,5,5-tetramethyl-1-pyrrolidinyloxy (PCA), 266mg N-hydroxysuccinimide (NHS) and 148mg N,N'-dicyclohexylcarbodiimide (DCC) were dissolved in 16ml dimethyl sulfoxide (DMSO) and stirred at room temperature for 24h. A 20mg/ml BSA solution in 45ml 0.1M sodium borate buffer pH 8.8 was prepared. 15ml of the DMSO solution was added to the protein solution, mixed well and incubated at room temperature for 4h. 24µl NH₄Cl was added and the solution was incubated at room temperature for 10min. A 2d dialysis against water at 4°C followed. Subsequently, the material was lyophilized (see 3.2.1.5).

3.1.5 Reagents and Buffers

Table 3-2 Reagents

Reagent	Description	Supplier
APMA	p-aminophenylmercuriacetate; catalogue # A9563	Sigma Aldrich Chemie GmbH (Taufkirchen, Germany)
Aprotinin	catalogue # 981532	Roche Diagnostics GmbH (Penzberg, Germany)
BCA Protein Assay	1 part CuSO ₄ 50 parts bicinchoninic acid (BCA)	KMF Laborchemie Handel GmbH, Lohmar, Germany
CaCl ₂ * 2H ₂ O	p.a.	VWR International GmbH (Darmstadt, Germany)
D ₂ O	heavy water; mind. 99.8%	VWR International GmbH (Darmstadt, Germany)
DCC	N,N'Dicyclohexylcarbodiimide; catalogue # 36650	Sigma Aldrich Chemie GmbH (Taufkirchen, Germany)
DMSO	dimethyl sulfoxide	Sigma Aldrich Chemie GmbH (Taufkirchen, Germany)
EDC	1-ethyl-3-(3-dimethyl- aminopropyl)carbodiimide; catalogue # 03449	Sigma Aldrich Chemie GmbH (Taufkirchen, Germany)
EnzCheck [®]	1mg/ml DQ gelatin in water	MoBiTec GmbH (Göttingen, Germany)
FALGPA	furylacryloyl-leucine-glycine-proline- alanine; catalogue # F5135	Sigma Aldrich Chemie GmbH (Taufkirchen, Germany)
HCl	1M	VWR International GmbH (Darmstadt, Germany)

NaCl	p.a.	Sigma Aldrich Chemie GmbH (Taufkirchen, Germany)
Na ₂ HPO ₄	1M	VWR International GmbH (Darmstadt, Germany)
NaN ₃	p.a.	Sigma Aldrich Chemie GmbH (Taufkirchen, Germany)
NaOH	1M	VWR International GmbH (Darmstadt, Germany)
NH ₄ Cl	ammonium chloride	VWR International GmbH (Darmstadt, Germany)
NHS	N-hydroxysuccinimide; catalogue # 56480	Sigma Aldrich Chemie GmbH (Taufkirchen, Germany)
PCA	3-carboxy-2,2,5,5-tetramethyl-1- pyrrolidinyloxy; catalogue # 25,332-4	Sigma Aldrich Chemie GmbH (Taufkirchen, Germany)
sodium borate	p.a.	VWR International GmbH (Darmstadt, Germany)
Tris*HCl	Tris(hydroxymethyl)aminomethane	VWR International GmbH (Darmstadt, Germany)
Trypsin	catalogue # 108919	Roche Diagnostics GmbH (Penzberg, Germany)
Water	demineralized water	

Table 3-3 Buffer systems

Buffer	pH	Composition
Sodium borate buffer	8.8	0.1M sodium borate
Tris buffer	6.8	1M Tris*HCl
Tris buffer	7.5	0.05M Tris*HCl, 0.2M NaCl, 0.01 CaCl ₂ * 2H ₂ O, 0.01% NaN ₃ in water
Tris buffer (D ₂ O)	7.5	0.05M Tris*HCl, 0.2M NaCl, 0.01 CaCl ₂ * 2H ₂ O, 0.01% NaN ₃ in D ₂ O

3.2 Methods

3.2.1 Matrix Preparation

3.2.1.1 Collagen Powder

Collagen powder was prepared by redispersion of lyophilized collagen material in water at 10% (w/w). The pH was adjusted to 7.4. After swelling at room temperature for 1h, the dispersion was centrifuged at 5000rpm (10°C, 10min). The residuum was split into portions of approximately 100mg, dried in a desiccator and finally dried under vacuum at 25°C. The dried material was ground with a Pulverisette 14 (Fritsch GmbH, Idar-Oberstein, Germany). Particle size was determined by sieve analysis and particles smaller than 180µm were used.

3.2.1.2 Collagen Mini rods

Mini rods were prepared by using a micro twin screw extruder (MiniLab[®] Micro Rheology Compounder, Thermo Haake GmbH, Karlsruhe, Germany) (see Figure 3-1). Extrusion could be controlled by the operation panel or by PC (Polylab MiniLab[®] software).

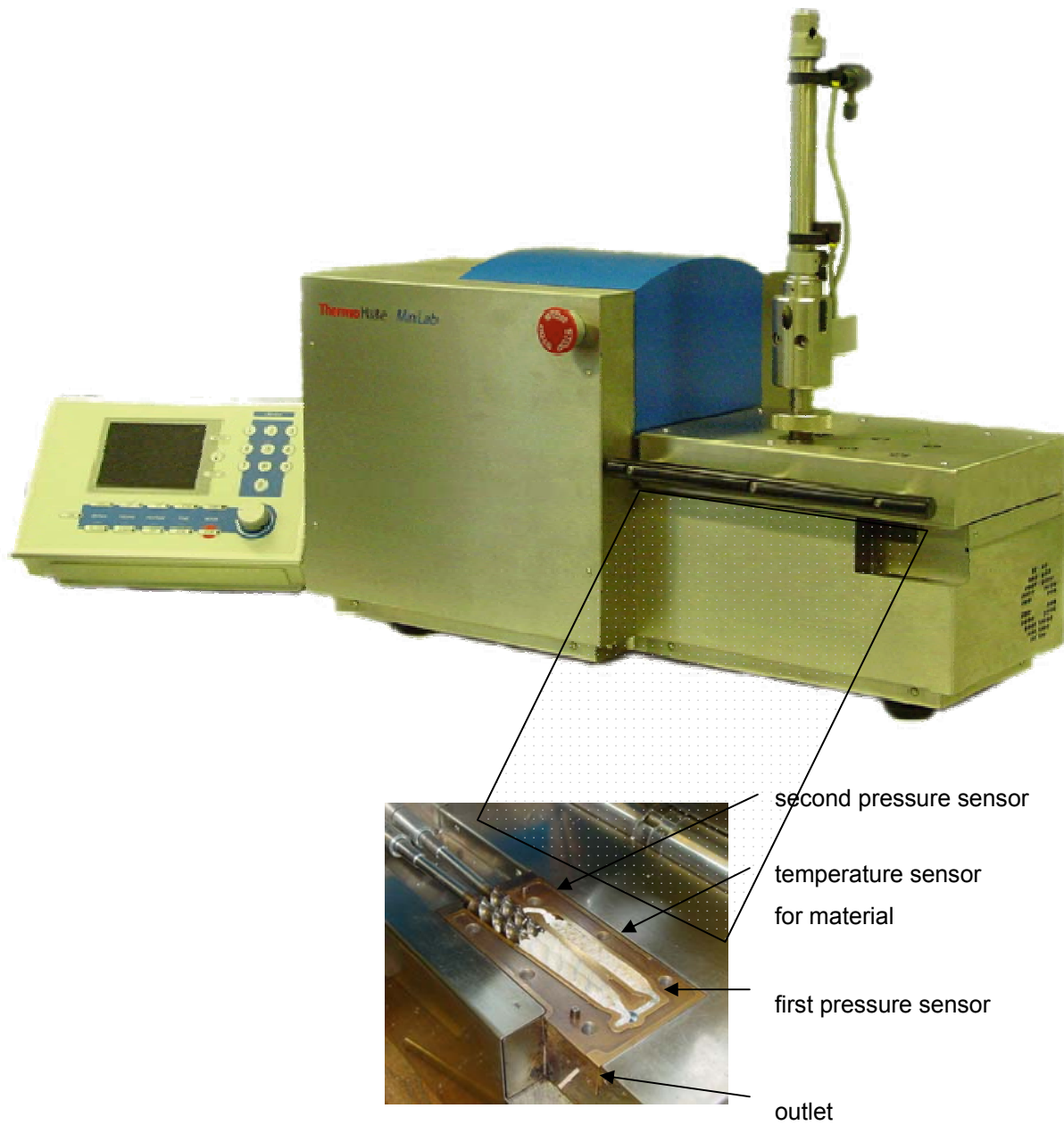


Figure 3-1 MiniLab[®] Micro Rheology Compounder (Thermo Haake GmbH, Karlsruhe, Germany)

Lyophilized collagen material was cut into pieces of approximately 0.25cm^3 . If pulverized collagen was used, the powder was inserted directly into the mini compounder. Without pre-swelling of the collagen pieces, the extruder was loaded with approximately 7g material by alternately adding collagen and water

or an aqueous PCA-BSA or FITC dextran 20, 70 and 150 solution, respectively. Loading of the extruder was performed until the second pressure in the bypass can be monitored. After homogenization for approximately 5min at 20°C, a strand was extruded. Obtained rods contained approximately 40% (w/w) collagen and 4% (w/w) PCA-BSA or 0%, 1% and 2% (w/w) FITC dextran, respectively. Collagen strands were dried hanging at room temperature, 55% r.h. for 5d. Subsequently, the rods were cut into pieces of 20mg weight, 10mm length and 1.7mm diameter. For release studies rods of 20mm, 30mm and 40mm length, respectively, and strands of 0.4mm, 0.8mm and 1.2mm diameter, respectively, were produced as well. Rods with reduced diameter were manufactured by fixing dies with a diameter of 0.5mm, 1mm and 1.5mm diameter, respectively, in front of the outlet (diameter 2mm). Mini-rods were stored in a desiccator (45% r.h.) at room temperature.

3.2.1.3 DHT Cross-linking

For dehydrothermal cross-linking (DHT), samples were placed in a vacuum chamber (Mettmert GmbH & Co. KG, Schwabach, Germany) and the following DHT protocol (see Table 3-4) was applied.

Table 3-4 DHT cross-linking program

Step	Time [h]	Temperature [°C]	Vacuum [mbar]
Start		25	--
Initial drying	0.5	25	0.1
Ramp	0.5	110	0.1
DHT cross-linking	120	110	0.1
Ramp		25	0.1
End		25	--

3.2.1.4 EDC Cross-linking

Cross-linking with EDC was performed before collagen matrices were prepared. 1% (w/w) collagen in water was adjusted to pH 3.5 with 1M HCl and pre-swollen for 1h. After dispersion for 10min with an Ultraturrax[®] (IKA-Werk, Staufen, Germany), the pH was adjusted to 5.1 with 1M Na₂HPO₄ and 10% stock solutions of EDC and NHS (molar ratio 5:2) were added. Four different collagen/EDC-ratios were used: 1g/0.0169mg, 1g/0.0677mg, 1g/0.2031mg and 1g/1.15mg. The dispersion was homogenized and the reaction was performed for 2h at 25°C under pH-control. Subsequently, the pH was adjusted to 9.1 by adding 1M Na₂HPO₄ and 1M NaOH. After another 2h, the pH was adjusted to 6.4 for both tendon materials and 6.6 for the bovine corium material, respectively, using 1M HCl. After 10 washing steps, using 100ml water each time, residues were lyophilized (see 3.2.1.5).

3.2.1.5 Lyophilization

Lyophilization was performed in a ε2-12D special freeze-dryer (Martin Christ Gefriertrocknungsanlagen GmbH, Osterode, Germany) with collagen dispersions of bovine corium raw material and all materials which were cross-linked with EDC. Collageneous materials were cast in plastic Petri dishes (diameter: 10cm) to a height of 1cm. Samples were lyophilized according to the following program:

Table 3-5 Lyophilization program

Step	Time [h]	Temperature [°C]	Vacuum [mbar]
Start		20	--
Ramp	2	-20	--
Freezing	2	-20	--
Ramp	3	15	0.1
Primary drying	25	15	0.1
Ramp	1	25	0.1
Secondary drying	15	25	0.1

3.2.2 Characterization of the Collagen Matrices

3.2.2.1 Macroscopic Studies

Pictures were taken with a Sony Cyber Shot 3.3 Mega Pixel camera.

3.2.2.2 Scanning Electron Microscopy (SEM)

Surface morphology of non-swollen and swollen minirods was investigated. Minirods were swollen without and with 0.1 µg/ml (0.04 Mandl units/ml) bacterial collagenase at 37°C. After 2d, minirods were shock frozen in liquid nitrogen and subsequently lyophilized (see 3.2.1.5). Dry minirods were sputtered with carbon (MED 020 coating system, BalTec GmbH, Liechtenstein) and analyzed with a SEM XL-20 (Philips, Eindhoven, The Netherlands).

3.2.2.3 Determination of Density

Density of minirods was calculated from the determined weight and calculated sample volume.

3.2.2.4 Karl-Fischer Titration

Residual moisture in dried minirods was determined by Karl-Fischer titration using a titrator with Head-Space oven (Analytik Jena AG, Jena, Germany).

Sealed samples were fixed in the oven chamber and heated to 60°C for 30min. Vaporized water was transported into the Karl-Fischer cell, determined coulometrically and calculated as water amount in % (w/w). Measurements were carried out at least in duplicate.

3.2.2.5 Differential Scanning Calorimetry (DSC)

Samples were analyzed with a DSC 204 Phoenix machine (Erich Netzsch GmbH & Co. Holding KG, Selb, Germany). Samples (3-7mg) were incubated in 1ml Tris buffer pH 7.5 at room temperature for at least 2h. Subsequently, samples were transferred in aluminum pans, 10µl buffer was added and containers were sealed. Samples were heated and cooled from 20 to 90°C at 5°C/min. Analyses were performed in triplicate against an empty reference pan. For statistical analysis the t-test was applied ($p < 0.001$).

3.2.2.6 Swelling Studies

Minirods of a length of 5mm were placed in a 24-well plate and incubated at 37°C in Tris puffer pH 7.5 without, with 0.1µg/ml (0.04 Mandl units/ml) and with 6.7µg/ml (2.06 Mandl units/ml) bacterial collagenase, respectively. For studies with collagenase, the enzyme was added after 30min swelling. The change in diameter was recorded with a digital video camera (JVC TK-C1380, JVC Professional Products GmbH, Friedberg, Germany; lens: Vivitar 55mm f2.8 macro) and pictures were analyzed with an image analysis system (Comet-Version 3.52a, Nikon GmbH) and Microsoft Photo Editor. Swelling was analyzed at least in triplicate.

3.2.2.7 Pulsed Field Gradient Nuclear Magnetic Resonance Spectroscopy (PFG-NMR)

The self-diffusion coefficient of water was determined by PFG-NMR coupled with magic angle spinning (MAS). Equine non cross-linked minirods were incubated at 37°C for 24h in a 10% (w/w) FITC dextran 70 solution in Tris buffer pH 7.5 (D₂O) and in pure Tris buffer pH 7.5 (D₂O), respectively, before NMR-measurements were performed according to Pampel et al. (Pampel et al.; 2002). Detection was conducted with a Bruker DMX 600 spectrometer operating at 600.13MHz for ¹H. A Bruker 4mm HR-MAS probe was used which is

equipped with ^1H , ^{13}C and ^2H lock channels and pulsed field gradient capabilities. The investigation was performed at 37°C with a typical 90° pulse length of about $10.5\mu\text{s}$, a rotating frequency of 3500Hz and a gradient pulse length of 1ms with a diffusion time of 50ms . The maximal gradient strength (0.48T/m) was calibrated using a water-filled HR-MAS rotor by recording the ^1H -spectrum with the gradient on. The self-diffusion coefficient of water was monitored using the HDO signal at 4.57ppm . Progressive gradient strengths of 4-85% of 0.48T/m were applied to obtain serial one-dimensional spectra, which were used to calculate the self-diffusion coefficient by plotting the integrated water signal intensity against the applied field gradient.

3.2.3 Characterization of the Model Drugs

3.2.3.1 Sodium Dodecyl Sulphate Polyacrylamide Gel Electrophoresis (SDS-PAGE)

SDS-PAGE was performed under non-reducing conditions using an XCell II Mini-Cell system (Novex, San Diego, USA). Samples were dissolved in Tris buffer pH 6.8 and heated for 15min at 95°C . After centrifugation, $10\mu\text{l}$ aliquots were loaded into NuPAGE[®] Novex 10% Bis-Tris Pre-Cast gels 1.0mm (Invitrogen GmbH, Karlsruhe, Germany). Gels were run with a constant current of 30mA in a MES running buffer (Invitrogen GmbH, Karlsruhe, Germany). After staining with a coomassie blue kit (Colloidal Blue Staining Kit; Invitrogen GmbH, Karlsruhe, Germany) according to the vendor's protocol, the gels were dried using a DryEasy[®] Gel Drying System (Invitrogen GmbH, Karlsruhe, Germany).

3.2.3.2 Fluorescence Correlation Spectroscopy (FCS)

Diffusion coefficients of FITC dextran 20, 70 and 150 in water were measured by FCS with a ConfoCor 2 (Carl Zeiss GmbH, Jena, Germany). Experiments were performed with an Argon laser (488nm) at room temperature. A standard solution of 10nM Alexa488 (diffusion time $26\mu\text{s}$) was used. Diffusion times were measured, analyzed with autocorrelation curves and converted into diffusion coefficients (Magde et al.; 1974). Diffusion coefficients at room temperature were converted by the Stokes-Einstein equation to diffusion coefficients at 37°C . Measurements were carried out in triplicate.

3.2.4 Characterization of the Enzymatic Reaction

3.2.4.1 Determination of Enzyme Activity

The enzymatic activity of CHC was determined for 2 weeks by incubating 10µg/ml (4 Mandl units/ml) collagenase in Tris buffer pH 7.5 at 37°C. The remaining enzymatic activity was determined in the supernatant by applying either a continuous FALGPA assay or the EnzCheck[®] assay kit. Time dependent activity of MMP-2 (19.1mg/ml or 1.67µg/ml dependent on the supplier), MMP-9 (6.8ng/ml) and CHC (0.1µg/ml) over 2h was determined by using the EnzCheck[®] assay kit only. Determinations were performed five fold.

3.2.4.1.1 FALGPA Assay

A specific activity assay for bacterial collagenase based on the enzymatic cleavage of FALGPA (Van Wart et al.; 1981) was used. The decrease in absorbance was measured over 6min at 345nm (25°C) using a ThermoSpectronic UV1 photometer (Thermo Electron Corporation, Egelsbach, Germany) and the change in absorption per minute was calculated.

3.2.4.1.2 EnzChek[®] Gelatinase / Collagenase Assay Kit

Activity of all three enzymes was investigated with the EnzChek[®] (MoBiTec GmbH, Göttingen, Germany) (Molecular Probes; 2001). Samples were incubated with DQ gelatin at room temperature, protected from light. Active enzymes cleave the fluorescent labeled gelatin and fluorescence was measured (493nm/518nm ± 10nm) after appropriated time intervals (MMP-2: 25h, MMP-9: 1h, bacterial collagenase: 3h) by using a Cary Eclipse fluorimeter (Varian Deutschland GmbH, Darmstadt, Germany).

3.2.4.2 Binding studies

Unless otherwise noted, 2mg matrices were incubated at 37°C for 120min in 1.1ml Tris buffer pH 7.5, containing 21ng or 1840ng (depending on the supplier) activated MMP-2, 7.5ng activated MMP-9 and 110ng bacterial collagenase, respectively. During incubation, samples from the supernatant were collected and analyzed at defined time points (0, 30, 60 and 120min). Bacterial collagenase binding was analyzed by two different assays. Binding of

gelatinases was determined by the EnzChek[®] only (see 3.2.4.1). For statistical analysis the t-test was applied ($p < 0.001$). Data for the mathematical model was determined with 20mg minirods. Investigations were performed five fold.

3.2.4.3 Sorption Studies

Sorption studies were performed in Tris buffer pH 7.5 at 37°C. 20mg minirods or collagen powder was incubated with 5µg/ml (2 Mandl units/ml) collagenase. Over 24h, the remaining enzymatic activity in the supernatant was determined by using the EnzChek[®] and the adsorbed enzyme amount was calculated. To verify the amount of collagenase which is bound unspecifically in the matrix, samples were incubated for distinct time intervals and washed several times with Tris buffer pH 7.5. The supernatant and all washing solutions were investigated for remaining enzymatic activity. Furthermore, the sorption isotherm and sorption constants were determined. Different amounts of collagenase (2.5 – 30µg/ml) were incubated with minirods for 1h. The enzymatic activity in the supernatant was measured with the EnzChek[®] and the adsorbed enzyme amount was calculated. Analyses were carried out in triplicate.

3.2.4.4 Determination of the Degradation Constants

Samples, containing 5-200mg collagen powder or 5-100mg minirods were incubated with 0.1µg/ml (0.04 Mandl units/ml), 0.4µg/ml (0.16 Mandl units/ml), 1.25µg/ml (0.5 Mandl units/ml) and 2µg/ml (0.8 Mandl units/ml) collagenase, respectively, at 37°C. Samples were taken periodically and stored at -80°C to stop the enzymatic degradation process. Degraded soluble collagen fragments were quantified by a BCA-assay (Smith et al.; 1985) at 562nm using a densitometer (CS 9301 PC; Shimadzu Corp., Tokyo, Japan). The amount of soluble collagen was calculated from a standard curve obtained with gelatin A 180, because the standard BSA calibration curve can not be used for the determination of collagen fragments (Geiger; 2001; Smith et al.; 1985). The Michaelis-Menten constants and k_{cat} 's were calculated. Investigations were performed in duplicate.

3.2.5 In vitro Degradation Studies

10mm minirods were incubated in 2ml Tris buffer pH 7.5 at 37°C (20mm: 5ml; 30mm: 7ml; 40mm: 15ml). After addition of 0.1µg/ml (0.04 Mandl units/ml) and 6.7µg/ml (2.06 Mandl units/ml) collagenase, respectively, the complete incubation medium was replaced at designated time points. FITC dextran release (see 3.2.6.1) and collagen degradation were determined simultaneously. Supernatants were analyzed for soluble collagen fragments in 96 well plates using the BCA assay (see 3.2.4.4). Degradation was determined in triplicate.

3.2.6 In vitro Release Studies

3.2.6.1 FITC Dextrans

10mm minirods were incubated in 2ml Tris buffer pH 7.5 at 37°C (20mm: 5ml; 30mm: 7ml; 40mm: 15ml). At designated time points, the complete incubation medium was replaced and the FITC dextran release and the matrix degradation (see 3.2.5) were determined simultaneously. FITC dextran release was determined by fluorescence measurement (495nm/525nm ± 10nm; Cary Eclipse fluorimeter (Varian Deutschland GmbH, Darmstadt, Germany)) in 96 well plates. With respect to the development of the mathematical model, different experimental setups were performed. No collagenase, 0.1µg/ml (0.04 Mandl units/ml) or 6.7µg/ml (2.06 Mandl units/ml) enzyme was added to the samples. Enzyme was added after 0.25h pre-swelling or after 6d FITC dextran release in absence of collagenase. FITC dextran release was analyzed in triplicate.

3.2.6.2 BSA

10mm minirods were incubated in 2ml Tris buffer pH 7.5 at 37°C with 0.1µg/ml (0.04 Mandl units/ml) or without collagenase. At designated time points, minirods were removed and the water film at the surface was removed carefully by blotting with an adsorbent paper. The samples were loaded into an eppendorf cap and placed inside the loop-gap resonator of an L-band ESR spectrometer (1GHz, RadicalScope mt 500-L, Magnettech GmbH, Berlin, Germany). Measurements were performed in triplicate at room temperature with

the following parameters: central magnetic field 49mT, sweep of the central magnetic field 15mT, microwave 3dB, frequency of modulation 100kHz, amplitude of modulation 0.14mT and scan time 30sec.

3.2.7 In vivo Studies

In vivo studies were conducted in adult domestic pigs. Six pigs were available and observations were made at six different time points (3, 5, 7, 14, 28 and 56d). Minirods were implanted subcutaneously into the ear backs. For surgery protocol see Thorwarth et al. (Thorwarth et al.; 2005). One ear per pig was used for samples intended for ESR measurements and the other for histological investigations. After sacrificing, the ears were immediately frozen at -80°C.

3.2.7.1 Electron Spin Resonance Spectroscopy (ESR)

The frozen blocks were thawed and stippled into thin layer chromatography (TLC) capillaries for investigation of different parts of the explanted material. Distinction was made between interior and exterior parts of the minirods, tissue next (1-2mm) to and distant (>5mm) from the minirods and cartilage. Samples between day 5 and 56 were investigated. Measurements were performed with an X-band ESR spectrometer (9.3GHz, MiniScope MS 200, Magnettech GmbH, Berlin, Germany) at 37°C using the following parameters: central magnetic field 335.6mT, microwave 10dB, amplitude of modulation 0.2mT and scan time 30sec. Determinations were performed in triplicate.

3.2.7.2 Histology

Histological evaluations were also performed at day 3. The frozen blocks were thawed and fixed in paraffin and 4% formalin. For staining, specimens were dehydrated with an ascending alcohol series at room temperature and were intermediary fixed on Xylol. For a general overview, slides were stained with hemalaun and eosin (HE). Additionally, the sectioned samples were stained with antibodies against collagen type I, collagen type III, transforming growth factor (TGF) β and interleukin 1 β , respectively. Stained samples were examined under a light microscope (Axiovert 25, Carl Zeiss AG, Göttingen, Germany) and pictures were taken with a Sony Cyber Shot 3.3 Mega Pixel camera.

3.2.8 Mathematical Discretization

A mathematical model to describe drug release from collagen matrices undergoing enzymatic degradation was established. For a numerical simulation the resulting equations were discretized in space by the mixed Raviart-Thomas finite element method of lowest order and in time by the backward Euler scheme. The mixed finite element method locally preserves mass which is an appreciable advantage of this approach. The equations are fully coupled and therefore solved simultaneously by a damped version of Newton's method. The linear systems of the Newton iteration are solved by a multigrid algorithm. Having determined the concentration of the collagen at the n -th time point, the drug release equation can be solved and it can be proceed to the next time step. The problem was implemented in the software package UG, version 3.8. Two dimensional simulations were performed on a SUN BLADE 100 workstation.

4 Results and Discussion

For the development of an adequate mathematical model, it is important to characterize physical and chemical changes of device properties during drug release (Siepmann et al.; 2001). Drug liberation from hydrophilic polymers like collagen is governed by different mechanisms (see 1.2.3). Before diffusion controlled release or release by enzymatic and/or non-enzymatic degradation can take place, swelling occurs after contact with aqueous incubation media (Gombotz et al.; 1995). Since dense collagen matrices were investigated in this study, it must also be dealt with a drug fraction whose delivery is hindered by the collagen matrix structure. This part can not to be released until collagen linkages are digested.

4.1 Characterization of Collagen Matrices

Initially, dry matrices and swelling of collagen matrices had to be analyzed, to define the fundamental features of the mathematical model. Furthermore, early stages of the drug device development were mainly based on swelling investigations (see 4.1.2.1).

4.1.1 Characterization of Dry Collagen Matrices

Monolithic implants often have a cylindrical shape and are commonly produced by extrusion (Kissel et al.; 1991). Extrusion of collagen is easy in handling and gentle for incorporated drugs, because neither heating, nor the use of organic solvents is required. In general, aqueous collagen masses can be extruded directly and resulting strands can be dried at room temperature (Fujioka et al.; 1998). Collagen drug devices, named minirods, were prepared by extrusion of approximately 40% (w/w) aqueous collagen dispersions (water content of raw material: approximately 9% (w/w)). Resulting strands were dried for 5d at room temperature, 55% r.h. to obtain rods with approximately 1.7mm in diameter and 10mm in length (see Figure 4-1).

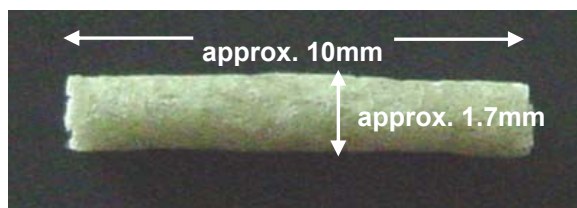


Figure 4-1 Dry equine EDC 1 cross-linked collagen minirod

The residual moisture of the hydrophilic matrix, determined by Karl-Fischer titration, is important with respect to the stability of potentially incorporated drugs. Furthermore, these values were necessary to feed the mathematical model and to determine release and degradation data correctly. After storage in a desiccator (45% r.h.) at room temperature, minirods had a residual water content of approximately 6% (w/w). No change in the water content was observed for cross-linked materials or if a model compound, e.g. FITC dextran or BSA, was incorporated. These results were in agreement with Kutz who investigated the water sorption of collagen hydrolysates (Kutz; 1988). He determined 8.5% (w/w) water content at 20°C/45% r.h. for Gelita Collagel[®].

4.1.1.1 Matrix Density

The surface of dry extrudates was studied by scanning electron microscopy (SEM) (see Figure 4-2). The lateral surface of equine and bovine tendon materials was dense before contact with liquids. A parallel orientated surface pattern according to the direction of extrusion was observed, resulting from the stress applied during the extrusion process (Sano et al.; 2003). A similar surface morphology was observed for both tendon materials independent of cross-linking (see Figure 4-2a-d), whereas the lateral surface of bovine corium EDC 1 cross-linked minirods appeared slightly scallier (see Figure 4-2e-f). The cross-section looked similar for all minirods. A longitudinal orientation of collagen bundles and small cavities could be observed (see Figure 4-2g-h).

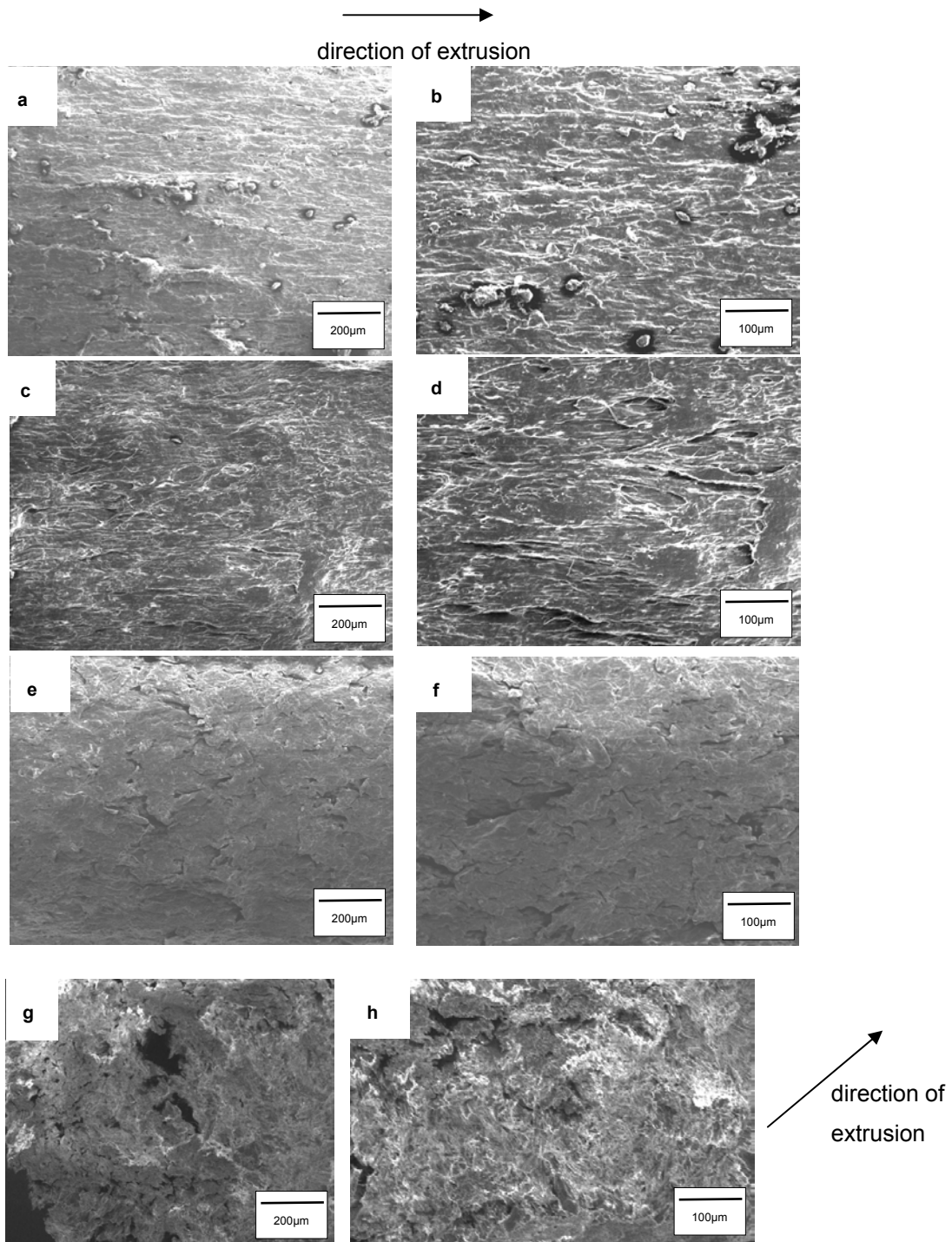


Figure 4-2 SEM micrographs of the surface of dry collagen minirods
 a; b: lateral surface of equine non cross-linked minirods
 c; d: lateral surface of equine EDC 1 cross-linked minirods
 e; f: lateral surface of bovine corium EDC 1 cross-linked minirods
 g; h: cross-section of bovine corium EDC 1 cross-linked minirods

Beyond optical investigations, the minirod density was calculated. In general, extruded devices show a density close to their particle density (Ghebre-Sellassie; 2003). Consequently, the calculated density values had to be compared to an apparent collagen density of 1.32g/cm^3 reported in the literature (Weadock et al.; 1984) and to an apparent density of 1.3g/cm^3 determined for dense collagen minipellets (Maeda et al.; 1999). All minirods had lower densities than values reported in literature (see Table 4-1). Unloaded minirods showed densities between 1.008 and 1.109g/cm^3 . No significant differences in apparent density were observed for non cross-linked and EDC 1 cross-linked matrices and between collagen materials extracted from different animal sources. If minirods prepared from tendon collagen were loaded with FITC dextran, device density remained almost constant if FITC dextran 70 was incorporated (unloaded equine non cross-linked minirods: 1.098g/cm^3 , FITC dextran 70 loaded extrudates: 1.109g/cm^3). The density decreased with a FITC dextran 20 load (0.983g/cm^3) or a FITC dextran 150 load (0.899g/cm^3). Increasing the FITC dextran 70 content to 2% (w/w) led also to a decrease in the apparent density of equine non cross-linked minirods (0.829g/cm^3), as did the incorporation of FITC dextran 70 in bovine corium EDC 1 cross-linked matrices (0.927g/cm^3). Thus, loading with FITC dextran affected the matrix structure and induced a reduced minirod density.

In summary, the presented observations showed that the extrusion of high concentrated collagen masses was possible and yielded dense, homogeneous matrices with a highly orientated structure (resembling the structure of tendon (Maeda et al.; 1999)). Apparent densities were decreased compared to the apparent collagen density.

Table 4-1 Calculated apparent densities of collagen minirods

Minirods	Density [g/cm ³]
Bovine corium non cross-linked	1.008
Bovine corium EDC 0.25 cross-linked (loaded with 1% FITC dextran 70)	0.717
Bovine corium EDC 1 cross-linked	1.025
Bovine corium EDC 1 cross-linked (loaded with 1% FITC dextran 70)	0.927
Bovine corium EDC 3 cross-linked (loaded with 1% FITC dextran 70)	1.089
Bovine tendon non cross-linked	1.075
Bovine tendon non cross-linked (loaded with 1% FITC dextran 70)	1.055
Bovine tendon EDC 1 cross-linked (loaded with 1% FITC dextran 70)	1.154
Equine non cross-linked	1.098
Equine non cross-linked pulverized	0.598
Equine non cross-linked (loaded with 1% FITC dextran 70)	1.109
Equine non cross-linked (loaded with 2% FITC dextran 70)	0.829
Equine non cross-linked (loaded with 1% FITC dextran 20)	0.983
Equine non cross-linked (loaded with 1% FITC dextran 150)	0.899
Equine EDC 1 cross-linked	1.109
Equine EDC 1 cross-linked (loaded with 1% FITC dextran 70)	1.011
Equine EDC 1 cross-linked (loaded with 1% FITC dextran 20)	0.791
Equine EDC 1 cross-linked (loaded with 1% FITC dextran 150)	0.804
Equine EDC 3 cross-linked (loaded with 1% FITC dextran 70)	0.948
Equine EDC 17 cross-linked (loaded with 1% FITC dextran 70)	0.999

4.1.1.2 Differential Scanning Calorimetry (DSC)

In order to identify the midpoint of transition, also known as melting temperature (T_m) of the collagen devices, DSC investigations were performed. Knowledge of this temperature is important to understand the physicochemical changes during in vitro and in vivo tests and to avoid temperature induced variations during storage. Furthermore, the degree of cross-linking can be judged indirectly, because the melting point of swollen collagen samples raises with an increase in cross-linkages due to stronger interactions between collagen fibers (Frieß et al.; 1996a; Geiger; 2001). In the dry state, a T_m of approximately 103°C was determined by Frieß (Frieß; 1999), indicating that collagen can be stored under dry conditions at room temperature without temperature induced changes. For fully swollen collagenous materials, incubated in Tris buffer pH 7.5 before DSC analysis, an endothermal peak in DSC spectra between 40 and 65°C was observed (see Figure 4-3, Figure 4-4 and Table 4-2). No additional peaks were detected during subsequent cooling and second heating (see Figure 4-3), indicating the complete and irreversible denaturation during the first run (Frieß et al.; 1996a).

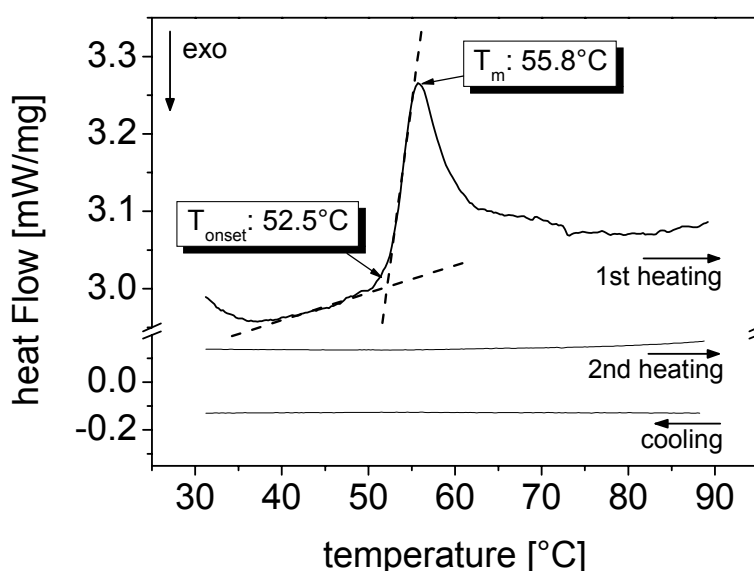


Figure 4-3 DSC scan of a pre-swollen bovine corium EDC 1 cross-linked collagen minirod

The difference between T_m of dry and fully swollen collagen materials was in agreement with Kopp et al., who observed higher denaturation temperatures, when the water content of collagen matrices was reduced (Kopp et al.; 1989).

DSC measurements of equine non cross-linked raw material and minirods (T_m (raw material) = $53.2^\circ\text{C} \pm 0.9^\circ\text{C}$ and T_m (mini-rods) = $53.6^\circ\text{C} \pm 0.2^\circ\text{C}$) showed, that extrusion did not affect the denaturation temperature significantly ($p > 0.001$). Overall, the observed thermal behavior corresponded to data presented by Piez, who proposed a single melting temperature at 55°C for homogeneous fibrillar collagen from rat tail tendon and calf skin (Piez; 1985).

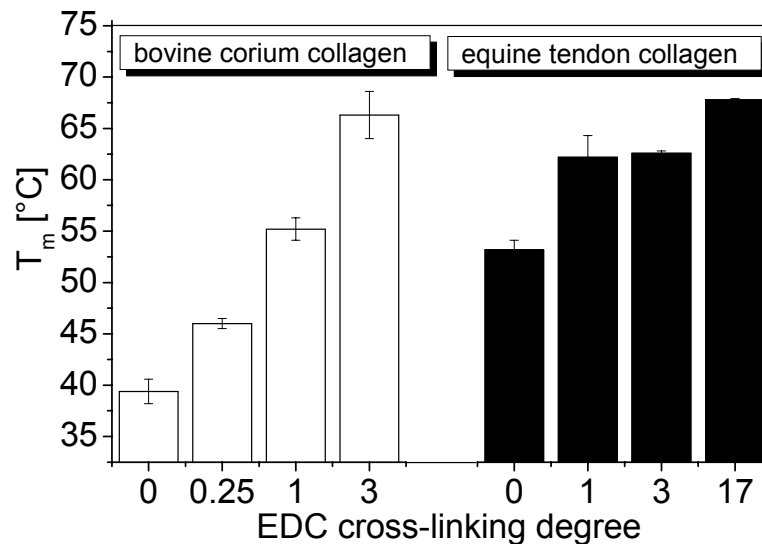


Figure 4-4 Melting temperatures of bovine corium and equine collagen raw materials cross-linked with different EDC ratios determined by DSC (average \pm SD; $n=3$)

EDC cross-linking resulted in an increase in the denaturation temperature (Pieper et al.; 1999) for all three investigated materials (see Figure 4-4 and Table 4-2). The upper limit of 17 was adapted from Olde Damink et al. (Olde Damink et al.; 1996b). Changing the cross-linking ratio of collagen is a potent tool to control the physicochemical properties of the manufactured delivery devices. Cross-linking is limited due to the number of reacting amino acids

(Frieß et al.; 1996a; Geiger; 2001). This could be manifested by an increase in T_m of EDC cross-linked collagens which leveled off between 62°C and 68°C (see Figure 4-4). Especially for preparation of equine EDC cross-linked matrices, ratios above 1 did not enhance stabilizing properties.

Table 4-2 Melting temperatures, determined by DSC, of different kinds of collagen type I raw materials (average \pm SD; n=3)

Sample	T_m [°C]
Equine DHT cross-linked	52.0 \pm 1.3
Bovine tendon non cross-linked	50.8 \pm 0.9
Bovine tendon EDC 1 cross-linked	60.3 \pm 0.7

The T_m of equine DHT cross-linked material did not increase compared to non cross-linked collagen (see Table 4-2). This was also observed by Pieper et al. for bovine tendon collagen type I and it was concluded that no distinct matrix stabilization takes place due to simultaneous cross-linking and denaturation (Pieper et al.; 1999). Gorham et al. even determined a decreased T_m for bovine corium collagen cross-linked at 120°C compared to cross-linked materials at 60°C, 80°C and 100°C, respectively. This was attributed to an increase in denaturation with increasing cross-linking temperatures (Gorham et al.; 1992).

Natural cross-linking depends on animal species, animal age and type of tissue (Frieß; 1999). Two different bovine collagens were compared with the equine tendon collagen. One bovine material was extracted from corium (= bovine corium collagen), whereas the bovine tendon material is composed of tendon collagen. Compared to equine non cross-linked collagen, lower denaturation temperatures were determined for both bovine non cross-linked materials (T_m (equine material) = 53.2 \pm 0.9°C; T_m (bovine corium material) = 39.4 \pm 1.2°C and T_m (bovine tendon collagen) = 50.8°C \pm 0.9°C). This indicated that these materials had a lower number of natural cross-links than the equine samples.

The decrease of T_m of bovine corium collagen compared to the bovine tendon material can be explained by a higher natural cross-linking in tendon than in corium, by different grades in purification and the different collagen fiber arrangement. In general, tendon materials consists of almost exclusively collagen type I after extraction and collagen fibers are orientated in parallel, whereas collagen materials extracted from skin may still contain remainders of other protein components and the fibers are arranged across each other (Gilbert; 1988b; Ruszczak et al.; 2003). Geiger detected denaturation temperatures of 55 – 59°C for insoluble bovine tendon non cross-linked collagen type I, similar to our bovine tendon collagen material. The variation in T_m was attributed to different cross-linking protocols (Geiger; 2001). Due to the low T_m and an onset temperature of $32.1 \pm 0.5^\circ\text{C}$, bovine corium non cross-linked collagen devices are less suitable for preparing drug delivery devices, because during incubation at 37°C physicochemical properties change and no constant release conditions can be provided for the complete investigation interval. Hence, this type of collagen was only used as cross-linked material in further investigations.

4.1.2 Transport of Water in Collagen Matrices

After characterization of the collagen material and the dry collagen matrices, the behavior in aqueous environment was investigated. Since collagen is a hydrogel, which swells after contact with water, the water penetration was studied in more detail.

4.1.2.1 Swelling of Collagen Matrices

Diffusion controlled drug release can be restricted e.g. by cross-linking, increasing the polymer concentration or by increasing the matrix dimensions (see 1.2.3.1). If swelling of collagen devices is minimized, a denser matrix structure is preserved longer and the release can be reduced due to a tighter diffusion barrier (Fujioka et al.; 1995; Sano et al.; 2003). Consequently, besides changing the matrix dimensions, variations in swelling properties and cross-linking ratios can be used to control release rates. The exclusion criterion in early matrix development was the swelling behavior in pure Tris buffer pH 7.5 at

37°C. The influence of bacterial collagenase (CHC) on swelling behavior was investigated as well, to gain information about the interplay of swelling and enzymatic degradation which is important for fitting the mathematical model (see 4.5).

4.1.2.1.1 Swelling Without Addition of Collagenase

Since tablets, produced by dry compaction, disintegrated already after 0.75h incubation at 37°C, further drug delivery devices were produced by extrusion. In general, minirods exhibited a two stage swelling process (see Figure 4-5). After fast initial swelling, a first plateau mostly of constant diameter and weight was reached, during which water distribution within the device takes place. This was followed by a second swelling phase, occurring more slowly than the first one, which is characterized by rearrangement of collagen structures (Frieß et al.; 1996b). After reaching the second plateau, the minirods started to disintegrate.

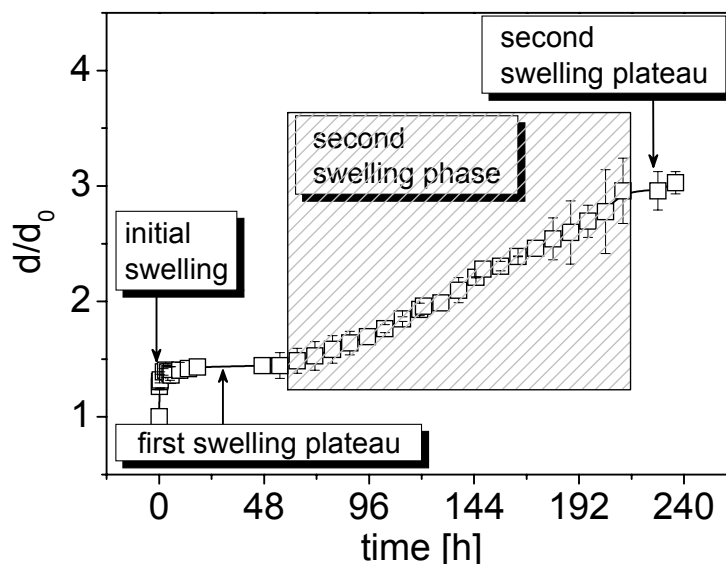


Figure 4-5 Schematic swelling process, demonstrated on the swelling profile of bovine corium EDC 1 cross-linked collagen minirods in Tris buffer pH 7.5 at 37°C (average \pm SD; n=3)

Initially, two preparation methods were tested: minirods were prepared with pulverized equine non cross-linked collagen (particle size < 180 μ m) or with the lyophilized raw material. Swelling can be reduced compared to tablets, but still was too pronounced for minirods prepared from the pulverized collagen material. As can be seen in Figure 4-6, minirods disintegrated already after 5h. To obtain powdered collagen, lyophilized raw material must be dispersed in water, subsequently air dried and finally grinded. Strong intra- and interhelical interactions resulted, which led to dense and hard matrices. These were transferred into particles by milling. Prior to extrusion, collagenous powder was hydrated again. But the dense particles showed only minor swelling and no homogeneous viscous collagen mass could be produced. Ductile deformation was also reduced which resulted in poor collagen cohesion during extrusion. Hence, interconnection inside the extrudates were less compared to minirods prepared directly from lyophilized collagen raw material (see Figure 4-6).

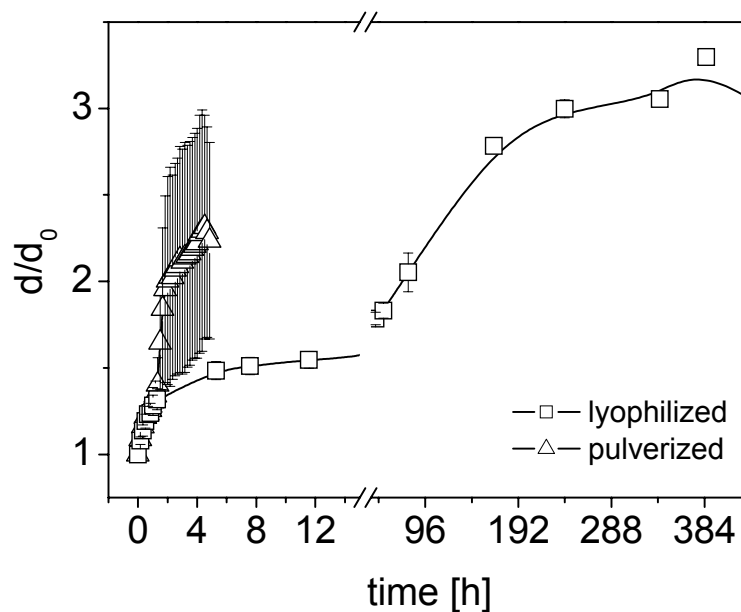


Figure 4-6 Swelling profiles of equine non cross-linked collagen minirods prepared from lyophilized and pulverized material in Tris buffer pH 7.5 at 37°C (average \pm SD; n=3)

This could also be manifested by the calculated apparent densities (see Table 4-1). Mini rods composed of lyophilized collagen showed a density of 1.098g/cm^3 , whereas pulverized starting material led to extrudates with a density of 0.598g/cm^3 . Hence, further mini rods were manufactured directly from raw material. Mini rods prepared from lyophilized equine collagen reached their first swelling plateau after 5h and remained at this level for another 18h. Subsequently, a swelling rate of $0.008/\text{h}$ was observed before the second swelling equilibrium was entered (see Figure 4-6).

For comparison, extrudates containing atelocollagen which were prepared by Japanese groups were used (Fujioka et al.; 1995). These extrudates are named minipellets. Swelling at 37°C was investigated for 24h (Maeda et al.; 1999). A fast swelling during the first 3h was observed, before the diameter and weight remained constant over the next 24h (increase in diameter: 50–100%, maximal change in weight: approximately 300%). The swelling profile and the change in weight during the 24h were almost similar to our mini rods. However, swelling of our mini rods was slightly delayed and less pronounced (60% increase in diameter at the first swelling plateau after 5h) and the matrices disintegrated later than the Japanese minipellets. As was demonstrated by Fujioka et al. (Fujioka et al.; 1995) and Maeda et al. (Maeda et al.; 1999), the swelling rate of collagen drug devices is influenced by the manufacturing and drying method and the concentration of the basic collagen dispersion. The Japanese minipellets, as well as our mini rods, were prepared by extrusion and subsequent air drying. They differ in the used collagen, insoluble equine collagen type I and soluble atelocollagen (dermal bovine collagen type I with removed telopeptides) for mini rods and minipellets, respectively, and in the collagen concentration (40% (w/w) versus 30% (w/w) collagen). The slightly delayed swelling of our mini rods can be attributed to the higher degree in natural cross-links and the higher concentration of collagen. In contrast to minipellets, our mini rods showed significant longitudinally ($l/l_0=1.3$ after 24h) and diagonally swelling. Since the swelling direction is related to the direction of shrinkage during drying (Maeda et al.; 1999), it was consistent that mini rods swelled in both directions, because during drying a uniform shrinkage of

approximately 0.85 in length (l/l_0) and diameter (d/d_0) was observed. Minipellets, prepared by the Japanese group, were dried lying on a plate and consequently only shrinkage in diameter was detected (Maeda et al.; 1999).

To investigate the influence of natural cross-linking on the swelling behavior, three different collagen qualities were used to prepare minirods. As was already demonstrated by DSC analysis (see 4.1.1.2), natural cross-linking in tendon is more pronounced than in corium, and equine collagen is more cross-linked than the two bovine materials. The fast swelling of the bovine corium material corresponded to the low T_m (T_m (bovine corium) = $39.4 \pm 1.2^\circ\text{C}$) and the slightly lower apparent matrix density (see Table 4-1). Since an onset temperature of $32.1 \pm 0.5^\circ\text{C}$ was measured, matrix disintegration started almost instantaneously after contact with buffer at 37°C . This manifested itself in a very short equilibration time (1h) and a fast rearrangement of the collagen structures before disintegration of the minirods started after approximately 10h (see Figure 4-7).

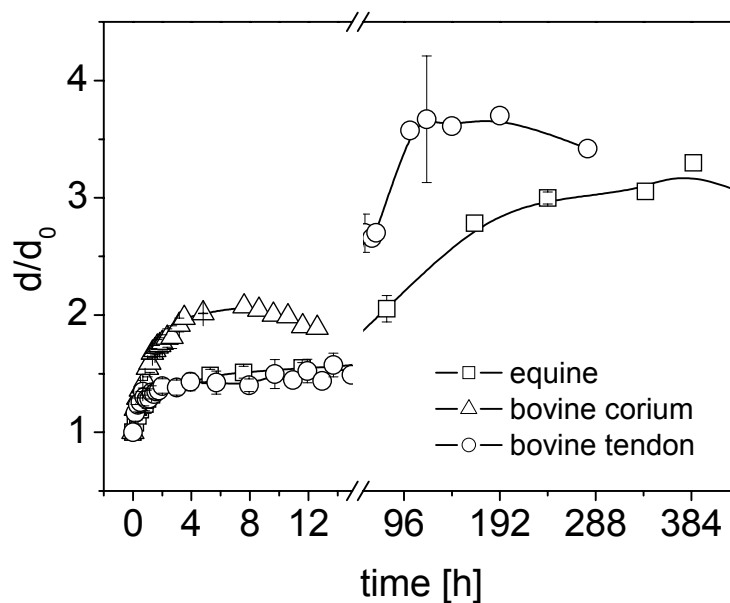


Figure 4-7 Swelling profiles of non cross-linked collagen minirods prepared from different collagen sources in Tris buffer pH 7.5 at 37°C (average \pm SD; $n=3$)

Due to a higher natural cross-linking degree in tendon, the collagen fiber structure is closer and penetration of the incubation medium is more hindered (Frieß et al.; 1996b). Bovine tendon extrudates showed a smaller increase in diameter than bovine corium minirods (1.4 compared to 1.8) during the first swelling phase (see Figure 4-7). This observation was consistent with the slightly higher calculated apparent matrix density (see Table 4-1) and the higher T_m (see 4.1.1.2) for the bovine tendon material. Natural cross-linking is even more pronounced in the equine collagen, because this material is in general prepared from older animals (Schlapp; 2001). Since the two dry tendon matrices had almost the same apparent density (see Table 4-1), the first swelling phase was similar for both minirods. The difference in number of natural, age-dependending cross-links became apparent in the second swelling phase. Equine minirods exhibited a second swelling rate over 140h with 0.008/h, whereas bovine tendon matrices had a swelling rate of 0.021/h for 77h. This indicated that an increase in cross-links delayed the rearrangement of collagen structures by fixation of collagen fibers (Frieß et al.; 1996b). Based on the observed swelling behavior, both tendon collagen variations appeared to be suited as matrix material for drug delivery devices in the non cross-linked state.

In order to further improve mechanical properties and reduce swelling, collagen was additionally cross-linked. Two different methods were carried out. Physical cross-linking was performed by DHT treatment after extrusion. During DHT cross-linking, interchain bonds are formed throughout the matrix by reducing the distances between neighboring molecules (Wang et al.; 1994; Weadock et al.; 1984). However, this method is accompanied by partial denaturation (Weadock et al.; 1996). Since this treatment results in fixation of the three dimensional collagen network without destruction of the triple helix (Weadock; 1986), it can only be performed with the final drug loaded minirods. In contrast, collagen was cross-linked with EDC before extrusion. Raw material was swollen and incubated with the cross-linking reagents. EDC diffuses into the collagen matrix and reaction times between 1h and 7h are sufficient to achieve a homogeneous cross-linking structure (De Paoli Lacerda et al.; 2005). EDC cross-linking results in intra- and interhelical, but no intermicrofibrillar, linkages (Zeeman et al.;

1999). After drying, the cross-linked material was extruded and loaded with drugs. If this preparation step would be performed with loaded minirods, side reactions with incorporated drug molecules and drug depletion due to diffusion processes may occur.

The effect of EDC cross-linking on swelling behavior was investigated with bovine corium collagen minirods (see Figure 4-8). At a low cross-linking ratio (EDC 0.25), the first swelling rate was similar to non cross-linked minirods, but water equilibration required more time. The second swelling rate occurred at less than half the rate of non cross-linked matrices (0.076/h compared to 0.195/h) and took place over a longer time period. This reflected the hindered rearrangement of the collagen structure (Frieß et al.; 1996b) and corresponded to the higher T_m detected for the cross-linked minirods (see Figure 4-4). However, this slight cross-linking did not lead to a pronounced improvement of the mechanical properties of the matrices. If the cross-linking degree was further increased, a decrease in the amount of penetrating solvent and in swelling were detected. These effects were described in literature as well (Charulatha et al.; 2003; Frieß et al.; 1996a; Frieß et al.; 1996b; Radu et al.; 2002; Rehakova et al.; 1996). The extent of the first swelling plateau was reduced by increased cross-linking, as was already observed for different degrees in natural cross-linking (see Figure 4-7). During the first swelling phase, EDC 1 and EDC 3 cross-linked minirods showed similar swelling, whereas differences could be detected by entering the second swelling phase (see Figure 4-8). The second swelling rate of EDC 1 cross-linked matrices (0.009/h) was similar to the swelling rate of equine non cross-linked minirods (see Figure 4-7). Since the swelling ratio correlates inversely to the cross-linking density (Pek et al.; 2003), the number of cross-links for both materials was comparable (Weadock et al.; 1984). DSC data (see Figure 4-4) indicated a similar tendency, because melting temperatures were approximately the same (T_m (equine non cross-linked material) = $53.2 \pm 0.9^\circ\text{C}$ and T_m (bovine corium EDC 1 cross-linked collagen) = $55.2^\circ\text{C} \pm 1.1^\circ\text{C}$). With further cross-linking, more collagen fibers were fixed through intra- and interhelical linkages and structure rearrangement was further delayed. This became apparent in a lower swelling rate (0.002/h) of

EDC 3 cross-linked extrudates. Comparison to equine material showed that the bovine corium EDC 3 cross-linked swelling rate was similar to the swelling rate of equine EDC 1 cross-linked minirods (see Figure 4-9) as were their denaturation temperatures (T_m (equine EDC 1 cross-linked material) = $62.2 \pm 2.1^\circ\text{C}$ and T_m (bovine corium EDC 3 cross-linked collagen) = $66.3^\circ\text{C} \pm 2.3^\circ\text{C}$). Hence, more additional cross-links had to be introduced into the bovine corium raw material to receive materials which are equally stabilized as the equine material.

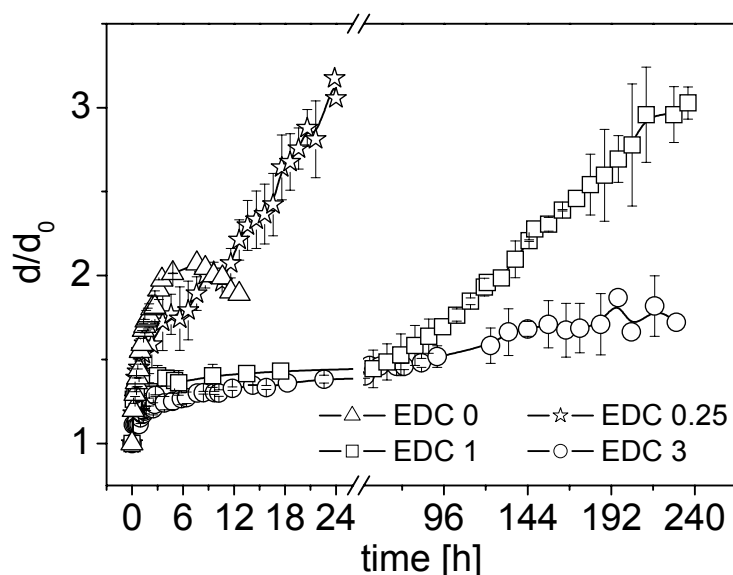


Figure 4-8 Influence of the cross-linking ratio on the swelling of bovine corium EDC cross-linked collagen minirods in Tris buffer pH 7.5 at 37°C (average \pm SD; $n=3$)

Variation in EDC cross-linking degree was also investigated for equine minirods. Due to the higher number in natural cross-links, ratios higher than EDC 1 had no additional positive effect on the minimization of swelling, because the maximal number in cross-links was already reached. The same conclusion could be drawn from DSC data (see Figure 4-4). A similar saturation effect was observed by Frieß et al. for differently GTA cross-linked bovine collagen films

(Frieß et al.; 1996b) and by Geiger for EDC, GTA and HMDIC (hexamethylene-diisocyanate) cross-linked bovine collagen sponges (Geiger; 2001).

The influence of DHT cross-linking on the swelling behavior was examined for equine minirods. Both cross-linking procedures, EDC and DHT treatment, reduced strongly swelling compared to non cross-linked minirods (see Figure 4-9). The first swelling phase was almost similar for both cross-linked materials resulting in an increase of diameter to approximately $d/d_0=1.2$ after 1h. The subsequent water equalization in EDC devices was slower than in DHT minirods (154h compared to 28h). EDC cross-linked minirods showed a second swelling rate (0.002/h) and a second plateau at $d/d_0=2$, which was higher than that of DHT minirods (0.001/h, $d/d_0=1.5$). This difference could be explained by the fixed three dimensional matrix structures after DHT treatment, which limit the rearrangement of collagen structures. EDC cross-linked minirods retained their flexibility, because no stabilizing intermicrofibrillar cross-links were introduced (Zeeman et al.; 1999) and a faster structure rearrangement could be detected. The less pronounced swelling of DHT treated collagen was in agreement with Pieper et al., who observed a reduced water binding capacity compared to non cross-linked or EDC cross-linked collagen (Pieper et al.; 1999). Wang et al. also observed a reduced swelling ratio of DHT collagen and attributed this phenomenon to occupied or removed water binding sites and to a more hindered water penetration into the dense matrix structure. The interfibrillar slipping is limited and the matrix is fixed three-dimensionally (Wang et al.; 1994). Geiger and Gorham et al. concluded that DHT treatment with increasing temperatures results in lower collagen solubility and consequently in increased collagen hydrophobicity (Geiger; 2001; Gorham et al.; 1992). The second swelling rate of cross-linked matrices was significantly lower than that of non cross-linked minirods due to fixation of collagen fibers and consequently slower rearrangement of the collagen inner structures (Frieß et al.; 1996b). This was consistent with DSC observations, because higher T_m -values were determined for equine EDC 1 cross-linked collagen than for the non cross-linked material. T_m of equine DHT treated collagen was almost similar to that of

the non cross-linked material, because of partially collagen denaturation (see 1.2.1.2 and 4.1.1.2).

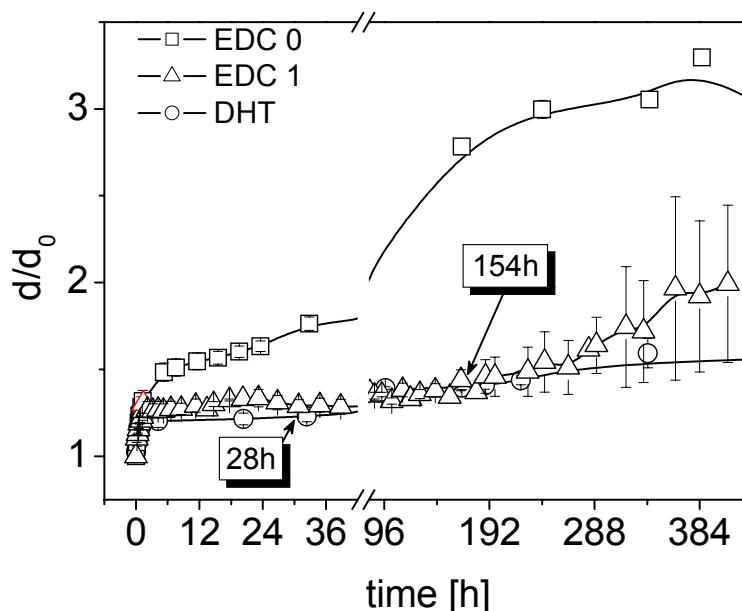


Figure 4-9 Influence of the cross-linking method on the swelling of equine collagen minirods in Tris buffer pH 7.5 at 37°C (time points indicate start of the second swelling phase) (average \pm SD; n=3)

Summarizing the presented results showed that swelling of minirods can be controlled by different ways. Starting with non cross-linked collagen material demonstrated that swelling could be suppressed by preparing extrudates from lyophilized raw material instead from pulverized material. Furthermore an effective tool to control the swelling properties of minirods was to use different insoluble collagen type I flavors which vary in their natural cross-linking degree. Least swelling was obtained with equine tendon material. To further reduce swelling, two different cross-linking methods were investigated. DHT treated minirods showed less swelling than EDC cross-linked extrudates. However, EDC cross-linked material was used in further experiments, since EDC cross-linking was performed prior to drug loading and preparation of minirods without damaging the drug as compared to the 110°C treatment of drug loaded

matrices. Increasing the EDC cross-linking ratio resulted in maximal stabilizing effects for a ratio of 1.

4.1.2.1.2 Swelling in the Presence of Collagenase

In vivo and in vitro drug release depends on swelling and enzymatic matrix degradation (see 1.2.3). Therefore, water uptake was studied in the presence of 0 µg/ml, 0.1 µg/ml (0.04 Mandl units/ml) and 6.7 µg/ml (2.06 Mandl units/ml) bacterial collagenase, respectively. Different enzyme concentrations were used, because the in vivo concentration of collagenase is not constant in all tissues and changes with disease (Parks; 1999). For example, intestinal collagenase (MMP-1) is increased 65-fold in chronic foot ulcers compared to traumatic wounds (Lobmann et al.; 2002). In vivo / in vitro - correlation of collagenase concentration is not well documented in the literature. Okada et al. investigated the degradation of Catgut (Okada et al.; 1992a) and found a correlation between in vivo and in vitro concentration of bacterial collagenase of 2.5 µg/ml. But data for enzymatic activity of CHC was missing and therefore, adaptation of this concentration had to be handled with care. Frieß set 2.5 µg/ml (1.15 Mandl units/ml) as in vitro concentration and concluded after subcutaneous implantation of dense collagen matrices in mice, that this concentration was chosen too high to receive good in vivo / in vitro – correlation of degradation rates (Frieß; 1999). Another approach was made by Yannas et al., who investigated the degradation of bovine tendon collagen tapes (Yannas et al.; 1975). Good in vivo / in vitro - correlation was found by using 3.5 Mandl units/ml bacterial collagenase. Nevertheless, this enzymatic concentration appeared to be extremely high. To bracken the range of possible concentrations of collagenase, two extreme enzymatic concentrations were used to observe the influence of enzymatic degradation on swelling. 6.7 µg/ml collagenase was set as the high end enzymatic concentration due to fast matrix degradation and simple preparation by dilution. 0.1 µg/ml collagenase was chosen as minimal concentration, because this concentration still allowed investigations of enzymatic activity with the EnzCheck® (detection limit: 7ng/ml (Molecular Probes; 2001), see 4.2.1 and 4.2.2).

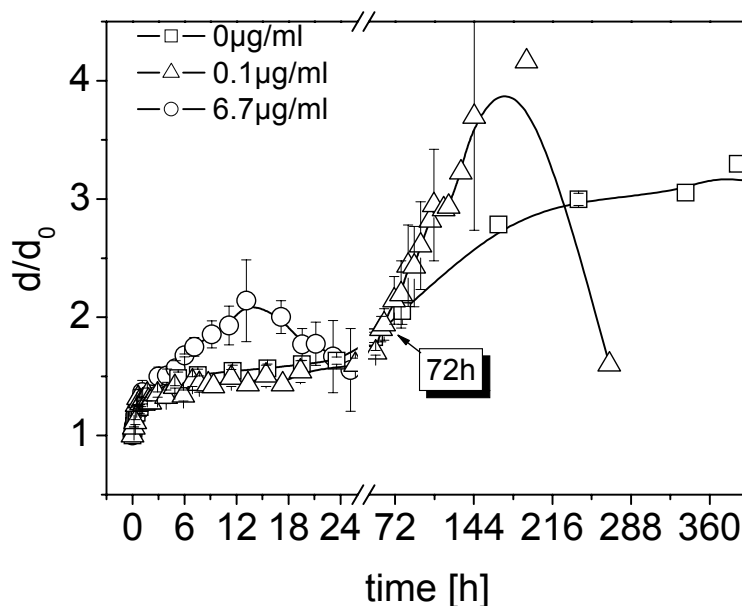


Figure 4-10 Swelling profiles of equine non cross-linked collagen minirods in the presence of 0, 0.1 and 6.7 µg/ml bacterial collagenase, respectively, at 37°C (time point indicates point of separation in swelling profiles between 0 and 0.1 µg/ml enzyme) (average \pm SD; n=3)

In general, penetration of collagenase can be considered to be very slow due to adsorption phenomena (see 4.2.2.4) and slow diffusion through the dense matrix structure. As can be seen in Figure 4-10, the influence on swelling behavior could be neglected for the first 3d for low enzymatic concentrations which were used in release and degradation studies. The second swelling rate was more than doubled when minirods were incubated with 0.1 µg/ml collagenase (0.02/h compared to 0.008/h). Due to enzymatic degradation of cross-links, minirods became less dense and a faster rearrangement of the collagen fibers could take place. If incubation was performed with higher concentrations of collagenase, extensive degradation overlaid swelling and the swelling behavior could not be followed anymore. The matrix became less dense due to simultaneous pronounced cleavage of collagen fibrils and the second swelling rate of 0.064/h indicated a fast collagen fiber rearrangement.

The maximum in matrix diameter ($d/d_0=2.1$) was already reached after 12h, followed by disintegration of the minirods (see Figure 4-10).

Since incubation of equine non cross-linked minirods showed no distinct difference in swelling kinetics during the first 3d if collagenase was present or not, the effect of $0.1\mu\text{g/ml}$ collagenase on the swelling behavior of EDC 1 cross-linked minirods was also investigated. The first swelling phase followed the same profile for experiments without and with $0.1\mu\text{g/ml}$ collagenase, resulting in a plateau of $d/d_0=1.25$ for equine EDC 1 cross-linked minirods and 1.4 for bovine corium EDC 1 cross-linked extrudates, respectively. As was already observed for equine non cross-linked minirods (see Figure 4-10), differences occurred in the second swelling phase. Again, the swelling rate increased by a factor of more than 2 when collagenase was added (bovine corium EDC 1: 0.024/h to 0.009/h; equine EDC 1: 0.004/h to 0.002/h).

Changes in surface morphology during swelling were investigated by SEM. The orientated structure of equine non cross-linked minirods was preserved during incubation in Tris buffer pH 7.5 at 37°C . Compared to dry minirods (see Figure 4-2), the surface was more porous, the collagen material was defibrated (Sano et al.; 2003) and collagen strands stuck out of the minirod surface (see Figure 4-11a, c). Minirods, exposed to $0.1\mu\text{g/ml}$ collagenase, also exhibited a smoother surface (see Figure 4-11b, d). Fringed collagen fiber bundles were missing, because they could be easily reached by collagenase, degraded and removed. Additionally, very small pores could be observed beneath the first surface layer, indicating that the enzyme attacked collagen inside the swollen device as well.

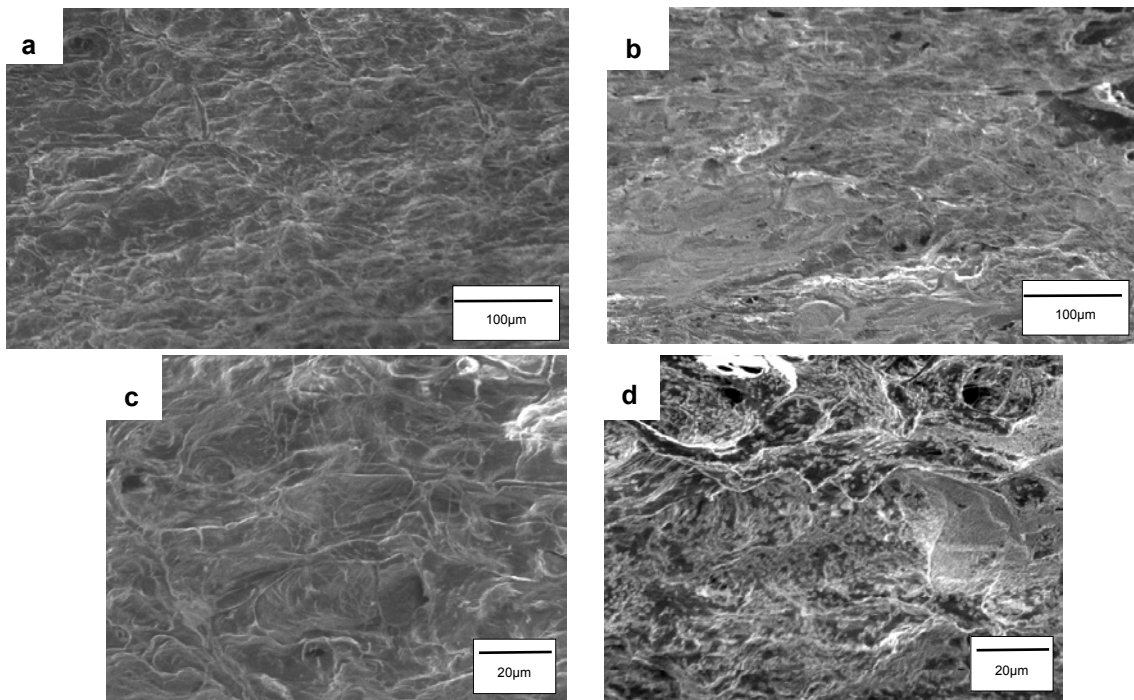


Figure 4-11 SEM micrographs of the lateral surface of equine non cross-linked collagen minirods after 2d swelling at 37°C
a; c: without collagenase
b; d: in the presence of 0.1µg/ml collagenase

The cross-section of minirods incubated with collagenase exhibited larger pores than minirods swollen in pure buffer (see Figure 4-12).

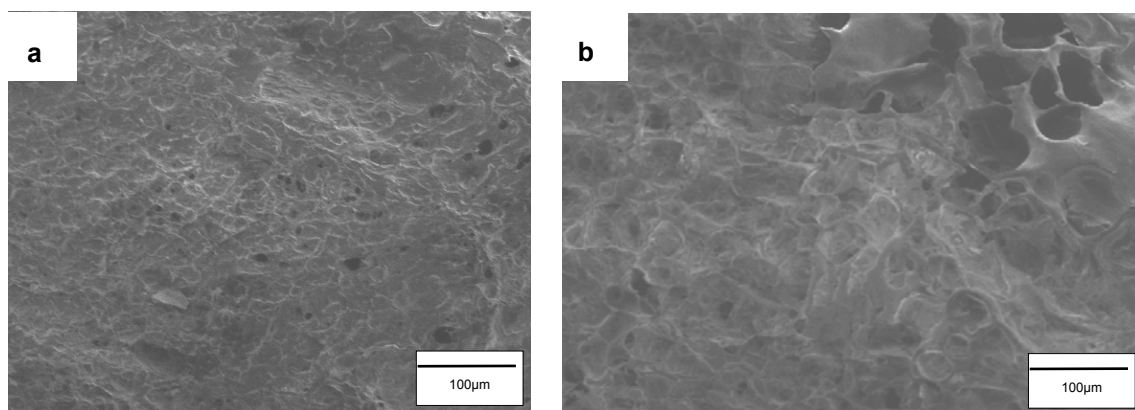


Figure 4-12 SEM micrographs of the cross-section of equine non cross-linked collagen minirods after 2d swelling at 37°C
a: without collagenase
b: in the presence of 0.1µg/ml collagenase

4.1.2.2 Diffusion Coefficient of Water in Mini-rods

The self-diffusion coefficient of water in equine non cross-linked collagen mini-rods was determined by PFG-NMR (pulsed field gradient nuclear magnetic resonance) coupled with magic angle spinning (MAS) to receive a higher spectral resolution. The resulting ^1H NMR spectrum is shown in Figure 4-13.

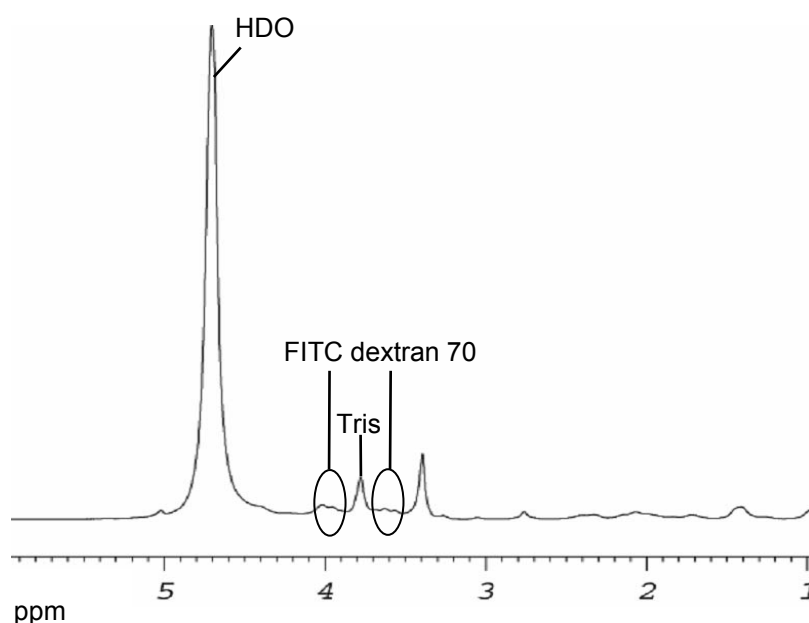


Figure 4-13 ^1H NMR spectrum of water in equine non cross-linked mini-rods

The signal of water appears at 4.57 ppm. A self-diffusion coefficient of $5.76 \cdot 10^{-2} \text{ cm}^2/\text{h}$ inside the mini-rods was obtained by plotting the integrated water signals against the applied field gradient (see Figure 4-14). The determined self-diffusion coefficient was in the range of the water self-diffusion coefficient in cartilage, e.g. determined as $7.0 \cdot 10^{-2} \text{ cm}^2/\text{h}$ by Knauss et al. (Knauss et al.; 1999), and the self diffusion coefficient of bulk water in hydrated collagen ($7.92 \cdot 10^{-2} \text{ cm}^2/\text{h}$) (Traore et al.; 2000). This indicated that the matrix structure of equine non cross-linked collagen mini-rods resembles the composition of cartilage, as was already demonstrated by Maeda et al. for minipellets containing atelocollagen (Maeda et al.; 1999). Compared to the diffusion

coefficient of pure water ($8.64 \cdot 10^{-2} \text{cm}^2/\text{h}$) (Pampel et al.; 2002), the diffusion of water inside the collagen minirods was only slightly restricted ($D(\text{solution})/D(\text{minirod})=0.67$). Hence, water interacts with the collagen structures during swelling and its mobility becomes restricted.

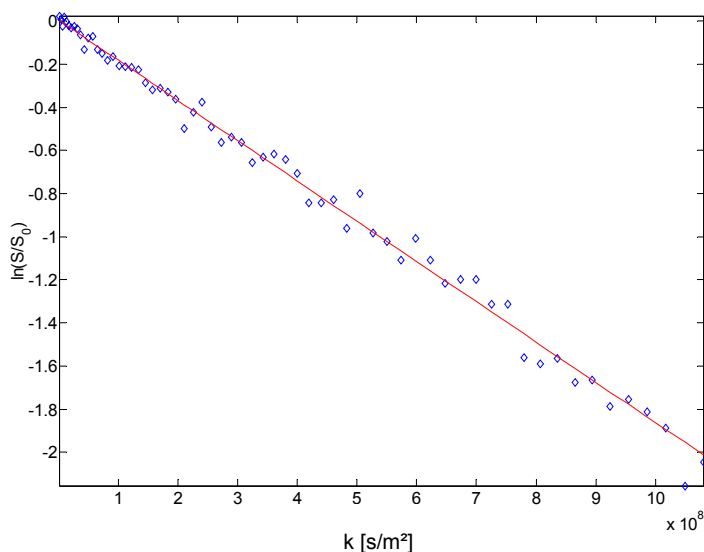


Figure 4-14 Determination of the self-diffusion coefficient of water in equine non cross-linked minirods (the slope is equivalent to the self-diffusion coefficient)

In an attempt to measure the self-diffusion coefficient of FITC dextran 70 inside equine non cross-linked minirods by PFG-NMR, the matrices were pre-swollen in Tris buffer pH 7.5 (D_2O) containing 10% (w/w) FITC dextran 70. However, the used MAS setup does not provide a gradient strength which enables the detection of the rather slow diffusing FITC dextran 70. If the minirods were loaded using the highly concentrated dextran solution, the rotational experimental setup made the unambiguous detection impossible, because the FITC dextran 70 solution was squeezed out of the collagen matrix during the diffusion measurement. In minirods pre-swollen in pure Tris buffer pH 7.5 (D_2O), the FITC dextran 70 concentration was too low to be detectable (see Figure 4-13). In conclusion, the applied experimental setup was not adequate for the measurement of FITC dextran 70 diffusion in dense collagen minirods.

4.1.3 Summary

Collagen is a member of the group of hydrophilic biodegradable polymers and swells in contact with aqueous solutions. It is important to investigate the physicochemical properties of collagen devices for a correct description and modeling of drug release. Implant manufacturing was optimized in the early matrix development stages mainly on data obtained by DSC and swelling investigations. Except for bovine corium non cross-linked collagen ($T_m=39.4 \pm 1.2^\circ\text{C}$) all materials have a T_m above 40°C , indicating that these kinds of collagen were stable during in vivo and in vitro examinations and could be used to prepare drug devices. Implants, prepared by extrusion, exhibited a highly orientated collagen fiber bundle structure, according to the direction of extrusion, which was even preserved during swelling. Water uptake was reduced, matrix disintegration delayed and diffusion barriers for drug release were maintained longer than e.g. in compressed tablets.

Different collagen type I materials were compared and it was concluded from swelling and DSC analysis that the number of natural cross-links is lower in corium than in tendon collagens and increases with animal age (T_m (equine material) = $53.2 \pm 0.9^\circ\text{C}$, matrix disintegration after 24d; T_m (bovine tendon collagen) = $50.8^\circ\text{C} \pm 0.9^\circ\text{C}$, matrix disintegration after 12d; T_m (bovine corium material) =: $39.4 \pm 1.2^\circ\text{C}$, matrix disintegration after 0.5d). The mechanical stability of collagen minirods was further enhanced by additional cross-links, introduced by physical (DHT) or chemical (EDC) treatment. Although lesser swelling was observed for DHT cross-linked matrices (DHT: swelling rate of 0.001/h, second plateau at $d/d_0=1.5$; EDC: swelling rate of 0.002/h, second plateau at $d/d_0=2$), EDC cross-linked extrudates were used in further experiments, because incorporated drugs may be damaged by the high temperatures applied during DHT treatment. Increasing the molar EDC cross-linking ratio led to an increase in number of cross-links. This was accompanied by an increase in T_m (e.g. T_m (bovine corium collagens): EDC 0 = $39.4 \pm 1.2^\circ\text{C}$; EDC 0.25 =: $46.0 \pm 0.5^\circ\text{C}$; EDC 1 =: $55.2 \pm 1.1^\circ\text{C}$; EDC 3 = $66.3 \pm 2.3^\circ\text{C}$) and a delay and reduction in swelling (matrix disintegration of bovine corium collagens after 0.5d (EDC 0); after 1d (EDC 0.25), after 10d (EDC 1) and after 9.5d (EDC

3), respectively). However, this effect was limited by available cross-linking sites, especially for the equine collagen, at a ratio of 1.

To obtain deeper insight into the behavior of water inside the minirods, the self-diffusion coefficient was determined by pulsed field gradient nuclear magnetic resonance (PFG-NMR). The self-diffusion coefficient inside the matrices was decreased compared to the self-diffusion coefficient in solution ($D(\text{solution})/D(\text{minirod})=0.67$), because water interacts with the collagen structures during swelling.

In summary, the presented data showed that the swelling properties of collagen drug delivery devices, and in consequence the diffusion barriers delaying the drug release, could be controlled by using different collagen type I materials and/or by introducing additional cross-links. For release and degradation studies, collagen matrices will be prepared by extrusion with either non cross-linked or EDC 1 cross-linked, lyophilized, non-grinded collagen. A concentration of $0.1\mu\text{g/ml}$ CHC will be used in the in vitro investigations to simulate in vivo conditions.

For development and implementation of the mathematical model of drug release from dense collagen matrices, an initial water content of 6% (w/w) of dry minirods and swelling data of minirods incubated in pure buffer were used, because of a similar swelling behavior in the presence of low bacterial collagenase concentrations.

4.2 Characterization of Degradation

Besides swelling, the second reason for changes in matrix dimensions is degradation of the collagenous matrix material. Especially release from devices with a higher cross-linking density is also controlled by erosion. Because of this important influence, matrix digestion by collagenases and gelatinases was studied in more detail to collect data for feeding the mathematical model (see 4.5). The most important group of MMPs which is responsible for collagen degradation is the group of collagenases. Enzymatic cleavage of insoluble substrates can only occur after enzyme adsorption (see 1.3.1). Binding to

different collagen matrices, including determination of sorption isotherms had to be investigated, before the degradation constants were determined. These data were used to fit and verify the mathematical model presented in section 4.5. Beyond these detailed investigations for collagenase, loss in activity and binding to several matrices were examined for human gelatinase A (=MMP-2) and human gelatinase B (=MMP-9). In former times, it was assumed that gelatinases can not cleave the helical parts of collagen and that they initiate only the second step of collagen digestion, the degradation of collagenous fragments into amino acids (see 1.2.2.2). But Okada et al. demonstrated that “MMP-9 plays a key role in the initial depolymerization step of collagen fibrils” by attacking the telopeptides of collagen type I (Okada et al.; 1995). Aimes et al. were able to proof that MMP-2 can cleave collagen type I even within its helical parts (Aimes et al.; 1995) Consequently, nowadays the synergistic action of collagenases and gelatinases is assumed to be important for in vivo collagen cleavage. Another reason for expanding the investigations was the important role of MMP-2 and MMP-9 in wound healing, especially their behavior in chronic wounds. Delayed healing often corresponds with an elevated level of gelatinase A and B (Tregrove et al.; 1999; Wysocki et al.; 1993).

4.2.1 Time Dependency of Activity of MMPs

Enzymes loose their activity during in vitro incubation (Cullen et al.; 2002a), depending on buffer system and temperature. In vivo this loss is not as important as in vitro due to continuous re-production. Consequently, the time dependency of enzymatic activity had to be taken into account, especially if sorption and degradation studies were performed over longer time periods. In the mathematical model (see 4.5), this degradation kinetics was incorporated to overcome the difference between in vitro – in vivo circumstances.

The loss in activity of bacterial collagenase during incubation was determined by two different activity assays (an assay with FALGPA (furylacryloyl-leucine-glycine-proline-alanine) and the EnzCheck[®]). After 24h incubation at 37°C in Tris buffer pH 7.5, enzymatic activity was reduced to 90% of the initial activity. Subsequently, the activity decreased to 80% after 48h and remained constant

at this level over 2 weeks (see Figure 4-15). This was in agreement with Olde Damink who determined a loss in enzymatic activity of 10% after incubation for 24h and 30% loss after 48h incubation at 37°C (Olde Damink et al.; 1995). The loss in enzymatic activity corresponded also to observations from Soru et al., who reported that collagenase was stable at least for one hour at 40°C and assumed that after 24h at this temperature 20% of activity was lost (Soru et al.; 1972).

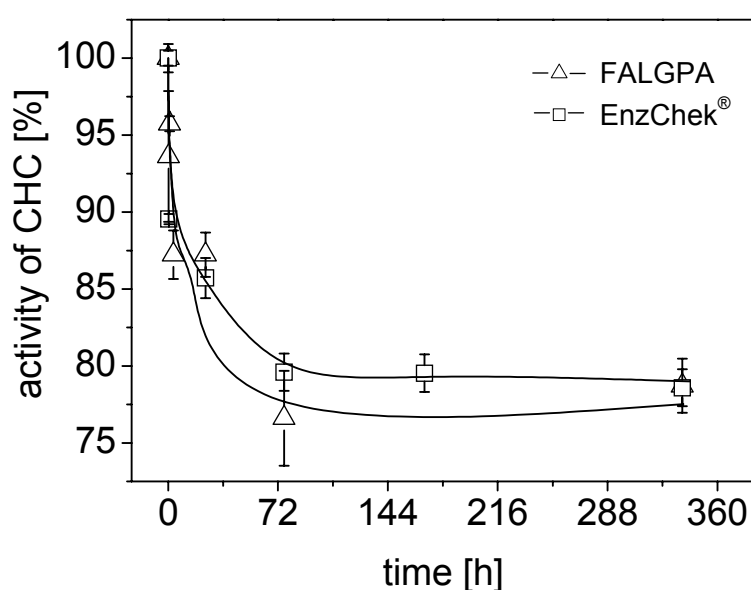


Figure 4-15 Time dependence of the activity of 10µg/ml bacterial collagenase at 37°C, determined by FALGPA and EnzChek[®] analysis, respectively (average ± SD; n=5)

Human MMPs are secreted in vivo as zymogens (see 1.2.2.2). During activation, an approximately 10kDa fragment is cleaved (Overall; 1991). In vitro, human MMPs have to be activated as well; commercially available zymogens of MMP-2 by reaction with APMA (p-aminophenylmercuriacetate) and MMP-9 with trypsin / aprotinin. For organomercurial agents, chelating with the conserved prodomain cystein residue is proposed. The cystein is displaced (Okada et al.; 1992b) and the zinc ion of the active site becomes available for substrate binding, leading to autocatalytic activity (Shapiro et al.; 1995). By

using trypsin activation, a subsequent stop of activation is necessary. Otherwise the enzyme would be degraded completely (Okada et al.; 1992b).

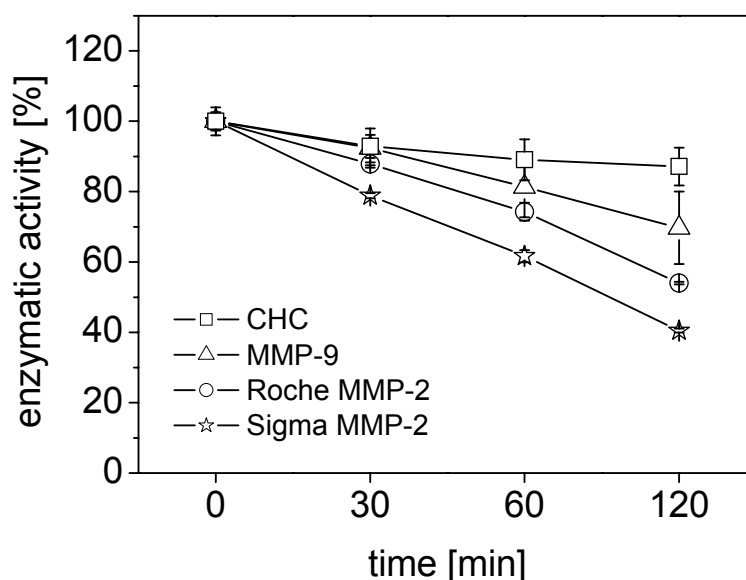


Figure 4-16 Time dependence of the activity of 100ng/ml bacterial collagenase, 1672.7ng/ml (Sigma) or 19.1ng/ml (Roche) MMP-2 and 6.8ng/ml MMP-9, respectively, at 37°C (average \pm SD; n=5)

The time dependent change in enzymatic activity was investigated over 2h which represented the incubation time for sorption studies (see Figure 4-16). Compared to collagenase both gelatinases were rather instable. This was in agreement with Cullen et al., who determined a loss of combined MMP activity in diabetic wound fluids of approximately 30% after 30min and 45% after 1h incubation (Cullen et al.; 2002a). In our studies, MMP-9 lost 30% of its initial activity within 2h. For gelatinase A two different qualities were used. The enzyme supplied from Roche showed a higher initial activity and a more stable behavior than the Sigma quality. These results suggested that the human gelatinases could only be used for short time studies, whereas with bacterial collagenase investigations over a longer time period than 2h could be performed without pronounced reduction in enzymatic activity.

4.2.2 Enzymatic Binding Studies on Collagenous Materials

To characterize the enzyme-substrate interaction properly, binding studies on collagenous materials for all three enzymes were performed. For method development, binding on two wound dressings, available on the German market (Vasel-Biergans; 2004), was determined. Due to their porous structure, enzymes can penetrate easily into the sponges and consequently a large surface area was available for binding. As examples for collagenous sponges, used in chronic wound therapy, Suprasorb[®] C (Lohmann & Rauscher GmbH & Co. KG, Rengsdorf, Germany), composed exclusively of bovine corium collagen type I, and Promogran[®], containing bovine corium collagen type I and oxidized regenerated cellulose (ORC) (ratio 45/55; Johnson & Johnson Medical Limited, Gargrave, Skipton, UK), were chosen. Bovine corium non cross-linked minirods (prepared from the same collagen as Suprasorb[®] C) were also investigated, to have the possibility to compare collagen sponges with dense collagen matrices.

4.2.2.1 Development of Test Conditions

The first set of experiments was performed with the FALGPA assay. This assay is one of the most frequently used activity assays for bacterial collagenase because of a rapid and simple test protocol (Van Wart et al.; 1981). Gaspers et al. mentioned that the FALGPA analysis is near the sensitivity limit, but reported repeatable results with approximately 10% standard derivation for each individual investigation (Gaspers et al.; 1995). When the supernatant was investigated directly, many visible degradation products were in the tested sample which interfere the UV measurement. After 60min, approximately 25% active collagenase for both wound dressings was recovered (see Figure 4-17a). To enhance sensitivity and reproducibility, two different setups were tested. On the one hand the supernatant was centrifuged prior to measurement and on the other hand a filtration step was performed before analysis. Filtration was slightly superior to centrifugation, but variability in the results was still high (see Figure 4-17b, c). To obtain more reliable results, we replaced the FALGPA assay by a more sensitive fluorimetric assay (EnzChek[®] (Molecular Probes; 2001)). Due to easier handling, samples were centrifuged before measurement to avoid

interference of degradation products. Reproducibility was strongly enhanced (see Figure 4-17d).

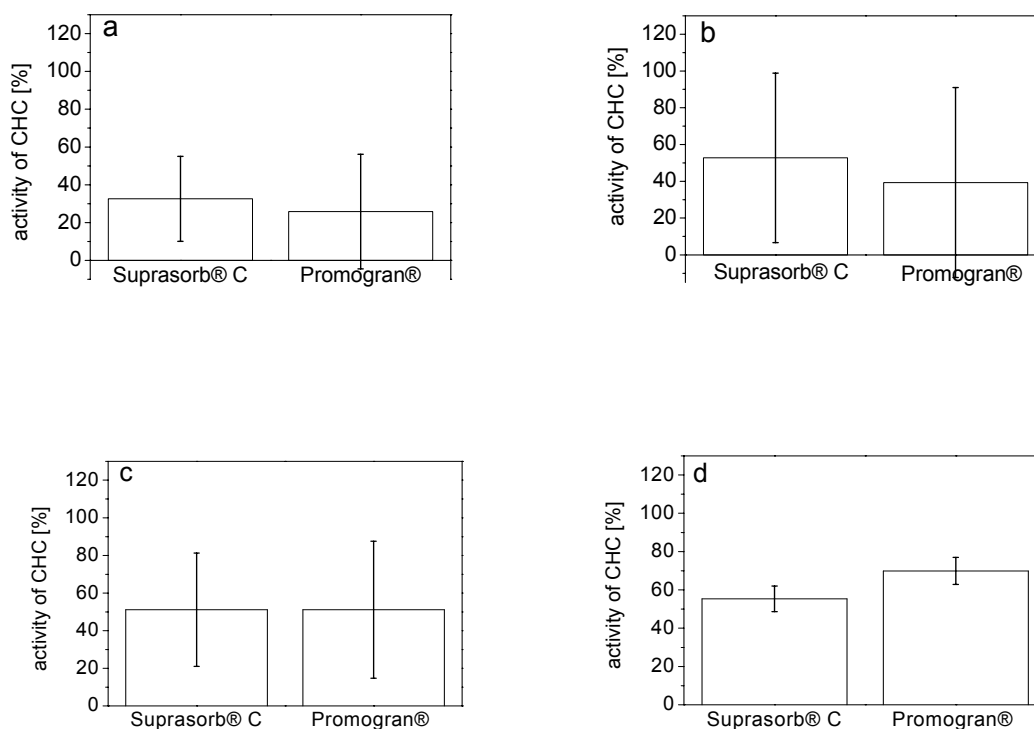


Figure 4-17 Activity of collagenase after 60 minutes incubation with 2mg Suprasorb® C and 2mg Promogran®, respectively, at 37°C (average \pm SD; n=5)

a: untreated sample; determined by FALGPA analysis

b: centrifuged sample (7500rpm; 5min); determined by FALGPA analysis

c: filtrated sample (0.2µm); determined by FALGPA analysis

d: centrifuged sample (7500rpm; 5min); measured with the EnzCheck®

Because enzymes were investigated separately in these setups, the EnzChek® assay could be used for all three. If all enzymes would be investigated together in one sample, no differentiation would be possible. Simultaneous degradation of fluorescent labeled gelatin would take place and even more specific methods, such as gelatin zymography for MMP-2 and 9, have to be applied (Cullen et al.; 2002a).

4.2.2.2 Gelatinase B (MMP-9)

Adsorption of gelatinase B was more pronounced than binding of collagenase (see Figure 4-17d; Figure 4-18). Although, MMP-9 is not as specific for collagen type I as collagenase, Okada et al. demonstrated that cleavage in the telopeptide region of the $\alpha 2$ chain takes place (Okada et al.; 1995). In consequence, the pretreatment of the collagen material is very important, because MMP-9 can only form specific binding complexes with collagen telopeptides. Already after 30min approximately 54% enzyme was bound to Suprasorb[®] C (see Figure 4-18). This effect was slightly more evident with Promogran[®]. The amount of enzyme (30% of the initial MMP-9 concentration) bound on Promogran[®] remained constant over 2h indicating that after 30min maximal binding of approximately 60% was reached. In diabetic wound fluids, Cullen et al. also observed after 2h a binding of approximately 30% of initial activity on Promogran[®] (Cullen et al.; 2002a). The residual enzymatic activity of MMP-9 after 30min in the presence of Suprasorb[®] C decreased at the same rate as the loss in activity of gelatinase B in buffer. Thus, binding was also completed after 30min and during the residual observation period equilibrium between bound and unbound enzyme was established. Binding of MMP-9 on collagen minirods was investigated as well. During the first hour no significant binding could be measured ($p < 0.001$). After 2h the extent of binding was comparable with the binding capacity of Promogran[®]. For both materials a binding of approximately 40% was observed. This delay in binding could be explained by the denser matrix structure and in consequence the more hindered access to the binding sites.

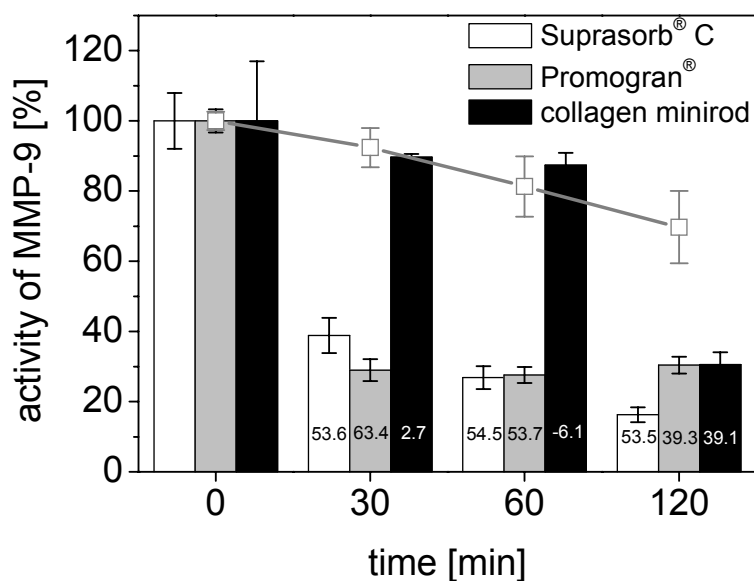


Figure 4-18 Binding of 7.5ng gelatinase B on 2mg collagenous matrices at 37°C (line: enzyme activity in buffer, numbers: difference of enzymatic activity without and in the presence of matrices; average \pm SD; n=5)

4.2.2.3 Gelatinase A (MMP-2)

Due to differences in stability (see Figure 4-16) and in specific activity of MMP-2 from different suppliers, these experiments were carried out with two different qualities. The first experiments were performed with gelatinase A from Roche. Both wound dressings showed no pronounced binding of MMP-2 (see Figure 4-19). Data obtained for gelatinase A from Sigma indicated slight binding after 30min incubation for both wound dressings (see Figure 4-20). However, the residual MMP-2 activity remained constant over the complete observation period in the presence of collagenous wound dressings (Suprasorb® C: approximately 60%; Promogran®: approximately 50% of the initial activity), indicating that no MMP-2 was bound after 2h. No binding of MMP-2 was detected in the presence of the collagen minirods as well.

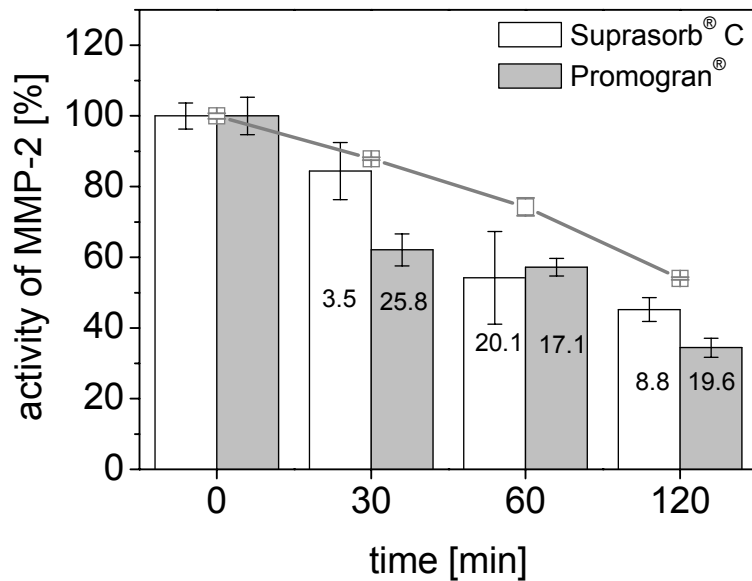


Figure 4-19 Binding of 21ng gelatinase A (Roche) on 2mg collagenous matrices at 37°C (line: enzyme activity in buffer, numbers: difference of enzymatic activity without and in the presence of matrices; average \pm SD; n=5)

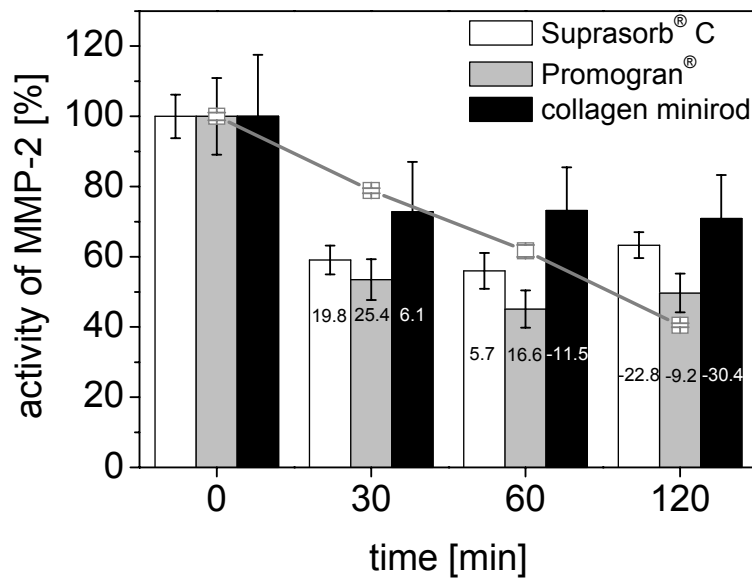


Figure 4-20 Binding of 1.84 μ g gelatinase A (Sigma) on 2mg collagenous matrices at 37°C (line: enzyme activity in buffer, numbers: difference of enzymatic activity without and in the presence of matrices; average \pm SD; n=5)

Since MMP-2 digests collagen type I (Aimes et al.; 1995) and degradation could be made visible by comparing Suprasorb[®] C incubated with and without gelatinase A (see Figure 4-21), the enzyme has to interact with the substrate.

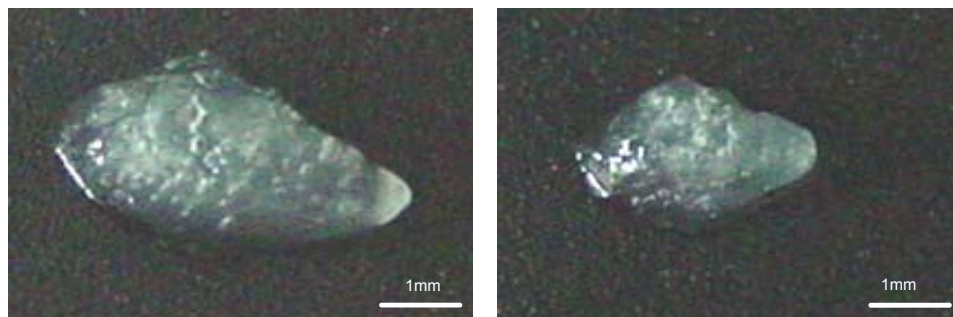


Figure 4-21 Suprasorb[®] C incubated without (left) and with 1.84µg (right) gelatinase A (Sigma) for 2 hours at 37°C

However, binding could not be quantified with the applied test conditions. A possible explanation might be, that the used enzymatic concentrations, 21ng (Roche) and 1840ng (Sigma) per 1.1ml, respectively, strongly exceed the concentration of gelatinase A in vivo (e.g. 103pg/ml active enzyme in diabetic foot ulcers (Lobmann et al.; 2002)). Hence, binding effects were too low to be detected. The detection limit of the EnzChek[®] does not allow a variation in MMP-2 concentration. Therefore, the substrate – enzyme ratio was reduced by increasing the collagen concentration (10mg matrices instead of 2mg collagen). With this modification, binding could be made visible (see Figure 4-22). After 30min incubation, Suprasorb[®] C could bind approximately 35% enzyme. Reduction in MMP-2 activity in the medium was more pronounced in the presence of Promogran[®], approximately 50% of the enzyme was bound after 30min. The binding capacity was nearly constant for one hour for both wound dressings (Suprasorb[®] C: approximately 35%; Promogran[®]: approximately 50%). After 2h, 10% less binding was observed for both materials (Suprasorb[®] C: approximately 20%; Promogran[®]: approximately 40%).

In literature it is documented that the growth of several cell types, e.g. fibroblasts, can be enhanced in the presence of collagen type I (Pachence et al.; 1987). Furthermore, MMP-2 secretion and activation is more pronounced, when fibroblasts are cultured with collagen type I (Azzam et al.; 1992).

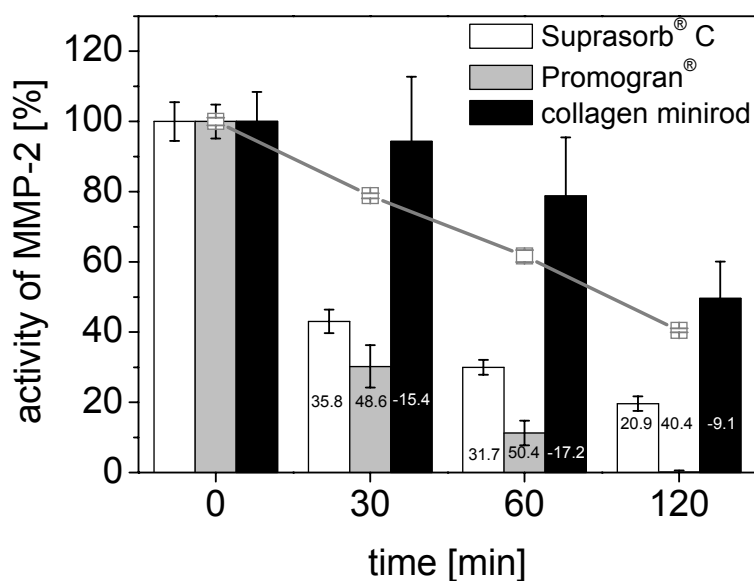


Figure 4-22 Binding of 1.84µg gelatinase A (Sigma) on 10mg collagenous matrices at 37°C (line: enzyme activity in buffer, numbers: difference of enzymatic activity without and in the presence of matrices; average ± SD; n=5)

It was concluded, that MMP-2 might maintain its activity when it is bound to this type of collagen. By assuming equilibrium between unbound and bound gelatinase A, the increase in enzymatic activity in the incubation medium after 2h could be traced back to an exchange of detached active enzymes with MMP-2 molecules which lost their activity by remaining in the incubation medium. Thus, the increased enzyme activity in the medium did not necessarily indicate a release of enzyme. This effect was not as pronounced for gelatinase A from Roche than for the Sigma quality, because MMP-2 from Roche was in general more stable (see Figure 4-16). Still, no binding of gelatinase A was detected in the presence of collagen minirods (see Figure 4-22). This could be explained by the denser matrix which hinders the penetration of enzyme molecules. The

specific binding in the interior of the collagen helix becomes more difficult and fewer enzyme molecules can be adsorbed on minirods.

4.2.2.4 Bacterial Collagenase (CHC)

Both wound dressings do bind collagenase due to the specificity of the enzyme towards collagen (see Figure 4-23). Incubating Suprasorb[®] C with CHC resulted in a more pronounced decrease of collagenolytic activity in the medium as compared to collagenase incubated in buffer. This indicated that the enzyme was bound onto to wound dressing and could be detracted from the simulated wound fluid. Promogran[®] bound collagenase to a similar degree. After 30min incubation, the extent of binding (approximately 18%) was similar for both wound dressings. After incubation for 60min, the amount of enzyme bound to Suprasorb[®] C increased to approximately 34% collagenase and was slightly, but not significantly ($p < 0.001$), higher as compared to Promogran[®]. At the 120min time point, approximately 62% enzyme was adsorbed on both wound dressings.

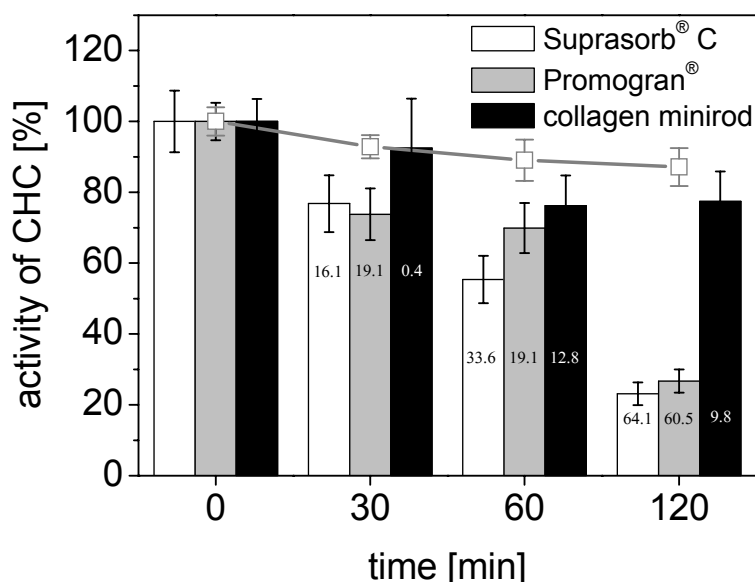


Figure 4-23 Binding of 110ng collagenase on 2mg collagenous matrices at 37°C (line: enzyme activity in buffer, numbers: difference of enzymatic activity without and in the presence of matrices; average \pm SD; n=5)

The dense collagen minirods showed delayed and less pronounced binding. Only approximately 10% of collagenase was bound over the complete observation period. The enzyme binds to specific binding sites inside the collagen fibers, but due to the dense matrix structure, penetration is hampered, the surface area is reduced and binding sites become limited (Steven; 1976).

In summary, the binding of bacterial collagenase and human gelatinase A and B on collagenous surfaces was investigated. In vitro, bacterial collagenase was more stable than the two human MMPs. Still, after 2 weeks approximately 80% of its initial activity could be measured and CHC can therefore be used for the longer investigations periods required in release and detailed binding and degradation studies. After establishment of adequate test conditions, adsorption on collagen wound dressings and collagen minirods was determined. Both wound dressings, Suprasorb[®] C and Promogran[®], approved for chronic wound treatment, did not differ much in their sorption profiles for all enzymes. In general, binding was enhanced with longer incubation times. Up to now, the binding mechanism is not completely identified. It is generally agreed, that collagen acts as a competitive substrate for all three enzymes. By presenting additional binding sites, the elevated enzymatic breakdown of tissue in chronic wounds can be repressed (Cullen et al.; 2002b). Besides this, the granulation phase can be enhanced by adsorption of wound fluid and the repair process may be initiated again (Vasel-Biergens; 2004). The second component of Promogran[®], ORC, is negatively charged at pH 7.5 and can bind positively charged atoms, such as the zinc and calcium ions in MMPs (Cullen et al.; 2002b). Therefore, a non-specific binding mechanism was proposed for Promogran[®]. It was assumed, that proteases bind physically without participation of their active sites and that their active sites are only obstructed by sterical features (Cullen et al.; 2002a). Almost no binding of MMP-2 and MMP-9 can be observed on minirods, prepared from the same collagen as Suprasorb[®] C. This indicated that the density of the device and in consequence the accessible surface area is a crucial factor for adsorption.

After investigation of the binding of MMP-2 and -9 on three different samples, the focus was put on the interaction of bacterial collagenase with collagen

minirods. For the development of the mathematical model (see 4.5), sorption isotherms of CHC on collagen surfaces were needed.

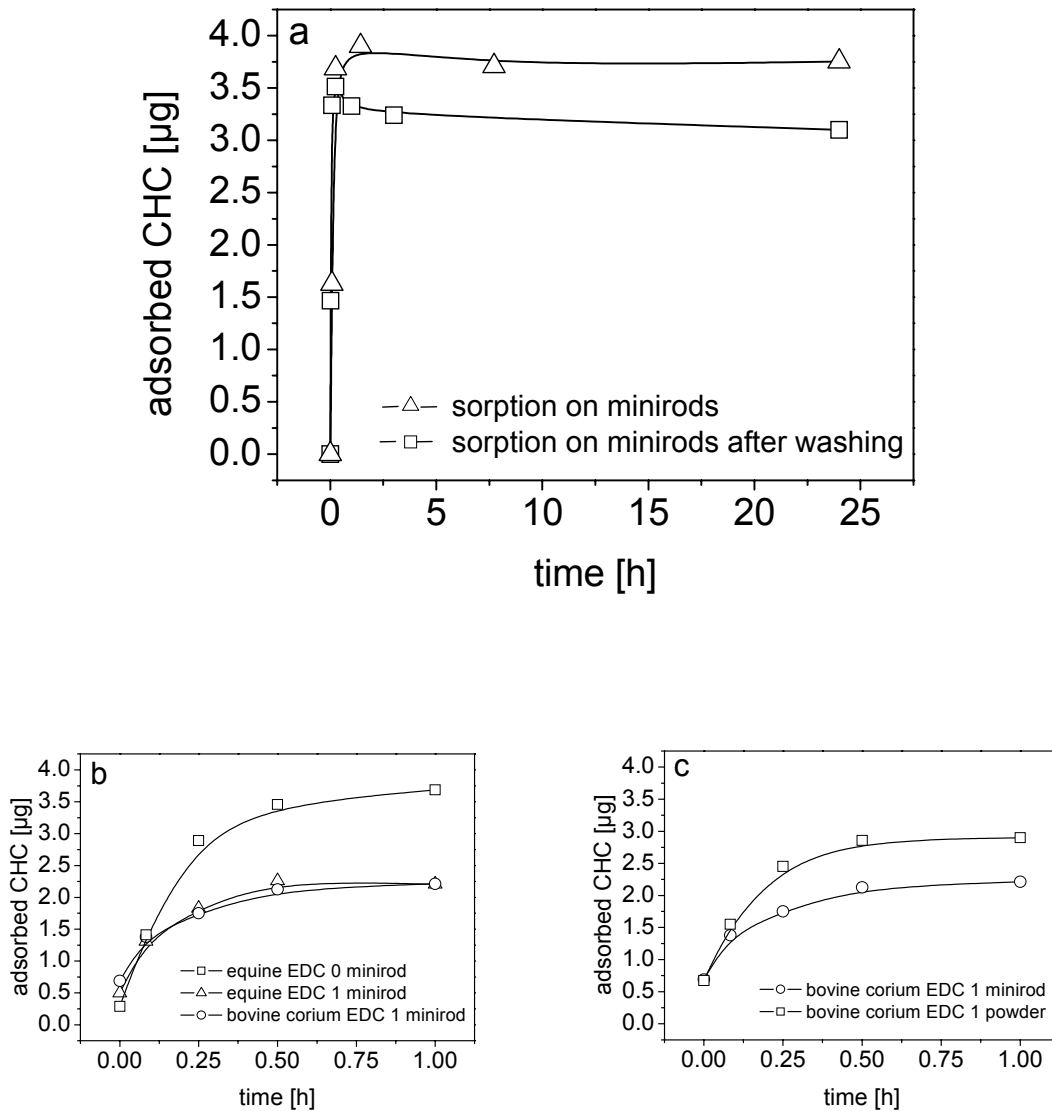


Figure 4-24 Sorption of 5µg/ml collagenase at 37°C on 20mg equine non cross-linked collagen minirods (a), on different collagen minirods (20mg) (b) and on 20mg bovine corium EDC 1 cross-linked minirods and powder (c) (n=3)

Therefore, the time interval of investigation was expanded to 24h and the sorption on collagen powders and minirods prepared from the three different raw materials was investigated. Before sorption isotherms could be determined,

the time of equilibrium in enzyme – substrate complexes must be known. In general, after a fast binding of collagenase, the adsorbed enzymatic amount remained constant for at least 24h (see Figure 4-24a), irrespectively whether collagen powder or minirods was used. Focusing on the first hour of adsorption (see Figure 4-24b, c), it was demonstrated that all accessible reaction sites were reached within this time interval, irrespectively of the used matrix form or collagen. Subsequently the number of enzyme-substrate complexes was almost constant due to simultaneously occurring sorption and desorption. After adsorption, CHC moved along the collagen fibers, until a specific binding site was reached. Cutting of the collagen helix could take place and subsequently diffusion along the collagen fibers continued (Gaspers et al.; 1994; Paige et al.; 2002). Binding sites within the matrix which were inaccessible at the beginning became accessible due to matrix swelling and degradation (Steven; 1976). Consequently, collagenase would not be released before the number of binding sites became less than enzyme molecules (Gaspers et al.; 1994; Welgus et al.; 1980). Sorption on EDC 1 cross-linked minirods was less pronounced than on non cross-linked minirods (see Figure 4-24b). Collagenase still diffused towards the collagenous surface, but enzymatic binding sites were blocked by cross-links (Zeeman et al.; 1999). The new linkages also restricted binding, because the pre-requisite untwisting of tropocollagen (French et al.; 1992) became more difficult. Similar adsorption on equine and bovine corium EDC 1 cross-linked minirods was observed. Another factor which highly influenced adsorption is the density of the device. By comparing minirods and powder prepared from bovine corium EDC 1 cross-linked collagen, this effect became obvious (see Figure 4-24c). The collagen powder exhibits a greater surface area than the minirods, consequently more binding sites were accessible and the extent of sorption was higher.

The strength of adsorption was investigated by washing equine non cross-linked minirods with Tris buffer pH 7.5 after incubation with CHC. The amount of collagenase, detectable in the supernatant at the end of incubation, decreased over time (see Figure 4-25), indicating that with longer incubation times more collagenase was attached onto collagen minirods. Analyzing the washing

solutions showed that with longer incubation periods, more washing steps were needed to free collagenase. Hence, it was assumed that a longer contact of collagenase with collagen led to a more specific manner in binding. On the one hand more binding sites got accessible due to swelling and on the other hand more enzyme molecules were able to reach specific binding sites after diffusion along the collagen fibers.

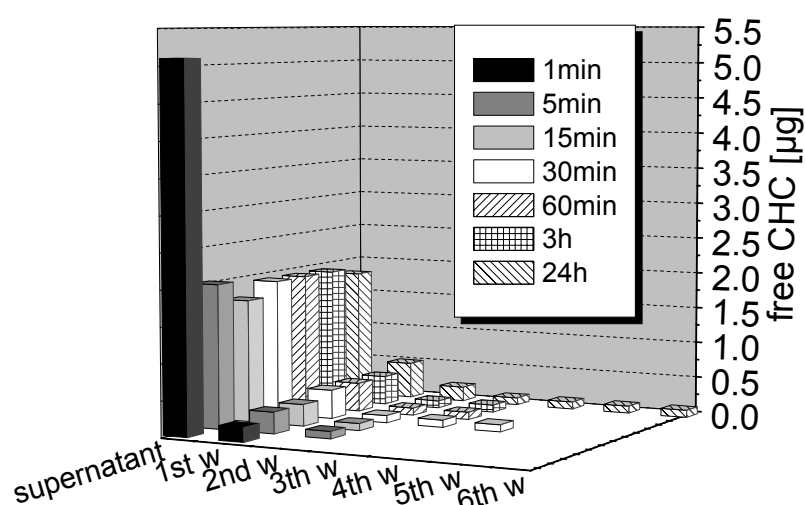


Figure 4-25 Detectable amount of collagenase in washing solutions after incubation of 20mg equine non cross-linked minirods with 5µg/ml collagenase at 37°C (w: washing step)

Since in average approximately 1µg collagenase could be removed by subsequent washing steps (see Figure 4-24a and Figure 4-25), it was concluded that this amount was only entrapped physically in the collagen matrix, but not bound specifically onto the collagen surface.

4.2.3 Determination of Sorption Isotherms

Similar time courses of adsorbed collagenase were observed for concentrations between 0.005 – 0.08mg/ml enzyme. Since only a fraction of complete added enzyme can be bound on collagen (e.g. approximately 10% within 2h, see

Figure 4-23) and the maximal amount of collagenase was already adsorbed between 0.5h and 1h (see Figure 4-24), sorption isotherms can be studied after 1h incubation. The first approach of a sorption isotherm was a linear relationship between adsorbed enzymatic amount and added CHC concentration (see Figure 4-26).

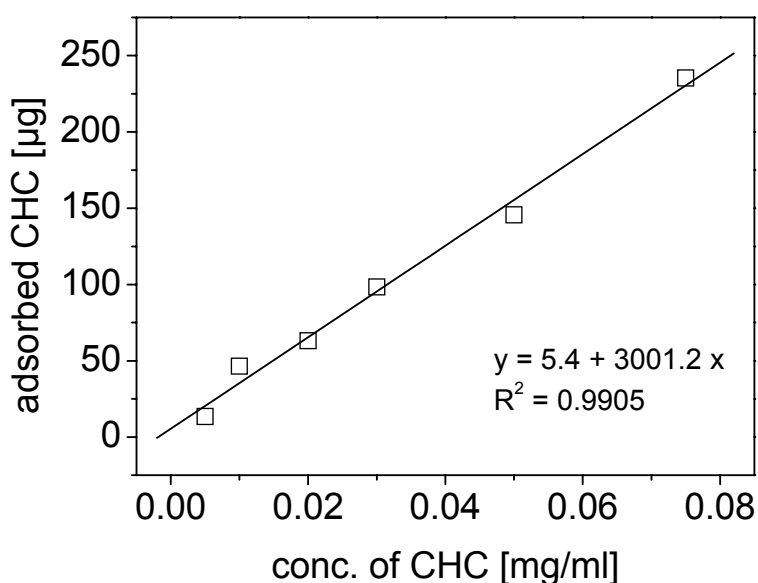


Figure 4-26 Linear fit of adsorbed collagenase on 20mg equine non cross-linked minirods after 1h incubation at 37°C

The approximate molar ratio of collagenase to collagen was calculated and a linear relationship ($R^2=0.9831$) with no upper limit could be detected (see Table 4-3). Seifter et al. noticed 150-200 cuts per α -chains, depending on the kind of used collagen (Seifter et al.; 1971) and French et al. identified at least 4 cuts per α -chain (French et al.; 1992). The calculated ratios indicated that more enzymes than available binding sites could be bound. Consequently, adsorption was not described sufficiently by a linear correlation and more complex isotherms had to be considered.

As was already discussed in section 1.3.1.1, several proposals based on either the Langmuir or Freundlich isotherm for adsorption of collagenase on collagen

surfaces were made in literature. Combining the two observations, maximum in binding after 0.5h to 1h (see Figure 4-24) and no upper adsorption limit (see Table 4-3), led to the conclusion that a Freundlich isotherm described adsorption best.

Table 4-3 Concentration dependent molar ratio of adsorbed collagenase on collagen equine non cross-linked minirods

Concentration of collagenase [mg/ml]	Molar ratio (collagenase : collagen)
0.0001	210 : 1
0.005	489 : 1
0.01	1720 : 1
0.02	2331 : 1
0.03	3640 : 1
0.05	5385 : 1

Sorption isotherms were determined after 1h incubation with 0.005 – 0.03mg/ml collagenase. At this time point, the equilibrium in enzyme-substrate complexes was established and no distinct degradation was observed. Experimental data were fitted with the Freundlich equation (see Figure 4-27).

The influence of the surface area on the extent of sorption could be seen by comparison of equine non cross-linked minirods with powder. Collagen powder has a larger relative surface area than minirods. Hence, more enzyme molecules could be bound (see Figure 4-27b).

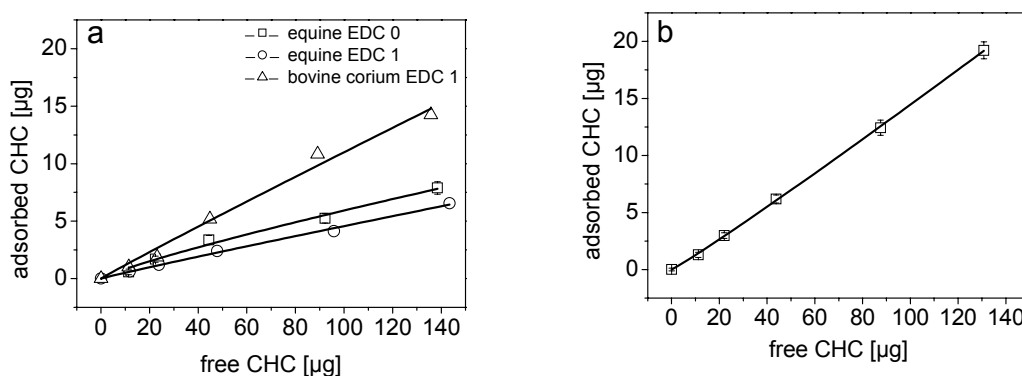


Figure 4-27 Sorption isotherms on 20mg collagen minirods (a) and on 20mg equine non cross-linked collagen powder (b) at 37°C (average \pm SD; $n=3$)

For low enzyme concentrations, sorption isotherms were nearly identical for all investigated minirods, irrespectively of cross-linking degree or collagen source (see Figure 4-27a). If the enzymatic concentration was increased, a slightly higher sorption of collagenase on equine non cross-linked minirods was observed compared to equine EDC 1 cross-linked extrudates. This was consistent with the assumption that additional cross-links restrict enzymatic binding (Zeeman et al.; 1999). However, bovine corium EDC 1 cross-linked minirods adsorbed higher amounts of collagenase than the other two kinds of minirods. A slightly higher surface area than in equine EDC 1 cross-linked matrices was accessible for enzymes, because bovine corium EDC 1 cross-linked minirods exhibited a similar swelling as equine non cross-linked minirods (see 4.1.2.1.1). Additionally, the lowest Michaelis-Menten constant of minirods was detected for bovine corium EDC 1 cross-linked minirods (see Table 4-5), indicating that a strong interaction between substrate and enzyme took place.

For all samples, n -values greater than 2/3 were observed (see Table 4-4). This indicated that the enzyme can penetrate into the collagen matrix (McLaren; 1963).

Table 4-4 Parameters of the Freundlich fits of Figure 4-27 (average \pm SD; $n=3$)

Sample	$y=k_1 x^n$	R^2
equine non cross-linked minirod	$k_1 = 0.12 \pm 0.04$ $n = 0.85 \pm 0.07$	0.989
equine EDC 1 cross-linked minirod	$k_1 = 0.06 \pm 0.01$ $n = 0.95 \pm 0.01$	0.997
bovine corium EDC 1 cross-linked minirod	$k_1 = 0.13 \pm 0.05$ $n = 0.97 \pm 0.09$	0.988
equine non cross-linked powder	$k_1 = 0.11 \pm 0.01$ $n = 1.05 \pm 0.01$	1

According to the literature (Gyani; 1945), different extreme Freundlich sorption exponents are defined (see 1.3.1.2).

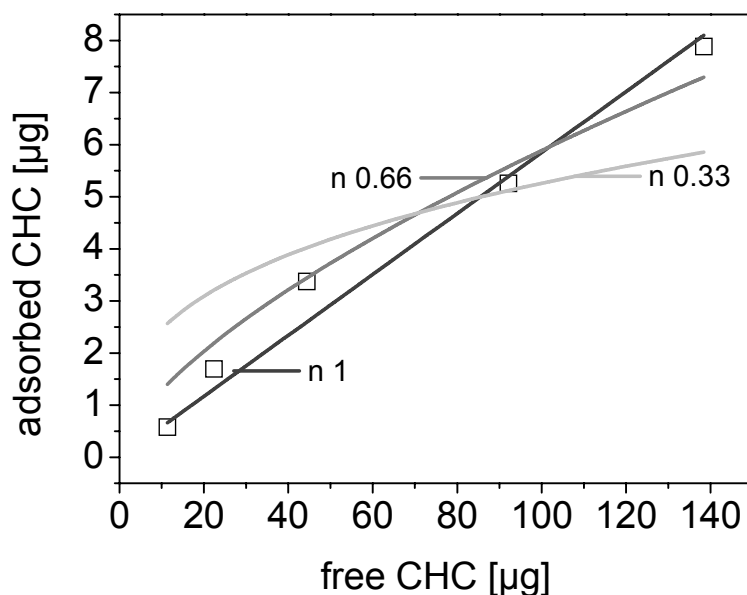


Figure 4-28 Theoretical evaluation of the Freundlich sorption exponent n of the collagenase sorption on equine non cross-linked minirods (dots represent experimental data)

For the development of the mathematical model (see 4.5), the complete range of possible n -values was fitted to the experimental data (see Figure 4-28). It was observed that the adsorption was described best, if n was in the range of $2/3 < n < 1$. For lower n -values, simulated results were not consistent with experimental observations. Since n was fitted in the mathematical model, solely n -values in the range of $2/3 < n < 1$ were tested in the mathematical model (see 4.5).

4.2.4 Determination of Degradation Constants

After adsorption and binding of collagenase on collagen surfaces, enzyme-substrate complexes can be formed and degradation starts. To investigate whether it is sufficient to describe the degradation of insoluble collagen by using the original Michaelis-Menten kinetic without consideration of adsorption phenomena, the degradation constants of collagen powder and minirods were determined.

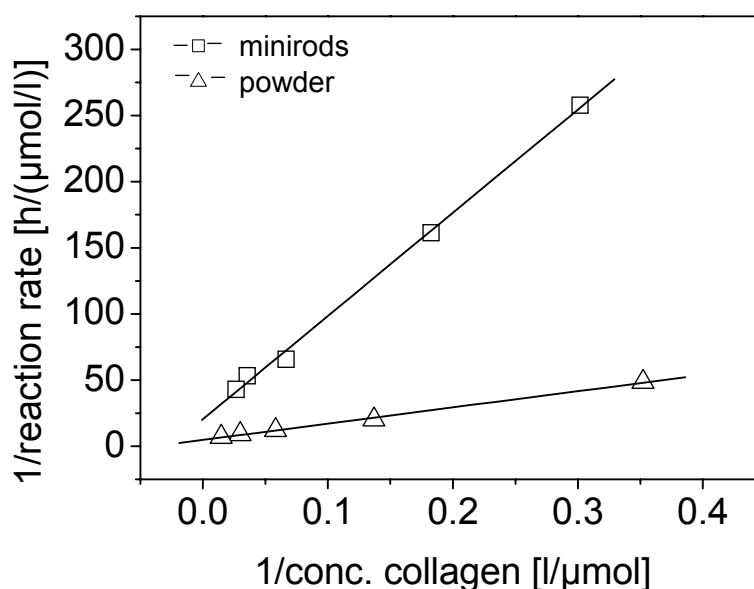


Figure 4-29 Lineweaver-Burk plots of 2 μg/ml collagenase acting on equine non cross-linked collagen matrices ($n=2$)

Although a heterogeneous enzymatic reaction took place, kinetics similar to the usual homogeneous Michaelis-Menten kinetic could be observed (Okada et al.; 1992a). Hence, typical Lineweaver-Burk diagrams were used to assess degradation constants (see Figure 4-29). The stability of the enzyme-substrate complex can be characterized by K_M and is dependent on the enzyme-substrate combination (Stryer; 1996).

For insoluble non cross-linked equine collagen, K_M values were in the range of $2.5 - 3.8 \cdot 10^{-5}$ mol/l, whereas K_M values of cross-linked collagens were lower (see Table 4-5). This indicated that the binding on cross-linked collagen was stronger and more specific. For comparison of different enzyme-substrate combinations, the turnover number k_{cat} is more suitable. This constant provides information about the reaction velocity of the enzymatic reaction. The degradation rate of equine non cross-linked collagen powder ($k_{cat}=750h^{-1}$) was in the range of values of soluble rat collagen type I gels ($k_{cat}=900-2100h^{-1}$ (Mallya et al.; 1992) and $k_{cat}=1000h^{-1}$ (Lin et al.; 1999)), whereas degradation rates of non cross-linked minirods and EDC 1 cross-linked matrices were lower (see Table 4-5).

Table 4-5 Collagenolytic degradation constants of collagen powder and minirods (n=2)

Sample	Powder		Minirods	
	K_M [mol/l]	k_{cat} [h^{-1}]	K_M [mol/l]	k_{cat} [h^{-1}]
equine non cross-linked	$2.55 \cdot 10^{-5}$	750	$3.8 \cdot 10^{-5}$	174
equine EDC 1 cross-linked	$1.33 \cdot 10^{-5}$	51.1	$1.97 \cdot 10^{-5}$	33.4

Due to a less compact matrix structure, collagen powders have a higher relative surface area and more reaction sites are accessible for collagenase (see Figure 4-24c). Hence, collagen powders were degraded faster than the minirods of the same material. This assumption could be manifested by several publications:

Bicsak et al. investigated the degradation of soluble and fibrillar guinea pig skin collagen type I by tadpole back-skin collagenase (Bicsak et al.; 1984) and Birkedal-Hansen et al. determined the catalytic properties of human fibroblast-type collagenase acting on bovine collagen type I (Birkedal-Hansen et al.; 1993). Both detected lower k_{cat} values for fibrillar than for soluble substrates (e.g. 1653h^{-1} for the degradation of soluble bovine collagen type I by human fibroblast-type collagenase and 11.4h^{-1} for the degradation of bovine collagen type I fibrils; (Birkedal-Hansen et al.; 1993)). McLaren observed a higher k_{cat} for trypsin degradation of a gelatin solution than for a gelatin gel (McLaren et al.; 1970). This phenomenon was attributed to the tertiary structure of the fibrils and the gel, respectively, which hampers the binding of the enzymes (McLaren et al.; 1970) and the access of water molecules to the hydrolysis site (Hasty et al.; 1987). Since number in cross-links increased from equine non cross-linked collagen to EDC 1 cross-linked materials (see 4.1.1.2), a similar conclusion to McLaren's proposal could be drawn from the presented experimental data.

Summarizing these results, one can conclude that the enzymatic degradation of insoluble collagen is not described sufficiently by using only the Michaelis-Menten equation. The enzymatic reaction rate of insoluble substrates is not exclusively dependent on the substrate concentration, but also on the matrix surface. Consequently, the adsorption process of the enzyme (see 4.2.2.4 and 4.2.3) and the reaction rate of the cleavage itself must be considered to characterize the enzymatic reaction properly and both processes had to be incorporated into the mathematical model (see 4.5).

4.2.5 Summary

In the first part of this section, the binding of bacterial collagenase (CHC) and human gelatinase A and B on different collagen matrices was investigated. Wound dressings which contain collagen exhibited a more pronounced enzyme binding than dense bovine corium non cross-linked minirods. Due to a higher accessible binding surface approximately 60% CHC, approximately 30% MMP-2 and approximately 45% MMP-9, respectively, were bound on the two collagen

sponges after 2h, whereas significant binding was only detected for MMP-9 on dense collagen extrudates ($p < 0.001$).

In the second part, interaction of CHC with dense collagen matrices was investigated in more detail. Adsorption was completed between 0.5h and 1h, irrespectively of collagen preparation and matrix shape, and the extent of sorption maintained constant for at least 24h. With longer incubation times, the fraction of specifically bound CHC increased. It was demonstrated that the extent of adsorption is influenced by the relative surface area and additional cross-linking. In this equilibrium state, sorption isotherms were measured and experimental data were fitted with the Freundlich isotherm. Since n -values greater than $2/3$ were detected, it was assumed that collagenase can penetrate into the collagen matrix. According to literature (Bailey; 1986), simple Michaelis-Menten kinetic can only be applied to soluble substrates. Hence, degradation of insoluble collagen substrates by CHC was studied by dividing the enzymatic reaction in two stages: a prerequisite adsorption step, followed by the true degradation. To verify whether enzyme adsorption is a necessary step for degradation, degradation constants for insoluble collagen powders and minirods were determined. Equine non cross-linked powder had a degradation rate in the range of soluble collagens (k_{cat} (equine non cross-linked powder) = 750h^{-1} versus $900\text{h}^{-1} < k_{cat}$ (soluble rate collagen type I) $< 2100\text{h}^{-1}$). An increase in cross-linking degree and a decrease in surface area (investigation of minirods) resulted in lower reaction rates ($33\text{h}^{-1} < k_{cat} < 175\text{h}^{-1}$). From the presented data it was concluded that the enzymatic reaction was dependent on adsorption and that this process had to be included into a precise description of the degradation mechanism. The obtained results from adsorption and degradation studies were incorporated in the mathematical model by using a Freundlich sorption isotherm and by inserting the measured k_{cat} ($=k_2$ in chapter 4.5) values and the calculated adsorption rates ($k_1 = \frac{k_{cat}}{K_M}$; (Tzafiri et al.; 2002)).

4.3 In vitro Release of FITC Dextran

In the previous section, the collagen matrix was characterized in more detail. Especially the interaction between collagenase and collagen was investigated, because parenterally implanted collagen drug devices undergo enzymatic degradation. The next step towards a mathematical model for drug release from dense collagen matrices was to investigate the release of model drug compounds from collagen extrudates. Two different experimental protocols were followed. On the one hand, a special experimental setup for the development of a model exclusively describing drug release controlled by erosion was needed. For this purpose, release was monitored for 6d in absence of collagenase. On day 6, 0.1µg/ml collagenase was added and release and degradation were determined in parallel. This setup was applied to eliminate the contribution of drug release by diffusion and swelling and to guarantee a fully swollen matrix. Consequently, the parameters which are necessary to develop the part of the mathematical model describing the drug release due to matrix degradation could be obtained. On the other hand, an experimental setup was chosen to simulate in vivo circumstances: 0.1µg/ml bacterial collagenase was already added to the minirods after a 0.25h pre-swelling phase in pure Tris buffer pH 7.5 at 37°C. Here, the release profile was more complex than in the first setup, because swelling, diffusion and erosion dependent drug release occurred simultaneously. To cover these complex mechanisms, the diffusion equations from the model of swelling controlled release presented by Radu et al. (Radu et al.; 2002) and the model of erosion controlled drug release, developed in this thesis (see 4.5), were combined. Data from the second experimental setup was used to test the mathematical model.

Since collagen devices swell in contact with aqueous liquids, water penetrates into the matrix and water soluble drugs dissolve (Sano et al.; 2003). Maeda et al. postulated that after drug dissolution the drug solution retains inside the hydrated collagen matrix (Maeda et al.; 1999), before release through water filled pores can occur (Gilbert et al.; 1988a). Weadock postulated that the gaps between staggered collagen tropocollagens (see Figure 1-1) build the pores which are prerequisite for diffusional drug release of water soluble compounds

(Weadock; 1986). Since collagen extrudates became highly hydrated after contact with water (approximately 70% water), a main part of drug delivery is covered by diffusion controlled release (Radu et al.; 2002). Hence, the diffusion coefficients in water of three model compounds were determined, before influences of experimental setup, collagen raw material, matrix dimensions and drug properties on drug release were investigated.

4.3.1 Diffusion Coefficient of FITC Dextrans

Movement of water soluble drugs inside and out of collagen matrices can be described by diffusion. After dissolution, these drugs can either diffuse directly out of the swollen matrix or their diffusion is hindered because either the collagen mesh is too tight or the molecular weight of the drug is too high (Rosenblatt et al.; 1989). In the second case the matrix has to be degraded, before drug diffusion can occur. To cover these processes, diffusion phenomena were implemented in the mathematical model (see 4.5). Since direct measurement of diffusion coefficients in dense non-transparent matrices is very challenging (see 4.1.2.2), the diffusion coefficients of FITC dextran 20, 70 and 150 were determined in water by fluorescence correlation spectroscopy (FCS). The diffusion coefficient of FITC dextran 70 at 23°C was determined with $1.7 \cdot 10^{-3} \text{cm}^2/\text{h}$. Similar results were obtained by Singh and Shenoy (Shenoy et al.; 1995; Singh; 1994). For FITC dextran 20 $2.1 \cdot 10^{-3} \text{cm}^2/\text{h}$ and for FITC dextran 150 $1.27 \cdot 10^{-3} \text{cm}^2/\text{h}$ were obtained. The diffusion coefficient is particularly dependent on the temperature and the molecular size of the investigated drug. By applying the Stokes-Einstein equation the diffusion coefficients can be converted to 37°C, the temperature at which release and degradation studies were performed (FITC dextran 70: $2.4 \cdot 10^{-3} \text{cm}^2/\text{h}$; FITC dextran 20: $3 \cdot 10^{-3} \text{cm}^2/\text{h}$ and FITC dextran 150: $1.8 \cdot 10^{-3} \text{cm}^2/\text{h}$). Besides movement of drugs, collagenase also has to diffuse towards the collagen surface, before binding and degradation can take place. Because fluorescent labeling of collagenase may alter its properties, FITC dextran 70 was used to simulate collagenase in these experiments. To verify whether the diffusion coefficient of FITC dextran 70 could be used for modeling collagenase, results were compared with literature. Seifert et al. measured a diffusion coefficient of collagenase A (MW:

105kDa) of $1.55 \cdot 10^{-3} \text{cm}^2/\text{h}$ at 20°C in water (Seifter et al.; 1959). By conversion with the Stokes-Einstein equation a diffusion coefficient of $2.2 \cdot 10^{-3} \text{cm}^2/\text{h}$ at 37°C was obtained. Gaspers et al. determined, by two different methods, a diffusion coefficient of collagenase of $2.4 \cdot 10^{-3} \text{cm}^2/\text{h}$ in bulk solution and different buffers (Gaspers et al.; 1994). The diffusion coefficients of collagenase, given in literature, were in good agreement with the measured FITC dextran 70 diffusion coefficient. Consequently, this diffusion coefficient could be used for both, collagenase and FITC dextran 70, in the mathematical model (see 4.5). Furthermore, the diffusion coefficient of the degradation products was necessary. According to French et al. (French et al.; 1992), degradation of the collagen triple helix resulted in fragments of a maximal molecular weight of approximately 70kDa. Therefore, the diffusion coefficient of FITC dextran 70 was used as the upper limit for the diffusion coefficient of the products (see 4.5).

4.3.2 Influence of Experimental Setup

4.3.2.1 Variation in Concentration of Collagenase

Initial experiments were conducted with collagen minirods of a length of 40mm. FITC dextran 70 release was observed in the presence of $6.7 \mu\text{g}/\text{ml}$, $0.1 \mu\text{g}/\text{ml}$ collagenase and without addition of enzyme (see Figure 4-30a). The matrix degradation was analyzed simultaneously in collagenase containing samples (see Figure 4-30b). In absence of collagenase drug release was incomplete. Only approximately 55% FITC dextran 70 was released by swelling and diffusion during the observation period. Adding $0.1 \mu\text{g}/\text{ml}$ enzyme resulted in complete matrix disintegration after 21d (see Figure 4-30b) which led to further drug release by erosion. 50% of the drug fraction which was initially immobilized inside the minirods could be delivered, but still not the complete drug load could be released. In the presence of $6.7 \mu\text{g}/\text{ml}$ collagenase FITC dextran 70 was delivered completely after 72h and the collagen matrix was entirely eroded at this time point. Matrix erosion started after a short lag phase of approximately 0.5h which is necessary to reach equilibrium in adsorption of collagenase on the matrix surfaces (see 4.2.2.4). The more enzymes were added, the more enzyme molecules could bind and cleave the collagen helices (see Table 4-3)

and a faster digestion was the consequence (see Figure 4-30b). A similar observation was made by Park et al., who investigated the in vitro degradation of collagen - hyaluronic acid scaffolds (Park et al.; 2002). Increasing the concentration of collagenase resulted in a decrease of the remaining scaffold weight after 24h. In conclusion, the release rate and the immobilized drug fraction could be controlled by addition of collagenase.

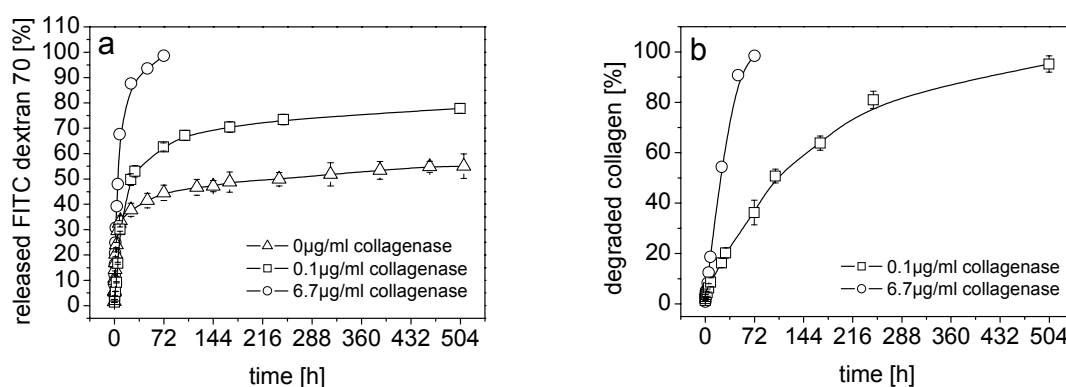


Figure 4-30 Effect of the concentration of collagenase on FITC dextran 70 release (a) and collagen degradation (b) of 40mm equine non cross-linked minirods (0 / 0.1 / 6.7 $\mu\text{g/ml}$ enzyme was added after 0.25h; average \pm SD; n=3)

Maeda et al. investigated the release of HSA from collagen minipellets, prepared from a 30% (w/w) atelocollagen dispersion. Almost complete release occurred within 2d from his standard formulation with 20% HSA in absence of collagenase (Maeda et al.; 1999). Investigating the release mechanism in more detail showed that a 3h swelling controlled release phase was followed by 36h of diffusion control which was dependent on the simultaneous matrix swelling and drug dissolution (Maeda et al.; 1999). No drug was immobilized inside the minipellets, suggesting that these drug devices were less compact after contact with aqueous solutions than our minirods, because non cross-linked atelocollagen was used for manufacturing (Fujioka et al.; 1995). These observations led to the conclusion that the release from our minirods must be diffusion, swelling and erosion controlled.

To determine whether the entrapped drug fraction could be released erosion controlled, collagenase was added after 6d, because at this time point drug release by swelling and diffusion control was finished (see Figure 4-30a). A second release stage was observed (see Figure 4-31a) and the remaining drug fraction was released. The hindering inter- and intramolecular bonds of the collagen mesh were enzymatically cleaved and the formerly immobilized FITC dextran 70 could diffuse out of the drug device.

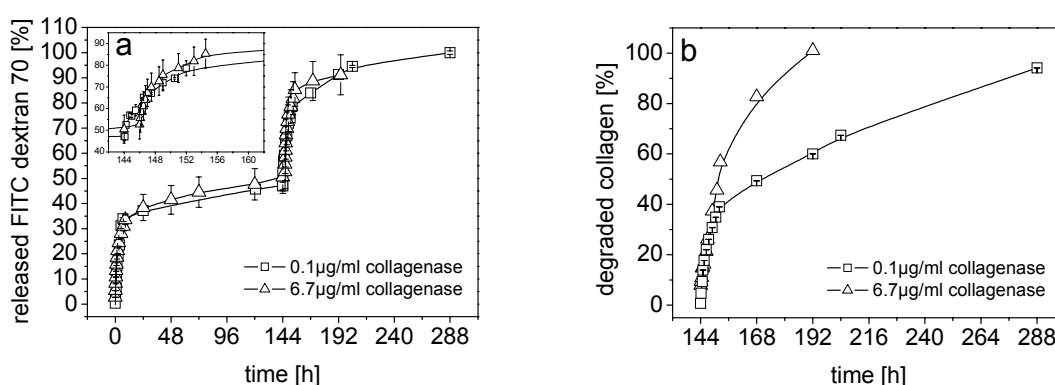


Figure 4-31 Effect of the concentration of collagenase on FITC dextran 70 release (a) and collagen degradation (b) of 40mm equine non cross-linked minirods (0.1 / 6.7 µg/ml enzyme was added after 6d; average \pm SD; n=3)

The initial release rates of the second release phase were similar for both enzyme concentrations (see Figure 4-31a), but matrix degradation was faster in the presence of 6.7 µg/ml collagenase (see Figure 4-31b). Hence, drug release was completed earlier, when more enzymes were present, because the hindering collagenous mesh was untightened earlier (completion after 8d for 6.7 µg/ml collagenase, compared to 12d in the presence of 0.1 µg/ml collagenase).

In this section, experiments were performed with 40mm minirods, because for investigations with 6.7 µg/ml collagenase a high substrate concentration is required to monitor the collagen degradation properly. This enzyme concentration was chosen rather high and did not represent in vivo circumstances. In further in vitro experiments only the 0.1 µg/ml concentration

was used. Furthermore, implants of a length of 40mm are not suitable for parenteral applications in humans. Consequently, unless otherwise noted, the following investigations were conducted with 10mm extrudates.

4.3.2.2 Variation in Time of Collagenase Addition

By comparing two different enzyme addition time points (0.25h versus 6d) almost congruent release profiles were observed (see Figure 4-32a). In contrast to 40mm extrudates (see Figure 4-30), 100% drug recovery was achieved for 10mm minirods. Differences in release curves occurred between day 2 and 6 due to depletion of mobile drug inside the matrix in absence of collagenase. If collagenase was present during the complete observation period, no such stagnancy in release rates could be detected.

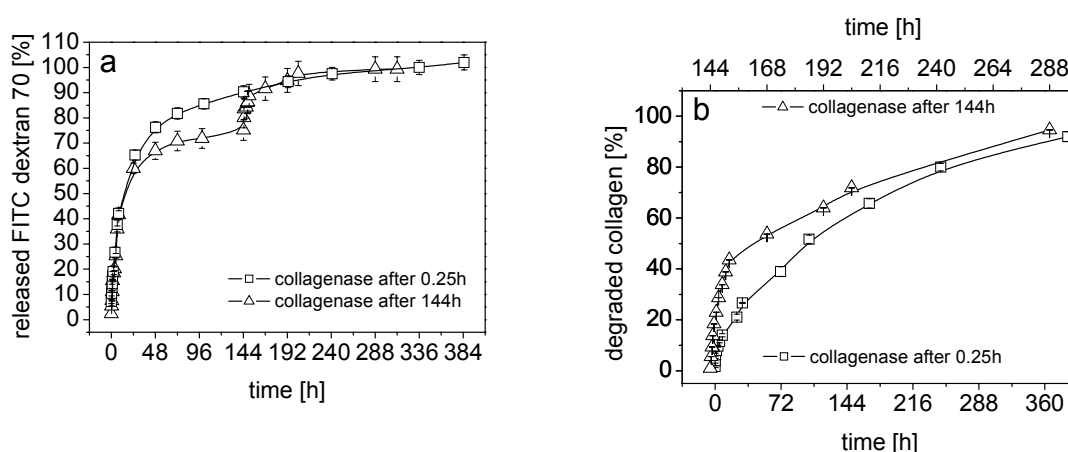


Figure 4-32 Effect of the time point of collagenase addition on FITC dextran 70 release (a) and collagen degradation (b) of 10mm equine non cross-linked minirods (0.1 μ g/ml enzyme was added after 0.25h or 6d; x-axes in the right graph: enzyme addition after 6d (top) and enzyme addition after 0.25h (bottom); average \pm SD; n=3)

A surface erosion process for the degradation of lyophilized collagen devices was proposed from Olde Damink et al., because a zero-order weight loss was determined in the presence of collagenase (Olde Damink et al.; 1996a). This assumption was based on observations by Steven, who postulated that collagen is digested by degradation of individual tropocollagen filaments (Steven; 1976). Similar conclusions were made by Okada et al., who assumed

that collagen suture fibers were eroded from the surface to the core (Okada et al.; 1992a). They attributed their proposal to the low water content of the fiber and the large size of collagenase which limits enzyme penetration into the dense fiber.

Looking closer at the erosion of equine non cross-linked minirods (see Figure 4-32b), a two-step degradation could be observed. This was also described for the degradation of insoluble collagens by cathepsins and pepsin (Etherington; 1977). In the beginning swelling takes place and rapid digestion, mainly of collagen filaments at the surface, occurs. Due to this combined effect of swelling and degradation, an almost linear degradation could be observed (Frieß et al.; 1996b). This stage was more pronounced for completely swollen equine non cross-linked minirods (see Figure 4-32b), because enzyme molecules can penetrate more easily into the collagen matrix (Lenz; 1993) and degradational turnover increased. In contrast, if collagenase was added after 0.25h, penetration was more restricted, because of coinciding matrix swelling. The next degradation stage is dominated by a slower occupation of the remaining free reaction sites due to sorption phenomena and slower enzyme penetration into the matrix. This phase is regulated by steric factors, by the rate of product release and the decreased number of enzyme cleavage sites. For some materials Etherington even observed a third phase with no further digestion due to collagen resistance (Etherington; 1977). The observed degradation profiles, neither zero- nor first-order kinetic over the complete degradation range, led to the conclusion that equine non cross-linked minirods were not degraded by a simple surface erosion process. Since profiles resembled the digestion curves presented by Etherington (Etherington; 1977), a combination of surface and bulk erosion of collagen minirods was assumed.

Summarizing the influences of addition of different collagenase concentrations at two different time points showed that a higher concentration of collagenase led to faster release and degradation profiles and that the addition to fully swollen matrices even enhanced this effect due to easier enzyme penetration and binding.

4.3.3 Influence of Collagen Raw Material

After evaluation of the test conditions, influences of matrix material, matrix dimensions and drug properties on release were examined. The purpose was to achieve a matrix system which controlled drug delivery mainly by erosional mechanisms and which consequently showed reduced drug release by instantaneous diffusion.

4.3.3.1 Variation in Pretreatment of Collagen Material

As was already detected by swelling studies, minirods prepared from pulverized equine collagen material showed a more pronounced swelling than extrudates prepared from lyophilized raw material (Figure 4-6). Minirods prepared from pulverized equine collagen material exhibited an apparent density which was on half of the density of minirods of lyophilized collagen material (0.598g/cm^3 compared to 1.098g/cm^3 ; see Table 4-1). Due to this less compact matrix structure, more aqueous channels can be built and drug release is enhanced (Maeda et al.; 1999).

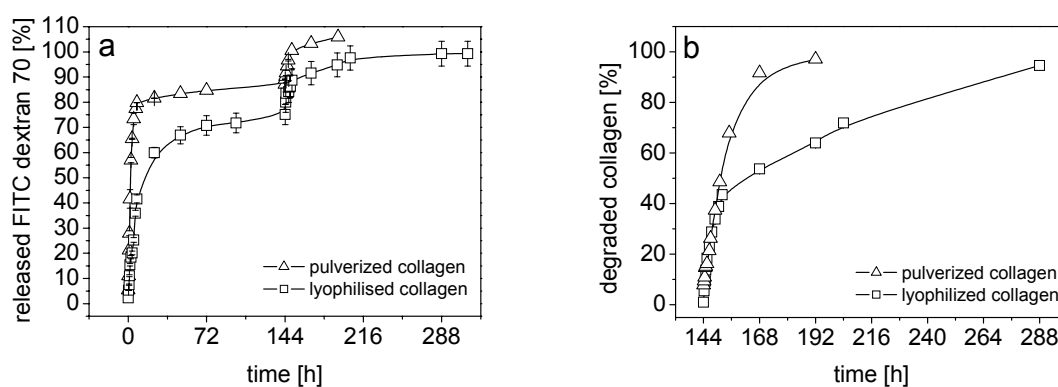


Figure 4-33 Effect of the collagen material pretreatment on FITC dextran 70 release(a) and collagen degradation (b) of 10mm equine non cross-linked minirods ($0.1\mu\text{g/ml}$ enzyme was added after 6d; average \pm SD; $n=3$)

The release was determined with the “two interval” setup, to study the change in drug release controlled by diffusion. Release by diffusion became enhanced and a higher initial burst release occurred if minirods were prepared from

pulverized equine collagen. A similar observation was made by Maeda et al. for the release from three different collagen preparations (Maeda et al.; 1999). A porous collagen sponge, a collagen film and the collagen minipellet were investigated and it was demonstrated that lower swelling properties reduce the initial release rates. After 24h approximately 80% FITC dextran 70 was released compared to 60% from minirods produced of lyophilized collagen (see Figure 4-33a). The lack in matrix cohesion became also apparent in the fast degradation after addition of 0.1µg/ml collagenase. The devices were degraded completely within 2d, whereas minirods prepared from lyophilized raw collagen were resistant for approximately one week (see Figure 4-33b).

4.3.3.2 Variation in Animal Source

To verify whether the matrix material itself or only the preparation technique influences the drug release, different collagen materials were used to produce minirods. With non cross-linked material, drug loaded minirods of equine and bovine tendon collagen were manufactured. Extrudates of bovine corium non cross-linked collagen were not suited as delivery devices, due to a fast disintegration at 37°C (see Figure 4-7). Release of FITC dextran 70 was slower from equine minirods than from bovine tendon matrices (see Figure 4-34a): 65% dextran was released during the first 24h from equine minirods, whereas 85% was delivered from the bovine tendon extrudates.

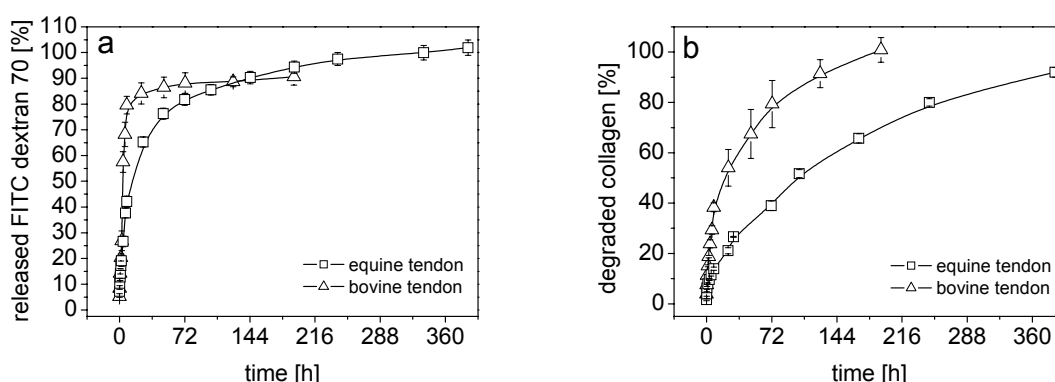


Figure 4-34 Effect of the animal source on FITC dextran 70 release (a) and collagen degradation (b) of 10mm non cross-linked minirods (0.1µg/ml enzyme was added after 0.25h; average ± SD; n=3)

Since natural cross-linking of bovine materials was less pronounced than in equine collagen types (see 4.1.1.2) (Schlapp; 2001), diffusion of FITC dextran 70 was less hindered and a higher amount of drug was free to diffuse. Due to the lower cross-linking degree in the bovine tendon collagen material, fewer linkages had to be cleaved before a degraded collagen fragment could be solubilized (Olde Damink et al.; 1996a) and degradation became faster (see Figure 4-34b) (Schlapp; 2001).

In conclusion, the equine collagen material appeared to be more appropriate to produce collagen minirods with controllable properties, because matrix erosion and (diffusion controlled) FITC dextran 70 release were less pronounced than of bovine materials.

4.3.3.3 Variation in Cross-linking

Release could further be reduced by collagen cross-linking with EDC (see Figure 4-35a). New intra- and interhelical bonds are built (Zeeman et al.; 1999), which led to reduced swellability (see Figure 4-8), increased matrix stability (Zeeman et al.; 1999) and denser matrices (see Table 4-1) (Frieß et al.; 1996b). For 3d, similar release profiles were observed for equine non cross-linked and both bovine EDC 1 cross-linked minirods. During the first 24h, 45% FITC dextran 70 was released from equine EDC 1 cross-linked implants, whereas 60% was delivered from the other three kinds of minirods (see Figure 4-35a). Release was completed after 19d for bovine corium minirods and after one month for both tendon materials. Due to the additional cross linkages, equine and bovine tendon EDC 1 cross-linked minirods became more resistant against collagenolytic attack than bovine corium EDC 1 cross-linked extrudates and equine non cross-linked devices (see Figure 4-35b). Bovine corium EDC 1 cross-linked minirods were degraded completely after 19d, whereas bovine tendon EDC 1 cross-linked extrudates were digested after 51d and equine EDC 1 cross-linked matrices after 59d. The penetration of collagenase was more restricted (Olde Damink et al.; 1996a) and the available binding surface was reduced, because binding and cleavage sites were partially blocked by cross-links (Gilbert et al.; 1990). Besides this, degradation was analyzed by

quantification of collagen fragments in the supernatant. Thus, retarded degradation was also measured, because cleavage products could only diffuse out of the matrix inside at a reduced rate due to the hindering cross-links (Charulatha et al.; 2003) and more scissions are needed to release a collagen fragment (Gilbert; 1988b). A more distinct two step degradation profile could be observed for all EDC 1 cross-linked minirods than for the equine non cross-linked matrices. Especially the second degradation phase, which was slowest for equine EDC 1 cross-linked matrices, indicated that digestion was reduced due to a more hindered diffusion of collagenase and collagen fragments. Similar conclusions were drawn by Schurr et al. for the degradation of a non cross-linked and disulfide cross-linked gelatin gel (Schurr et al.; 1966). A homogeneous digestion was observed for the non cross-linked gel, whereas the dimensions of the cross-linked matrix decreased steadily. This was attributed to the restricted enzyme penetration resulting in surface degradation.

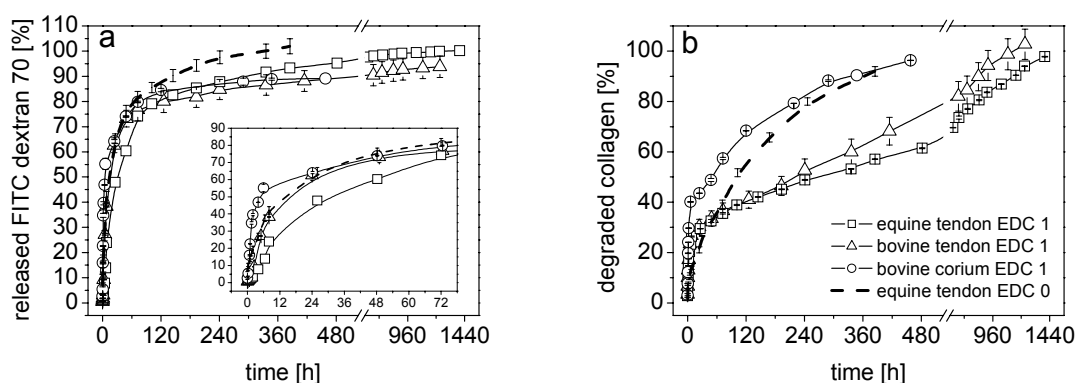


Figure 4-35 Effect of the animal source on FITC dextran 70 release (a) and collagen degradation (b) of 10mm EDC 1 cross-linked minirods (0.1 μ g/ml enzyme was added after 0.25h; similar legend for release and degradation; average \pm SD; n=3)

To characterize the release properties of our minirods in more detail, comparison with release data from minipellets was made. Release of BSA from minipellets, prepared from a 2% (w/w) atelocollagen dispersion, was studied by Maeda et al. at 5°C in absence of collagenase (Maeda et al.; 2003). Within the first day, the same drug portion (approximately 60-70%) was released as from

our equine non cross-linked, bovine corium and bovine tendon EDC 1 cross-linked minirods (approximately 60% for each kind of minirod; see Figure 4-35a), incubated at 37°C in the presence of 0.1 µg/ml collagenase. The remaining drug was delivered over 3d from minipellets (Maeda et al.; 2003), whereas the release was slower for our minirods. Consequently, minirods showed superior release kinetics, because even at higher temperatures and in an enzymatic environment the release could be more prolonged. The same group prepared minipellets from 30% (w/w) atelocollagen dispersions and investigated the release of different HSA loads at 37°C in absence of collagenase for 2 and 3 days, respectively (Maeda et al.; 1999). During the first 24h approximately 35% HSA was released from minipellets loaded with 5% HSA. This initial release was only slightly lower compared to our equine EDC 1 cross-linked minirods which released approximately 45% during this time period (see Figure 4-35a). The retardation in drug release could be explained by two effects. On the one hand, the higher viscosity of concentrated formulations delays drug release by diffusion compared to devices prepared from 2% (w/w) collagen dispersions. On the other hand, Fujioka et al. postulated that drugs can only be taken up into collagen fibers if low concentrated collagen dispersion are used (Fujioka et al.; 1998). Therefore, a pre-lyophilization step of a low concentrated collagen-drug mixture was performed, before minipellets containing 30% collagen were prepared. Consequently, both effects of retardation in delivery could be combined in the 30% minirods (Fujioka et al.; 1998). The slightly faster release during the first 24h from our equine EDC 1 cross-linked minirods can be explained by the fact that the delay in release was achieved only by the denser collagen mesh due to the high concentrated collagen mixture with additional inter- and intrahelical cross-linkages and not by drug incorporation into collagen fibers, because a pre-lyophilization step was not performed.

4.3.3.3.1 Variation in EDC Cross-linking Ratio

Variation in EDC cross-linking ratio was performed for equine tendon and bovine corium collagen. As was already demonstrated by swelling studies, increasing the EDC ratio from 1 to 3 or 17 for equine minirods did not lead to

further stabilizing effects (see 4.1.2.1.1). Such saturation effects in cross-linking were also observed by Frieß et al. (Frieß et al.; 1996b) and Geiger (Geiger; 2001). Degradation studies and investigation of FITC dextran 70 release confirmed these results, because higher rates occurred with cross-linking ratios of 3 and 17 (see Figure 4-36). Drug release by diffusion occurred even slightly faster than from equine non cross-linked minirods. Since in highly cross-linked collagen materials (EDC 3 and 17) many new intra- and interhelical bonds are introduced, interfibrillar interlockings due to compression during extrusion could become difficult. This resulted in extrudates which exhibited lower cohesion, detectable by the slightly decreased apparent density (see Table 4-1; EDC 0: 1.109g/cm³, EDC 1: 1.011g/cm³, EDC 3: 0.948g/cm³, EDC 17: 0.999g/cm³), and consequently a faster swelling and degradation.

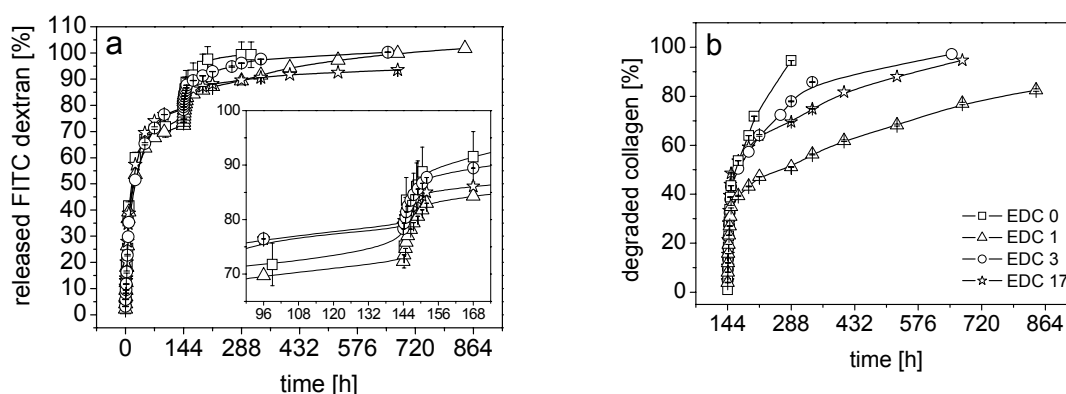


Figure 4-36 Effect of the EDC cross-linking ratio on FITC dextran 70 release (a) and collagen degradation (b) of 10mm equine minirods (0.1µg/ml enzyme was added after 6d; similar legend for release and degradation; average ± SD; n=3)

Drug release from EDC cross-linked bovine corium minirods was compared to release from equine non cross-linked matrices. Since natural cross-linking in the bovine corium material was less pronounced than in equine tendon collagen, additional cross-linkages had to be introduced into the bovine material to improve its mechanical properties (see 4.1.1.2). However, release and degradation rates of all investigated EDC cross-linking ratios were increased compared to equine non cross-linked minirods (see Figure 4-37). This was

attributed to the lower apparent matrix density (see Table 4-1) and the different pattern in cross-linkages. EDC cross-linking does only introduce new inter- and intramolecular bonds (Zeeman et al.; 1999), whereas the natural cross-links in equine extrudates are also located interfibrillarly. The fastest drug release from EDC cross-linked bovine corium minirods was observed for the EDC 0.25 ratio and was already completed after 4d (see Figure 4-37a). Since DSC measurements showed that completely swollen EDC 0.25 cross-linked bovine corium minirods started to undergo thermal changes at 40°C (see Figure 4-4), rapid disintegration and degradation at 37°C (see Figure 4-37b) was the logical consequence. This behavior was analogous to bovine corium non cross-linked matrices which even had a T_m below 40°C. As was already observed for equine EDC cross-linked minirods (see Figure 4-36), an increase in EDC cross-linking degree could decrease matrix stabilization. For bovine corium EDC cross-linked extrudates the highest investigated ratio of 3 resulted in a more pronounced initial FITC dextran 70 release than from EDC 1 cross-linked minirods, because degradation was elevated during the first 6h (see Figure 4-37).

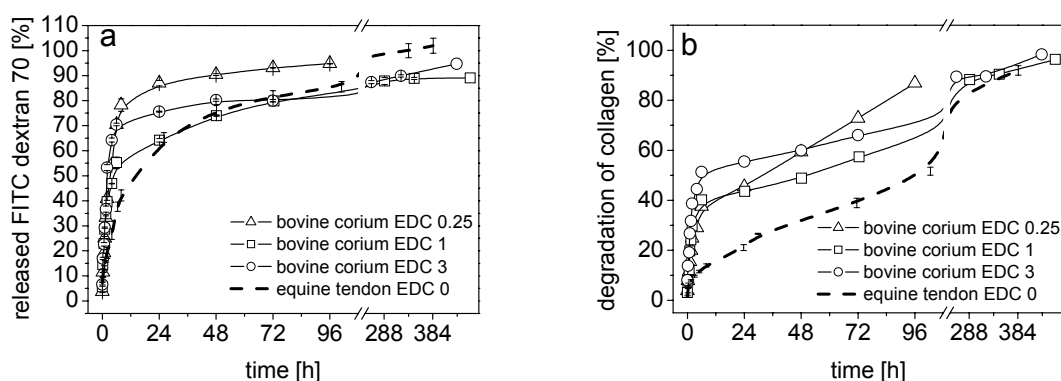


Figure 4-37 Effect of the EDC cross-linking ratio on FITC dextran 70 release (a) and collagen degradation (b) of 10mm bovine corium minirods (0.1µg/ml enzyme was added after 0.25h; average ± SD; n=3)

Consequently, the EDC 1 cross-linking degree was assumed to be the most appropriate cross-linking ratio for bovine corium minirods (and for equine matrices) to prepare dense drug delivery devices with reduced release and degradation properties.

4.3.3.3.2 Variation in Cross-linking Method

Besides chemically, equine minirods were also cross-linked physically by DHT treatment of the final minirods after extrusion of the collagen material. Since this method was solely applied in an early matrix development stage, only release data of 40mm extrudates in the presence of 6.7 μ g/ml collagenase were collected. Compared to non cross-linked equine minirods, release and degradation was delayed for the DHT cross-linked matrices (see Figure 4-38).

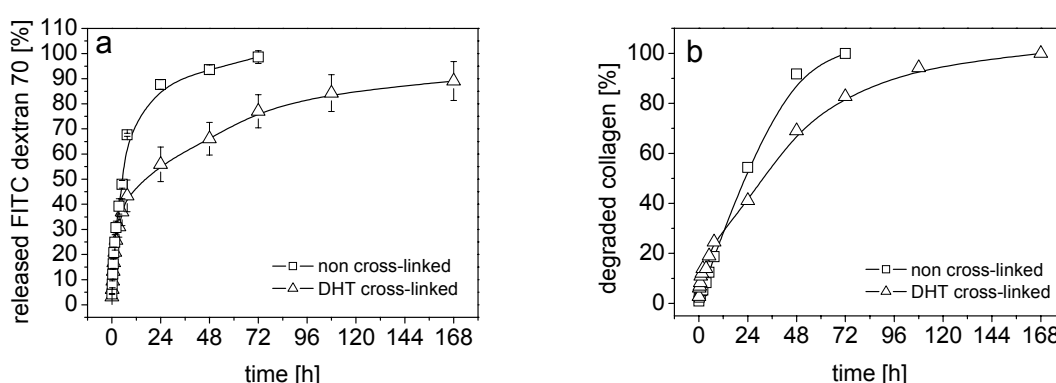


Figure 4-38 Effect of the cross-linking method on FITC dextran 70 release (a) and collagen degradation (b) of 40mm equine minirods (6.7 μ g/ml enzyme was added after 0.25h; average \pm SD; n=3)

The FITC dextran 70 load was released completely after one week, whereas release from non cross-linked extrudates already reached 100% within 3d. These time intervals were identical to the time necessary for complete digestion of the matrices. Degradation of DHT cross-linked minirods was not as markedly suppressed as for EDC treated materials and the digestion rates during the second degradation phase were higher than for EDC collagens, indicating that penetration of collagenase was less restricted. This was in agreement with Pieper et al., who determined a similar degradation behavior in the presence of collagenase for non cross-linked and DHT cross-linked porous collagen matrices, but an enhanced resistance of EDC cross-linked materials (Pieper et al.; 1999). As was already discussed in 4.1.2.1.1, DHT cross-linking was not

used for further preparation of minirods due to potential thermal damages of the incorporated drug.

In this section it was demonstrated that release and degradation behavior of collagen minirods could be controlled on the one hand by the used collagen raw material and on the other hand by the introduction of additional cross-linkages. Minirods prepared from lyophilized equine EDC 1 cross-linked collagen showed the lowest release and degradation profiles in the presence of collagenase.

4.3.4 Influence of Matrix Dimensions

Another approach to control the delivery properties of collagen minirods is to vary the matrix dimension or geometry. Since the surface area is a crucial factor for drug delivery by diffusion and enzyme binding, devices with a low ratio of surface area to volume should show reduced release and degradation rates. However, implant dimensions are often restricted by the application method and drug load (Sano et al.; 2003). Extruded minirods were chosen as most promising matrices. For cylinders either the length or the diameter could be changed. Different aspect ratios (length/diameter) were produced and tested with respect to FITC dextran 70 release and collagen degradation.

4.3.4.1 Variation in Length of Minirods

Longer minirods, which had a higher aspect ratio, exhibited a slower release of FITC dextran 70 (see Figure 4-39a). This was in agreement with Maeda et al., who also observed this trend for HSA delivery (Maeda et al.; 1999). Due to extrusion, collagen fibers were highly orientated in the drug device and consequently the lateral side surface was higher in density than the cross-section (see Figure 4-2, Figure 4-11, Figure 4-12). Maeda et al. postulated that the slower release from longer extrudates was also related to this phenomenon, because drug delivery is more difficult from the smoother lateral side surface of the minipellet than from the more porous cross-section (Maeda et al.; 1999). The release was determined with the “two interval” setup, to study the change in drug release controlled by diffusion. With elongating, the portion of the lateral side surface increased relatively (from 93.1% for 10mm minirods to 97.6% for 40mm matrices) and the release during the first 24h without addition of

collagenase was decreased from approximately 60% from 10mm minirods to 35% from 40mm matrices.

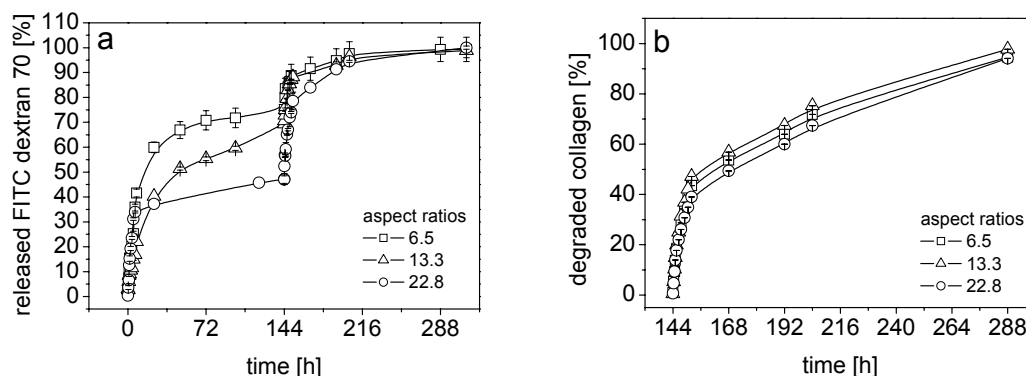


Figure 4-39 Effect of the minirods length on FITC dextran 70 release (a) and collagen degradation (b) of equine non cross-linked minirods (0.1 μ g/ml enzyme was added after 6d; 10mm (aspect ratio of 6.5); 20mm (aspect ratio of 12.3); 40mm (aspect ratio of 22.8); average \pm SD; n=3)

The entrapped drug portion after 6d was increased from 25% in 10mm extrudates to 50% in 40mm minirods. After addition of collagenase, similar release rates during the first 8h occurred for all three minirods, resulting from similar degradation profiles (see Figure 4-39). A two phase degradation profile was observed (Etherington; 1977), which was similar for all minirods because of the same cross-linking degree.

If collagenase was added already at the beginning of the experiments, the same effects were observed. Elongation resulted in a slower release profile (see Figure 4-40a) due to the anisotropic release behavior of the extrudates. Compared to the pure swelling and diffusion controlled drug delivery (see Figure 4-39a), release was faster for all minirods, because erosion dependent release occurred additionally. During the first 24h approximately 65%, 60% and 50% FITC dextran 70 was liberated from 10mm, 20mm and 30mm matrices, respectively (compared to 60%, 40% and 35% released by diffusion from 10mm, 20mm and 40mm matrices, respectively).

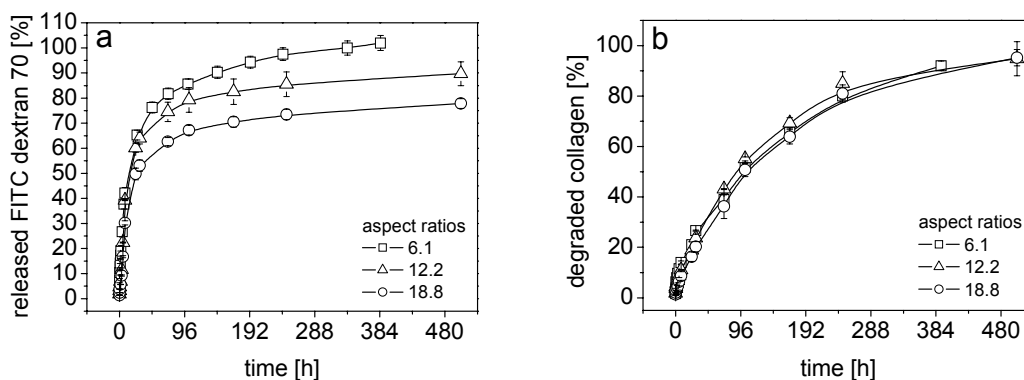


Figure 4-40 Effect of the minirods length on FITC dextran 70 release (a) and collagen degradation (b) of equine non cross-linked minirods (0.1 μ g/ml enzyme was added after 0.25h; 10mm (aspect ratio of 6.1); 20mm (aspect ratio of 12.2); 30mm (aspect ratio of 18.8); average \pm SD; n=3)

Degradation occurred at a similar rate for all three lengths (see Figure 4-40b). The two stage degradation was not as pronounced as for the fully swollen matrices (see Figure 4-39b), because less tropocollagens were accessible in the beginning and the first degradation phase was diminished. Since the specific surface of all minirods was almost similar (surface/volume approximately 2.6mm^{-1}) and the degradation of minirods differing in length was identical within each setup (see Figure 4-39b and Figure 4-40b), the proposal of Maeda et al. that the change in release occurred due to the variation in relative proportion of the dense lateral surface to the overall surface area could be confirmed.

4.3.4.2 Variation in Diameter of Minirods

For in vivo applications, implants should be as small as possible to avoid foreign-body reactions and to achieve good patient compliance (Fujioka et al.; 1994). However, drug dosage and administration method limit the range of possible implant diameters (Sano et al.; 2003). Reduction in diameter led to an extreme increase of aspect ratios, which represented an increase in proportion of lateral to overall surface area. With decreasing the diameter of minirods, an augmentation in initial drug release rates took place (see Figure 4-41a). A

similar observation was made for the HSA release from minipellets (Sano et al.; 2003). This could be explained by the shorter diffusion pathways for water and drug molecules and the increased specific surface area (surface/volume ratio: 2mm: 2.8mm^{-1} ; 1.5mm: 3.4mm^{-1} ; 1mm: 4.9mm^{-1} ; 0.5mm: 9.1mm^{-1}). Water penetration and swelling were accelerated (Maeda et al.; 2004b) and a higher specific surface is available through which release can occur and at which collagenase can bind. However, observed degradation profiles indicated only a minimal increase in degradation rate with reduction in extrudate diameter (see Figure 4-41b).

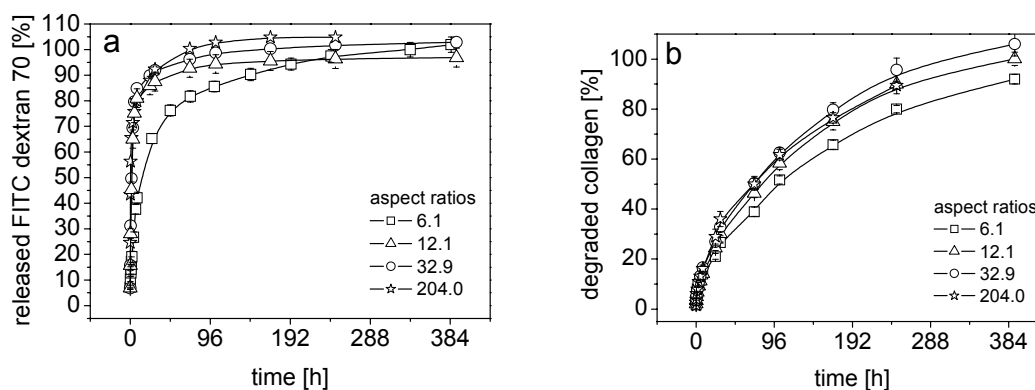


Figure 4-41 Effect of the diameter of minirods on FITC dextran 70 release (a) collagen degradation (b) of 20mg equine non cross-linked minirods ($0.1\mu\text{g/ml}$ enzyme was added after 0.25h; 2mm (aspect ratio of 6.1); 1.5mm (aspect ratio of 12.1); 1mm (aspect ratio of 32.9); 0.5mm (aspect ratio of 204.0); average \pm SD; $n=3$)

Based on the observed results, it was concluded that release kinetics can be controlled by adjusting the dimensions of minirods. Besides the specific surface area, important for enzyme binding and drug release by diffusion, the ratio of lateral- to cross-section influences the drug delivery due to the different surface structures and in consequence anisotropic release properties.

A further change in matrix geometry, e.g. towards a collagen slab, was not performed experimentally, but could be simulated with the developed mathematical model (see 4.5).

4.3.5 Influence of FITC Dextran

4.3.5.1 Variation in Molecular Weight

Since drug release from collagen devices is partially diffusion controlled, drug release should become slower with increasing molecular weight (Gilbert et al.; 1988a) and a higher drug fraction should be entangled inside the matrix in absence of collagenase. Therefore, the influence of the molecular weight of the model compound on drug release was investigated. FITC dextrans of different molecular weight were used to avoid drug dependent collagen – drug - interactions. Their diffusion coefficients in water were determined by FCS (see 4.3.1), as were their hydrodynamic radii (r_H (FITC dextran 20): 3.97nm; r_H (FITC dextran 70): 4.91nm; r_H (FITC dextran 150): 6.56nm). Before the complex release mechanism composed of swelling, diffusion and erosion dependent delivery was investigated, pure swelling and diffusion controlled release was monitored (see Figure 4-42a). Similar release profiles were observed for FITC dextran 70 and 150. FITC dextran 20 was released faster than the other two model drug compounds: approximately 80% was liberated during the first 24h compared to 60% of FITC dextran 70 and 150. After this fast initial release no further significant release over the next 5d could be detected for all three minirods. Consequently, the molecular size of the drug primarily influenced the extent of the initial release by diffusion. Release profiles indicated that during the initial swelling the pore diameter was greater than the hydrodynamic radius of FITC dextran 20, because of its fast unhindered diffusional delivery. Initial swelling was completed after 23h (see Figure 4-9) and the molecular size has no more significant influence on the release kinetic. This was in agreement with the measured diffusion coefficients in water which were nearly identical for all three compounds (see 4.3.1). Furthermore, Fujioka et al. postulated that there does not need to be a relationship between the molecular size of proteins and their in vitro release rate observed in this phase of release (Fujioka et al.; 1998) and Weadock et al. suggested that at low swelling ratios, e.g. ratios of wet to dry matrix weight of 4, drug diffusion through collagen barriers can be insensitive to variations in molecular drug size (Weadock et al.; 1987). After 6 days, 15% of FITC dextran 20 and 25% of FITC dextran 70 and 150 were

entrapped within the matrix and could only be released after matrix degradation. After addition of collagenase, this immobilized drug portion was delivered over 5d (FITC dextran 20 and 150) and 6d (FITC dextran 70), respectively (see Figure 4-42a).

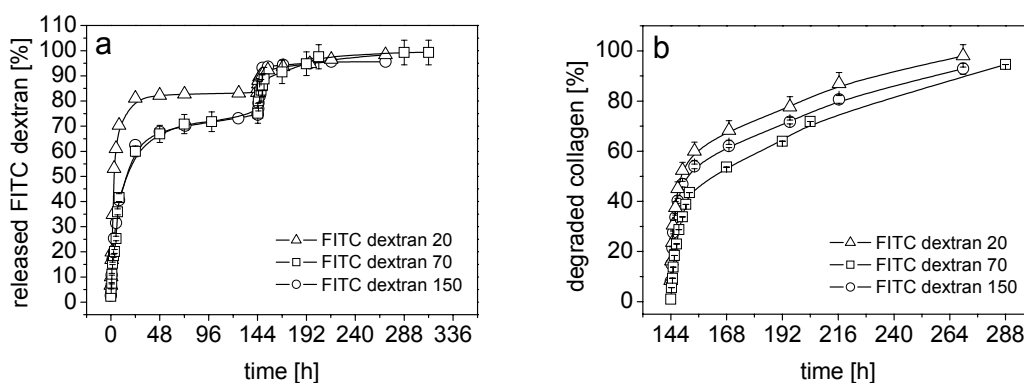


Figure 4-42 Effect of the molecular weight of FITC dextran on drug release (a) and collagen degradation (b) of 10mm equine non cross-linked minirods (0.1 μ g/ml enzyme was added after 6d; average \pm SD; n=3)

Degradation profiles were almost similar for all three incorporated dextran flavors, suggesting that the degradation of completely swollen extrudates is independent of the incorporated drug and that the molecular weight of the incorporated compound did not affect the structural integrity of the swollen minirods (see Figure 4-42b). During the first 8h a rapid linear degradation occurred. Afterwards, the degradation rate slowed down due to a decrease in enzymatic binding sites on the collagen surface.

Drug release in the presence of collagenase followed an almost identical profile for all three types of FITC dextrans (see Figure 4-43a). FITC dextran 70 delivery was slightly slower (release after 24h 60%, compared to 80% for FITC dextran 150 and 20), because these minirods had the highest apparent density (see Table 4-1; FITC 20: 0.983g/cm³, FITC dextran 70: 1.109g/cm³, FITC dextran 150: 0.899g/cm³) and were consequently degraded at a lower degradation rate (see Figure 4-43b). Almost no difference in release pattern was observed for FITC dextran 20 and 150 devices. Assuming homogeneous drug distribution,

more FITC dextran 150 than FITC dextran 20 was immobilized per matrix volume (see Figure 4-42a). Since erosion behavior was similar for these minirods, proportionally more immobilized FITC dextran 150 than FITC dextran 20 could be set free and FITC dextran 150 made up the difference from the diffusion dependent drug release.

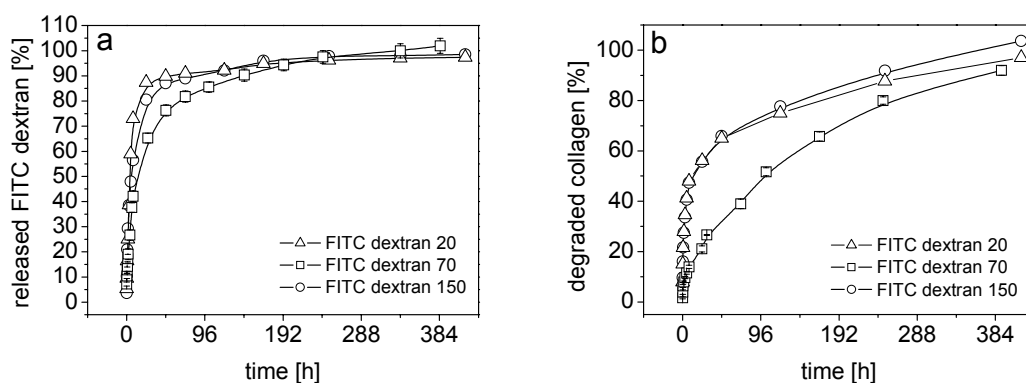


Figure 4-43 Effect of the molecular weight of FITC dextran on drug release (a) and collagen degradation (b) of 10mm equine non cross-linked minirods ($0.1\mu\text{g/ml}$ enzyme was added after 0.25h; average \pm SD; $n=3$)

Summarizing the effects of variation in molecular weight of incorporated drug compounds in equine non cross-linked minirods showed that FITC dextran 20 could freely diffuse in these matrices, because similar release profiles during the first 24h were observed in absence and presence of $0.1\mu\text{g/ml}$ collagenase (see Figure 4-42a and Figure 4-43a). In contrast, diffusion was restricted for FITC dextran 70 and 150 due to a higher hydrodynamic radius than matrix pore size. Initial release of FITC dextran 150 from equine non cross-linked matrices could be enhanced if collagenase was added, whereas this effect was less pronounced for FITC dextran 70 containing extrudates, because of their high apparent density (see Table 4-1). Comparing the release behavior after the first day, showed that erosion dependent release became important for all three kinds of dextran. Degradation of fully swollen equine non cross-linked minirods was similar irrespectively of the incorporated drug. If digestion of collagen extrudates was monitored in the presence of collagenase added already after

0.25h, the difference in apparent matrix density became more dominant, because the denser FITC dextran 70 minirods showed the slowest degradation profile.

The influence of the molecular weight on drug release was more pronounced for equine EDC 1 cross-linked minirods than for equine non cross-linked matrices. Again, first of all pure swelling and diffusion controlled release was investigated, before release dependent on swelling, diffusion and matrix erosion was studied in more detail. According to their hydrodynamic radius, FITC dextran 20 was delivered faster than FITC dextran 70. FITC dextran 150 showed the slowest release during the first 6d when no collagenase was present (see Figure 4-44a). After 24h, 75% drug was released from minirods containing FITC dextran 20, whereas release of FITC dextran 70 and 150 was approximately 55%. After 2d, no further drug was delivered from FITC dextran 20 and 150 extrudates indicating that the complete mobile drug fraction was already released. In contrast, FITC dextran 70 delivery went on until approximately 70% was released after 6d.

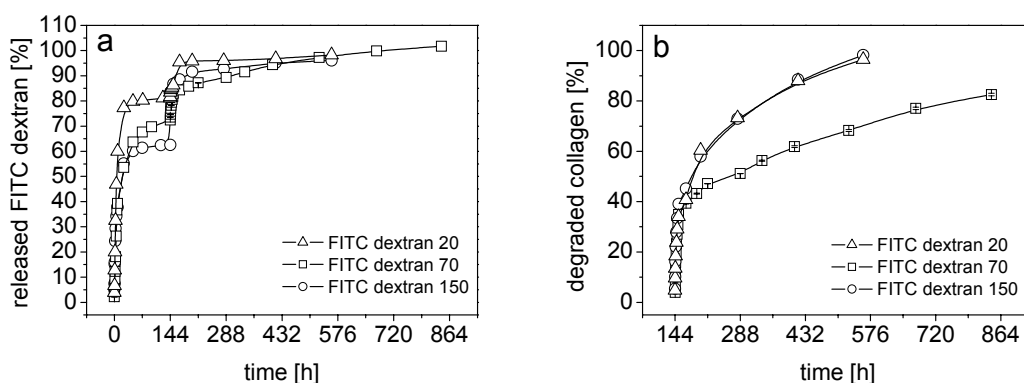


Figure 4-44 Effect of the molecular weight of FITC dextran on drug release (a) and collagen degradation (b) of 10mm equine EDC 1 cross-linked minirods (0.1 μ g/ml enzyme was added after 6d; average \pm SD; n=3)

Compared to equine non cross-linked minirods (see Figure 4-42a), higher drug contents were immobilized inside the cross-linked collagen matrices. For FITC dextran 20 and 70 5% drug was added to the immobile fraction, whereas the

portion of FITC dextran 150 could be increased from 25% to 40%. This indicated that with additional cross-linking of the collagen drug device, the pore size was reduced and drug release by diffusion could be repressed which became effective especially for FITC dextran 150. Besides this, cross-linking of equine minirods resulted in a higher resistance against enzymatic attack and erosion controlled FITC dextran release could be reduced as compared to drug release from non cross-linked matrices (see Figure 4-42 and Figure 4-44). Complete FITC dextran 20 load was delivered from equine EDC 1 cross-linked matrices after 8d, whereas already after 5d 100% FITC dextran 20 could be detected in the supernatant of equine non cross-linked minirods. Due to the higher molecular weight of FITC dextran 150, more drug molecules were immobilized by the collagen matrix and FITC dextran 150 could not be delivered completely before day 22 (compared to 5d from non cross-linked minirods). Since both EDC 1 cross-linked devices were degraded at similar rates (see Figure 4-44b), it was concluded that for the delivery of the remaining immobilized FITC dextran fractions less collagen had to be digested to obtain complete FITC dextran 20 release (approximately 50% matrix degradation was sufficient) than for the FITC dextran 150 minirods (100% digestion was required). This confirmed the assumption that more drug molecules were immobilized in dense collagen matrices when their molecular weight was increased. As was already observed for equine non cross-linked minirods (see Figure 4-43b), equine EDC 1 cross-linked FITC dextran 70 extrudates showed a slower degradation behavior (see Figure 4-44b) than equine EDC 1 cross-linked matrices loaded with FITC dextran 20 and 150, respectively. Since swelling of EDC 1 cross-linked matrices was not as pronounced as for non cross-linked minirods after 6d (see Figure 4-9) and FITC dextran 70 matrices were denser than the other drug loaded matrices (see Table 4-1; FITC 20: 0.791g/cm³, FITC dextran 70: 1.011g/cm³, FITC dextran 150: 0.804g/cm³), penetration of collagenase and drug diffusion were more restricted. This resulted in a delayed complete FITC dextran 70 release from equine EDC 1 cross-linked minirods over 34d (see Figure 4-44a).

In the presence of collagenase, higher initial release rates were detected for equine EDC 1 cross-linked FITC dextran 20 and 150 matrices (see Figure 4-45a) than in absence of the enzyme (see Figure 4-44a), because swelling, diffusion and erosion controlled delivery occurred simultaneously. Within 24h 90% FITC dextran 20 and 65% FITC dextran 150, respectively, were delivered when 0.1 μ g/ml collagenase was present (compared to 75% FITC dextran 20 and 55% FITC dextran 150 liberation when collagenase was absent). Similar FITC dextran 70 delivery within the first 24h (approximately 55% release) was observed for equine EDC 1 cross-linked matrices, irrespectively of collagenase presence. Since these minirods exhibited the highest apparent density (see Table 4-1) the lowest degradation profile was the consequence (see Figure 4-45b) and release was independent of erosion during the first 72h.

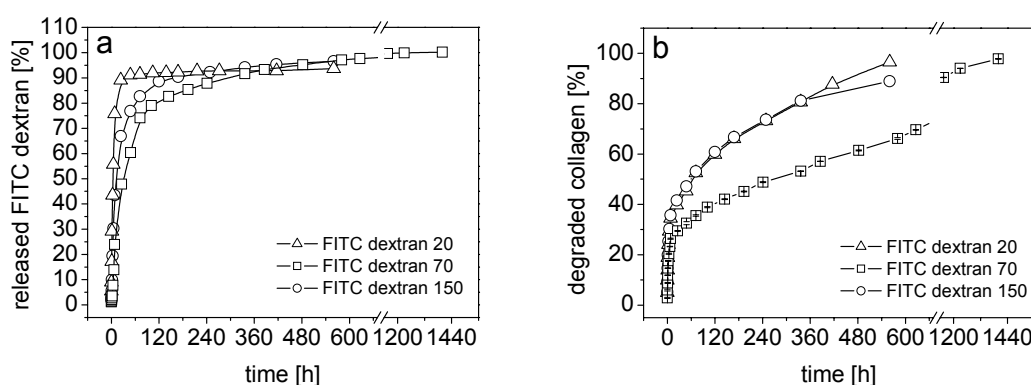


Figure 4-45 Effect of the molecular weight of FITC dextran on drug release (a) and collagen degradation (b) of 10mm equine EDC 1 cross-linked minirods (0.1 μ g/ml enzyme was added after 0.25h; average \pm SD; n=3)

For equine EDC 1 cross-linked FITC dextran 20 and 150 devices a more pronounced digestion was detected and both types of minirods were degraded in a similar fashion. This resulted in a more delayed release of FITC dextran 150 due to more interactions with the cross-linked collagen structure (Weadock et al.; 1987).

For bovine corium material, the influence of different EDC cross-linking ratios on release of FITC dextran 20 and 70 were tested (see Figure 4-46a). The drug

release profiles indicated a fast release from EDC 0.25 minirods independent of the molecular weight of FITC dextrans, because of a fast matrix erosion in the presence of $0.1\mu\text{g/ml}$ collagenase at 37°C (see Figure 4-37 and Figure 4-46b). This suggested that this cross-linking treatment did not create enough linkages to reduce the free diffusion of the drugs as was also concluded for the FITC dextran 20 release from equine non cross-linked minirods. At a cross-linking ratio of 1 sufficient hindrances were incorporated into the collagen material to delay the FITC dextran 70 release more significantly than the FITC dextran 20 delivery. Incorporated FITC dextran did only affect the degradation behavior of bovine corium EDC cross-linked matrices fractionally for both cross-linked ratios (see Figure 4-46b).

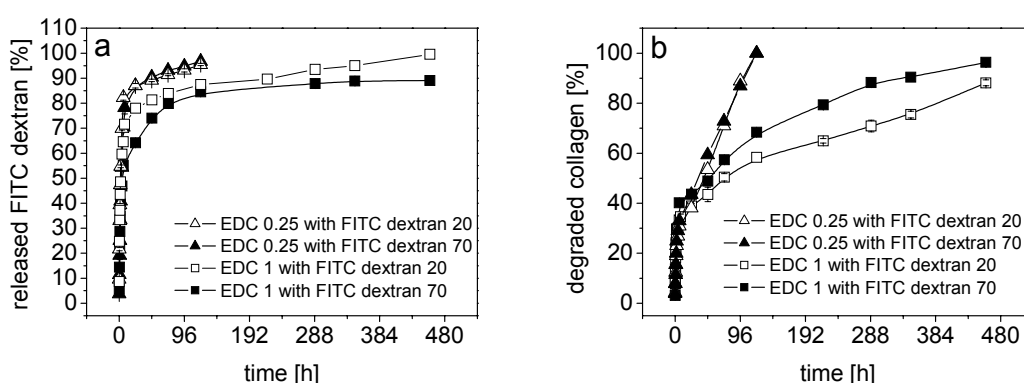


Figure 4-46 Effect of the molecular weight of FITC dextran on drug release (a) and collagen degradation (b) of 10mm bovine corium EDC 0.25 and EDC 1 cross-linked minirods ($0.1\mu\text{g/ml}$ enzyme was added after 0.25h; average \pm SD; $n=3$)

The influence of the molecular weight on drug release could be clearly shown for EDC cross-linked matrices. Pure swelling and diffusion controlled release from equine EDC 1 cross-linked extrudates decreased with an increase in molecular weight of FITC dextran. If $0.1\mu\text{g/ml}$ collagenase was added release was enhanced for FITC dextran 20 and 150, but not for FITC dextran 70. This indicated that the higher apparent density of FITC dextran 70 loaded equine EDC 1 cross-linked devices is responsible for the suppression of release by diffusion and not exclusively the molecular drug size. The investigation of

different EDC cross-linking degrees of bovine corium extrudates showed that delivery could only be controlled if sufficient new cross-links were introduced by an EDC cross-linking of 1.

4.3.5.2 Variation in Drug Concentration

Finally, the influence of total drug load on FITC dextran 70 release was investigated. Numerous studies on various delivery systems have shown that this parameter may substantially influence the release behavior, e.g. for collagen minipellets (Sano et al.; 2003), collagen discs (Gilbert; 1988b), poly(orthoester) discs (Sparer et al.; 1984), EVAc matrices (Saltzman; 2001) and tristearin implants (Mohl; 2004).

Maeda et al. investigated the incorporation of HSA into minipellets (Maeda et al.; 1999). HSA was found as fine particulated clusters inside the matrices which were homogeneously distributed throughout the complete collagen extrudate. After water contact, these clusters dissolve and the drug could be released. As a result, small cavities remained inside the matrix at the areas where HSA was located before dissolution (Maeda et al.; 1999; Sano et al.; 2003). Although Gilbert et al. postulated that drug loads higher than 10% inulin were necessary to create additional cavities (Gilbert et al.; 1990), Maeda et al. could demonstrate that even 1% HSA was sufficient to observe small pores in the surface of collagen extrudates during release (Maeda et al.; 1999). Since the structure of our minirods resembled more Maeda's extrudates and because model drugs with higher molecular weights were used, it was assumed that new pores could be built during FITC dextran release as well. A 2% FITC dextran 70 concentration was used as highest model drug concentration. FITC dextran solutions with higher concentrations show markedly increased viscosity which may lead to inhomogeneous drug distribution. Furthermore, the intense fluorescence may cause trouble in fluorescent investigations. As was also observed for HSA, interferon alpha and G-CSF release from collagen minipellets (Sano et al.; 2003), an increase in drug concentration resulted in a relative increase in drug liberation (for FITC dextran 70 see Figure 4-47a), because more cavities could be built. The density of the FITC dextran 70 loaded

devices (see Table 4-1; 1%: 1.109g/cm³, 2%: 0.829g/cm³) and consequently the thickness of the diffusion barrier decreased and a faster release took place (Sano et al.; 2003). This observation was made with highly water soluble compounds which are readily released by diffusion. Besides “normal” diffusion through water filled pores, diffusion through the swollen matrix itself could take place. This was observed for the release of hGH from air dried 2% collagen films (Maeda et al.; 2001). A 3% drug load resulted in Fickian diffusion, whereas release of 30% hGH was accelerated and became dependent on diffusion through water filled pores as well as the swollen matrix itself. If the drug is less soluble under physiological conditions or if interactions between drug and collagen occur, drug loading and diffusion controlled release becomes less important. This effect was observed for rh-BMP 2 (recombinant human bone morphogenetic protein 2) release from minipellets (Maeda et al.; 2004b). For rh-BMP 2, diffusion controlled delivery could be amplified if glutamic acid was added which lowers the pH value inside the collagen matrix and increases the solubility of collagen and rh-BMP 2 (Maeda et al.; 2004a).

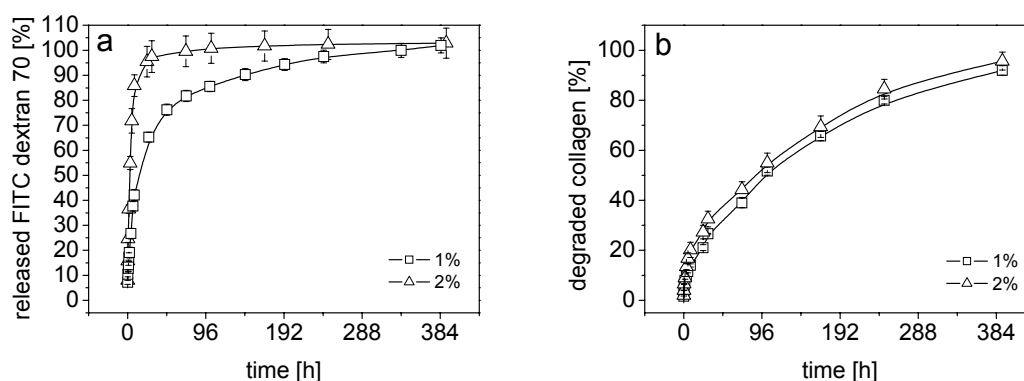


Figure 4-47 Effect of the FITC dextran 70 concentration on drug release (a) and collagen degradation (b) of 10mm equine non cross-linked minirods (0.1µg/ml enzyme was added after 0.25h; average ± SD; n=3)

Since degradation of 1% and 2% minirods was identical the assumption of pore formation and additional diffusion controlled release through these new

cavities could be accepted for our minirods. This resulted in a higher initial release for the 2% devices (see Figure 4-47).

4.3.6 Summary

The objective of this chapter was to investigate the in vitro release of FITC dextrans from collagen minirods. Since drug release from collagen devices is mainly governed by diffusion dependent liberation (Radu et al.; 2002), diffusion equations had to be implemented into the mathematical model (see 4.5). Therefore, the diffusion coefficients in water of FITC dextran 20, 70 and 150 were determined by FCS. According to their molecular weights, the diffusion coefficient decreased from $3 \cdot 10^{-3} \text{cm}^2/\text{h}$ for FITC dextran 20 to $1.8 \cdot 10^{-3} \text{cm}^2/\text{h}$ for FITC dextran 150. The observed diffusion coefficient of FITC dextran 70 ($2.4 \cdot 10^{-3} \text{cm}^2/\text{h}$) corresponded well with the diffusion coefficient of collagenase, described in the literature, and was consequently used for the enzyme in the mathematical model as well.

Drug release was investigated with respect to the used collagen matrix quality, the incorporated drug and the added enzyme. If higher amounts of collagenase were added, FITC dextran 70 release and collagen degradation became faster (24h release: 0 $\mu\text{g}/\text{ml}$ collagenase: 35%, 0.1 $\mu\text{g}/\text{ml}$ collagenase: 50%, 6.7 $\mu\text{g}/\text{ml}$ collagenase: 85%, 24h degradation: 0.1 $\mu\text{g}/\text{ml}$ collagenase: 15%, 6.7 $\mu\text{g}/\text{ml}$ collagenase: 55%) and less drug was entrapped inside the collagen matrix, suggesting that a distinct drug portion could only be released by matrix erosion. It was demonstrated that the addition of collagenase to a fully swollen matrix resulted in faster collagen digestion, because more enzyme binding and cleavage sites became accessible.

Using different collagen materials for minirod preparation gave a tool to control drug release. A fast release (and degradation) was observed for pulverized equine non cross-linked collagen and bovine tendon non cross-linked minirods. Delivery could be delayed by using lyophilized equine material. Further retardation in drug liberation was achieved by cross-linking. DHT treatment resulted in lower enzymatic resistance than EDC cross-linking (Pieper et al.; 1999) and in consequence release was not as suppressed as from chemically

cross-linked matrices. Different ratios of EDC cross-linking were examined. Both investigated types of collagen, equine and bovine corium, showed the most promising results for EDC 1 cross-linked materials.

With changing the dimensions of the extrudates, drug release could also be controlled. Increasing the length or diameter of the cylindrical rods resulted in a decrease of FITC dextran 70 delivery. This was attributed on the one hand to an increase of the smooth lateral surface area, if minirods were elongated, which exhibit a more hindered release pattern than the porous cross-section. On the other hand, if extrudates were thickened, diffusion ways increased and the specific surface area decreased which resulted in a lower particle release by diffusion.

The last parameters which can influence drug release derive from the incorporated drug itself. In general, it is assumed that increasing the molecular weight lead to slower release by diffusion. However, the theoretical order FITC dextran 20 - 70 - 150 could only be detected for the diffusion based release from equine EDC 1 cross-linked minirods. The other collagen matrices met another order: FITC dextran 70 was always released slowest followed by FITC dextran 150 and 20. This change in sequence was attributed to the higher apparent density of FITC dextran 70 extrudates resulting in a lower degradation behavior. Since the other two FITC dextran loads exhibited almost identical matrix densities, the liberation of FITC dextran 150 was delayed due to more pronounced interactions with the collagen mesh. This indicated that the influence of the matrix structure on the release and degradation pattern was more pronounced than the effect of the molecular size of the incorporated drugs. If the incorporated drug portion was increased, faster release occurred. It was assumed that the faster release from 2% matrices derive from diffusion controlled release through newly formed cavities built at positions formerly filled by drug, because 1% and 2% minirods were degraded identically.

4.4 In vitro and in vivo Release of PCA-BSA

After characterization of the in vitro release of FITC dextrans, the in vitro and in vivo release of bovine serum albumin (BSA) from collagen minirods was investigated. BSA was chosen as a model protein compound, because no interactions with collagen, which could affect the release profile, are known (Maeda et al.; 1999). Furthermore, spin labeling of BSA, necessary for ESR investigations, is fast and simple (Katzhendler et al.; 2000a) and due to its molecular weight (MW (BSA): 66kDa), comparison with the in vitro release data of FITC dextran 70 is possible.

4.4.1 Introduction to Electron Spin Resonance (ESR) Spectroscopy

Release of BSA was observed using ESR spectroscopy. In literature, synonyms for this method are “electron paramagnetic resonance” (EPR) and “electron magnetic resonance” (EMR). This technique is closely related to the better known nuclear magnetic resonance (NMR), because in both methods magnetic dipoles interact with an externally applied magnetic field (Swartz et al.; 1972). The main difference is the detected particle species: with ESR, unpaired electron spins are quantified, whereas in NMR measurements the behavior of protons in the applied magnetic field is monitored (Mäder; 1998).

4.4.1.1 Physical Principles

Electrons can be regarded as small bar magnets with north and south poles, because they have own magnetic moments arising to 99% from their quantum-mechanical “spin” (called spin magnetic moment) (Lurie et al.; 2005; Swartz et al.; 1972). In general, stable chemical bonds consist of paired electrons with opposite spins, according to the Pauli exclusion principle (Swartz et al.; 1972). This is imperative in order to coexist in such close vicinity. The magnetic moment of paired electrons is erased (Lurie et al.; 2005). In contrast, unpaired electrons have a magnetic moment which can interact with the externally applied magnetic field B_0 during ESR measurements.

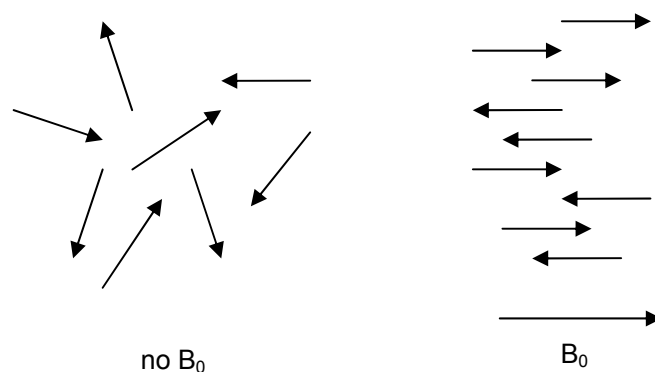
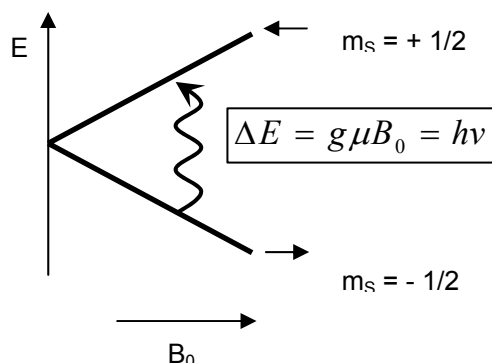


Figure 4-48 Electron spins without (left) and with externally applied magnetic field (right) (modified from (Mäder; 1998))

Two orientations of the electron spins in the presence of an externally applied magnetic field are possible (see Figure 4-48). Spins can either be aligned along the externally applied magnetic field or against it. This effect, known as the Zeeman splitting, results in two different energy states for the electron spins, a low energy state ($m=-1/2$) and a high energy state ($m=+1/2$) (see Figure 4-49). The energetic difference ΔE between these two states is dependent on the strength of the applied magnetic field B_0 and the molecular weight of the excited species. Due to the lower mass of electrons, the Bohr magneton is larger than that of protons and a higher energetic difference ΔE between the two states results which increase the sensitivity of ESR compared to NMR measurements (Mäder; 1998). In ESR investigations, electromagnetic radiation with frequencies between 0.3 - 10GHz are used to excite unpaired electrons (Lurie et al.; 2005). At the resonance conditions, the photon energy of the electromagnetic radiation matches the difference between the two energy states ΔE (see Figure 4-49). Electrons can now adsorb energy and jump from the low- to the high-energy state by flipping their electron spins by 180° (Lurie et al.; 2005).



- ΔE : energy difference between the two spin states
 h : Planck constant
 ν : microwave frequency
 g : g-factor or Zeeman splitting factor ($e^- = 2.0023$; $H^+ = 5.5856$)
 μ : Bohr magneton ($e^- = 9.274 \cdot 10^{-24} \text{ JT}^{-1}$; $H^+ = 5.051 \cdot 10^{-27} \text{ JT}^{-1}$)
 B_0 : applied magnetic field
 m_S : quantum number

Figure 4-49 Electronic energy level diagram with resonance conditions (modified from (Mäder; 1998))

Since all physical systems prefer the low-energy state, electrons fall back at this level within $0.1 - 1 \mu\text{s}$ and simultaneously release electromagnetic radiation at the same frequency as the excitation frequency (Lurie et al.; 2005). If many electrons pass through this scenario at the same time, the resulting electron magnetism is strong enough to alter the externally applied magnetic field by reflecting parts of the applied microwaves. This change is detected during ESR measurements (Swartz et al.; 1972) and is monitored either as adsorption spectrum (amplitudes of the reflected microwaves versus magnetic field strength) or as first derivative spectrum (slope of the adsorption spectrum against magnetic field strength) (see Figure 4-50) (Lurie et al.; 2005).

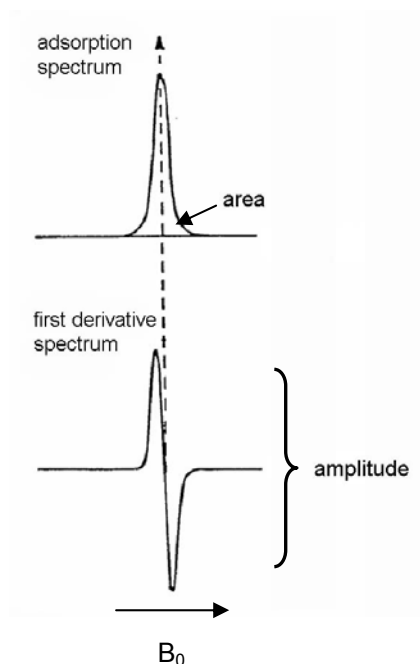


Figure 4-50 Adsorption (top) and first derivative (bottom) ESR spectrum (modified from (Palmer; 1999))

In general, ESR spectra consist of more than one individual line, because unpaired electrons interact not only with the externally applied magnetic field, but also with the magnetic moments of nuclei (Katzhendler et al.; 2000b). The electron-nucleus interaction can take place between unpaired electrons and its own nucleus or a neighboring nucleus (Palmer; 1999). Since the nitrogen nucleus has a nuclear spin of 1, three orientations in the applied magnetic field are possible, resulting in three different magnetic moments (Katzhendler et al.; 2000b). Unpaired electrons in nitroxides are exposed to a magnetic field composed of the strong externally applied magnetic field and a weaker local magnetic field of the nitrogen nucleus. The consequence is a “hyperfine splitting” of the ESR signal e.g. a three line spectrum for nitroxides, because the resonance condition is satisfied at three different values of the externally applied magnetic field (see Figure 4-51) (Swartz et al.; 1972). Hydrogen nuclei in vicinity of the nitrogen nucleus also influence the ESR spectrum. Their effect

is far less pronounced than that of the nitrogen nucleus, due to a greater distance to the unpaired electron, and results in line broadening instead of additional hyperfine splitting (Lurie et al.; 2005).

Besides the permanent magnetic electron-nucleus interactions, orbital-orbital coupling effects occur as well, which depend on the symmetry of the electron orbital (Assenheim; 1966). This effect, known as the orbital magnetic moment, contributes the remaining 1% to the total magnetic moment of electrons (Swartz et al.; 1972) and is displayed in the ESR spectrum shape. If electrons of a spherical orbital (s-orbital) take part, isotropic interactions occur and the ESR spectrum is composed of identical lines. If a conical orbital (p-orbital) participates, the ESR signal is influenced by the three different planes (x, y and z). An anisotropic environment results, reflected by different, broadened line shapes which superpose to the finally observed spectra (see Figure 4-51 bottom). These anisotropic effects can only be averaged out, if the detected electron can tumble very fast (see Figure 4-51 top) (Palmer; 1999).

Summarizing the presented influences on electrons shows that the spectrum shape and width provide information about the molecule structure (Swartz et al.; 1972).

4.4.1.2 Samples

A main advantage of ESR measurements is that a high variety of samples can be examined without any pre-treatment. All states of aggregation (liquid, solid or gaseous) can be studied. Furthermore, samples can be investigated without destruction and they must not be transparent or homogenous, as in other commonly used spectroscopic techniques. Due to the high sensitivity of this method, concentrations down to the nanomolar region can be detected (Mäder; 1998). Samples for ESR measurements must have almost only one unique property: they must be paramagnetic, that means they must contain free electron spins arising from unpaired electrons. Otherwise they are ESR “silent” and no signal can be detected. In general, two kinds of paramagnetic samples are possible. On the one hand, samples which already contain unpaired electrons, e.g. oxygen, metals and transition metals or where radicals are

introduced by e.g. γ -irradiation (Mäder; 1998). Especially free radicals often exist only at a small number and have very short life times. Consequently, they can only be detected at low temperatures or with spin trapping techniques (Lurie et al.; 2005). On the other hand, stable free radicals can be incorporated into ESR silent diamagnetic samples as spin probes (physical incorporation) or spin labels (chemical incorporation) (Mäder; 1998). Due to their higher stability, measurement at room temperature is possible. Spin probes, like nitroxides can either be used directly, e.g. to simulate small model drugs, or can be used to label larger molecules, like polysaccharides or proteins (Lurie et al.; 2005). Pyrrolidine derivatives, e.g. 3-carboxy-2,2,5,5-tetramethyl-1-pyrrolidinyloxy (PCA), are more stable than piperidine radicals, e.g. 4-hydroxy-2,2,6,6-tetramethyl-1-piperidinyloxy (TEMPO) (Mäder; 1998; Yoshioka et al.; 1995). Limitations in sample selection are the size, restricted by the cavity dimensions, and the water content due to non-resonant dielectric loss (Lurie et al.; 2005). Samples of approximately 3mm in diameter and 10mm in length are normally used in X-band spectrometers. The water content is often the limiting factor if biological samples are examined. Water is electrically conductive, strongly interacts with the applied microwaves and limits the penetration depth to approximately 1mm for X-band spectrometers (Mäder et al.; 1996). Consequently, often only the outer surface of the sample can be investigated (Katzhendler et al.; 2000b). To overcome these limitations, low frequency spectrometers have been developed. The penetration depth is increased to e.g. 16mm for L-band spectrometers (1GHz) (Mäder et al.; 1994) and direct in vivo studies of mice become possible (Lurie et al.; 2005; Saito et al.; 1997). A decrease in frequency goes along with a lower splitting of the energy levels which results in a remarkable decrease in sensitivity (Mäder et al.; 1994).

4.4.1.3 Spectra Analysis

In general, the first derivate spectrum is used for analysis. Different information can be drawn from ESR signals to characterize the homo- or heterogeneity of the investigated sample. Information about the molecule structure and its environment can be obtained. Using the phenomenon of hyperfine splitting, the microviscosity and the micropolarity can be determined. For this purpose, the

order parameter S and the hyperfine coupling constant a_n are used (see Figure 4-51).

To monitor the rotational freedom of the spin probe, the order parameter S is used. Values of 1 correspond to an entirely immobilized spin probe, whereas values approaching 0 indicate complete spin probe mobility (see Figure 4-51) (Katzhendler et al.; 2000b). Besides the change in S parameter, the value of a_n increases as well, when spin probes exhibit low mobility.

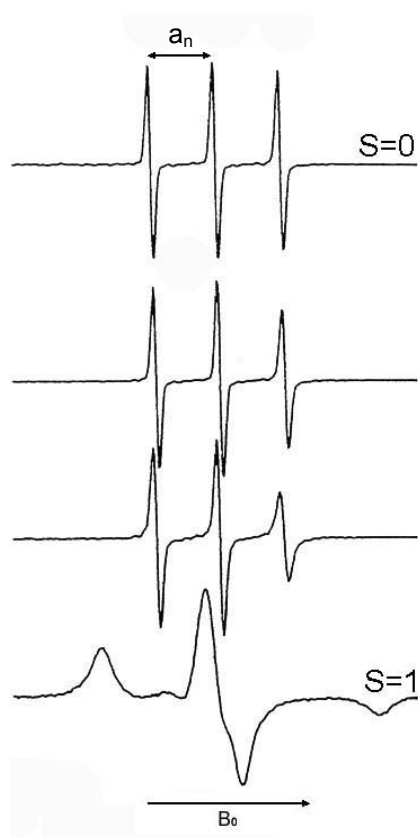


Figure 4-51 PCA dissolved in water, 50/50 water/glycerol, 30/70 water/glycerol and in dry state (from top to bottom) with corresponding S parameters and hyperfine coupling constant a_n (modified from (Katzhendler et al.; 2000b))

The spectrum is a superposition of many individual spectra which arise from the slightly shifted orientation of electrons to the externally applied magnetic field. At low viscosities, effective averaging of the anisotropic spin-lattice interactions

is possible due to a fast molecular tumbling of the radical. This results in three narrow lines, known as the Lorentzian line shape (Katzhendler et al.; 2000b). Increased viscosity is reflected by line broadening of the spectrum accompanied by a decrease in signal amplitude (see Figure 4-51 middle). Anisotropic effects can not be averaged as completely as in low viscosity systems (Capancioni et al.; 2003). This results in a Gaussian line shape. At this stage, the influence of nuclei becomes very important (Katzhendler et al.; 2000b). In the solid state, an asymmetric line shape is obtained, named “glass” or “powder” spectrum (see Figure 4-51 bottom).

The absolute concentration of spin probes can be determined by the peak area of the adsorption spectra. Relative concentrations can be estimated by comparison of the spectra amplitudes of the first derivative spectra (see Figure 4-50). In most cases, relative concentrations are determined, because for measuring absolute concentrations tremendous demands on experimental setup and analysis are necessary, including e.g. an internal standard (Mäder; 1998). Determination of spin probe concentrations can be used e.g. to monitor drug release.

Further insights into the mechanism of drug release can be gained by focusing on the changes in spectra intensity and shape during the observation period. Drug release controlled by surface erosion results in a decrease of spectra intensity with identical signal shape over the complete time, because the mobility of the radical remains constant. In contrast, spectra of drugs released by diffusion, swelling and/or bulk erosion change in intensity and shape due to a change in drug mobility (Lurie et al.; 2005). Spectra of dissolved and unsolved molecules superimpose. The S parameter changes over time, similar as observed for variation in viscosity (see Figure 4-51). Beyond this, degradation of the polymer and/or penetration of water are associated with a decrease in spectrum intensity because of reduction in the stabilizing environmental effects (Mäder; 1998).

Due to adequate ESR spectrometers (see 4.4.1.2), *in vivo* investigations can be performed as well. Non-invasive *in vivo* drug release studies can be conducted

to correlate *in vitro* and *in vivo* data (Lurie et al.; 2005). Furthermore, all these investigations can be detected 2- or 3-dimensionally by simultaneously using different nitroxides (or different isotopes of the same nitroxide) or by applying imaging techniques (Lurie et al.; 2005).

4.4.2 Labeling of BSA

For ESR measurements, BSA was spin labeled with PCA. To verify that labeling had taken place, spectra of PCA-BSA were compared with spectra of pure PCA. PCA showed three identical narrow lines (see Figure 4-52), indicating high mobility of the small molecule in solution. If the spin label is bound to the protein, its mobility is reduced and lines in the spectra, especially in the high-field, become broadened (Yoshioka et al.; 1995). This effect was observed for PCA-BSA, indicating that binding had taken place.

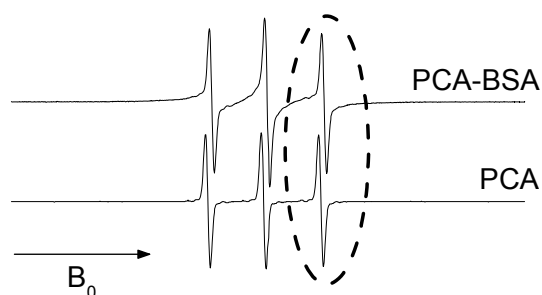


Figure 4-52 ESR spectra of PCA-BSA (top) and PCA (bottom) in water (determined by an L-band ESR spectrometer)

During spin labeling protein aggregation can take place. An increase in aggregate level would limit the *in vivo* application, because of potentially increased immunogenicity and formation of antibodies on the one hand (Hermeling et al.; 2004) and interferences in release kinetics on the other hand. As could be seen with SDS-PAGE (see Figure 4-53), the amount of monomers and aggregates were similar before and after labeling. This indicated that labeling did not induce aggregation and PCA-BSA could be used for *in vivo* studies.

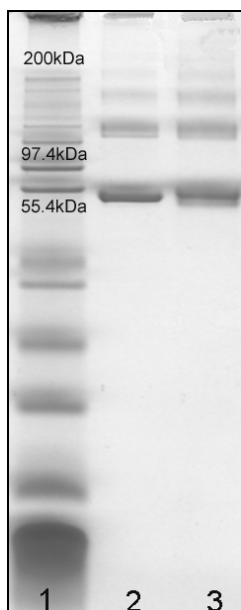


Figure 4-53 Stability of BSA after labeling with PCA (lane 1: MW marker, lane 2: BSA, lane 3: PCA-BSA)

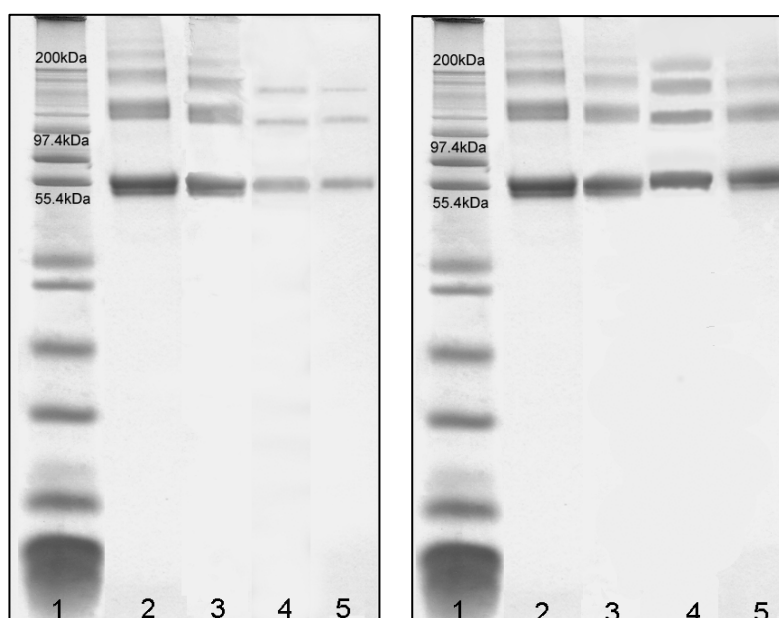


Figure 4-54 Stability of PCA-BSA during incubation without (left) and with 0.1 µg/ml collagenase (right) at 37°C (lane 1: MW marker, lane 2: non-incubated PCA-BSA, lane 3: PCA-BSA incubated for 1h, lane 4: PCA-BSA incubated for 12h, lane 5: PCA-BSA incubated for 24h)

Before in vitro and in vivo drug release tests from collagen devices could be carried out, the possibility of enzymatic hydrolysis of BSA had to be considered. Collagenases are enzymes which only cleave collagen at specific amino acid sequences within its helical parts (Harrington; 1996). For in vitro studies we used a commercially available crude bacterial collagenase mixture which also exhibits caseinase activity (Sigma Aldrich; 1998). In vivo, proteinases which may cleave PCA-BSA are present as well. SDS-PAGE of labeled BSA incubated with and without crude bacterial collagenase indicated, that PCA-BSA was stable against enzymatic attack, because no enzymatic hydrolysis products could be observed in the presence of collagenase (see Figure 4-54).

4.4.3 In vitro Release of BSA

Since drug release from collagen devices is swelling, diffusion and erosion controlled (see 1.2.3.1), two different experimental setups were conducted. On the one hand, exclusively swelling and diffusion controlled release in the absence of collagenase was studied. On the other hand, bacterial collagenase was added to investigate the influence of matrix degradation on drug release. For measurements, minirods as a whole had to be transferred from the incubation buffer into the ESR spectrometer and the end of experiments was determined by the compactness of the minirods. Investigations were performed as long as it was possible to handle minirods properly. PCA-BSA release was estimated relatively by comparison of spectra amplitudes. Signal amplitudes decreased over time (see Figure 4-55, Figure 4-56 and Figure 4-57), indicating that the concentration of PCA-BSA decreased inside the minirods and that drug release occurred.

Before contact to Tris buffer pH 7.5, a “powder” PCA-BSA spectrum was observed for all minirods (see Figure 4-55 and Figure 4-56). This indicated that the labeled BSA was immobilized inside the dry collagen matrices. After contact with the aqueous solution, water penetrated into the device and the ESR spectra changed to spectra of more mobile PCA-BSA, because the anisotropy of the hyperfine interaction was partially averaged and reorientation times decreased. However, the mobility was not as pronounced as that of PCA in

water (see Figure 4-52 top), because a_n was larger. In absence of collagenase, drug release was expected to be mainly diffusion controlled. This should result in a change in ESR spectra shape. With $0.1\mu\text{g/ml}$ collagenase, drug release might be dependent on matrix erosion as well. In case of pure erosion controlled release, no change in spectra shape should be observed (see 4.4.1.3).

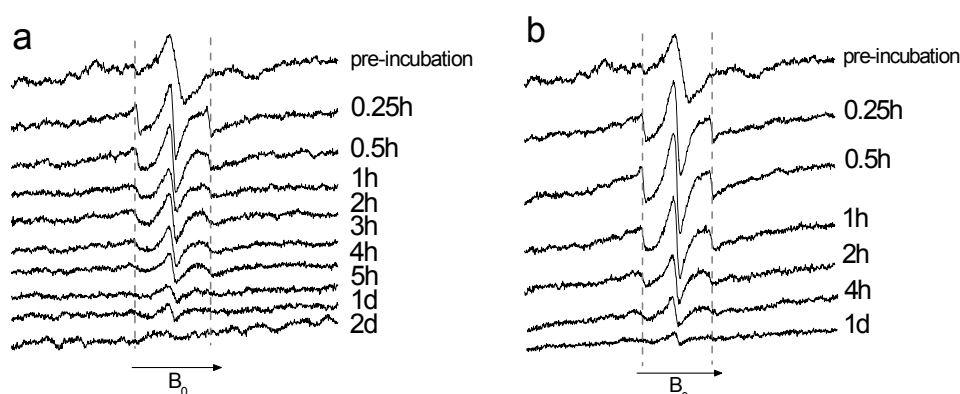


Figure 4-55 ESR spectra of 10mm PCA-BSA loaded bovine tendon non cross-linked minirods incubated without (a) and with $0.1\mu\text{g/ml}$ collagenase (b) at 37°C

Significant changes in spectra form and S parameter were observed for bovine tendon non cross-linked minirods with and without addition of collagenase (see Figure 4-55). Lines became broadened with longer observation time, as can be seen e.g. in the 4h spectra. A similar observation was made for bovine tendon EDC 1 cross-linked minirods in absence of collagenase (see Figure 4-56a). a_n increased from day 1 until the end of investigation. In the beginning, drugs which were not immobilized by the matrix could diffuse freely inside the matrix and spectra superimposed with the spectra of the less mobile drugs. Consequently, spectra of mobile PCA-BSA were observed with reorientation times between the time required in pure solution and in solid state. If the mobile PCA-BSA was released, the observed spectra were more and more dominated by the remaining immobilized drug fraction and the spectra shape changed. This indicated on the one hand that an environment with intermediate viscosity

was created and on the other hand that diffusion control was the dominating factor of PCA-BSA release.

In contrast, for PCA-BSA signals of bovine tendon EDC 1 cross-linked matrices incubated with collagenase only a decrease in amplitude could be detected, but hardly no variation in spectra shape (see Figure 4-56b). This indicated that the environment inside the collagen minirods and in consequence the mobility of labeled BSA changed only marginally in these EDC cross-linked minirods over the complete observation period. Hence, besides swelling and diffusion phenomena, BSA delivery was also erosion controlled in bovine tendon EDC 1 cross-linked minirods. This could be attributed to the higher number in hindrances compared to non cross-linked extrudates (see 4.1.1.2 and Table 4-2). Reduced swelling and a more pronounced PCA-BSA immobilization was the result, and the immobilized drug fraction could only be released by erosion mechanism.

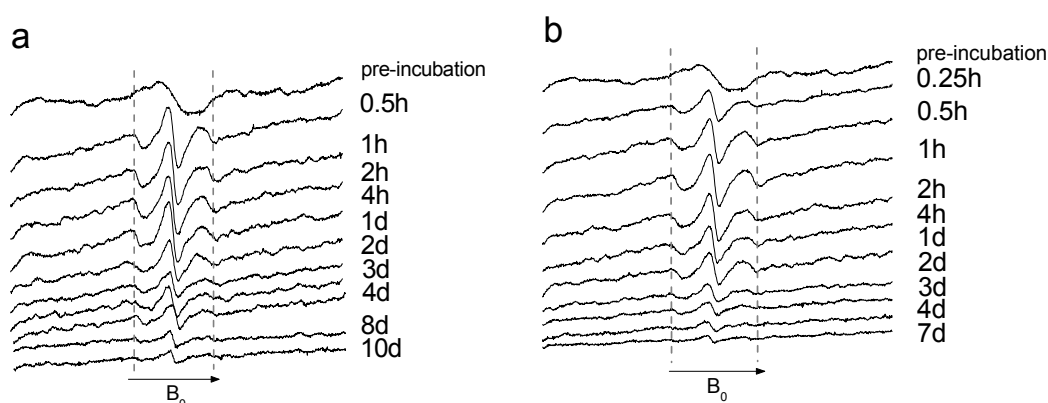


Figure 4-56 ESR spectra of 10mm PCA-BSA loaded bovine tendon EDC 1 cross-linked bovine tendon minirods incubated without (a) and with 0.1µg/ml collagenase (b) at 37°C

Diffusional drug release is dependent on the cross-linking degree of minirods, because a higher number of cross-links hampers diffusion of macromolecules (Frieß et al.; 1996b; Gilbert et al.; 1988a). As was already demonstrated by DSC measurements (see 4.1.1.2), the extent of cross-linking increased from bovine tendon non cross-linked over bovine corium EDC 1 cross-linked to

bovine tendon EDC 1 cross-linked collagen. The in vitro PCA-BSA release in pure Tris buffer pH 7.5 decreased in the same order (see Figure 4-57a), because a lower number of cross-links led to a more rapid swelling and more pronounced diffusion controlled release within the first day. This confirmed the assumption that a higher cross-linking degree delayed the PCA-BSA release.

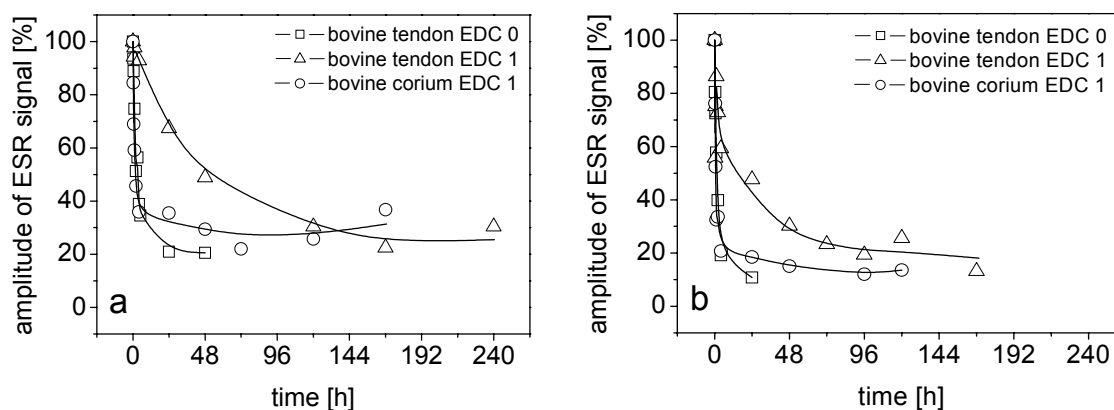


Figure 4-57 Signal amplitudes of ESR spectra of 10mm PCA-BSA loaded minirods incubated without (a) and with 0.1µg/ml collagenase (b) at 37°C (n=3)

For all three types of minirods a change in spectra shape was observed, indicating that the major fraction of labeled BSA release was governed by diffusion of the mobile BSA. In the presence of collagenase, swelling, diffusion and erosion controlled drug release occurred simultaneously. Again, bovine tendon non cross-linked minirods showed the fastest release and bovine tendon EDC 1 cross-linked the slowest (see Figure 4-57b). Differences to the release without enzyme were observed. PCA-BSA delivery became faster, because minirods started earlier to disintegrate in the presence of collagenase (see 4.1.2.1.2 and 4.3.2.1). More PCA-BSA could be released, because the PCA-BSA fraction which was entrapped in the collagen matrix by cross-links could now be liberated by erosion. The extent of the erosion controlled delivery was lower for bovine tendon non cross-linked minirods than for EDC 1 cross-linked extrudates (10% versus 20%). By investigation of the spectra shape it became

evident that the release from EDC 1 cross-linked minirods is partly erosion controlled, because no change in spectra shape could be detected. At later incubation time points, measurements became impossible, because matrices were too instable to guarantee a complete transfer of the minirods into the ESR cavity. Consequently, only approximately 80-90% labeled BSA could be recovered, because PCA-BSA which remained inside the matrix until complete matrix disintegration could not be detected by this method.

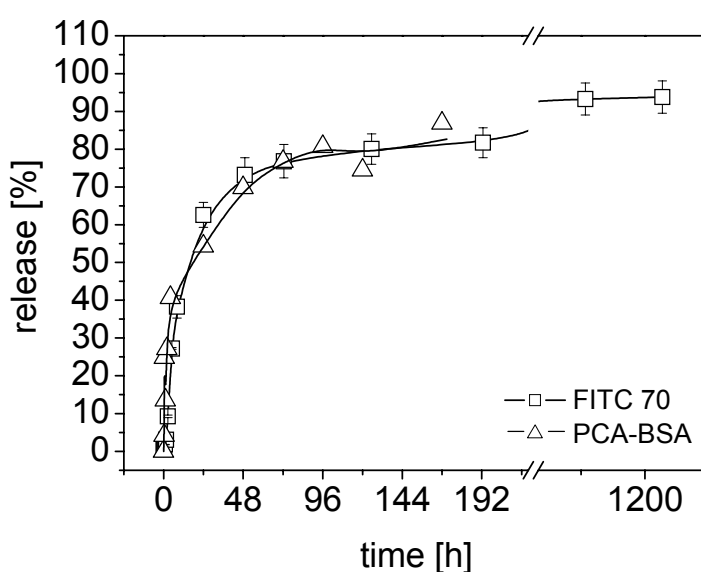


Figure 4-58 In vitro drug release from 10mm bovine tendon EDC 1 cross-linked minirods incubated with 0.1 μ g/ml collagenase added after 0.25h (average \pm SD; n=3)

Good correlation was found for the first week between the PCA-BSA release and the in vitro release of FITC dextran 70 from bovine tendon EDC 1 cross-linked minirods (see Figure 4-58). FITC dextran 70 delivery was followed until matrices were completely disintegrated and 100% of the incorporated FITC dextran 70 was recovered compared to 80-90% PCA-BSA.

From this observation two conclusions could be drawn: FITC dextran 70 also shows only low interactions with collagen due to a congruent release profile with

labeled BSA during the first week, and the PCA-BSA fraction which was not recovered, remains inside the devices until the matrix disintegrates completely.

4.4.4 In vivo Release of BSA

The in vivo release of PCA-BSA was investigated in adult domestic pigs due to close resemblance to human histology (Burke et al.; 1983) and metabolism (Hönig et al.; 1993). Furthermore as a large animal, morphological and anatomical features are quite similar to humans. This is prerequisite for a good result transfer to humans (Thorwarth et al.; 2005). Implants can be injected subcutaneously by a trocar (Kissel et al.; 1991) to achieve a systemic effect or they can be administered directly in or nearby a superficial lesion, e.g. during surgery, for local treatment (Fujioka et al.; 1995). In the performed in vivo study, minirods were implanted subcutaneously into ears by surgery. After sacrificing the animals at designated time points, minirods were explanted and divided into two groups. Drug release was investigated by ESR measurements and in vivo compatibility by histology.

In vivo ESR measurements are more challenging than in vitro experiments. The high water content of biological tissue reduces the penetration depth due to a high dielectric loss (Mäder; 1998). This dielectrical loss occurred by the measurement of the complete explanted tissues as well. Therefore, measurements were conducted in an X-band spectrometer (9.3GHz). Interference of water from the surrounding tissue was avoided and an overview of drug transportation was provided by introducing explants into TLC capillaries before ESR assessment. Distinction between the interior and the exterior of minirods, near (< 1mm) and distant (2-5mm) tissue and cartilage was made. As can be seen in Figure 4-59, the amplitudes of PCA-BSA signal decreased from the center to the minirods boundaries. This indicated that PCA-BSA was at first released near the matrix surface, before release occurred in the matrix interior. For tissue and cartilage only marginal ESR signals were observed with an additional change towards spectra of higher mobility. Hence, the labeled BSA was removed fast from the implantation site by diffusion phenomena after release from the collagen matrix.

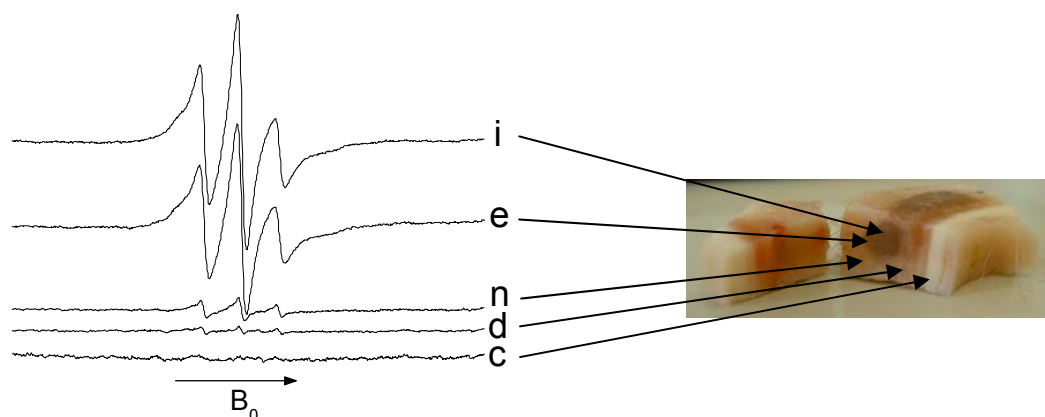


Figure 4-59 ESR spectra of 10mm PCA-BSA loaded bovine tendon EDC 1 cross-linked minirod 7d post implantation (i: center of the minirod, e: boundary of the minirod, n: tissue near the minirod, d: tissue distant from the minirod, c: cartilage)

The in vivo release of PCA-BSA was monitored for 56d. The spectral shape of PCA-BSA loaded extrudates before implantation represented a so called “powder” ESR spectrum (see Figure 4-60; pre-implantation). It indicates a “frozen state” of the label, e.g. a very low degree of mobility. These spectral shapes are expected in dry and solid matrices. The spectral shape of the implants changed significantly within the first 5d after implantation for all collagen species (see Figure 4-60; 5d). The anisotropy of the hyperfine interaction was partially averaged and the nitroxide reorientation time was in the range of few nanoseconds. The mobility was significantly increased compared to day zero, but still much lower compared to an aqueous solution, where the molecule reorients in the order of several hundred picoseconds (see Figure 4-52 top). It was concluded that water penetration into the implant occurred in vivo within 5d, going along with creation of an environment with intermediate viscosity. The resulting spectral changes of the first 5 days were comparable for all minirods. However, significant differences between the non cross-linked and EDC 1 cross-linked samples were found in the following days.

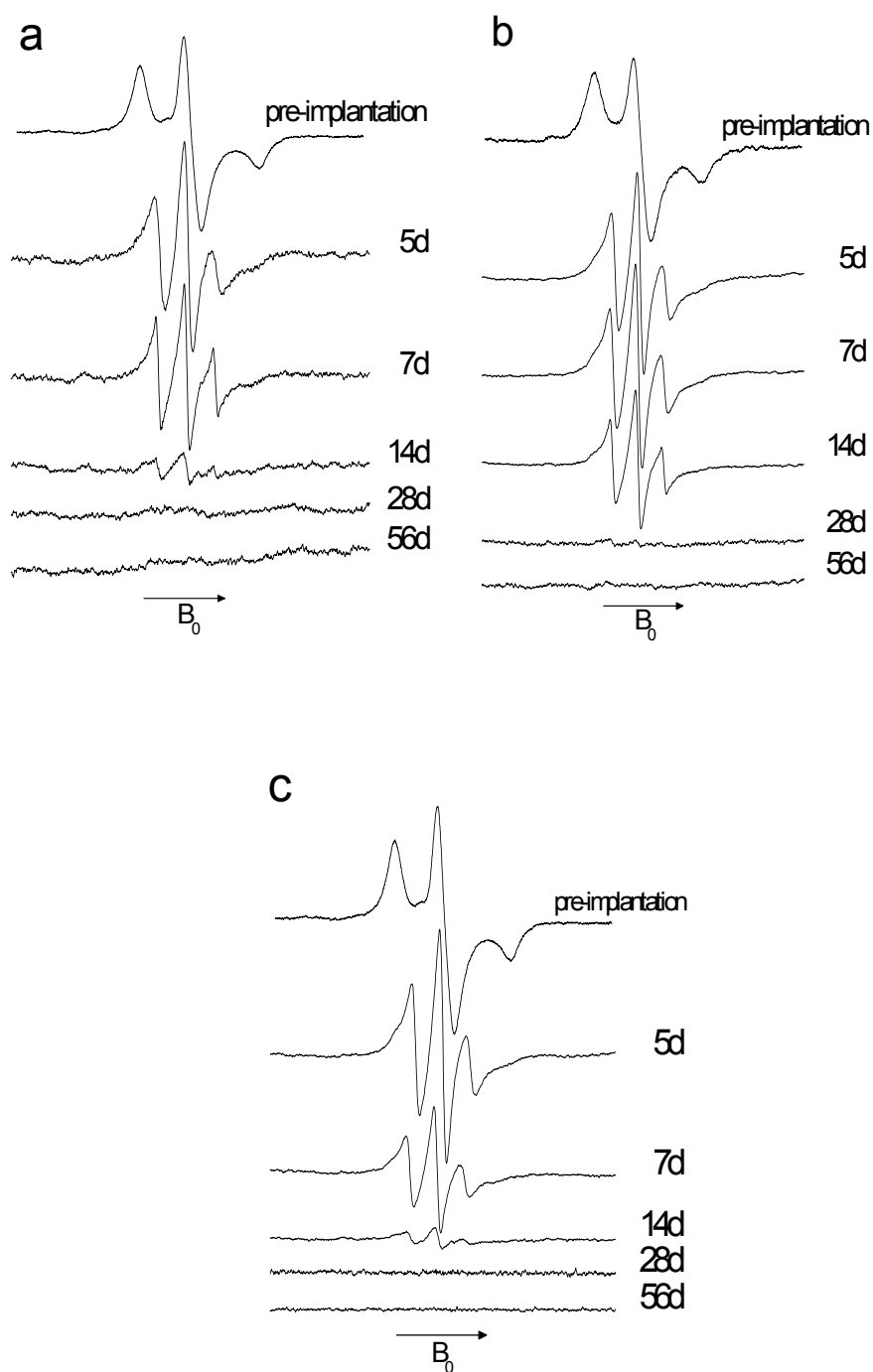


Figure 4-60 “Interior” ESR spectra of 10mm PCA-BSA loaded bovine tendon non cross-linked (a) and EDC 1 cross-linked (b) minirods and bovine corium EDC 1 cross-linked (c) minirods

The drug retention in the implant was determined by relative comparison of the signal amplitudes of the interior spectra. Signal amplitudes decreased over time for all three minirods until day 14. At day 28, only for bovine tendon EDC 1 cross-linked minirods a signal in the magnitude of the detection noise was detectable and after 56d no signal could be measured for any minirods (see Figure 4-60). Besides the decrease in signal amplitudes, only the spectra shape of PCA-BSA in non cross-linked bovine tendon extrudates altered (see Figure 4-60a). As was observed for the in vitro release (see 4.4.3), PCA-BSA mobility changed because release was mainly diffusion controlled. Almost no modifications in spectra shape were detected for PCA-BSA in EDC 1 cross-linked minirods (see Figure 4-60b, c), indicating that the model protein was immobilized and delivery after 5d was also dependent on matrix erosion. This observation was consistent with the conclusion drawn from the in vitro drug release from EDC 1 cross-linked matrices in the presence of collagenase (see 4.4.3).

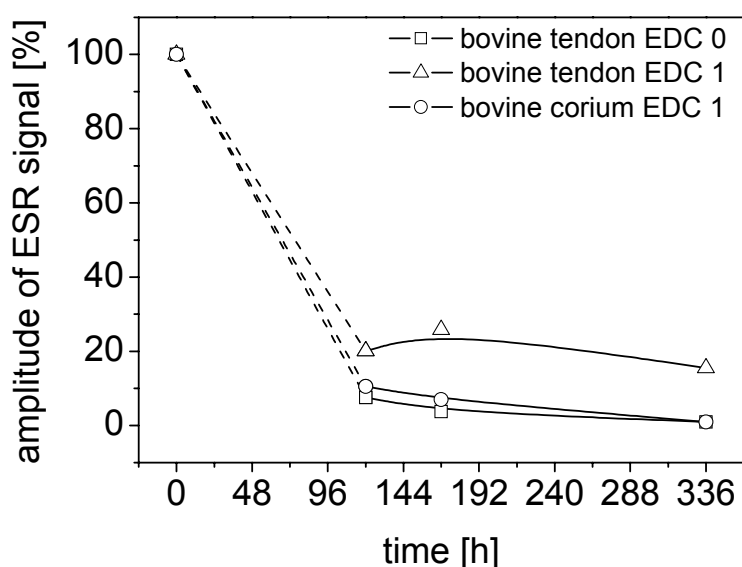


Figure 4-61 Signal amplitudes of ESR spectra of 10mm PCA-BSA loaded minirods post implantation (n=3)

After 7d, approximately 90% PCA-BSA was liberated from bovine tendon non cross-linked and bovine corium EDC 1 cross-linked minirods and release was completed within 14d (see Figure 4-61). In contrast, 20% PCA-BSA was still present in bovine tendon EDC 1 cross-linked minirods after 5d and release was finished not until 28d. The same rank order of in vivo release rates was observed as in the in vitro studies (see Figure 4-57).

Comparison of in vitro (see Figure 4-57) with in vivo data (see Figure 4-61) showed that besides the same release mechanism and the same order in release profiles, a similar magnitude in release time was observed. In general, in vivo release is often slower than in vitro, because water accessibility can be decreased and/or pH values can vary due to differences in buffer capacity (Lurie et al.; 2005). However, the main difference responsible for slower release in vivo is the implant encapsulation and consequently an additional diffusion barrier which hampers drug release (Anderson et al.; 1981). For our minirods only slight encapsulation was observed (see 4.4.5) and therefore the major reason for the slower in vivo release was the slightly restricted swelling and the slower degradation in pigs compared to the in vitro setups. Swelling was suppressed by surrounding tissue and the lower water content at the implantation site. Degradation was minimized because the restricted swelling hindered enzyme penetration and due to the lower in vivo enzyme concentrations. Analyzing all collected in vitro and in vivo data showed that in vitro and in vivo results were comparable. However, an in vitro - in vivo - correlation according to USP standards was not performed, because in vivo release data during the first 5d could not be collected.

4.4.5 Biocompatibility

In vivo performance of equine and bovine tendon non cross-linked and EDC 1 cross-linked and bovine corium EDC 1 cross-linked minirods were analyzed macroscopically and microscopically. In macroscopic studies, implants could be observed over 28d. The implants could be differentiated well from the surrounding tissue, because minirods were darker and denser than the

surrounding tissue. Miniroids were swollen, but their cylindrical shape was retained (see Figure 4-62).

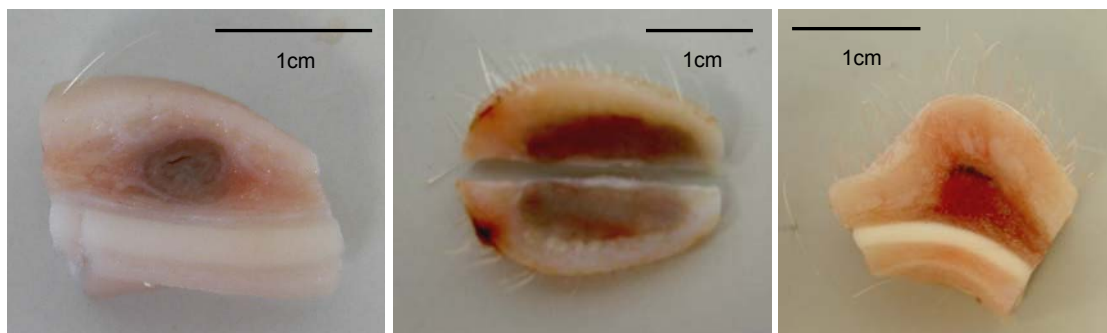


Figure 4-62 Sections of equine non cross-linked miniroid 7d (cross-section), 14d (lateral section) and 28d (cross-section) post implantation (from left to right)

To evaluate the biocompatibility of a material, in general two histological investigations are performed (Anderson; 1994). On the one hand the tissue response is evaluated with respect to degeneration of necrotic changes, inflammation, foreign body reactions and fibrosis. On the other hand, the cell types are characterized in more detail (Anderson; 1994). Histological evaluations of the miniroids were more difficult than macroscopic examinations, because the collagen extrudates contain collagen type I with traces of collagen type III. Since these collagen types are also present in tissue, differentiation between implants and surrounding tissue was challenging, especially because pig dermal collagen appears denser than human collagen structures (Burke et al.; 1983). Miniroids were identified by denser, more stained areas with atypical, non-native collagen bundle structures (Burke et al.; 1985). Additionally, especially at the later time points, cell accumulations gave hints where the miniroids had been implanted.

After surgical implantation acute and chronic inflammation reactions occur dependent on the implanted material, implantation site and the size, shape and motion of the device (Anderson et al.; 1981; Anderson; 1994). Usually antigenic reactions are detected during the first 72h post implantation (Soo et al.; 1993).

The first response to an injury is the migration of leukocytes, predominantly neutrophils, and the exudation of fluids and plasma proteins within minutes to days. This is followed by a chronic inflammation characterized by an increase in macrophages, monocytes and lymphocytes and proliferation of blood vessels and connective tissue. If normal wound healing takes place, the healing response is initiated by proliferation of macrophages and monocytes followed by appearance of fibroblasts and vascular endothelial cells and formation of granulation tissue. Subsequently, the foreign body reaction follows in which macrophages, fibroblasts and foreign body giant cells take part. This may lead finally to fibrosis or the formation of a fibrous capsule when particles with a size greater than 10 μ m were implanted (Medlicott et al.; 2004). If biomaterials are less biocompatible, body response ends at the stage of chronic inflammation and no further healing process is initiated (Anderson; 1994).

Almost no inflammation could be detected by interferon 1 β staining for all investigated insoluble collagen materials between day 5 and 56. Only superficial, slight inflammatory areas were observed, resulting from the administration of the solid, but rapidly swollen matrix (Hirasawa et al.; 1997) and the motion of the implant (Anderson et al.; 1981). Inflammatory reactions could be detected by TGF β staining and cell accumulations, most likely leucocytes.

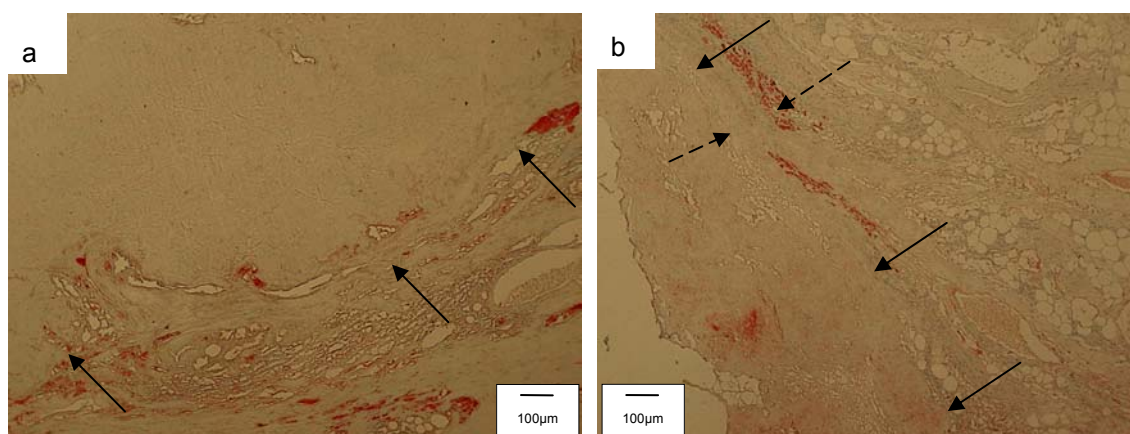


Figure 4-63 Equine non cross-linked (a) and EDC 1 cross-linked (b) minirod 3d post implantation (TGF β staining, solid arrows indicate boundaries of implant, dashed arrows: capsule)

TGF β staining was performed between day 3 and 28. Positive TGF β stained areas were detected near the implant boundaries up to day 14 (see Figure 4-63). This observation corresponded to the interferon 1β staining studies. Differentiation between mono-, lympho- and granulocytes was difficult, because no cell specific staining was performed. However, it was assumed that the observed cells were mainly mono- or lymphocytes due to the short life time of granulocytes. The immunogenic response was slightly more pronounced for non cross-linked materials which could be due to less washing steps during raw material preparation (Park et al.; 2002) and a faster collagen degradation. Since gelatin and gelatin peptides are chemotactic for neutrophils, an acute inflammatory response can be elevated (Weadock et al.; 1984). No further increase in cell number was observed for EDC 1 cross-linked matrices, indicating that this cross-linking ratio was suitable for in vivo applications (van Wachem et al.; 1994a). In general, equal performance was observed for materials with and without PCA-BSA, indicating that the in vivo performance of minirods was mainly dependent on the matrix material and not on the incorporated labeled model compound.

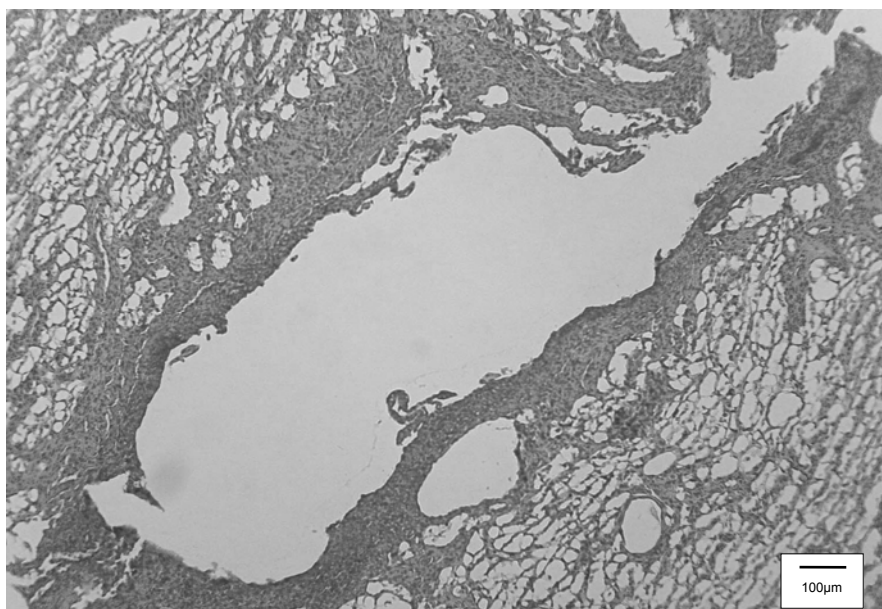


Figure 4-64 Remaining pocket of a bovine tendon non cross-linked minirod 5d post implantation (HE staining)

At days 3 and 5 post implantation, difficulties in cutting of bovine tendon specimens occurred. The minirods were pressed out during this preparation step, resulting in a cavity with sharp, cell rich boundaries from the implantation procedure (see Figure 4-64). The increase in cell number gave evidence that cells were attracted by the collagen minirods. Both equine and bovine corium EDC 1 cross-linked minirods were attached firmly enough to the surrounding tissue, to remain at their position. At day 3, cells were already attracted by the equine and bovine corium EDC 1 cross-linked minirods. This resulted in formation of a cellular capsule around the implants (see Figure 4-65b), because the additionally cross-links hindered cells to penetrate into the matrix core. Equine non cross-linked extrudates were also attached well to the surrounding tissue. Cells already started to invade the devices and consequently no distinct capsule around the implants could be detected (see Figure 4-65a).

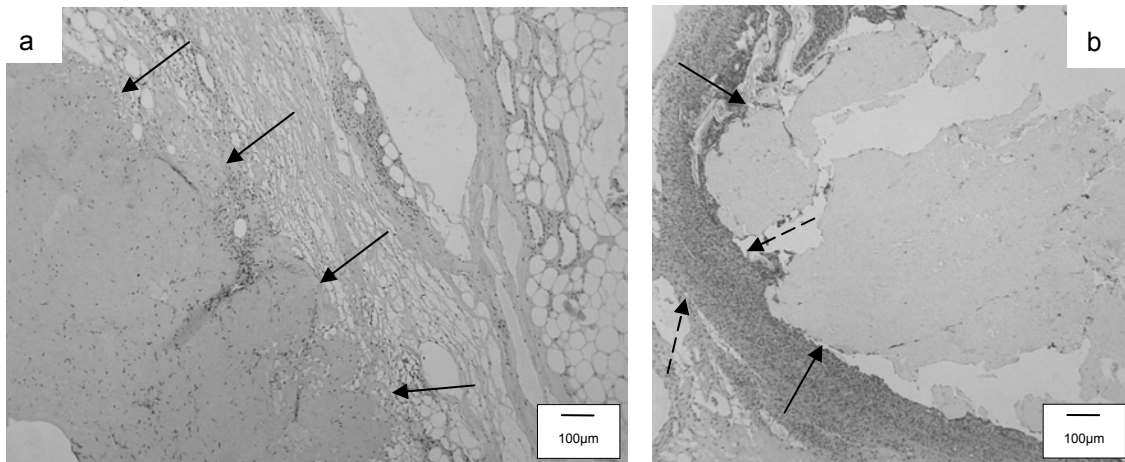


Figure 4-65 Equine non cross-linked (a) and EDC 1 cross-linked (b) minirod 3d post implantation (HE staining, solid arrows indicate boundaries of implant, dashed arrows: capsule)

After 7d, all materials were incorporated well and cells infiltrated the minirods (see Figure 4-66). Since minirods were swollen and fragmented, a mixed immune response could be observed. In the interior of the implant an acute inflammatory reaction, with a high number of presumably polymorphonuclear leukocytes, occurred. The cell number at the implant boundary decreased

slightly compared to day 3 and a chronic immune reaction with monocytes and lymphocytes took place (Anderson; 1994), which resulted in the formation of a thin capsule around the minirods.

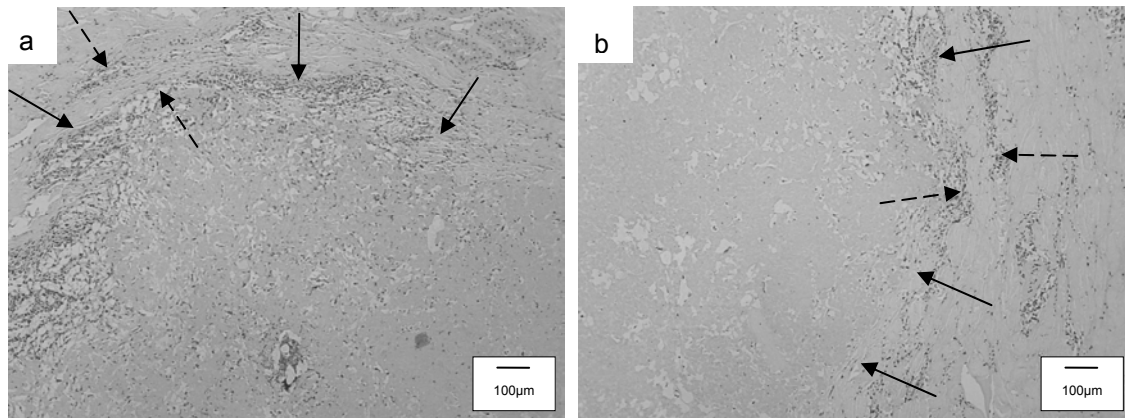


Figure 4-66 Equine non cross-linked (a) and EDC 1 cross-linked (b) minirod 7d post implantation (HE staining, solid arrows indicate boundaries of implant, dashed arrows: capsule)

Still a lower number of cells could be detected in the interior of equine EDC 1 cross-linked minirods compared to equine non cross-linked matrices (see Figure 4-66).

Looking closer at bovine tendon EDC 1 minirods, it was observed that the implant itself exhibited a porous structure which was surrounded by tissue with numerous cells (see Figure 4-67a). In spite of the different structure, incorporation had taken place, as can be seen by collagen I staining (see Figure 4-67b). Extrudate fragments were stronger stained than tissue. Cells, presumably monocytes, infiltrated the minirods and the implants were degraded. An exact boundary could not be detected anymore. The remodeling process could also be observed with this sample. During wound healing processes, collagen type III is the prevalent collagen type (Burke et al.; 1985) and can already be detected between day 2 and 7 after injury. In later wound healing phases, collagen type III is replaced by collagen type I (Sedlarik; 2005).

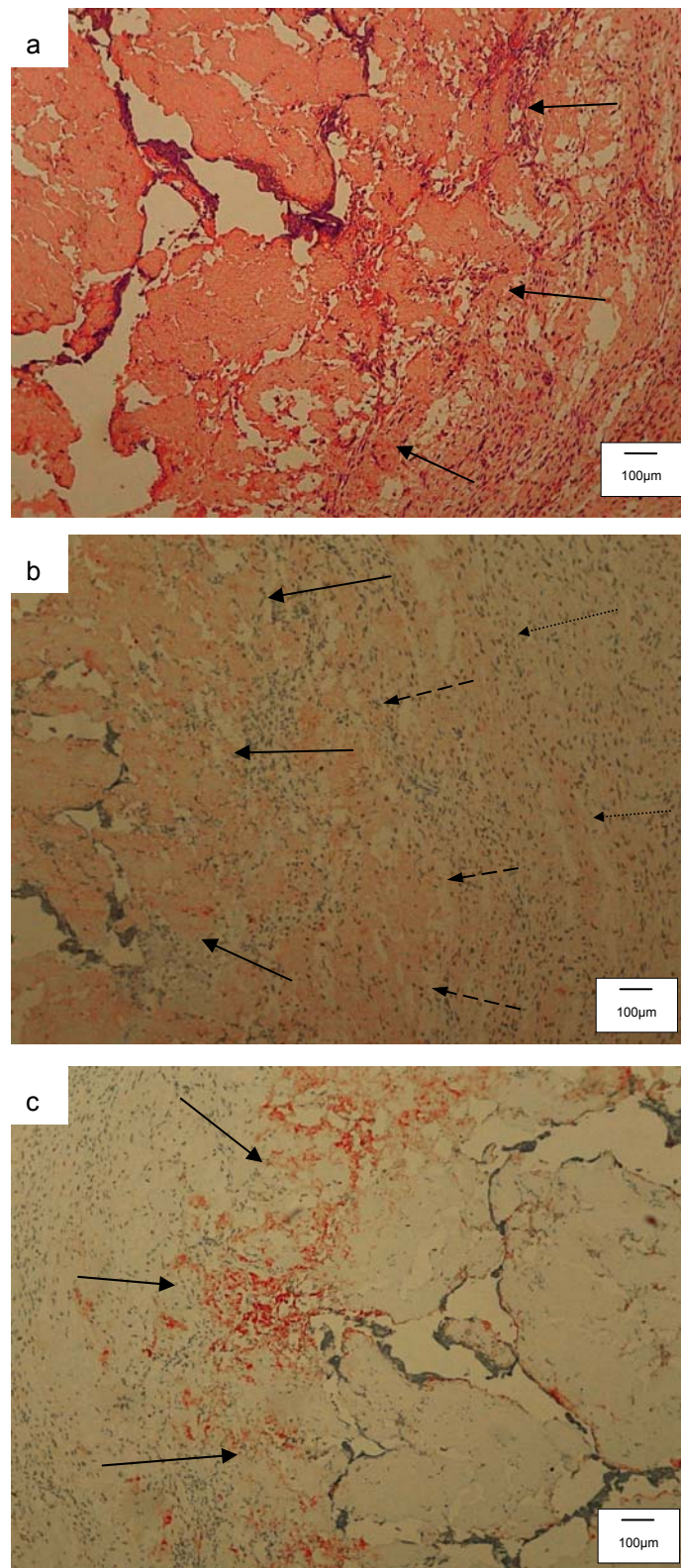


Figure 4-67 Bovine tendon EDC 1 minirod 7d post implantation (a) HE staining, (b) collagen I staining, (c) collagen III staining (arrows indicate boundaries of implant; in figure (b): solid arrows: inner implant, dashed arrows: transition, dotted arrows: tissue)

Collagen III staining showed, that inside the original extrudate boundaries, collagen type III was present and it was concluded that new collagen structures had been built (see Figure 4-67c).

After two weeks, the bovine corium EDC 1 minirods were degraded completely and at the site at which the sample had been implanted only a large cell accumulation could be detected (see Figure 4-68). This indicated that bovine corium EDC 1 extrudates stimulated a host response which caused fast implant degradation and replacement by newly formed collagen. A similar effect was observed by Burke et al. for a bovine dermal type I collagen (Zyderm[®]) suspension implanted in pigs (Burke et al.; 1983).

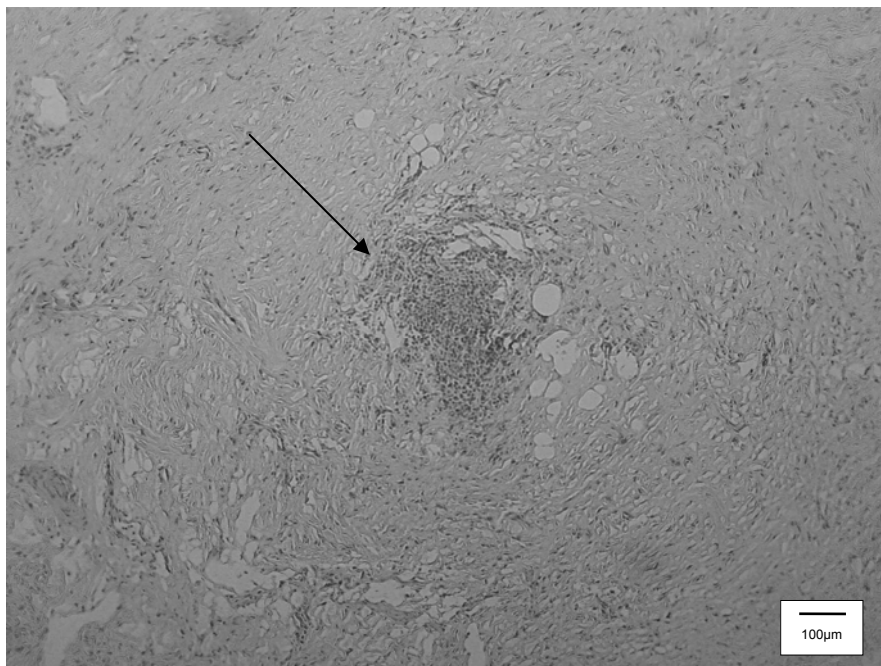


Figure 4-68 Bovine corium EDC 1 minirod 14d post implantation (HE staining, arrow indicates cell accumulation)

Bovine and equine tendon non cross-linked minirods were still present after two weeks and showed good incorporation into the surrounding tissue (see Figure 4-69a).

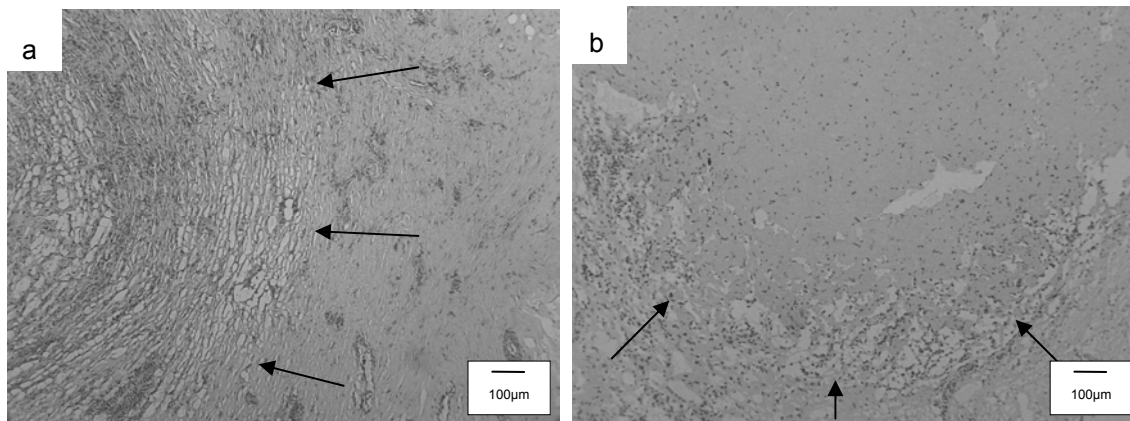


Figure 4-69 Equine non cross-linked (a) and EDC 1 cross-linked (b) minirod 14d post implantation (HE staining, arrows indicate boundaries of implant)

Both tendon EDC 1 cross-linked extrudates were also incorporated well and retained their homogeneous structure even longer than non cross-linked matrices. Only at the boundaries small cavities were observed, whereas still a compact implant core with several invaded cells existed (see Figure 4-69b).

After 28d, equine implants, independent of cross-linking, were infiltrated by many cells and extensive remodeling had taken place (see Figure 4-70). However, in contrast to bovine corium EDC 1 cross-linked extrudates after 14d (see Figure 4-68) shapes of minirods could still be detected.

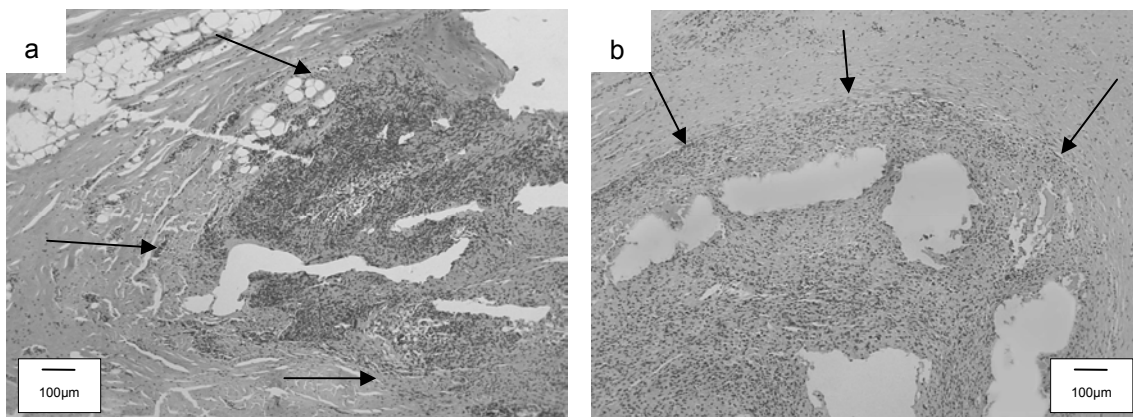


Figure 4-70 Equine non cross-linked (a) and EDC 1 cross-linked (b) minirod 28d post implantation (HE staining, arrows indicate boundaries of implant)

Collagen forms a swollen hydrogel after contact with physiological fluids. The swollen matrix is soft and elastic and minimizes mechanical and frictional irritation of the surrounding tissue (Anderson et al.; 1981). Consequently, a normal wound healing process was observed for collagen minirods. Additionally, protein adsorption can be prevented because of the hydrophilic mobile surface and the low adverse interaction between collagen and the aqueous biological environment (Park et al.; 1996). Taken these facts together, collagen has a good biocompatibility. Based on the histological data, the *in vivo* persistence of minirods was put in the following chronological order: bovine corium EDC 1 cross-linked minirods were taken up first (after 14d), followed by bovine tendon non cross-linked and EDC 1 cross-linked matrices and equine tendon non cross-linked extrudates. As was expected from DSC data (see 4.1.1.2), swelling (see 4.1.2.1.1) and degradation studies (see 4.3.3), the slowest degradation was observed for equine EDC 1 cross-linked minirods. All materials were degraded in a comparable way. Digestion occurred simultaneously to formation of new collagen structures without abnormally high inflammatory reactions. This was in agreement with the common assumption that only low inflammation takes place after collagen implantation, because of almost similar amino acid sequences of collagen flavors extracted from different species (Gilbert; 1988b). Consistent observations were made for the *in vivo* digestion of minipellets (Hirasawa et al.; 1997).

4.4.6 Summary

In vitro and *in vivo* studies were performed with BSA loaded minirods. For drug release studies, BSA was labeled with PCA. During labeling no protein aggregation occurred and BSA was not hydrolyzed in the presence of a crude bacterial collagenase mixture. *In vitro*, 80% PCA-BSA was released from bovine tendon non cross-linked minirods within 48h in absence of collagenase and after 7h in the presence of 0.1 μ g/ml enzyme. Bovine corium EDC 1 cross-linked matrices released 80% drug within approximately 80h and 12h, respectively. From bovine tendon EDC 1 cross-linked devices 80% release occurred after 168h without addition of collagenase and after 95h if 0.1 μ g/ml collagenase was present. The sequence of drug release was consistent for both experimental

setups. Hence, drug release and degradation were dependent on the used collagen material; more cross-links led to lower matrix degradation and decreased PCA-BSA release rates. In vitro drug release of FITC dextran 70 was compared with the in vitro PCA-BSA delivery and good correlation was found. This indicated that FITC dextran 70 is suitable as a model “protein” drug and correlations based on the molecular weight can be made. In vivo PCA-BSA release was slightly more delayed than in vitro, because swelling of the minirods was more restricted and the devices were degraded more slowly in pigs compared to the in vitro setup. 80% PCA-BSA was delivered after 96h from bovine tendon non cross-linked and bovine corium EDC 1 cross-linked extrudates, whereas bovine tendon EDC 1 cross-linked minirods showed 80% release after 120h.

Mechanistic studies, performed in vitro, showed that swelling and diffusion controls the drug release in pure Tris buffer pH 7.5 for minirods, irrespective of cross-linking degree. For bovine tendon non cross-linked matrices this was also the dominating mechanism if collagenase was present. In contrast, EDC 1 cross-linked devices exhibited a release which was also dependent on matrix erosion. In the in vivo studies, similar release mechanisms as in the in vitro investigations with 0.1µg/ml collagenase were detected for all three collagen materials. Since it was possible to investigate different parts of the minirods in the in vivo experiments, it could further be demonstrated that the PCA-BSA release started at the matrix surface before release occurred inside the minirods. In vitro - in vivo – comparison demonstrated that minirods behave equally in vitro and in vivo and that the period of release was in the same magnitude of time.

Histological investigations of seven different minirods were performed (bovine tendon non cross-linked and EDC 1 cross-linked, bovine corium EDC 1 cross-linked and equine tendon non cross-linked and EDC 1 cross-linked collagen matrices with incorporated PCA-BSA and drug free equine and bovine tendon non cross-linked collagen minirods). All devices were tolerated well, because no severe foreign body reaction was detected. The time course of the observed host digestion, resembling normal tissue turnover, was dependent on the

collagen material. Bovine corium EDC 1 cross-linked minirods were taken up fastest, followed by the bovine tendon non cross-linked, the bovine tendon EDC 1 cross-linked and the equine non cross-linked matrices. The slowest adsorption was observed for equine EDC 1 cross-linked minirods. This order was consistent with the increase in cross-links from bovine to equine collagen materials. Since this remodeling process is required to avoid a surgical implant removal after drug depletion, prospects for in vivo application were promising.

4.5 Mathematical Model of the Erosion Controlled Drug Release from Collagen Devices

Since therapy with higher molecular weight drugs, e.g. proteins, attains more and more attraction, a mechanistic model for the release of macromolecules was developed. Swelling and diffusion controlled drug release of indomethacin and gentamicin from dense collagen devices were modeled by Radu et al. (Radu et al.; 2002). Fickian diffusion and concentration dependent diffusion coefficients of water and drug were assumed. If collagenous matrices are implanted parenterally, several processes occur simultaneously. Besides drug release by swelling and diffusion, delivery dependent on matrix erosion takes places (see 1.2.3.2). To adapt the model of Radu et al. to in vivo circumstances the influence of device erosion on drug release has to be incorporated into the mathematical model. A model dealing exclusively with drug release controlled by matrix erosion was developed, using experimental results obtained in the previous chapters. Subsequently, both models could be combined to achieve a model which describes the entire drug delivery properly.

4.5.1 Model Development

The model is designed for a matrix of cylindrical geometry with length l and diameter d , which consists of a homogeneous polymer (= collagen) with uniformly dispersed drug. Collagen is a hydrogel and swells after contact with aqueous solutions and a collagen fiber mesh with aqueous (drug) solution is assumed during the drug release (see Figure 4-71). Due to the assumed uniform collagen and drug distribution inside the collagen minirods, only the radial degradation and release was simulated.

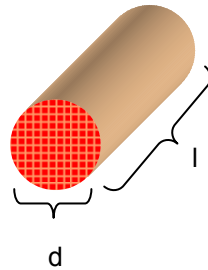


Figure 4-71 Schematic illustration of a cylindrical drug device with diameter d and length l (bright mesh symbolizes collagen network, dark areas drug solution)

In the model dealing exclusively with drug release controlled by matrix erosion a fully swollen matrix is assumed to eliminate the effect of swelling on the drug release. To describe the interaction between collagenase and collagen properly, three steps have to be considered: diffusion of collagenase towards the collagen substrate, adsorption onto the collagen surface and subsequently collagen degradation (see Figure 4-72).

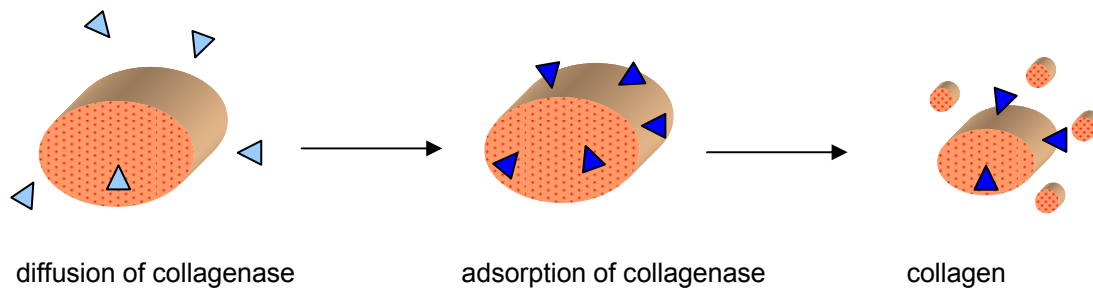
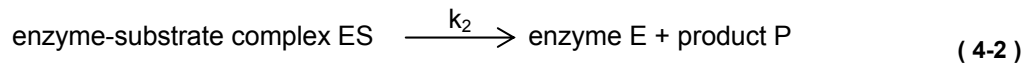
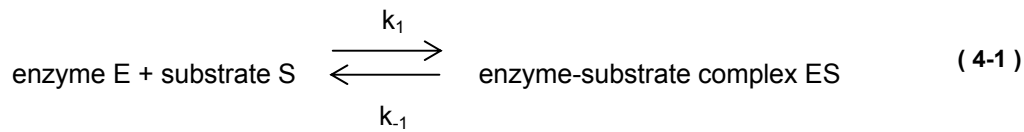


Figure 4-72 Schematic illustration of degradation of collagen minirods (\triangle free collagenase, \blacktriangle adsorbed collagenase)

The common reaction scheme for an enzymatically catalyzed degradation process was proposed by Michaelis and Menten (Cornish-Bowden; 1999) and can be summarized by:



k_1, k_{-1}, k_2 are rate parameters: k_1 describes the adsorption of collagenase onto the collagen fiber, k_{-1} the dissociation of the ES complex without degradation (in general zero (Tzafriri et al.; 2002)) and k_2 the degradation process. The degradation was assumed to be the rate-limiting step, because equilibrium in adsorption was already obtained within 1h (see 4.2.3), whereas degradation last longer (see 4.3). This was in agreement with Tzafriri et al., who modeled the degradation of sparsely fibrillar collagen gels by human skin fibroblast collagenase (Tzafriri et al.; 2002). Hydrolytic erosion of a solid polymer matrix can occur by two extreme mechanisms (see 1.2.3.1). Heterogeneous erosion is restricted to the surface of the device and the undegraded carrier remains chemically intact during degradation. Homogeneous erosion, such as erosion of non cross-linked collagen matrices, involves random cleavage at a uniform rate throughout the complete matrix. While the molecular weight of the polymer decreases steadily, the matrix can remain essentially mechanically intact until 90% of the polymer is degraded. Then mass loss and disintegration of the device starts. In the model for the release of chlorhexidine gluconate from a cross-linked gelatin chip, Tzafriri assumed solely matrix bulk erosion (Tzafriri; 2000). For our dense collagen matrices a combination of surface and bulk erosion is assumed (see 4.3.2.2). Due to enzyme binding at its reaction sites and the dense matrix structure, which hinders diffusion of enzymes and degradation products, it would be incorrect to consider pure bulk erosion. A pure surface erosion, as was proposed by Tzafriri et al. for the degradation of dense collagen fibers (Tzafriri et al.; 2002), would also not reflect the complete digestion process properly, because it was demonstrated that a fully swollen matrix showed a higher degradation rate than a still swelling device (see

4.3.2.2). From these observations it was concluded that a limited collagenase penetration into the collagen matrix is possible and that both processes must be combined. On the one hand tropocollagens can only be eroded at their surface (Steven; 1976), whereas on the other hand the complete collagen extrudate undergoes bulk erosion. Further basic assumptions in the model are that the diffusion of collagenase towards the collagen surface is assumed to be Fickian and that the Michaelis-Menten scheme does not describe the degradation in sufficient detail. The degradation rate k_2 is dependent on the concentration of collagen and collagenase and increased with higher concentration of collagenase (see 4.5.2.1). Because the enzymatic reaction of an insoluble substrate is modeled, degradation is limited by the enzyme reaction sites on the surface of collagen (see 1.3.1.2). These effects are taken into account by equation (4-3).

$$\partial_t C_E - \nabla \cdot (D_E(C_C) \nabla C_E) + k_{act} C_E = -k_1(C_E)^n C_C + k_2 C_{ES}^{\gamma} \quad \text{in } J \times \Omega \quad (4-3)$$

$$\partial_t C_{ES} = k_1(C_E)^n C_C - k_2 C_{ES}^{\gamma} \quad \text{in } J \times \Omega \quad (4-4)$$

$$C_E = C_E^{ext} \quad \text{in } J \times \Gamma \quad (4-5)$$

$$C_E = 0 \quad \text{on } 0 \times \Omega \quad (4-6)$$

$$C_{ES} = 0 \quad \text{on } 0 \times \Omega \quad (4-7)$$

$$\partial_t C_C = -k_1(C_E)^n C_C \quad \text{in } J \times \Omega \quad (4-8)$$

$$C_C = C_C^0 \quad \text{on } 0 \times \Omega \quad (4-9)$$

C_E, C_{ES}, C_C denote the concentrations, expressed in mole per volume, of free enzyme E , enzyme-collagen complex ES and collagen C , respectively. Ω is a bounded domain in \mathbb{R}^2 with a sufficiently smooth boundary $\Gamma = \partial\Omega$. $J = (0, T]$ denotes a finite interval with final time T . In (4-3) k_{act} represents a constant rate modeling the loss in enzymatic activity over time in the incubation medium

which was determined in 4.2.1. In contrast to Tzafriri et al. (Tzafriri et al.; 2002), a Freundlich isotherm is implemented (see (4-8)). Based on experimental results (see 4.2.3), it was demonstrated that the Langmuir adsorption isotherm does not describe the adsorption process adequately. n represents the index of the adsorption reaction, which is often set as a positive number (e.g. 2/3 (McLaren et al.; 1970)). γ describes the dependency of the degradation rate on the concentration of the ES complex. This relationship was investigated in 4.5.2.1. The initial concentration of the enzyme and of the ES complex in the matrix is zero and at the boundary $C_E = C_E^{ext}$ is prescribed, where C_E^{ext} denotes the enzymatic concentration in the ambient medium. For the diffusion coefficient of the enzyme in the matrix (D_E) a Fujita like dependence on the concentration of collagen C_C is assumed (free volume theory (Fujita; 1961)), i.e.

$D_E = D_E^0 \exp(-\beta_E \frac{C_C}{C_C^0})$, where D_E^0 is the diffusion coefficient of the enzyme in water, C_C^0 the initial concentration of collagen and β_E a dimensionless parameter (Thombre et al.; 1985). An almost free diffusion of enzyme inside the completely swollen matrix was assumed (Siepmann et al.; 1999a; Tzafriri; 2000).

After matrix digestion, degraded collagen fragments P and drug molecules A are released by diffusion. Diffusion is instantaneously compared to the time scale of degradation (Tzafriri et al.; 2002).

$$\partial_t C_P - \nabla \cdot (D_P \nabla C_P) = k_2 C_{ES}^\gamma \quad \text{in } J \times \Omega \quad (4-10)$$

$$C_P = 0 \quad \text{in } J \times \Gamma \quad (4-11)$$

$$C_P = 0 \quad \text{on } 0 \times \Omega \quad (4-12)$$

C_P denotes the concentration of the hydrolyzed collagen fragments which can diffuse out of the matrix. A constant diffusion coefficient of the collagen fragments is assumed and the initial concentration of the product in the matrix is zero.

According to Tzafriri (Tzafriri; 2000), the drug load is composed of two pools: one part which can diffuse freely inside the swollen matrix and the other part which is immobilized by the polymer due to physical or chemical entrapment and can only diffuse after matrix degradation. Weadock drew a similar conclusion from adsorption studies (Weadock; 1986) and assumed that drugs in collagen membranes exhibit a dual sorption behavior; one drug fraction can diffuse freely inside the collagen membrane, whereas the diffusion of the other part is restricted because of reversible interactions with the collagen device. Since for FITC dextrans and BSA no chemical interactions with collagen could be detected (see 4.4.3), it was assumed that the drugs were only immobilized physically and drug liberation is proportional to the number of cross-links. Drug delivery is governed by a diffusion equation with a source term due to liberation of the immobilized drug by matrix degradation. Thus, writing a mass balance the following equation is obtained.

$$\partial_t C_A - \nabla(D_A(C_C)\nabla C_A) = -\partial_t C_{Ai} \quad (4-13)$$

C_A, C_{Ai} denote the concentrations of free (A) and immobilized drug (A_i), respectively. The incorporated drug is released by a diffusion mechanism influenced by a concentration gradient. The diffusion is restricted because of the physical entrapment. This effect is represented by the source term $\partial_t C_{Ai}$. Due to matrix degradation occurring simultaneously, the matrix phase through which the diffusion takes place, changes continuously as a function of the extent of collagen hydrolysis. The diffusion coefficient of the drug within the matrix can not be considered as constant, but as a function of the fluid and/or collagen concentration. According to the free volume theory (Fujita; 1961) the diffusion coefficient is given by $D_A = D_A^0 \exp(-\beta_A \frac{C_C}{C_C^0})$, where D_A^0 denotes the diffusion coefficient of the drug in water and β_A a dimensionless constant (Thombre et al.; 1985).

To complete the model, a relation between the concentrations of free and immobilized drug is needed (see Figure 4-73). A general functional dependency

$C_{Ai} = \sigma C_C^\ominus$ is assumed. σ is a dimensionless constant, which was determined in 4.3, denoting the immobilizing capacity of the polymer which is equal to the number of hindering cross-links or entanglements per mole of the fully swollen substrate and θ is a correlation factor, determined in 4.5.2.2. In contrast to Tzafriri (Tzafriri; 2000), a non-linear relationship between the immobilized drug and substrate concentration is valid.

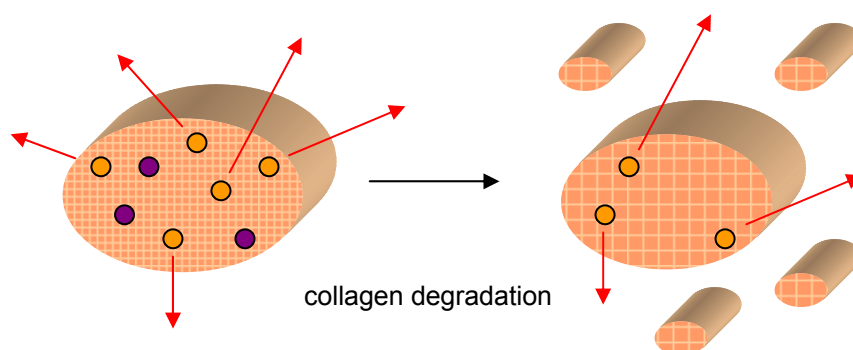


Figure 4-73 Schematic illustration of the mobile ● and immobile ● drug pool; hindrances are reduced after matrix degradation and the immobilized drug fraction becomes mobile

The model is completed by implementing Dirichlet boundaries. Calculations were performed with the software package “UG”.

In summary, a mathematical model was developed which describes the drug release controlled by matrix erosion from dense collagen extrudates. In some parts, similar assumptions were made as in the models proposed by Tzafriri (Tzafriri; 2000; Tzafriri et al.; 2002). With our model additional applications are possible, because equations for higher molecular weight drugs are implemented and the erosion of a dense collagen matrix is modeled.

4.5.2 Additional Parameters Needed for the Model

4.5.2.1 Dependency of k_2 on the Enzyme Concentration

In general, a linear relationship between enzyme concentration and degradation rate is observed, which levels off at very high enzyme concentrations (Gilbert; 1988b). In literature, several studies investigated this dependency. Mallya et al.

established a quantitative assay for the hydrolysis of different soluble collagen types by collagenase. A linear relationship between the initial reaction velocities and the collagenase concentrations was found and it was concluded that the reaction follows a first-order kinetic with respect to the enzyme concentration (Mallya et al.; 1986). Huang et al. investigated the degradation of insoluble bovine tendon collagen tapes and a first-order dependency with respect to the collagenase concentration was also detected (Huang et al.; 1977). Gilbert also assumed a linear relationship between the initial degradation rate of cross-linked atelocollagen matrices and collagenase concentrations between 0 and 200 units (Gilbert; 1988b). If a non-linear function would be fitted, even the complete range from 0 to 500 units is included (see Figure 4-74).

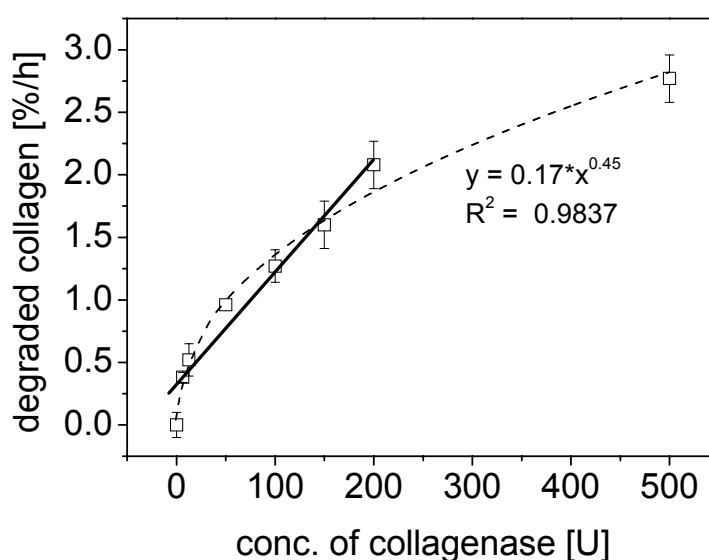


Figure 4-74 Initial degradation rate of GTA cross-linked random fibril collagen discs (45% ϵ -blocked amino groups) versus collagenase concentration (adapted from Figure 38 from (Gilbert; 1988b))

Rubingh differentiated between a soluble substrate (N-succinyl-alanine-proline-phenylalanine-p-nitroanilide) and an insoluble substrate (Azocoll) (Rubingh et al.; 1992). A linear dependency on the enzyme concentration was found for the degradation of the soluble substrate, whereas the relationship between enzyme

concentration and degradation rate was more complex for the insoluble Azocoll. For two enzymes a linear correlation was found, but for one protease an adsorption isotherm like function was observed. The adsorption isotherm type was assumed to describe the circumstances more precisely, because the degradation of insoluble substrates is dependent on the adsorption of the enzyme and on the substrate surface ((Rubingh et al.; 1992) and 4.2.4). This hypothesis was manifested by Rubingh et al., because a linear plot of the degradation rate versus the enzyme surface concentration was obtained (Rubingh et al.; 1992).

For our mathematical model, a function which describes the relationship between the turnover number k_2 and very low enzyme concentrations is needed. Since the ES complexes could not be measured directly, the dependency on the enzyme concentration was investigated. The degradation of equine non cross-linked minirods was investigated. A non-linear dependency on the enzyme concentration, which resembled the results obtained by Gilbert (Gilbert; 1988b) and Rubingh et al. (Rubingh et al.; 1992), was detected (see Figure 4-75).

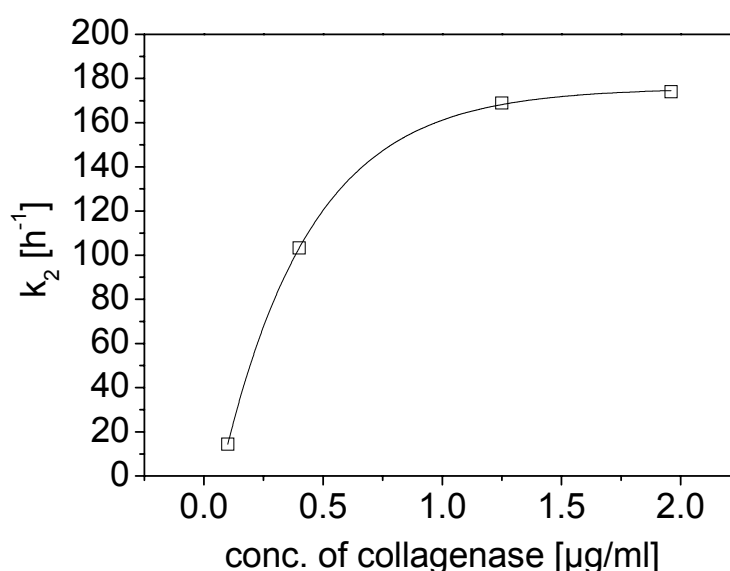


Figure 4-75 Dependency of the degradation rate of equine non cross-linked minirods on the concentration of collagenase

It was concluded that the degradation rate is also not linearly dependent on the concentration of ES complexes. This manifested indirectly the assumption that the Michaelis-Menten equation without consideration of adsorption phenomena would not describe the degradation of insoluble collagen properly. Therefore, a factor γ was introduced into equations (4-3) and (4-10) to describe the degradation process more precisely.

4.5.2.2 Correlation Between Immobile Drug and Degraded Collagen

Tzafiriri proposed a correlation between the immobilized drug fraction and the hindering properties of the drug matrix (Tzafiriri; 2000). It was demonstrated that both model compounds, FITC dextrans and BSA, showed no chemical interactions with the collagen matrix (see 4.4.3). Therefore, the immobilizing capacity σ of the dense collagen extrudates was attributed completely to physical interactions arising from the dense matrix structure and in particular from cross-linkages between the collagen bundles. A non-linear relationship between the immobilized drug fraction and the degraded collagen amount was found (see Figure 4-76 and Table 4-6).

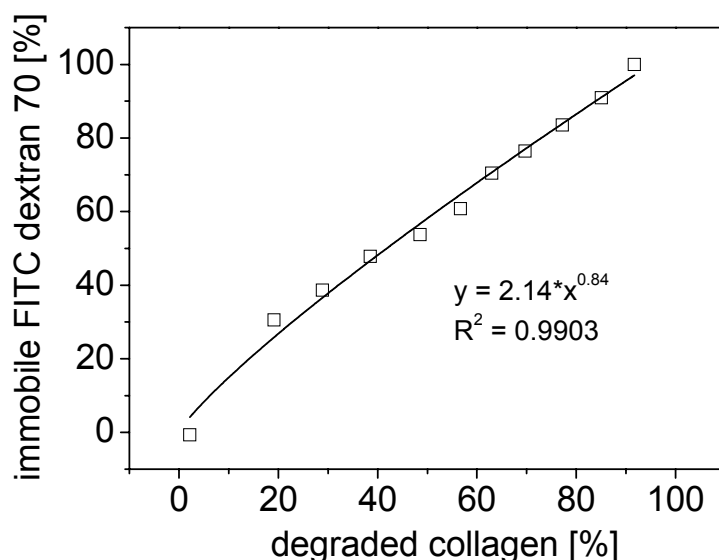


Figure 4-76 Determination of θ of bovine corium EDC 1 cross-linked minirods containing FITC dextran 70 (incubated with 0.1 μ g/ml collagenase)

Since values of σ and θ were dependent on the used collagen material and the incorporated FITC dextran, the proposal that the degradation is independent of the incorporated drug (Tzafiriri; 2000) could not be confirmed. In contrast, as was already assumed in 4.3.5, the degradation of our minirods was dependent on the incorporated drug, presumably due to the different apparent matrix densities (see Table 4-1).

Table 4-6 Immobilization constants of Figure 4-76 (average \pm SD; n=3)

Sample	1% FITC dextran load	Function $C_{Ai} = \sigma C_C^\theta$	R ²
equine non cross-linked minirod	FITC dextran 20	$\theta=0.84$	0.9839
	FITC dextran 70	$\theta=1.97$	0.9756
	FITC dextran 150	$\theta=1.36$	0.9584
equine EDC 1 cross-linked minirod	FITC dextran 20	$\theta=1.97$	0.9660
	FITC dextran 70	$\theta=1.51$	0.9629
	FITC dextran 150	$\theta=0.69$	0.9332
bovine corium EDC 1 cross-linked minirod	FITC dextran 70	$\theta=0.84$	0.9903

Based on the values of σ , determined in 4.3, the exact value of σ was calculated during the simulation according to $\sigma = C_C^\theta / C_{Ai}$ for each time point.

4.5.3 Data used for Fitting the Model

The following assumptions and parameters are used in the model.

Table 4-7 Fundamental assumptions of the model

Reaction	Assumption
Diffusion	Fick's second diffusion law with Fujita like diffusion coefficients
Adsorption	Freundlich adsorption isotherm
Degradation	Michaelis-Menten kinetic with adsorption dependencies
Release	two drug pools: <ul style="list-style-type: none"> ➤ mobile drug released by diffusion (and swelling) ➤ immobile drug released by matrix erosion and subsequent diffusion

Table 4-8 Experimentally determined parameter used in the model

Parameter	Value
Ω	matrix dimensions (length and diameter of the extrudate)
J	time interval during which the matrix is degraded
C_E^{ext}	enzyme concentration in the ambient medium
C_C^0	collagen concentration of the fully swollen matrix
C_A	drug concentration which can be released in absence of collagenase = mobile drug fraction (determined in 4.3)
C_{Ai}	drug concentration which is entrapped inside the matrix if no collagenase is added = immobile drug fraction (determined in 4.3)
k_{act}	rate of loss in enzymatic activity (determined in 4.2.1)

D_E^0	diffusion coefficient of collagenase in water (determined in 4.3.1)
D_P^0	diffusion coefficient of collagen fragments in water (determined in 4.3.1)
D_A^0	diffusion coefficient of FITC dextran 70 in water (determined in 4.3.1))
k_2	degradation rate (determined in 4.2.4)
θ	immobilization dependency (determined in 4.5.2.2)

4.5.4 Elaboration of the Implemented Parameters

To test the developed mathematical model, sensitivity analyses were performed. Based on an optimal parameter set for the release of FITC dextran 70 from bovine corium EDC 1 cross-linked minirods (see 4.5.5.2), the influence of individual parameters was simulated.

4.5.4.1 Sorption Parameters

The adsorption process was implemented in equations (4-3) and (4-8).

4.5.4.1.1 Type of Sorption Isotherm

In literature, three different types of enzyme adsorption isotherms on insoluble substrates were proposed (see 1.3.1.1). Therefore, the Freundlich sorption isotherm was compared with the Langmuir isotherm and a combination of Langmuir and Freundlich (see Figure 4-77). The Langmuir isotherm approached a maximum in adsorption, because only an enzyme monolayer can be adsorbed. This resulted in very slow collagen degradation. Implementing the Freundlich isotherm led to a faster digestion, because more enzyme molecules can be adsorbed and consequently more ES complexes can be built. A combination of both isotherms resulted in a collagen degradation between the individual sorption isotherms, because effects were combined.

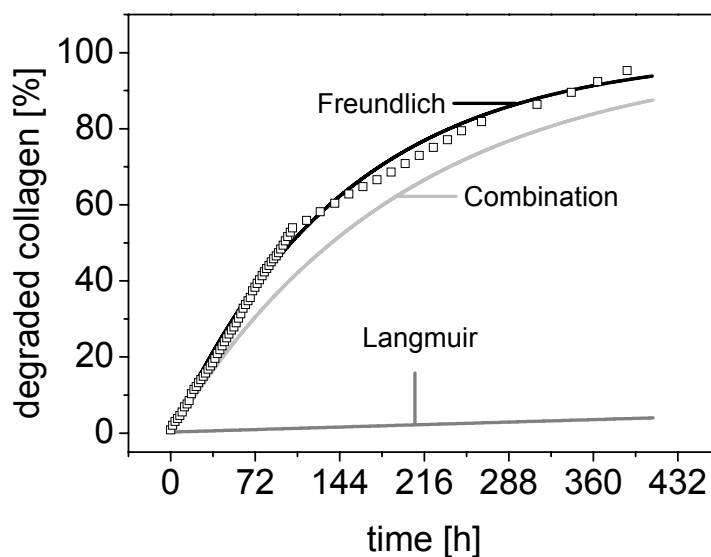


Figure 4-77 Variation in the sorption isotherm of collagenase on insoluble bovine corium EDC 1 cross-linked collagen minirods (dots represent experimental data)

On the basis of the experimental results (see 4.2.3) and the modeled adsorption variations (see Figure 4-77), a Freundlich sorption isotherm was implemented into the model. This isotherm contains two parameters which were tested for their influence: the Freundlich sorption exponent n and the sorption rate k_1 .

4.5.4.1.2 Freundlich Sorption Exponent n

If enzyme adsorption follows the Freundlich isotherm more than a monolayer of enzymes can be adsorbed on the collagen surface, resulting in different surface covering states. Consequently, Gyani defined four extremes of n (Gyani; 1945). The adsorption between two immiscible liquids yields $n=1$. Values lower than 1 are valid, when adsorption between a solid and a liquid is investigated. Complete surface coverage of a smooth solid is presented by $n=2/3$. When $n=1/3$ is observed, only adsorption on edges and cracks of the solid takes place and only distinct points are covered when $n=0$ (Gyani; 1945). If n is between $1/3$ and $2/3$, adsorption on edges and cracks and surface adsorption

occur simultaneously. If $n > 2/3$ is valid, penetration of the solute into the solid can take place (McLaren; 1963).

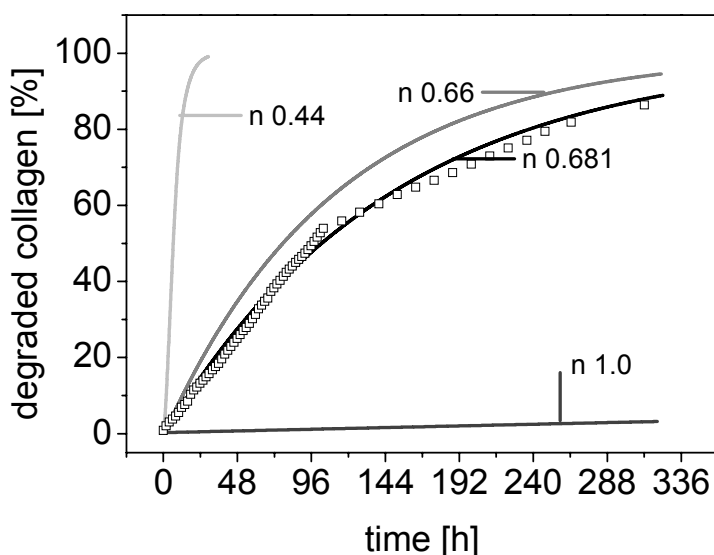


Figure 4-78 Variation in the sorption constant n : theoretical values and optimal fitted value for the degradation of bovine corium EDC 1 cross-linked minirods (dots represent experimental data)

For a theoretical evaluation, sorption constants of different levels were compared (see Figure 4-78). Based on the wrong assumption that the substrate is also soluble, $n=1$ resulted in almost no degradation. Digestion increased by reducing the value of n . The most promising results were obtained close to $n=2/3$. Further reduction, e.g. to $n=0.44$, led to a more pronounced degradation, which did not reflect the circumstances of the in vitro collagen minirod degradation. Experimental data indicated that n is in the range of $2/3 < n < 1$ (see Figure 4-28), and that collagenase can penetrate into the collagen minirods. This range was investigated in more detail and best results were found for n near $2/3$ (most promising value 0.681). Hence, the enzyme solution covered the complete collagen minirod surface and not only elevations which arise from the extrusion process. Furthermore, this observation

manifested the assumption that not only surface erosion took place, but that collagenase could also penetrate into the collagen device and could degrade collagen molecules inside the matrices.

4.5.4.1.3 Sorption Rate k_1

Variation in the sorption rate k_1 was based on the experimentally determined k_2 -value (k_2 (bovine corium EDC 1 cross-linked minirods) = 51.4h^{-1} , see Table 4-5). If adsorption is fast ($k_1 > k_2$), the influence of adsorption is diminished and the overall reaction rate is determined by the degradation itself. The adsorption process becomes the rate limiting step, if a lower value is used ($k_1 < k_2$). This indicated that adsorption had a strong influence on the degradation of collagen (see Figure 4-79). Based on the experimental results, degradation was assumed to be the rate limiting process, because adsorption already reached equilibrium within 1h (see 4.2.3).

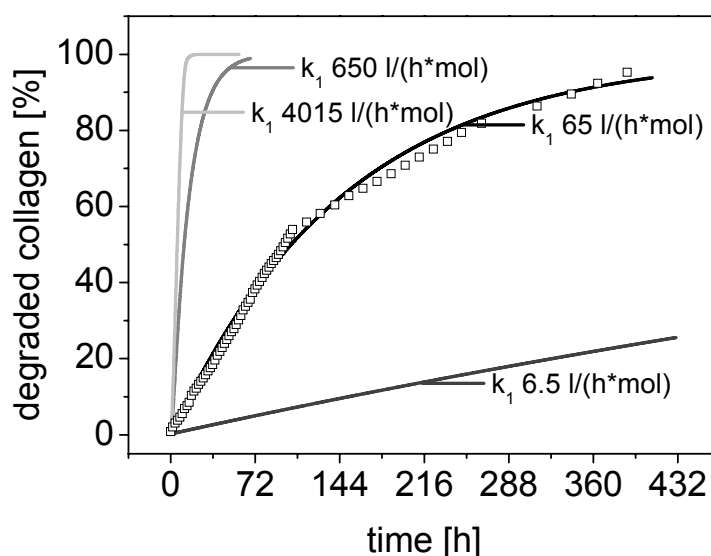


Figure 4-79 Variation in the sorption rate k_1 : calculated value (k_1 4015 l/(h*mol)) and fitted values for the degradation of bovine corium EDC 1 cross-linked minirods (dots represent experimental data)

Since the development of the intermediate ES complex could not be measured directly, k_1 was fitted. Two approaches were followed. In the first simulations, a typical Michael-Menten reaction is assumed and k_1 was determined by $k_1 = \frac{k_2}{K_M}$, similar as was done by Tzafirri (Tzafirri et al.; 2002). However, this approach must be handled with care, because the hydrolysis of insoluble collagen by bacterial collagenase did not follow the original Michael-Menten kinetics. Therefore, the next approaches were made by a direct fitting of k_1 .

If the k_1 -value was increased, collagen was degraded faster, because of an excess of adsorbed enzymes. $k_1=4015 \text{ l/(h}\cdot\text{mol)}$ was determined by $k_1 = \frac{k_2}{K_M}$ (Tzafirri et al.; 2002). This value did not reflect the in vitro collagen degradation properly, because digestion was too fast. In addition, the assumption that the Michaelis-Menten kinetic did not describe the degradation of insoluble collagen properly could be confirmed. The most promising value for k_1 was obtained for $65 \text{ l/(h}\cdot\text{mol)}$. Higher values resulted in a high degradational turnover, because enzyme adsorption is very fast and many enzyme molecules are adsorbed at the collagen surface and can build ES complexes. Lowering the k_1 -value decreased the digestion rate, because not enough ES complexes can be built to maintain the digestion rate and the degradation becomes adsorption dependent. $k_1=65 \text{ l/(h}\cdot\text{mol)}$ was implemented into the model, because this fitted value simulated the experimental observations best.

In summary, it was demonstrated that all parameters connected with the collagenase adsorption have a strong influence on the simulated collagen degradation.

4.5.4.2 Degradation Parameters

The degradation of collagen was modeled in equations (4-3) and (4-10).

4.5.4.2.1 Degradation Rate k_2

The turnover number k_2 ($=k_{cat}$) was determined experimentally for every collagen material (see Table 4-5) and this value was used in the simulations.

4.5.4.2.2 Dependency of the Degradation Rate on the ES Complex Concentration (γ)

For the determination of the turnover number k_2 higher enzyme concentrations ($2\mu\text{g/ml}$) were used than in the degradation and release studies ($0.1\mu\text{g/ml}$). The dependency of k_2 on the concentration of collagenase was investigated exemplarily for equine non cross-linked minirods (see 4.5.2.1). A non-linear correlation was found and it was assumed that k_2 is also a non-linear function of the ES complex concentration.

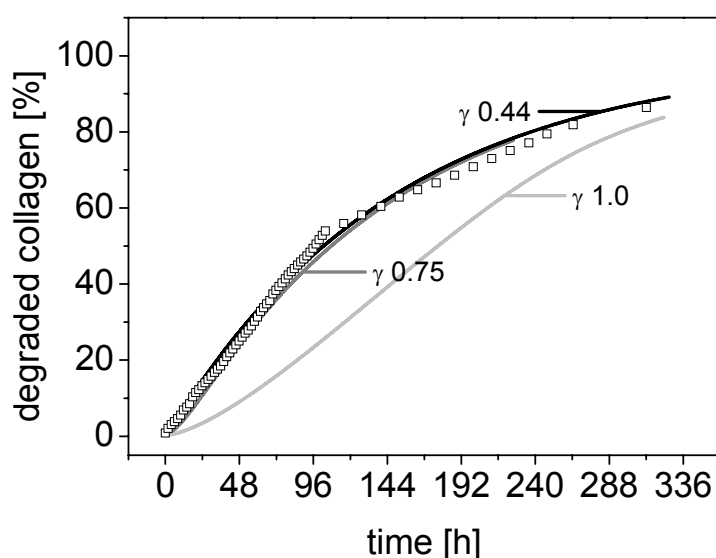


Figure 4-80 Variation in dependency of k_2 on the concentration of ES (γ): fitted values for the degradation of bovine corium EDC 1 cross-linked minirods (dots represent experimental data)

For soluble substrates, a linear relationship between enzyme concentration and degradation rate was observed in literature (Gilbert; 1988b; Huang et al.; 1977; Mallya et al.; 1986; Rubingh et al.; 1992), indicating that a correlation of $\gamma=1$ is correct. Due to the influence of the adsorption process, different dependencies were postulated for the digestion of insoluble substrates (Gilbert; 1988b; Rubingh et al.; 1992). For values of $\gamma < 1$ digestion became more enhanced (see Figure 4-80). Since a high initial degradation was observed in the

experimental studies (see 4.5.5.2), this indicated that a non-linear relation between k_2 and the concentration of ES complexes, i.e. $\gamma < 1$, describes the digestion of insoluble collagen better than a linear function. If a non-linear function was fitted to the data of Gilbert, $\gamma = 0.45$ was obtained (see Figure 4-74). A similar value ($\gamma = 0.44$) was also assumed to be the optimal value for the simulation of degradation of minirods.

Summarizing the effects of parameters concerning the degradation, it became evident that these constants did not influence the modeled collagen digestion as pronounced as the adsorption parameters.

4.5.4.3 Parameters of the Drug Release

The drug delivery was incorporated by equation (4-13) and the dependency $C_{Ai} = \sigma C_C^\ominus$ into the mathematical model.

4.5.4.3.1 FITC Dextran 70 Immobilization Inside the Collagen Minirods

An important parameter for erosion controlled drug release is the immobilization of the drug load. Two parameters have to be considered. On the one hand the immobilization capacity of the matrix restricts the drug release when a high drug fraction is embedded. On the other hand, the exponent θ , which provides information about the relationship between degraded collagen and still immobilized drug fraction, affects the delivery rate. A non-linear correlation between the immobilized drug fraction and the degraded collagen matrix was found for all matrices (see 4.5.2.2). Increasing the immobile drug fraction reduces the initial release rates (see Figure 4-81). Based on the in vitro release data obtained by the “two interval” experimental setup (addition of 0.1 $\mu\text{g/ml}$ collagenase after 6d), 25% FITC dextran 70 was detected to be immobilized inside the fully swollen bovine corium EDC 1 cross-linked minirods. Since the simulated data was compared with an in vitro release study in which collagenase was added already after 0.25h, the matrices were not swollen completely in the beginning. In this state the immobilized drug fraction could not be determined and it was assumed that the amount was higher than 25% FITC dextran 70 due to more physical entanglements in the non-swollen device. This

could be manifested by simulations. The best fit was obtained with 35% immobilized drug.

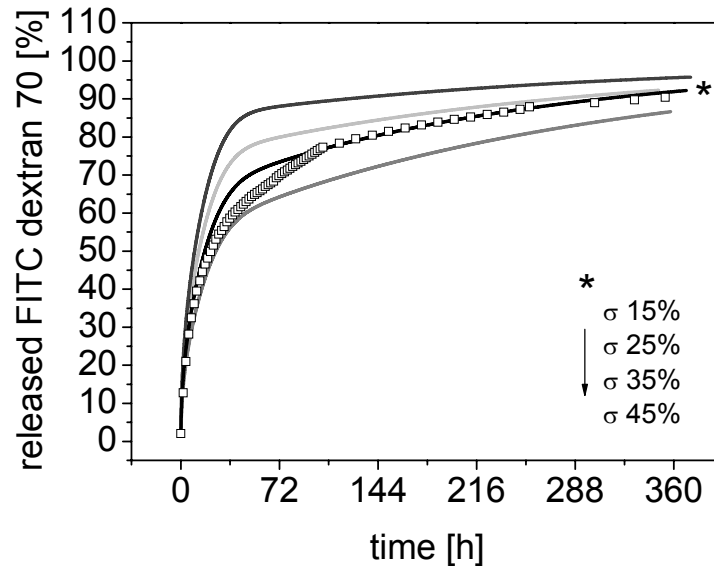


Figure 4-81 Variation in the immobilization capacity: experimentally determined value (25%) and fitted values for the FITC dextran 70 release from bovine corium EDC 1 cross-linked minirods (dots represent experimental data)

The dependency of immobilized drug on degraded collagen was implemented by $C_{Ai} = \sigma C_C^\theta$. An increase in θ enhanced drug release (see Figure 4-82). Depending on the used collagen matrix and the incorporated drug different exponents θ were obtained (see 4.5.2.2). For the release of FITC dextran 70 from bovine corium EDC 1 cross-linked minirods $\theta < 1$ was assumed and best correlation was found for $\theta = 0.6$.

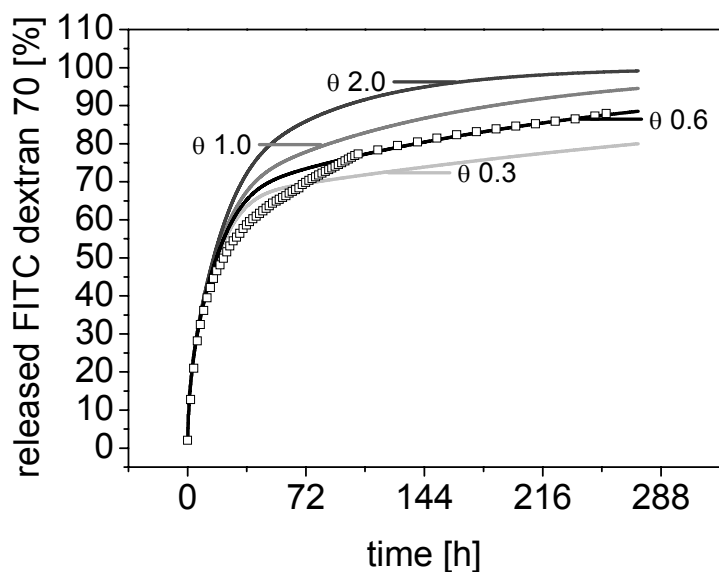


Figure 4-82 Variation in θ for the FITC dextran 70 release from bovine corium EDC 1 cross-linked minirods (dots represent experimental data)

4.5.4.3.2 Diffusion Coefficients of FITC Dextran 70 and Collagenase

Diffusion coefficients based on the free volume theory were assumed, because the diffusion coefficients are dependent on the degree of matrix degradation and the water content. The dimensionless constants β_E (for collagenase) and β_A (for FITC dextran 70) were fitted in order to get a correlation between the diffusion coefficient in the matrix and in solution. Siepmann et al. modeled the diffusion controlled drug release from hydroxypropyl methylcellulose tablets (Siepmann et al.; 1999b). A Fujita-type diffusion coefficient was assumed and it was emphasized that the value of the dimensionless constant is dependent on the molecular size of the diffusing agent and the water content. In our model, relations between the diffusion coefficient in solution and within the device were made. A fully swollen matrix and free diffusion inside the matrix were assumed. Best plots were obtained with $\beta_A = 3.5$ for FITC dextran 70 (see Figure 4-83a) and $\beta_E = 1$ for collagenase (see Figure 4-83b).

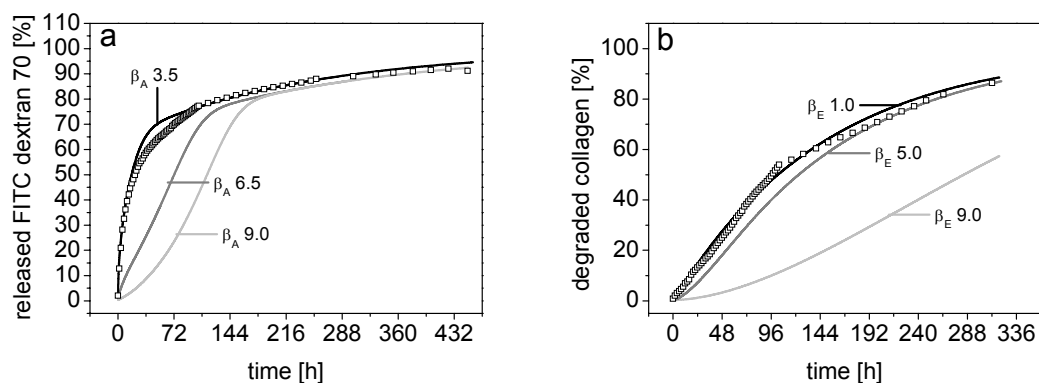


Figure 4-83 Variation in the fitted dimensionless constants of the diffusion coefficients:
 (a) β_A for the FITC dextran 70 release from bovine corium EDC 1 cross-linked minirods (dots represent experimental data)
 (b) β_E for the degradation of bovine corium EDC 1 cross-linked minirods (dots represent experimental data)

Increasing the values of β_E and β_A diminished the diffusion coefficients of collagenase and FITC dextran 70, respectively, which resulted in an initial lag time in drug release (see Figure 4-83a) and degradation (see Figure 4-83b) which did not reflect the observed in vitro circumstances (see 4.5.5.2). Despite molecular weights in the same range, a lower value β_E was chosen, because of adsorption phenomena which limit enzyme diffusion.

4.5.4.3.3 Matrix Dimensions

In order to extend the model to other geometries, simulations were performed for variations in the cylinder diameter. Because only 2D-simulations were modeled, variation in the length was not tested. However, this can be done if 3-dimensionally simulations would be performed.

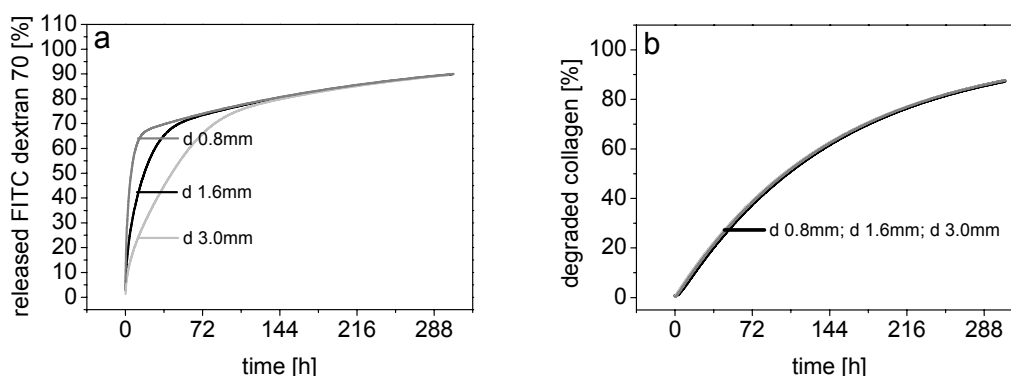


Figure 4-84 Variation in the minirod diameter for the FITC dextran 70 release (a) and the degradation (b) of bovine corium EDC 1 cross-linked minirods

As was already detected in the experimental studies (see 4.3.4.2), variation in the diameter of minirods did only affect the drug release behavior, but not the degradation profile (see Figure 4-84). With smaller diameters, release became enhanced because a higher specific surface area is available through which release can occur and diffusion pathways of water and drug are decreased (see Figure 4-84a). Consequently, the minirods swell faster and the collagen mesh untightens earlier. This resulted in increased drug liberation. Due to similar polymer properties, no variation in degradation profile could be detected.

4.5.5 Comparison of Modeled and Experimental Data

The development of an optimized simulation was performed in two steps. In the first stage (see 4.5.5.1), preliminary assumptions were made to get the possibility for fitting the values of n and γ . In the second dataset, optimized assumptions were implemented and the fitted parameters were tested (see 4.5.5.2).

4.5.5.1 FITC Dextran 70 Release from Equine Non Cross-linked Minirods

The first dataset was collected with the “two interval” setup to eliminate the contribution of drug release by diffusion and swelling and to guarantee a fully swollen matrix. Only the second part of this experiment was simulated, in order

to plot exclusively the drug release of the immobilized drug fraction. Simulated data were compared with results of FITC dextran 70 release from equine non cross-linked minirods (see Figure 4-85). Numerous simulations were performed and the best fit was obtained for the parameter set listed in Table 4-9.

In this set, k_1 was calculated by applying the assumption from Tzafiriri ($k_1 = \frac{k_2}{K_M}$; (Tzafiriri et al.; 2002)). n and γ were fitted and validated by the second experimental comparison (see 4.5.5.2). Good correlation was found for the first 3d (see Figure 4-85). Subsequently, simulated degradation and release were lower than the observed experimental results. This could be attributed to the used diffusion coefficients (used values were determined at room temperature) and the simplified boundaries of the enzyme concentration. In the simulation it was prescribed that the enzyme activity vanished within 7.5min after addition of collagenase which resulted in a restricted degradation behavior, especially during longer replacement intervals.

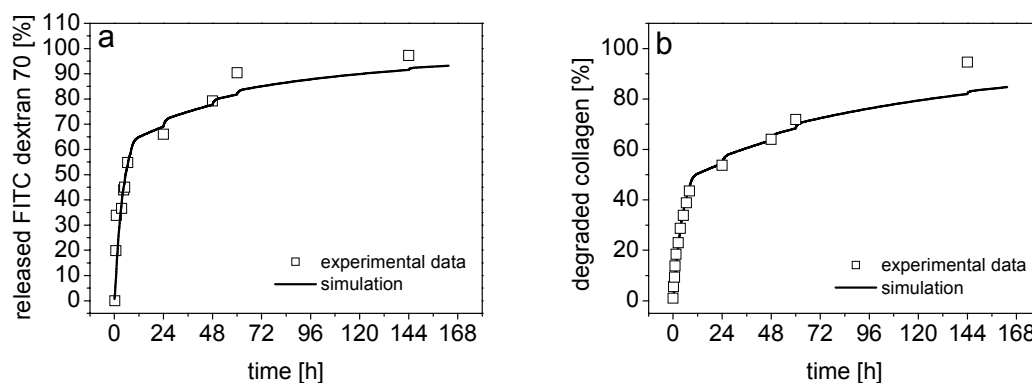


Figure 4-85 Simulation of (immobilized) FITC dextran 70 release (a) and collagen degradation (b) of 10mm equine non cross-linked minirods (0.1 μ g/ml enzyme was added after 6d; dots represent experimental data)

Table 4-9 Parameter set of FITC dextran 70 release from 10mm equine non cross-linked minirods

Parameter	Value
Ω	diameter: 0.278cm, length: 1.386cm
J	(0h, 164h]
C_E^{ext}	t=0: 0.1 μ g/ml t=between replacement of incubation medium: linear decrease to 0 μ g/ml within 0.125h t=replacement of incubation medium: 0.1 μ g/ml
C_C^0	1.12*10 ⁻⁶ mol/cm ³
$C_A^0 = C_{Ai}$	1.36*10 ⁻⁸ mol/cm ³
k_{act}	0
$D_E^0 = D_P^0 = D_A^0$	1.7*10 ⁻³ cm ² /h
sorption isotherm	Freundlich
k_1	4579 l/(h* μ mol)
n	0.681
k_2	174h ⁻¹
γ	0.44
β_E	1.0
β_A	1.0
θ	1.5

4.5.5.2 FITC Dextran 70 Release from Bovine Corium EDC 1 Cross-linked Mini-rods

FITC dextran 70 release and degradation of bovine corium EDC 1 cross-linked mini-rods were investigated in the presence of 0.1 µg/ml collagenase added after 0.25h. Consequently, the release of the mobile and the immobile FITC dextran 70 fractions were modeled simultaneously. The basic experimental setup was compared with a special experimental setup in which collagenase was changed and samples were drawn in regular intervals (every 2h during the first 100h, every 12h between 100h and 250h and every 24h until the end of the study, see Figure 4-86). This setup was conducted to verify whether a limit in degraded collagen fragments and liberated FITC dextran 70 was reached during the reaction intervals.

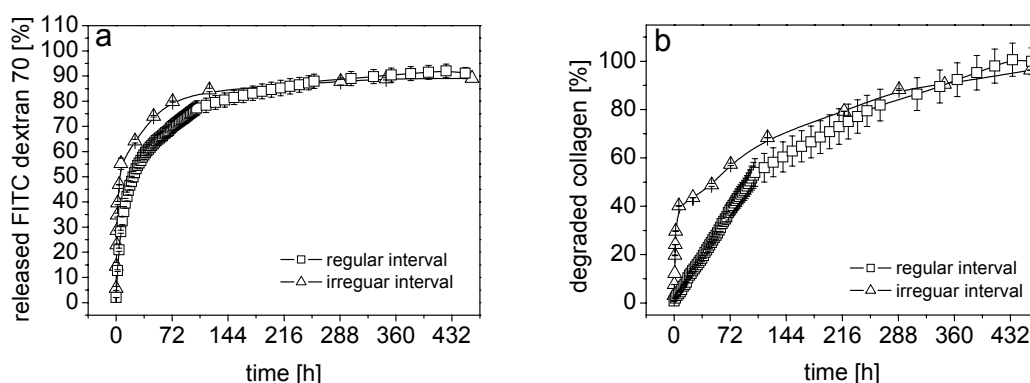


Figure 4-86 Effect of sample drawing on FITC dextran 70 release (a) and collagen degradation (b) of 10mm bovine corium EDC 1 cross-linked mini-rods (0.1 µg/ml enzyme was added after 0.25h; average ± SD; n=3)

Almost similar release profiles were observed for both experimental setups, irrespectively of the investigation intervals (see Figure 4-86a). The slightly lower drug delivery in the regular setup during the first 144h could be explained by the slower degradation (see Figure 4-86b). Since in the “irregular interval” setup the enzyme was replaced every hour during the first 6h, more collagenase was available in the beginning of the experiment and more collagen molecules could be degraded. After 40% and 60% collagen degradation in the irregular and the

regular experiment, respectively, almost similar degradation rates were reached for both setups. This indicated that a similar reaction occurred during a longer time interval between enzyme changes and a more often replacement.

Since it was assumed that the water soluble FITC dextran 70 was released by diffusion, the release data were plotted versus $t^{0.45}$. This exponent was used instead of the usually square root of time according to the Higuchi law, because circumstances in cylindrical matrices are better represented by 0.45 (Wise et al.; 2000). Comparison of the release profiles indicated that approximately 55% FITC dextran 70 was released in both experimental setups by diffusion (see Figure 4-87a). This drug fraction is composed of drug initially located at the device surface and the drug amount which is free to diffuse inside the collagen matrix. Subsequently, the release rate became dependent on matrix swelling (see Figure 4-87b). Due to water penetration, the mobility of collagen chains increases, the glassy barrier changes to a rubbery state and release can occur (Gilbert; 1988b). The release becomes strongly dependent on the diffusion coefficient in this phase, because the diffusion coefficients change as a function of water content. Since minirods were highly cross-linked, this phase should follow a Fickian dependency as well (Gilbert; 1988b). This assumption could be manifested by the linear dependency when the release was plotted against the time $t^{0.45}$ (see Figure 4-87b). After approximately 80% delivery, another reduction in release rate was observed (see Figure 4-87c). The remaining drug fraction corresponded to the drug fraction which is immobilized inside the matrix and can only be released by erosion processes.

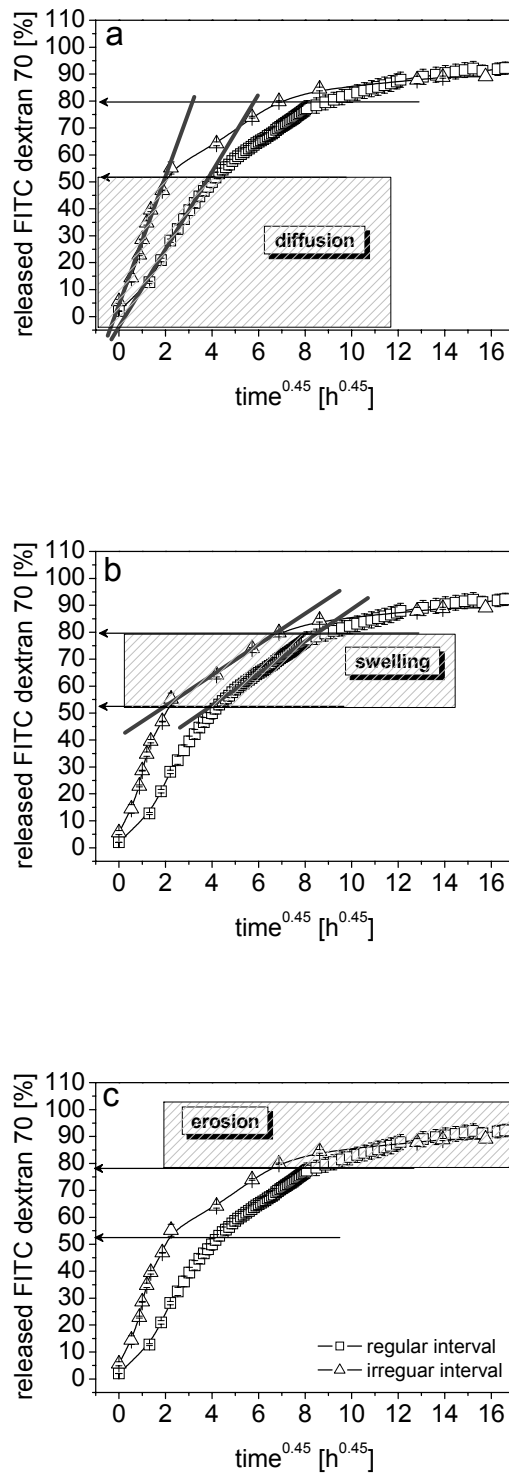


Figure 4-87 FITC dextran 70 release from 10mm bovine corium EDC 1 cross-linked minirods plotted against $t^{0.45}$: differentiation between diffusion (a), swelling (b) and erosion (c) control (0.1 μ g/ml enzyme was added after 0.25h; average \pm SD; n=3; similar legend for all graphs)

Exemplarily, the regular setup was simulated (parameter set see Table 4-10). Several assumptions were improved compared to the simulation of equine non cross-linked minirods (see 4.5.5.1). The adsorption rate k_1 was fitted, and not calculated according to Tzafriri (Tzafriri et al.; 2002), the enzyme concentration in the ambient medium remained constant and diffusion coefficients referred to 37°C were implemented. The parameters n and γ from 4.5.5.1 were used to validate their values.

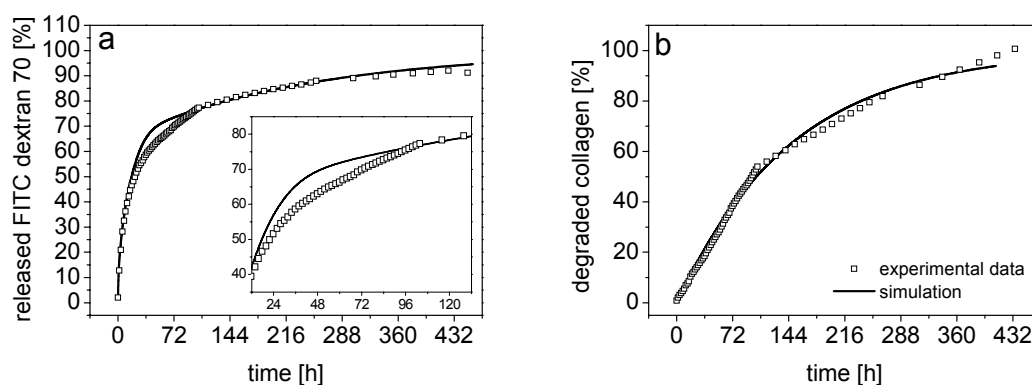


Figure 4-88 Simulation of FITC dextran 70 release (a) and collagen degradation (b) of 10mm bovine corium EDC 1 cross-linked minirods (0.1 μ g/ml enzyme was added after 0.25h; similar legend for release and degradation; dots represent experimental data)

Comparison to experimental data showed that good correlation was obtained for the matrix degradation (see Figure 4-88b) and the diffusion and erosion controlled release phase (see Figure 4-88a). The part of swelling controlled release was not plotted satisfactorily. This was not surprising, because swelling controlled release was not considered in the applied mathematical model. If the mathematical model would be combined with the model of swelling controlled release presented by Radu et al. (Radu et al.; 2002), good correlation for the complete drug release profile can be expected.

Table 4-10 Parameter set of FITC dextran 70 release from 10mm bovine corium EDC 1 cross-linked minirods

Parameter	Value
Ω	diameter: 0.159cm, length: 1.135cm
J	(0h, 456h]
C_E^{ext}	0.1 $\mu\text{g/ml}$ (constant during complete observation)
C_C^0	$2.18 \cdot 10^{-6} \text{ mol/cm}^3$
C_A^0	$8.17 \cdot 10^{-8} \text{ mol/cm}^3$
C_{Ai}	$2.86 \cdot 10^{-8} \text{ mol/cm}^3$
k_{act}	0
$D_E^0 = D_P^0 = D_A^0$	$2.4 \cdot 10^{-3} \text{ cm}^2/\text{h}$
sorption isotherm	Freundlich
k_1	65.0 l/(h* mol)
n	0.681
k_2	51.4 h^{-1}
γ	0.44
β_E	1.0
β_A	3.5
θ	0.6

4.5.6 Summary

In this chapter a mathematical model was presented which describes the drug release from dense collagen devices controlled by enzymatic matrix erosion. The challenging part within this model was to describe the degradation of an insoluble substrate properly. Based on experimental observations, a Freundlich sorption isotherm was incorporated into the Michaelis-Menten equation to describe the dependency of the degradation rate on the concentration of ES complexes correctly. It was assumed that the degradation reaction itself is the rate limiting step. A mixture of experimentally determined and fitted parameters was implemented and the model was tested. Since adsorption is the prerequisite step for the enzymatic reaction, a high influence of parameters related to the sorption process (i.e. k_1 and n) was observed. The degradation rate k_2 , which limits the value of k_1 , and the matrix dimensions did affect the degradation of collagen minirods only marginally. The simulated data were compared with experimentally performed degradation and release studies. Some parameters were fitted in the first experimental setup and validated in the second setup. Good correlation was found for the degradation studies. In the release studies good correlation was obtained for the diffusion and erosion dependent drug liberation, but the swelling controlled drug delivery was not plotted satisfactorily. This highlighted that the model is appropriate to simulate the release by erosion, but shows deficits in description of the release by swelling. A combination with the model for swelling controlled drug delivery presented by Radu et al. (Radu et al.; 2002) would be a promising attempt to model the drug release from dense collagen devices more precisely. Figure 4-89 summarizes such a combined mathematical modeling approach:

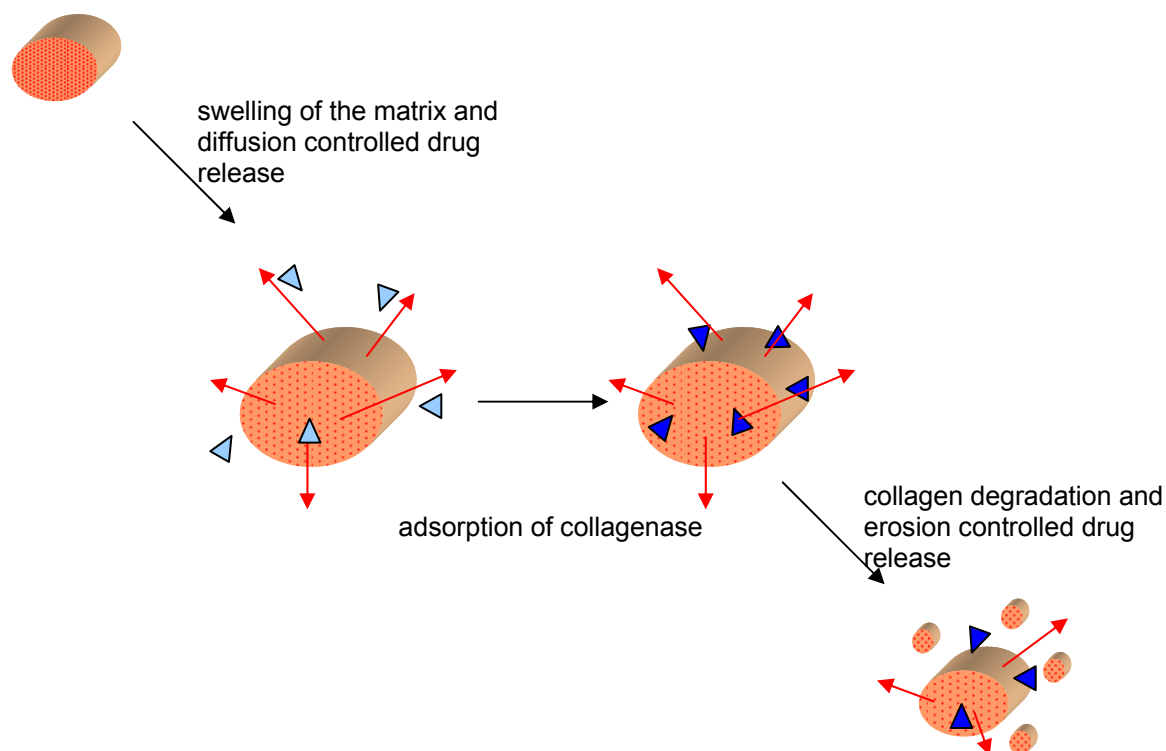


Figure 4-89 Schematic illustration of a combined mathematical model of dense collagen minirods (→ drug release, △ free collagenase, ▲ adsorbed collagenase)

This model would provide further insights into the release mechanism of erosion controlled drug delivery from dense collagen matrices. Using the combined mechanistic model, its application can be extended to other collagen materials or drugs and expensive experimental investigations for the development of new drug devices can be reduced. However, one has to keep in mind that the developed model is a rather simplified assumption of the reactions occurring during drug release and matrix erosion, which nevertheless describes the processes adequately. Further improvement could be obtained e.g. by implementation of a distinction between lateral and cross-section surface area which behave differently with respect to their liberation properties.

5 Final Summary

The aim of this thesis had been to develop collagen drug devices for higher molecular weight drugs, e.g. proteins, from which drug release is controlled by diffusion, swelling and matrix erosion. Besides this, the degradation of insoluble collagen type I by bacterial collagenase was studied in more detail to gain further insight into the enzymatic hydrolysis of collagen. Based on the obtained in vitro results a mathematical model was to be developed to describe drug release from collagen matrices undergoing enzymatic degradation. To achieve a matrix form, suitable for parenteral applications, cylindrical rods were prepared by extrusion. Since it was desired to obtain a delivery system which controls release mainly by erosion, insoluble collagen type I materials were used to enhance the resistance against enzymatic attack. Consequently, the developed implants, named “minirods”, combine the advantage of restricted drug diffusion and enzyme penetration, due to the chosen collagen and the high apparent matrix density with optimal dimensions for parenteral application. Finally, in vivo drug release, degradation and biocompatibility of the developed minirods were evaluated to provide further basis for future applications.

The physicochemical properties of collagen materials and matrices were investigated in chapter 4.1. A compact, parallel orientated surface pattern was observed by scanning electron microscopy which corresponded to the direction of extrusion. The apparent matrix density was lower than the apparent density of collagen reported in the literature (Weadock et al.; 1984). It was demonstrated that collagen materials extracted from equine sources showed higher melting temperatures (T_m) than bovine collagen qualities. Moreover, collagen materials which were extracted from tendon exhibited higher melting temperatures than corium collagen material. The lowest melting temperature was observed for bovine corium non cross-linked collagen ($T_m = 39.4 \pm 1.2^\circ\text{C}$; $T_{\text{onset}} = 32.1 \pm 0.5^\circ\text{C}$) which leads to rapid disintegration at 37°C . An increase in melting temperature was detected for increasing EDC (1-ethyl-3-(3-dimethylaminopropyl)carbodiimide) cross-linking ratios which leveled off between 62°C

and 68°C. Since collagen is a hydrogel, water interacts with the collagen structures during swelling. The self-diffusion coefficient (D) of water inside the collagen matrices, determined by pulsed field gradient nuclear magnetic resonance, was decreased ($5.76 \cdot 10^{-2} \text{cm}^2/\text{h}$) compared to the diffusion coefficient of pure water ($D(\text{solution})/D(\text{minirod})=0.67$). The swelling behavior of minirods during the first 3d was not affected by the presence of collagenase. Results obtained by differential scanning calorimetry, concerning the matrix stability, were confirmed by swelling studies and equine tendon collagen was chosen as most promising material for device manufacturing.

After finding the standard matrices, the degradation of insoluble collagen was characterized in chapter 4.2. A fundamental investigation of the degradation pattern was necessary, because this information is very important to describe the drug release by a mechanistic mathematical model properly. Collagenase can only form an enzyme-substrate complex with insoluble collagen after adsorption onto the substrate surface. Hence, besides the degradation, the adsorption profile and isotherm were examined. An adequate experimental setup to analyze the binding of bacterial collagenase and human gelatinases (A and B) was developed. The adsorption of bacterial collagenase reached equilibrium between 0.5h to 1h and followed a Freundlich sorption isotherm. The subsequent degradation was highly influenced by this adsorption process. The highest degradational turnover was detected for equine non cross-linked collagen powder ($k_{\text{cat}}=750\text{h}^{-1}$) and the lowest for equine EDC 1 cross-linked minirods ($k_{\text{cat}}=33.4\text{h}^{-1}$).

In chapter 4.3, the *in vitro* drug release of FITC (fluorescein isothiocyanate) dextrans, representing model “protein” drug compounds, was investigated. The diffusion coefficients of FITC dextrans in solution were determined by fluorescence correlation spectroscopy. The obtained value of $2.4 \cdot 10^{-3} \text{cm}^2/\text{h}$ for FITC dextran 70 was also used for the diffusion equations of collagenase in the mathematical model, because of a good correlation with coefficients reported in the literature (Gaspers et al.; 1994; Seiffter et al.; 1959). Several processes, i.e. diffusion, swelling and erosion, contribute to the overall release profile from collagen minirods. Therefore, different experimental setups were conducted to

separate swelling and erosion controlled drug release. The required release profile could be adapted by a change in collagen matrix material, e.g. animal source or cross-linking degree, or by variation of the matrix dimensions, either length or diameter of the minirods. Using these parameters, 80% FITC dextran 70 liberation could be extended from approximately 13h for bovine tendon non cross-linked minirods to approximately 3d for equine non cross-linked matrices and approximately 5d for equine EDC 1 cross-linked extrudates. A change in matrix dimensions of equine non cross-linked minirods resulted in an increase in retardation from approximately 8h (diameter: 0.5mm; length: 10mm) to 5d (diameter: 2mm; length: 20mm). Besides this, the drug load also influenced the release profile. Increasing the molecular weight of FITC dextrans led to retardation in release from equine non cross-linked minirods (e.g. after 24h 99% FITC dextran 20 delivery and 48% FITC dextran 70 liberation, respectively), because of a restricted diffusion. As a consequence, a higher drug fraction was entrapped inside the collagen matrix, which could only be released by matrix erosion. However, this effect was not valid for all minirods, because the matrix degradation was influenced by the apparent minirod density as well (e.g. after 24h 67% FITC dextran 150 versus 48% FITC dextran 70 liberation from equine non cross-linked minirods). Increasing the concentration of FITC dextran 70 resulted in a faster release. Equine non cross-linked matrices loaded with 2% (w/w) FITC dextran 70 showed 80% delivery already after approximately 7h, whereas 80% of a 1% (w/w) load was released within approximately 3d.

The *in vitro* release of PCA-BSA (bovine serum albumin labeled with 3-carboxy-2,2,5,5-tetramethyl-1-pyrrolidinyloxy) was investigated in chapter 4.4.3. Differentiation between swelling controlled release and delivery dependent on enzymatic erosion was made. Similar release profiles were obtained for FITC dextran 70 and PCA-BSA, manifesting the assumption that FITC dextrans could be used to model protein drug release from collagen devices and that previous results could be transferred. PCA-BSA release was monitored by electron spin resonance (ESR) spectroscopy. Besides the release profiles, insights into the release mechanism were obtained. It was demonstrated that water penetrated into the collagen devices within 0.25h. In absence of bacterial collagenase,

PCA-BSA release from minirods was mainly diffusion controlled. Addition of 0.1 µg/ml collagenase led to a differentiation between the investigated minirod variations. Non cross-linked extrudates still released PCA-BSA diffusion controlled, but EDC 1 cross-linked devices showed also an erosion dependent delivery. This confirmed the assumption that a mobile and an immobile drug pool was created inside dense collagen minirods and that a higher number in cross-linkages could immobilize drugs inside the device. The mobile drug fraction was released by diffusion and swelling, whereas the immobilized fraction could only be released by diffusion after matrix erosion.

In chapter 4.4.4 and 4.4.5, the *in vivo* release of PCA-BSA and the biocompatibility of minirods were monitored in adult domestic pigs. Results of protein delivery were comparable to the *in vitro* investigations. However, release was slightly delayed due to a lower swelling and degradation *in vivo*. Release started at the matrix surface, before a change in drug concentration occurred in the minirod interior. After PCA-BSA liberation fast diffusional remove from the implantation site took place. Mechanistic studies showed again that EDC 1 cross-linked minirods released PCA-BSA by diffusion, swelling and erosion phenomena, whereas the delivery from non cross-linked matrices was mostly independent of the erosion process. To achieve an even deeper insight into the mechanistic properties of the drug release from collagen devices, further ESR studies would have to be performed with spin labeled collagen matrix material.

Histological evaluations demonstrated that all minirods were tolerated well and that only minor inflammation reactions occurred, which were detectable by TGFβ-staining and cell accumulations. Cell penetration into non cross-linked minirods was facilitated, because of a slightly lower apparent matrix density and a lower number of cross-links. *In vivo* persistence was similar to the order of the *in vitro* degradation in the presence of 0.1 µg/ml bacterial collagenase. Cross-linked matrices were more stable than non cross-linked devices and the minirods prepared from equine collagen showed the highest resistance. Tissue remodeling, which resembled normal wound healing, took place and emphasized the assumption that collagen minirods can be used *in vivo* without surgical removal after drug depletion.

The presented experimental *in vitro* studies were used to develop a mathematical model in chapter 4.5, which describes the drug release by erosion from dense collagen minirods. Equations for the collagen degradation and the drug release were implemented. Adsorption and diffusion phenomena were incorporated and a mixture of experimentally determined and fitted parameters was used to feed the model. Parameters related to adsorption (i.e. k_1 and n) had a high influence on the digestion of the collagen matrix, whereas the degradation rate k_2 , which limits the value of k_1 , and the matrix dimensions did affect the degradation of collagen minirods only marginally. Good correlation was found for the collagen degradation. Simulated release of FITC dextran 70 reflected the diffusion and erosion controlled delivery phases well. The swelling dependent drug release was not modeled sufficiently, because this influence was not yet implemented into the model. To describe the *in vivo* drug release from dense collagen matrices completely, the developed mathematical model for erosion controlled drug release has to be combined with the model for swelling controlled release presented by Radu et al. (Radu et al.; 2002).

In conclusion, a promising dense collagen implant was developed which can be easily manufactured by extrusion at room temperature without the need of organic solvents. It was shown that high molecular weight drugs can be incorporated and that their release can be controlled by e.g. using different collagen variations. Besides the enhanced degradation and release properties compared to collagen devices prepared from soluble collagen, e.g. atelocollagen, the mechanism of release can be changed towards erosion control by the degree of matrix cross-linking. Furthermore, the developed minirods showed good biocompatibility, which provides the basis for potential applications *in vivo*.

6 Reference List

1. Aimes, R.T. and Quigley, J.P.; Matrix Metalloproteinase-2 Is an Interstitial Collagenase. Inhibitor-Free Enzyme Catalyzes the Cleavage of Collagen Fibrils and Soluble Native Type I Collagen Generating the Specific 3/4- and 1/4-Length Fragments; *Journal of Biological Chemistry*; 270 (1995) 5872 - 5876.
2. Anderson, J.M., Niven, H., Pelagalli, J., Olanoff, L.S. and Jones, R.D.; The Role of the Fibrous Capsule in the Function of Implanted Drug-Polymer Sustained Release Systems; *Journal of Biomedical Materials Research*; 15 (1981) 889 - 902.
3. Anderson, J.M.; In Vivo Biocompatibility of Implantable Delivery Systems and Biomaterials; *European Journal of Pharmaceutics and Biopharmaceutics*; 40 (1994) 1 - 8.
4. Assenheim, H.M.; *Introduction to Electron Spin Resonance* (1966).
5. Azzam, H.S. and Thompson, E.W.; Collagen-Induced Activation of the Mr 72,000 Type IV Collagenase in Normal and Malignant Human Fibroblastoid Cells; *Cancer Research*; 52 (1992) 4540 - 4544.
6. Bailey, J.E.; *Enzyme Reactions in Heterogeneous Systems in: Biochemical engineering fundamentals* (1986); 148 - 153.
7. Batycky, R.P., Hanes, J., Langer, R. and Edwards, D.A.; A Theoretical Model of Erosion and Macromolecular Drug Release From Biodegrading Microspheres; *Journal of Pharmaceutical Sciences*; 86 (1997) 1464 - 1477.
8. Bicsak, T.A. and Harper, E.; Purification and Characterization of Tadpole Back-Skin Collagenase With Low Gelatinase Activity; *Journal of Biological Chemistry*; 259 (1984) 13145 - 13150.
9. Birkedal-Hansen, H., Moore, W.G., Bodden, M.K., Windsor, L.J., Birkedal-Hansen, B., DeCarlo, A. and Engler, J.A.; Matrix Metalloproteinases: a Review; *Critical Reviews in Oral Biology and Medicine : an Official Publication of the American Association of Oral Biologists*; 4 (1993) 197 - 250.
10. Bond, M.D. and Van Wart, H.E.; Relationship Between the Individual Collagenases of *Clostridium histolyticum*: Evidence for Evolution by Gene Duplication; *Biochemistry*; 23 (1984) 3092 - 3099.
11. Brinckmann, J., Notbohm, H., Mueller, P.K. and Editors.; *Collagen: Primer in Structure, Processing and Assembly* (2005).
12. Burke, K.E., Naughton, G. and Cassai, N.; A Histological, Immunological, and Electron Microscopic Study of Bovine Collagen Implants in the Human; *Annals of Plastic Surgery*; 14 (1985) 515 - 522.

13. Burke,K.E., Naughton,G., Waldo,E. and Cassai,N.; Bovine Collagen Implant: Histologic Chronology in Pig Dermis; *Journal of Dermatologic Surgery and Oncology*; 9 (1983) 889 - 895.
14. Capancioni,S., Schwach-Abdellaoui,K., Kloeti,W., Herrmann,W., Brosig,H., Borchert,H.H., Heller,J. and Gurny,R.; In Vitro Monitoring of Poly(Ortho Ester) Degradation by Electron Paramagnetic Resonance Imaging; *Macromolecules*; 36 (2003) 6135 - 6141.
15. Charlier,A., Leclerc,B. and Courraze,G.; Release of Mifepristone From Biodegradable Matrixes: Experimental and Theoretical Evaluations; *International Journal of Pharmaceutics*; 200 (2000) 115 - 120.
16. Charulatha,V. and Rajaram,A.; Influence of Different Crosslinking Treatments on the Physical Properties of Collagen Membranes; *Biomaterials*; 24 (2003) 759 - 767.
17. Cheung,D.T., Perelman,N., Ko,E.C. and Nimni,M.E.; Mechanism of Crosslinking of Proteins by Glutaraldehyde III. Reaction With Collagen in Tissues; *Connective Tissue Research*; 13 (1984) 109 - 115.
18. Cleland,J.L.; Protein Delivery From Biodegradable Microspheres; *Pharmaceutical Biotechnology*; 10 (1997) 1 - 43.
19. Cornish-Bowden,A.; Basic Principles of Chemical Kinetics, Introduction to Enzyme Kinetics, Practical Aspects of Kinetic Studies in: *Fundamentals of Enzyme Kinetics* (1999); 1 - 72.
20. Cullen,B., Smith,R., McCulloch,E., Silcock,D. and Morrison,L.; Mechanism of Action of PROMOGRAN, a Protease Modulating Matrix, for the Treatment of Diabetic Foot Ulcers; *Wound Repair and Regeneration*; 10 (2002a) 16 - 25.
21. Cullen,B., Watt,P.W., Lundqvist,C., Silcock,D., Schmidt,R.J., Bogan,D. and Light,N.D.; The Role of Oxidised Regenerated Cellulose/Collagen in Chronic Wound Repair and Its Potential Mechanism of Action; *International Journal of Biochemistry & Cell Biology*; 34 (2002b) 1544 - 1556.
22. Danckwerts,M. and Fassihi,A.; Implantable Controlled Release Drug Delivery Systems: a Review; *Drug Development and Industrial Pharmacy*; 17 (1991) 1465 - 1502.
23. Dash,A.K. and Cudworth,G.C., II; Therapeutic Applications of Implantable Drug Delivery Systems; *Journal of Pharmacological and Toxicological Methods*; 40 (1998) 1 - 12.
24. De Paoli Lacerda,S.H., Ingber,B. and Rosenzweig,N.; Structure-Release Rate Correlation in Collagen Gels Containing Fluorescent Drug Analog; *Biomaterials*; 26 (2005) 7164 - 7172.
25. Esterbauer,H. and Janosi,A.; Effect of Mechanical and Thermal Pretreatment on the Enzymic Hydrolysis of Lignocelluloses; *Papier (Bingen, Germany)*; 38 (1984) 599 - 606.

26. Etherington, D.J.; The Dissolution of Insoluble Bovine Collagens by Cathepsin B1, Collagenolytic Cathepsin and Pepsin. The Influence of Collagen Type, Age and Chemical Purity on Susceptibility; *Connective Tissue Research*; 5 (1977) 135 - 145.
27. Federman, S., Miller, L.M. and Sagi, I.; Following Matrix Metalloproteinases Activity Near the Cell Boundary by Infrared Micro-Spectroscopy; *Matrix Biology*; 21 (2002) 567 - 577.
28. Fields, G.B. and Van Wart, H.E.; Unique Features of the Tissue Collagenase Cleavage Site in Interstitial Collagens; *Matrix (Stuttgart)*; Supplement 1 (1992) 68 - 70.
29. French, M.F., Bhowan, A. and Van Wart, H.E.; Identification of Clostridium Histolyticum Collagenase Hyperreactive Sites in Type I, II, and III Collagens: Lack of Correlation With Local Triple Helical Stability; *Journal of Protein Chemistry*; 11 (1992) 83 - 97.
30. Frieß, W. and Lee, G.; Basic Thermoanalytical Studies of Insoluble Collagen Matrixes; *Biomaterials*; 17 (1996a) 2289 - 2294.
31. Frieß, W.; *Drug Delivery Systems Based on Collagen* (1999).
32. Frieß, W.; Collagen. Biomaterial for Drug Delivery; *European Journal of Pharmaceutics and Biopharmaceutics*; 45 (1998) 113 - 136.
33. Frieß, W., Lee, G. and Groves, M.J.; Insoluble Collagen Matrixes for Prolonged Delivery of Proteins; *Pharmaceutical Development and Technology*; 1 (1996b) 185 - 193.
34. Fujioka, K., Hirasawa, K., Kajiwara, M., Sano, A., Sugawara, S. and Urabe, Y.; Rod-like controlled-release drug implants; Patent; 659406 (1994).
35. Fujioka, K., Maeda, M., Hojo, T. and Sano, A.; Protein Release From Collagen Matrixes; *Advanced Drug Delivery Reviews*; 31 (1998) 247 - 266.
36. Fujioka, K., Takada, Y., Sato, S. and Miyata, T.; Novel Delivery System for Proteins Using Collagen As a Carrier Material: the Minipellet; *Journal of Controlled Release*; 33 (1995) 307 - 315.
37. Fujita, H.; Diffusion in Polymer-Diluent Systems; *Fortschr. Hochpolymer. Forsch.*; 3 (1961) 1 - 47.
38. Gaspers, P.B., Gast, A.P. and Robertson, C.R.; Enzymes on Immobilized Substrate Surfaces: Reaction; *Journal of Colloid and Interface Science*; 172 (1995) 518 - 529.
39. Gaspers, P.B., Robertson, C.R. and Gast, A.P.; Enzymes on Immobilized Substrate Surfaces: Diffusion; *Langmuir*; 10 (1994) 2699 - 2704.
40. Geiger, M.; Porous Collagen/Ceramic Composite Carriers for Bone Regeneration Using Recombinant Human Bone Morphogenetic Protein-2 (RhBMP-2); PhD Thesis; FAU Erlangen, Germany (2001).

41. Gelse, K., Poschl, E. and Aigner, T.; Collagens - Structure, Function, and Biosynthesis; *Advanced Drug Delivery Reviews*; 55 (2003) 1531 - 1546.
42. Ghebre-Sellassie, I.; *Pharmaceutical Extrusion Technology* (2003).
43. Ghose, T.K. and Bisaria, V.S.; Studies on the Mechanism of Enzymic Hydrolysis of Cellulosic Substances; *Biotechnology and Bioengineering*; 21 (1979) 131 - 146.
44. Gilbert, D.L. and Kim, S.W.; Macromolecular Release From Collagen Monolithic Devices; *Journal of Biomedical Materials Research*; 24 (1990) 1221 - 1239.
45. Gilbert, D.L., Okano, T., Miyata, T. and Kim, S.W.; Macromolecular Diffusion Through Collagen Membranes; *International Journal of Pharmaceutics*; 47 (1988a) 79 - 88.
46. Gilbert, D.L.; *Collagen Macromolecular Drug Delivery Systems*; PhD Thesis; Univ. Utah, Salt Lake City, UT, USA (1988b).
47. Gombotz, W.R. and Pettit, D.K.; Biodegradable Polymers for Protein and Peptide Drug Delivery; *Bioconjugate Chemistry*; 6 (1995) 332 - 351.
48. Göpferich, A.; Mechanisms of Polymer Degradation and Erosion; *Biomaterials*; 17 (1996) 103 - 114.
49. Göpferich, A.; Mechanism of Polymer Degradation and Elimination in: *Handbook of Biodegradable Polymers* (1997a); 451 - 471.
50. Göpferich, A.; Polymer Bulk Erosion; *Macromolecules*; 30 (1997b) 2598 - 2604.
51. Gorham, S.D., Light, N.D., Diamond, A.M., Willins, M.J., Bailey, A.J., Wess, T.J. and Leslie, N.J.; Effect of Chemical Modifications on the Susceptibility of Collagen to Proteolysis. II. Dehydrothermal Crosslinking; *International Journal of Biological Macromolecules*; 14 (1992) 129 - 138.
52. Gorham, S.D.; Collagen As a Biomaterial in: *Biomaterials* (1991); 55 - 122.
53. Gyani, B.P.; Distribution Law, Adsorption, and Chemical Reaction; *Journal of Physical Chemistry*; 49 (1945) 442 - 453.
54. Haas, U.; *Physik Für Pharmazeuten Und Mediziner* (2002).
55. Harrington, D.J.; Bacterial Collagenases and Collagen-Degrading Enzymes and Their Potential Role in Human Disease; *Infection and Immunity*; 64 (1996) 1885 - 1891.
56. Harris, E.D., Jr. and Krane, S.M.; Collagenases (Second of Three Parts); *The New England Journal of Medicine*; 291 (1974) 605 - 609.
57. Hasty, K.A., Jeffrey, J.J., Hibbs, M.S. and Welgus, H.G.; The Collagen Substrate Specificity of Human Neutrophil Collagenase; *Journal of Biological Chemistry*; 262 (1987) 10048 - 10052.

58. He,C., Wilhelm,S.M., Pentland,A.P., Marmer,B.L., Grant,G.A., Eisen,A.Z. and Goldberg,G.I.; Tissue Cooperation in a Proteolytic Cascade Activating Human Interstitial Collagenase; Proceedings of the National Academy of Sciences of the United States of America; 86 (1989) 2632 - 2636.
59. Heller,J.; Biodegradable Polymers in Controlled Drug Delivery; Critical Reviews in Therapeutic Drug Carrier Systems; 1 (1984) 39 - 90.
60. Hendriks, M., Verhoeven, M., Cahalan, P.T., Zeeman, R., Dijkstra, P.J. and Feijen, J.; A method of making a crosslinked collagen-based material and bioprosthetic devices produced therefrom; Patent; 898973 (1998).
61. Hermeling,S., Crommelin Daan,J.A., Schellekens,H. and Jiskoot,W.; Structure-Immunogenicity Relationships of Therapeutic Proteins; Pharmaceutical Research; 21 (2004) 897 - 903.
62. Hirasawa,T., Sano,A., Fujioka,K., Inoue,K., Miyata,K., Nakano,M., Yamashita,K. and Hayakawa,T.; Biodegradability of "Minipellet," a New Drug Formulation Using Atelocollagen As a Drug Carrier Material, in the Rhesus Monkey; Journal of Biomedical Materials Research; 18 (1997) 149 - 159.
63. Hönig,J.F. and Merten,H.A.; Das Göttinger Miniaturschwein (GMS) Als VErsuchstier in Der Human-Medizinischen Osteologischen Grundlagenforschung; Zeitschrift Für Zahnärztliche Implantologie; 9 (1993) 244 - 254.
64. Huang,A.A.; Kinetic Studies on Insoluble Cellulose-Cellulase System; Biotechnology and Bioengineering; 17 (1975) 1421 - 1433.
65. Huang,C. and Yannas,I.V.; Mechanochemical Studies of Enzymic Degradation of Insoluble Collagen Fibers; Journal of Biomedical Materials Research; 11 (1977) 137 - 154.
66. Imai,S., Konttinen,Y.T., Jumppanen,M., Lindy,O., Ceponis,A., Kempainen,P., Sorsa,T., Santavirta,S., Xu,J.W. and Lopez-Otin,C.; High Levels of Expression of Collagenase-3 (MMP-13) in Pathological Conditions Associated With a Foreign-Body Reaction; Journal of Bone and Joint Surgery; 80 (1998) 701 - 710.
67. Jayakrishnan,A. and Jameela,S.R.; Glutaraldehyde As a Fixative in Bioprostheses and Drug Delivery Matrices; Biomaterials; 17 (1996) 471 - 484.
68. Junqueira,L.C. and Carneiro,J.; Histologie (1996).
69. Kamath,K.R. and Park,K.; Biodegradable Hydrogels in Drug Delivery; Advanced Drug Delivery Reviews; 11 (1993) 59 - 84.
70. Kanjickal,D.G. and Lopina,S.T.; Modeling of Drug Release From Polymeric Delivery Systems--a Review; Critical Reviews in Therapeutic Drug Carrier Systems; 21 (2004) 345 - 386.

71. Katzhendler, I., Mäder, K., Azoury, R. and Friedman, M.; Investigating the Structure and Properties of Hydrated Hydroxypropyl Methyl Cellulose and Egg Albumin Matrixes Containing Carbamazepine: EPR and NMR Study; *Pharmaceutical Research*; 17 (2000a) 1299 - 1308.
72. Katzhendler, I., Mäder, K. and Friedman, M.; Correlation Between Drug Release Kinetics From Protein Matrix and Matrix Structure: EPR and NMR Study; *Journal of Pharmaceutical Sciences*; 89 (2000b) 365 - 381.
73. Khor, E.; Methods for the Treatment of Collagenous Tissues for Bioprostheses; *Biomaterials*; 18 (1997) 95 - 105.
74. Kissel, T., Brich, Z., Bantle, S., Lancranjan, I., Nimmerfall, F. and Vit, P.; Parenteral Depot-Systems on the Basis of Biodegradable Polyesters; *Journal of Controlled Release*; 16 (1991) 27 - 41.
75. Knauss, R., Schiller, J., Fleischer, G., Karger, J. and Arnold, K.; Self-Diffusion of Water in Cartilage and Cartilage Components As Studied by Pulsed Field Gradient NMR; *Magnetic Resonance in Medicine*; 41 (1999) 285 - 292.
76. Kopp, J., Bonnet, M. and Renou, J.P.; Effect of Collagen Crosslinking on Collagen-Water Interactions (a DSC Investigation); *Matrix (Stuttgart, Germany)*; 9 (1989) 443 - 450.
77. Kutz, G.; Bedeutung Von Kollagenhydrolysaten Als Pharmazeutische Hilfsstoffe - Einsatz in Tablettenüberzügen, Tabletten Und Sprühtrocknungsprodukten; PhD Thesis; FAU Erlangen, Germany (1988).
78. Langer, R. and Folkman, J.; Sustained Release of Macromolecules From Polymers; *Midland Macromolecular Monographs*; 5 (1978) 175 - 196.
79. Lee, Y.H., Fan, L.T. and Fan, L.S.; Kinetics of Hydrolysis of Insoluble Cellulose by Cellulase; *Advances in Biochemical Engineering*; 17 (1980) 131 - 168.
80. Lenz, R.W.; Biodegradable Polymers; *Advances in Polymer Science*; 107 (1993) 1 - 40.
81. Lin, H., Clegg, D.O. and Lal, R.; Imaging Real-Time Proteolysis of Single Collagen I Molecules With an Atomic Force Microscope; *Biochemistry*; 38 (1999) 9956 - 9963.
82. Lobmann, R., Ambrosch, A., Schultz, G., Waldmann, K., Schiweck, S. and Lehnert, H.; Expression of Matrix-Metalloproteinases and Their Inhibitors in the Wounds of Diabetic and Non-Diabetic Patients; *Diabetologia*; 45 (2002) 1011 - 1016.
83. Lurie, D.J. and Mäder, K.; Monitoring Drug Delivery Processes by EPR and Related Techniques-Principles and Applications; *Advanced Drug Delivery Reviews*; 57 (2005) 1171 - 1190.
84. Mäder, K., Swartz, H.M., Stoesser, R. and Borchert, H.H.; The Application of EPR Spectroscopy in the Field of Pharmacy; *Pharmazie*; 49 (1994) 97 - 101.

85. Mäder,K.; Pharmazeutische Anwendungen Der Elektronenspinresonanzspektroskopie (ESR); PZ Prisma; 3 (1998) 202 - 212.
86. Mäder,K., Gallez,B., Liu,K.J. and Swartz,H.M.; Non-Invasive in Vivo Characterization of Release Processes in Biodegradable Polymers by Low-Frequency Electron Paramagnetic Resonance Spectroscopy; Biomaterials; 17 (1996) 457 - 461.
87. Maeda,H., Nakagawa,T., Adachi,N., Sakai,Y., Yamamoto,T., Matsuoka,A., Sano,A., Satoh,Y., Miyata,T. and Fujioka,K.; Design of Long-Acting Formulation of Protein Drugs With a Double-Layer Structure and Its Application to RhG-CSF; Journal of Controlled Release : Official Journal of the Controlled Release Society; 91 (2003) 281 - 297.
88. Maeda,H., Sano,A. and Fujioka,K.; Controlled Release of RhBMP-2 From Collagen Minipellet and the Relationship Between Release Profile and Ectopic Bone Formation; International Journal of Pharmaceutics; 275 (2004a) 109 - 122.
89. Maeda,H., Sano,A. and Fujioka,K.; Profile of RhBMP-2 Release From Collagen Minipellet and Induction of Ectopic Bone Formation; Drug Development and Industrial Pharmacy; 30 (2004b) 473 - 480.
90. Maeda,M., Tani,S., Sano,A. and Fujioka,K.; Microstructure and Release Characteristics of the Minipellet, a Collagen-Based Drug Delivery System for Controlled Release of Protein Drugs; Journal of Controlled Release; 62 (1999) 313 - 324.
91. Maeda,M., Kadota,K., Kajihara,M., Sano,A. and Fujioka,K.; Sustained Release of Human Growth Hormone (HGH) From Collagen Film and Evaluation of Effect on Wound Healing in Db/Db Mice; Journal of Controlled Release; 77 (2001) 261 - 272.
92. Magde,D., Elson,E.L. and Webb,W.W.; Fluorescence Correlation Spectroscopy. II. Experimental Realization; Biopolymers; 13 (1974) 29 - 61.
93. Mainardes,R.M. and Silva,L.P.; Drug Delivery Systems: Past, Present, and Future; Current Drug Targets; 5 (2004) 449 - 455.
94. Mallya,S.K., Mookhtiar,K.A. and Van Wart,H.E.; Accurate, Quantitative Assays for the Hydrolysis of Soluble Type I, II, and III 3H-Acetylated Collagens by Bacterial and Tissue Collagenases; Analytical Biochemistry; 158 (1986) 334 - 345.
95. Mallya,S.K., Mookhtiar,K.A. and Van Wart,H.E.; Kinetics of Hydrolysis of Type I, II, and III Collagens by the Class I and II Clostridium Histolyticum Collagenases; Journal of Protein Chemistry; 11 (1992) 99 - 107.
96. Mandl,I., MacLennan,J.D., Howes,E.L., DeBellis,R.H. and Sohler,A.; Isolation and Characterization of Proteinase and Collagenase From Clostridium Histolyticum; Journal of Clinical Investigation; 32 (1953) 1323 - 1329.

97. Martin,A., Swarbrick,J. and Cammarata,A.; Physical Pharmacy: Physical Chemical Principles in the Pharmaceutical Sciences (1983).
98. McLaren,A.D.; Enzyme Reactions in Structurally Restricted Systems. IV. The Digestion of Insoluble Substrates by Hydrolytic Enzymes; *Enzymologia*; 26 (1963) 237 - 246.
99. McLaren,A.D. and Packer,L.; Enzyme Reactions in Heterogeneous Systems; *Advances in Enzymology and Related Areas of Molecular Biology*; 33 (1970) 245 - 308.
100. Medicott,N.J., Waldron,N.A. and Foster,T.P.; Sustained Release Veterinary Parenteral Products; *Advanced Drug Delivery Reviews*; 56 (2004) 1345 - 1365.
101. Mohl,S.; The Development of a Sustained and Controlled Release Device for Pharmaceutical Proteins Based on Lipid Implants; PhD Thesis; LMU Munich, Germany (2004).
102. Molecular Probes; EnzCheck[®] Gelatinase/Collagenase Assay Kit; Internet (2001).
103. Mookhtiar,K.A. and Van Wart,H.E.; Clostridium Histolyticum Collagenases: a New Look at Some Old Enzymes; *Matrix (Stuttgart)*; Supplement 1 (1992) 116 - 126.
104. Nagase,H. and Woessner,J.F., Jr.; Matrix Metalloproteinases; *Journal of Biological Chemistry*; 274 (1999) 21491 - 21494.
105. Netzel-Arnett,S., Mallya,S.K., Nagase,H., Birkedal-Hansen,H. and Van Wart,H.E.; Continuously Recording Fluorescent Assays Optimized for Five Human Matrix Metalloproteinases; *Analytical Biochemistry*; 195 (1991) 86 - 92.
106. Okada,T., Hayashi,T. and Ikada,Y.; Degradation of Collagen Suture in Vitro and in Vivo; *Biomaterials*; 13 (1992a) 448 - 454.
107. Okada,Y., Gonoji,Y., Naka,K., Tomita,K., Nakanishi,I., Iwata,K., Yamashita,K. and Hayakawa,T.; Matrix Metalloproteinase 9 (92-KDa Gelatinase/Type IV Collagenase) From HT 1080 Human Fibrosarcoma Cells. Purification and Activation of the Precursor and Enzymic Properties; *Journal of Biological Chemistry*; 267 (1992b) 21712 - 21719.
108. Okada,Y., Naka,K., Kawamura,K., Matsumoto,T., Nakanishi,I., Fujimoto,N., Sato,H. and Seiki,M.; Localization of Matrix Metalloproteinase 9 (92-Kilodalton Gelatinase/Type IV Collagenase = Gelatinase B) in Osteoclasts: Implications for Bone Resorption; *Laboratory Investigation; a Journal of Technical Methods and Pathology*; 72 (1995) 311 - 322.
109. Olde Damink,L.H.H., Dijkstra,P.J., van Luyn,M.J.A., van Wachem,P.B., Nieuwenhuis,P. and Feijen,J.; Cross-Linking of Dermal Sheep Collagen Using a Water-Soluble Carbodiimide; *Biomaterials*; 17 (1996a) 765 - 773.

110. Olde Damink,L.H.H., Dijkstra,P.J., van Luyn,M.J.A., van Wachem,P.B., Nieuwenhuis,P. and Feijen,J.; In Vitro Degradation of Dermal Sheep Collagen Crosslinked Using a Water-Soluble Carbodiimide; *Biomaterials*; 17 (1996b) 679 - 684.
111. Olde Damink,L.H.H., Dijkstra,P.J., van Luyn,M.J.A., van Wachem,P.B., Nieuwenhuis,P. and Feijen,J.; Changes in the Mechanical Properties of Dermal Sheep Collagen During in Vitro Degradation; *Journal of Biomedical Materials Research*; 29 (1995) 139 - 147.
112. Overall,C.M.; Recent Advances in Matrix Metalloproteinase Research; *Trends in Glycoscience and Glycotechnology*; 3 (1991) 384 - 400.
113. Pachence,J.M., Berg,R.A. and Silver,F.H.; Collagen: Its Place in the Medical Device Industry; *Medical Device & Diagnostic Industry Magazine*; 9 (1987) 49 - 55.
114. Paige,M.F., Lin,A.C. and Goh,M.C.; Real-Time Enzymatic Biodegradation of Collagen Fibrils Monitored by Atomic Force Microscopy; *International Biodeterioration & Biodegradation*; 50 (2002) 1 - 10.
115. Palmer,G.; *Introduction to Electron Paramagnetic Resonance* (1999).
116. Pampel,A., Michel,D. and Reszka,R.; Pulsed Field Gradient MAS-NMR Studies of the Mobility of Carboplatin in Cubic Liquid-Crystalline Phases; *Chemical Physics Letters*; 357 (2002) 131 - 136.
117. Park,H. and Park,K.; Biocompatibility Issues of Implantable Drug Delivery Systems; *Pharmaceutical Research*; 13 (1996) 1770 - 1776.
118. Park,S., Park,J., Kim,H.O., Song,M.J. and Suh,H.; Characterization of Porous Collagen/Hyaluronic Acid Scaffold Modified by 1-Ethyl-3-(3-Dimethylaminopropyl)Carbodiimide Cross-Linking; *Biomaterials*; 23 (2002) 1205 - 1212.
119. Parks,W.C.; Matrix Metalloproteinases in Repair; *Wound Repair and Regeneration*; 7 (1999) 423 - 432.
120. Pek,Y.S., Spector,M., Yannas,I.V. and Gibson,L.J.; Degradation of a Collagen-Chondroitin-6-Sulfate Matrix by Collagenase and by Chondroitinase; *Biomaterials*; 25 (2003) 473 - 482.
121. Pieper,J.S., Oosterhof,A., Dijkstra,P.J., Veerkamp,J.H. and Van Kuppevelt,T.H.; Preparation and Characterization of Porous Crosslinked Collagenous Matrixes Containing Bioavailable Chondroitin Sulfate; *Biomaterials*; 20 (1999) 847 - 858.
122. Piez,K.A.; Collagen in: *Encyclopedia of Polymer Science and Engineering* 3 (1985); 699 - 727.
123. Pillai,O. and Panchagnula,R.; Polymers in Drug Delivery; *Current Opinion in Chemical Biology*; 5 (2001) 447 - 451.

124. Radu,F.A., Bause,M., Knabner,P., Lee,G.W. and Frieß,W.C.; Modeling of Drug Release From Collagen Matrices; *Journal of Pharmaceutical Sciences*; 91 (2002) 964 - 972.
125. Ranade,V.V., Hollinger,M.A. and Editors.; *Drug Delivery Systems* (2003).
126. Rehakova,M., Bakos,D., Vizarova,K., Soldan,M. and Jurickova,M.; Properties of Collagen and Hyaluronic Acid Composite Materials and Their Modification by Chemical Crosslinking; *Journal of Biomedical Materials Research*; 30 (1996) 369 - 372.
127. Roche Diagnostics; Gelatinase 92kDa; Internet (2004a).
128. Roche Diagnostics; Gelatinase 72kDa; Internet (2004b).
129. Rosenblatt,J., Rhee,W. and Wallace,D.; The Effect of Collagen Fiber Size Distribution on the Release Rate of Proteins From Collagen Matrixes by Diffusion; *Journal of Controlled Release*; 9 (1989) 195 - 203.
130. Rubingh,D.N. and Bauer,M.D.; Catalysis of Hydrolysis by Proteases at the Protein-Solution Interface; *Studies in Polymer Sciences*; 11 (1992) 445 - 464.
131. Ruszczak,Z. and Frieß,W.; Collagen As a Carrier for on-Site Delivery of Antibacterial Drugs; *Advanced Drug Delivery Reviews*; 55 (2003) 1679 - 1698.
132. Saito,K., Yoshioka,H., Ito,N., Kazama,S., Tanizawa,H., Lin,Y., Watanabe,H., Ogata,T. and Kamada,H.; Spatiotemporal ESR-CT Study on the Metabolism of Spin-Labeled Polysaccharide in a Mouse; *Biological & Pharmaceutical Bulletin*; 20 (1997) 904 - 909.
133. Saltzman,W.M.; *Drug Delivery: Engineering, Principles for Drug Therapy* (2001).
134. Sano,A., Maeda,M., Nagahara,S., Ochiya,T., Honma,K., Itoh,H., Miyata,T. and Fujioka,K.; Atelocollagen for Protein and Gene Delivery; *Advanced Drug Delivery Reviews*; 55 (2003) 1651 - 1677.
135. Sattler,W., Esterbauer,H., Glatter,O. and Steiner,W.; The Effect of Enzyme Concentration on the Rate of the Hydrolysis of Cellulose; *Biotechnology and Bioengineering*; 33 (1989) 1221 - 1234.
136. Schlapp,M.; *Kollagen/PLGA-Mikropartikel Komposite Zur Gesteuerten Freigabe Von Gentamicin*; PhD Thesis; FAU Erlangen, Germany (2001).
137. Schurr,J.M. and McLaren,A.D.; Enzyme Action: Comparison on Soluble and Insoluble Substrate; *Science (Washington, DC, United States)*; 152 (1966) 1064 - 1066.
138. Sedlarik,K.M.; *The Processes in Wound Healing*; *Wundforum* (2005) .
139. Seifter,S. and Harper,E.; *The Collagenases in: The Enzymes Bd. III* (1971); 649 - 697.

140. Seifter, S., Gallop, P.M., Klein, L. and Meilman, E.; Collagen. II. Properties of Purified Collagenase and Its Inhibition; *Journal of Biological Chemistry*; 234 (1959) 285 - 293.
141. Seifter, S. and Harper, E.; Collagenases; *Methods in Enzymology*; 19 (1970) 613 - 635.
142. Shapiro, S.D., Fliszar, C.J., Broekelmann, T.J., Mecham, R.P., Senior, R.M. and Welgus, H.G.; Activation of the 92-KDa Gelatinase by Stromelysin and 4-Aminophenylmercuric Acetate. Differential Processing and Stabilization of the Carboxyl-Terminal Domain by Tissue Inhibitor of Metalloproteinase (TIMP); *Journal of Biological Chemistry*; 270 (1995) 6351 - 6356.
143. Shastri, V.P.; Non-Degradable Biocompatible Polymers in Medicine: Past, Present and Future; *Current Pharmaceutical Biotechnology*; 4 (2003) 331 - 337.
144. Shenoy, V. and Rosenblatt, J.; Diffusion of Macromolecules in Collagen and Hyaluronic Acid, Rigid-Rod-Flexible Polymer, Composite Matrixes; *Macromolecules*; 28 (1995) 8751 - 8758.
145. Shingleton, W.D., Hodges, D.J., Brick, P. and Cawston, T.E.; Collagenase: a Key Enzyme in Collagen Turnover; *International Journal of Biochemistry & Cell Biology*; 74 (1996) 759 - 775.
146. Siegel, R.A. and Langer, R.; Controlled Release of Polypeptides and Other Macromolecules; *Pharmaceutical Research*; (1984) 2 - 10.
147. Siepmann, J. and Göpferich, A.; Mathematical Modeling of Bioerodible, Polymeric Drug Delivery Systems; *Advanced Drug Delivery Reviews*; 48 (2001) 229 - 247.
148. Siepmann, J., Kranz, H., Bodmeier, R. and Peppas, N.A.; HPMC-Matrices for Controlled Drug Delivery: a New Model Combining Diffusion, Swelling, and Dissolution Mechanisms and Predicting the Release Kinetics; *Pharmaceutical Research*; 16 (1999a) 1748 - 1756.
149. Siepmann, J., Podual, K., Sriwongjanya, M., Peppas, N.A. and Bodmeier, R.; A New Model Describing the Swelling and Drug Release Kinetics From Hydroxypropyl Methyl Cellulose Tablets; *Journal of Pharmaceutical Sciences*; 88 (1999b) 65 - 72.
150. Siepmann, J., Faisant, N. and Benoit, J.P.; A New Mathematical Model Quantifying Drug Release From Bioerodible Microparticles Using Monte Carlo Simulations; *Pharmaceutical Research*; 19 (2002) 1885 - 1893.
151. Sigma Aldrich; Collagenase C78051; Internet (1998).
152. Silver, F.H. and Garg, A.K.; Collagen. Characterization, Processing, and Medical Applications; *Drug Targeting and Delivery*; 7 (1997) 319 - 346.
153. Singh, M.; A Fundamental Study of Electrostatic Effects in Release of Polypeptides From Collagen Hydrogels (Drug Delivery); PhD Thesis; Univ. of Maryland Baltimore County, Baltimore, MD, USA (1994).

154. Sinha, V.R. and Trehan, A.; Biodegradable Microspheres for Protein Delivery; *Journal of Controlled Release*; 90 (2003) 261 - 280.
155. Smith, P.K., Krohn, R.I., Hermanson, G.T., Mallia, A.K., Gartner, F.H., Provenzano, M.D., Fujimoto, E.K., Goeke, N.M., Olson, B.J. and Klenk, D.C.; Measurement of Protein Using Bicinchoninic Acid; *Analytical Biochemistry*; 150 (1985) 76 - 85.
156. Soo, C., Rahbar, G. and Moy, R.L.; The Immunogenicity of Bovine Collagen Implants; *Journal of Dermatologic Surgery and Oncology*; 19 (1993) 431 - 434.
157. Soru, E. and Zaharia, O.; Clostridium Histolyticum Collagenase. II. Partial Characterization; *Enzymologia*; 43 (1972) 45 - 55.
158. Sparer, R.V., Shih, C., Ringeisen, C.D. and Himmelstein, K.J.; Controlled Release From Erodible Poly(Ortho Ester) Drug Delivery Systems; *Journal of Controlled Release*; 1 (1984) 23 - 32.
159. Steiner, W., Sattler, W. and Esterbauer, H.; Adsorption of Trichoderma Reesei Cellulase on Cellulose: Experimental Data and Their Analysis by Different Equations; *Biotechnology and Bioengineering*; 32 (1988) 853 - 865.
160. Steven, F.S.; Polymeric Collagen Fibrils. An Example of Substrate-Mediated Steric Obstruction of Enzymic Digestion; *Biochimica et Biophysica Acta*; 452 (1976) 151 - 160.
161. Stryer, L.; *Enzyme in: Biochemie* (1996); 191 - 217.
162. Suga, K., Van Dedem, G. and Moo-Young, M.; Enzymic Breakdown of Water Insoluble Substrates; *Biotechnology and Bioengineering*; 17 (1975) 185 - 201.
163. Swartz, H.M., Borg, D.C. and Bolton, J.R.; *Biological Applications of Electron Spin Resonance* (1972).
164. Thombre, A.G. and Himmelstein, K.J.; A Simultaneous Transport-Reaction Model for Controlled Drug Delivery From Catalyzed Bioerodible Polymer Matrixes; *AIChE Journal*; 31 (1985) 759 - 766.
165. Thorwarth, M., Schultze-Mosgau, S., Wehrhan, F., Kessler, P., Srour, S., Wiltfang, J. and Schlegel, K.A.; Bioactivation of an Anorganic Bone Matrix by P-15 Peptide for the Promotion of Early Bone Formation; *Biomaterials*; 26 (2005) 5648 - 5657.
166. Traore, A., Foucat, L. and Renou, J.P.; ¹H-NMR Study of Water Dynamics in Hydrated Collagen: Transverse Relaxation-Time and Diffusion Analysis; *Biopolymers*; 53 (2000) 476 - 483.
167. Trengove, N.J., Stacey, M.C., MacAuley, S., Bennett, N., Gibson, J., Burslem, F., Murphy, G. and Schultz, G.; Analysis of the Acute and Chronic Wound Environments: the Role of Proteases and Their Inhibitors; *Wound Repair and Regeneration*; 7 (1999) 442 - 452.

168. Tsuk,A.G. and Oster,G.; Determination of Enzyme Activity by a Linear Measurement; *Nature* (London, United Kingdom); 190 (1961) 721 - 722.
169. Tzafirri,A.R.; Mathematical Modeling of Diffusion-Mediated Release From Bulk Degrading Matrices; *Journal of Controlled Release*; 63 (2000) 69 - 79.
170. Tzafirri,A.R., Bercovier,M. and Parnas,H.; Reaction Diffusion Model of the Enzymatic Erosion of Insoluble Fibrillar Matrices; *Biophysical Journal*; 83 (2002) 776 - 793.
171. Uhrich,K.E., Cannizzaro,S.M., Langer,R.S. and Shakesheff,K.M.; Polymeric Systems for Controlled Drug Release; *Chemical Reviews* (Washington, D.C.); 99 (1999) 3181 - 3198.
172. van Wachem,P.B., van Luyn,M.J., Olde Damink,L.H., Dijkstra,P.J., Feijen,J. and Nieuwenhuis,P.; Biocompatibility and Tissue Regenerating Capacity of Crosslinked Dermal Sheep Collagen; *Journal of Biomedical Materials Research*; 28 (1994a) 353 - 363.
173. van Wachem,P.B., van Luyn,M.J., Olde Damink,L.H., Dijkstra,P.J., Feijen,J. and Nieuwenhuis,P.; Tissue Regenerating Capacity of Carbodiimide-Crosslinked Dermal Sheep Collagen During Repair of the Abdominal Wall; *International Journal of Artificial Organs*; 17 (1994b) 230 - 239.
174. Van Wart,H.E. and Steinbrink,D.R.; A Continuous Spectrophotometric Assay for *Clostridium Histolyticum* Collagenase; *Analytical Biochemistry*; 113 (1981) 356 - 365.
175. Vassel-Biergans,A.; *Kollagen-Wundauflagen in: Wundauflagen ; WVG* (2004); 166 - 174.
176. von Burkersroda,F., Schedl,L. and Gopferich,A.; Why Degradable Polymers Undergo Surface Erosion or Bulk Erosion; *Biomaterials*; 23 (2002) 4221 - 4231.
177. Wall,S.J., Bevan,D., Thomas,D.W., Harding,K.G., Edwards,D.R. and Murphy,G.; Differential Expression of Matrix Metalloproteinases During Impaired Wound Healing of the Diabetes Mouse; *Journal of Investigative Dermatology*; 119 (2002) 91 - 98.
178. Wallace,D.G. and Rosenblatt,J.; Collagen Gel Systems for Sustained Delivery and Tissue Engineering; *Advanced Drug Delivery Reviews*; 55 (2003) 1631 - 1649.
179. Wang,M.C., Pins,G.D. and Silver,F.H.; Collagen Fibers With Improved Strength for the Repair of Soft Tissue Injuries; *Biomaterials*; 15 (1994) 507 - 512.
180. Weadock,K.S., Olson,R.M. and Silver,F.H.; Evaluation of Collagen Crosslinking Techniques; *Biomaterials, Medical Devices, and Artificial Organs*; 11 (1984) 293 - 318.
181. Weadock,K.S., Miller,E.J., Keuffel,E.L. and Dunn,M.G.; Effect of Physical Crosslinking Methods on Collagen-Fiber Durability in Proteolytic Solutions; *Journal of Biomedical Materials Research*; 32 (1996) 221 - 226.

182. Weadock, K.S., Wolff, D. and Silver, F.H.; Diffusivity of Iodine-125-Labeled Macromolecules Through Collagen: Mechanism of Diffusion and Effect of Adsorption; *Biomaterials*; 8 (1987) 105 - 112.
183. Weadock, K.S.; *Macromolecular Diffusion Through Collagen Membranes*; PhD Thesis; Rutgers, State Univ., New Brunswick, NJ, USA (1986).
184. Weiss, J.B.; Enzymic Degradation of Collagen; *International Review of Connective Tissue Research*; 7 (1976) 101 - 157.
185. Welgus, H.G., Jeffrey, J.J., Stricklin, G.P., Roswit, W.T. and Eisen, A.Z.; Characteristics of the Action of Human Skin Fibroblast Collagenase on Fibrillar Collagen; *Journal of Biological Chemistry*; 255 (1980) 6806 - 6813.
186. Welgus, H.G., Kobayashi, D.K. and Jeffrey, J.J.; The Collagen Substrate Specificity of Rat Uterus Collagenase; *Journal of Biological Chemistry*; 258 (1983) 14162 - 14165.
187. Winzenburg, G., Schmidt, C., Fuchs, S. and Kissel, T.; Biodegradable Polymers and Their Potential Use in Parenteral Veterinary Drug Delivery Systems; *Advanced Drug Delivery Reviews*; 56 (2004) 1453 - 1466.
188. Wise, D.L. and Editor.; *Handbook of Pharmaceutical Controlled Release Technology* (2000).
189. Woessner, J.F.; Matrix Metalloproteinases and Their Inhibitors in Connective Tissue Remodeling; *FASEB Journal*; 5 (1991) 2145 - 2154.
190. Wysocki, A.B., Staiano-Coico, L. and Grinnell, F.; Wound Fluid From Chronic Leg Ulcers Contains Elevated Levels of Metalloproteinases MMP-2 and MMP-9; *Journal of Investigative Dermatology*; 101 (1993) 64 - 68.
191. Yannas, I.V., Burke, J.F., Huang, C. and Gordon, P.L.; Correlation of in Vivo Collagen Degradation Rate With in Vitro Measurements; *Journal of Biomedical Materials Research*; 9 (1975) 623 - 628.
192. Yoshioka, H., Tanizawa, H., Ogata, T. and Kazama, S.; A Novel Spin Probe With Long Life in Vivo for ESR Imaging; *Biological & Pharmaceutical Bulletin*; 18 (1995) 1572 - 1575.
193. Yoshizaki, T., Sato, H. and Furukawa, M.; Recent Advances in the Regulation of Matrix Metalloproteinase 2 Activation: From Basic Research to Clinical Implication (Review); *Oncology Reports*; 9 (2002) 607 - 611.
194. Zeeman, R., Dijkstra, P.J., Van Wachem, P.B., Van Luyn, M.J.A., Hendriks, M., Cahalan, P.T. and Feijen, J.; Successive Epoxy and Carbodiimide Crosslinking of Dermal Sheep Collagen; *Biomaterials*; 20 (1999) 921 - 931.

Presentations associated with this work

I. Metzmacher, F. Wehrhan, S. Schultze-Mosgau, K. Mäder, W. Frieß
Investigation of the In Vivo Drug Release from Collagen Minirods by ESR
Poster, 32nd Annual Meeting of the Controlled Release Society; Miami Beach (2005)

F. Radu, **I. Metzmacher**, M. Bause, W. Frieß, P. Knabner
Modeling drug release from collagen matrices undergoing enzymatic degradation
Poster, 32nd Annual Meeting of the Controlled Release Society; Miami Beach (2005)

I. Metzmacher, P. Ruth, M. Abel, W. Frieß
"Inaktivierung von bakterieller Kollagenase, MMP-2 und MMP-9 durch Suprasorb® C"
MedReport Nr. 36, 11 (2004)

I. Metzmacher, P. Ruth, M. Abel, W. Frieß
"Inaktivierung von bakterieller Kollagenase, MMP-2 und MMP-9 durch Suprasorb® C"
Oral presentation for the DGfW award of basic research, 8th Congress of the German Society of Wound Healing and Wound Treatment; Weimar (2004)

I. Metzmacher, P. Ruth, M. Abel, W. Frieß
Inactivation of MMP-2 and MMP-9 by Suprasorb® C
Poster, 2nd Congress of the World Union of Wound Healing Societies; Paris (2004)

I. Metzmacher, P. Ruth, M. Abel, W. Frieß
Swelling and Degradation of Collagen Minirods
Poster, 2nd Congress of the World Union of Wound Healing Societies; Paris (2004)

I. Metzmacher, W. Frieß
Studies on the Interaction between Insoluble Collagen and Collagenase
Poster, 18th European Conference of Biomaterials; Stuttgart (2003)

I. Metzmacher, W. Frieß
Collagen Minirods for Sustained Release
Poster, 30th Annual Meeting of the Controlled Release Society; Glasgow (2003)

M. Bause, W. Frieß, P. Knabner, **I. Metzmacher**, F. Radu
Modeling drug release from collagen matrices undergoing enzymatic degradation
Poster, 30th Annual Meeting of the Controlled Release Society; Glasgow (2003)

Curriculum Vitae

Iris Metzmacher, *nee* Krebs

PERSONAL DATA

date of birth: March 7th, 1977
place of birth: Munich, Germany
marital status: married (since 2002)
citizenship: German

EDUCATION

01/2002 – 10/2005 Ph.D. thesis; Department of Pharmacy, Pharmaceutical Technology and Biopharmaceutics, LMU; Munich, Germany
supervisor: Prof. Dr. W. Frieß
in cooperation with the Institute of Applied Mathematics, FAU; Erlangen, Germany

01/2002 licensed pharmacist

05/2001 – 10/2001 internship at Azupharma GmbH & Co.; Gerlingen, Germany
(division of pharmaceutical development)

11/2000 – 04/2001 internship at Apotheke am Forum; Munich, Germany

1996 - 2000 Study of Pharmacy, LMU; Munich, Germany

06/1996 graduation with Abitur

1987 – 1996 secondary school; Dachau, Germany